

**MODELLING HYDROLOGICAL RESPONSES TO LAND USE AND
CLIMATE CHANGE: THE MFOLOZI CATCHMENT**

ANDREW ZAWADI MARO

Submitted in partial fulfilment of the requirements for the degree of
Master of Science in Engineering
in the
Civil Engineering Programme
University of KwaZulu-Natal
Durban
2012

Supervisor: Professor Derek Stretch

ABSTRACT

St. Lucia is South Africa's largest and most important estuarine system. The Mfolozi and Mkuze catchments provide the main source of water to the system. Regional climate change may influence future water and sediment yields from the catchments. Other factors include human activities in the form of land use changes, forestation, urbanisation and/or unsustainable agricultural activities leading to land degradation.

In this study these changes were evaluated using an analysis of historical rainfall data for the region, and by applying the ACURU model to simulate water and sediment yields incorporating land use changes. Rainfall intensity was a particular focus since it affects the erosion process that underpins sediment yield by providing and maintaining the water-to-sediment ratio within the flow.

No consistent evidence of statistically significant changes in mean annual rainfall was found. However, an increase in average intensity of rainfall events across all gauging stations was supported by statistically significant reductions in the number of annual wet-days. An increase in the occurrence of high intensity rainfall (>30mm/day and 50mm/day) was found to be small but statistically significant.

Hydrological responses to present land-uses have been evaluated by comparing streamflows and sediment yields generated under natural and current land covers. It was determined that the Mfolozi catchment has undergone a 33% change in land-use from natural conditions. The hydrological impacts of this were a 38% reduction in streamflow accompanied by a 53% increase sediment yield from natural land cover conditions. Subcatchments with high proportions of commercial forest and sugarcane plantations have been identified as the major source of these changes.

Using a combination of empirically downscaled rainfall from global climate models, future projections assuming present day land-uses of catchment streamflow and sediment yield have been presented and compared against future projections assuming natural land covers. This was done so as to compare the effects of land-use and climate change on the hydrology of the Mfolozi catchment. Impacts of land-use change were found to be greater

than those due to climate change. In a scenario that assumed both occurred, it was found that land-use change was still the dominant driver of hydrological responses, with climate change providing either an amplification or attenuation effect.

The findings from this research will provide decision-makers with quantitative guidelines for effective management of the St Lucia Estuary system under different land-use and climatic scenarios.

PREFACE

I, Andrew Zawadi Maro, hereby declare that the whole of this dissertation is my own work and has not been submitted in part, or in whole to any other University. Where use has been made of the work of others, it has been duly acknowledged in the text. This research work was carried out in the Centre for Research in Environmental, Coastal and Hydraulic Engineering, School of Civil Engineering, Surveying and Construction, University of KwaZulu-Natal, Durban, under the supervision of Professor D. D. Stretch.

December 3, 2012

.....

.....

Andrew Zawadi Maro

Date

As the candidates supervisor I have approved this dissertation for submission

December 3, 2012

.....

.....

Professor D. D. Stretch

Date

Copyright © 2012 University of KwaZulu-Natal

All rights reserved.

ACKNOWLEDGEMENTS

I would like to express my sincere gratitude to the following:

- My family, for their unconditional love and unending motivation throughout the entire duration of the MSc Programme.
- My supervisor, Prof. Derek Stretch for his continued guidance and support.
- Mark Horan, for mentoring on ACRU.
- The Staff at the School of Bio-resources Engineering and Environmental Hydrology (University of KwaZulu-Natal, Pietermaritzburg).
- Prof. Renzo Perissinotto, for use of laboratory equipment from the School of Biological Sciences (University of KwaZulu-Natal, Westville).
- The South African Weather Service (SAWS) for providing rainfall and temperature data.
- The Mtubatuba Water Treatment Works for providing turbidity measurements.

The research was made possible by a grant from the South Africa Netherlands research Programme on Alternatives in Development (SANPAD).

TABLE OF CONTENTS

Abstract.....	i
Preface	iii
Acknowledgements.....	iv
Table of Contents.....	v
List of Figures	xi
List of Tables	xvi
Abbreviations.....	xvii
1. Introduction.....	1
1.1 Background and Motivation.....	1
1.2 Research questions	2
1.3 Aim.....	2
1.4 Objectives.....	2
1.5 Dissertation outline	3
2. General overview of Mfolozi-St Lucia Catchments	4
3. Literature review	7
3.1 Climate change, variability, trends and predictions: a critical review	7
3.1.1 An introduction to climate change.....	7
3.1.2 Observed changes in rainfall trends including extreme events: A global overview.....	12
3.1.2.1 Observed rainfall trends	12
3.1.2.2 Extreme precipitation	13
3.1.3 Observed and projected trends including extreme precipitation events in South Africa.....	18
3.1.3.1 Climate Context.....	18

3.1.3.2	Observed Trends.....	18
3.1.3.3	Observed extreme events.....	21
3.1.4	Summary of past rainfall trends across South Africa	23
3.1.5	Projected trends.....	23
3.2	Erosion and Sediment dynamics: a critical review	25
3.2.1	Soil erosion: concepts, processes and principles	25
3.2.2	Erosion due to rain drop impact and leaf drip	25
3.2.3	Physical process of raindrop erosion and sediment deposition	26
3.2.4	Sediment transport and Sediment Yield	28
3.3	Brief overview of Sediment transport formulae.....	29
3.3.1	Bed-load transport formulae	30
3.3.1.1	DuBoy's approach	30
3.3.1.2	Meyer-Peter approach	30
3.3.1.3	Einstein-Brown approach.....	31
3.3.1.4	Summary of bed-load sediment transport formulae	32
3.3.2	General approach to suspended load transport	32
3.3.3	Summary of sediment transport formulae	34
3.4	Sediment transport capacity, sediment load, and sediment yield	34
3.4.1	Mathematical modelling of sediment yield	36
3.4.1.1	Physical and empirical based models.....	36
3.4.1.2	The Revised Universal Soil Loss Equation (RUSLE).....	37
3.4.1.3	The Agricultural Catchments Research Unit (ACRU) model	39
3.4.1.4	The Water Erosion Prediction Project (WEPP) Model	41
3.4.1.5	The SHETRAN model	43

3.4.1.6	Summary and general comparison of the ACRU, WEPP, and SHETRAN models	44
3.5	Overview on Hydrological impacts of land-use change within South African catchments	45
3.6	Criteria for the selection of an appropriate hydrological model for land-use change in the Mfolozi catchment	50
3.7	Catchment Sediment yields: The Mfolozi catchment in a global and Southern African perspective	52
4.	Methodology	55
4.1	Introduction	55
4.1.1	Literature review	55
4.2	Methodological approach to analysis of hydrological data	55
4.2.1	Analysis of hydrological data	55
4.2.1.1	Suitable data set	56
4.2.1.2	Exploratory data analysis	57
4.2.1.3	Locally weighted regression	57
4.2.2	Application of statistical tests	58
4.2.2.1	Moving averages	58
4.2.2.2	Linear regression	58
4.2.2.3	Hypothesis testing	59
4.2.2.4	Using the T-test to test for homogeneity	59
4.2.2.5	Gamma distribution	60
4.2.3	Definition of heavy rainfall event	60
4.2.4	Summary of rainfall data collection and analysis procedure	61
4.2.5	Limitations of rainfall data analysis	62
4.3	Methodological approach to hydrological modelling with ACRU	62

4.3.1	Catchment configuration.....	63
4.3.2	Daily rainfall	65
4.3.3	Daily temperature and daily potential evaporation.....	66
4.3.4	Soils information.....	68
4.3.5	Baseline land cover and current land use scenarios.....	69
4.3.5.1	Baseline (pristine) land cover	70
4.3.5.2	Present day land-use	71
4.3.6	Streamflow simulation control variables	71
4.3.6.1	Stormflow generation in ACRU.....	72
4.3.6.2	Baseflow generation in ACRU.....	73
4.3.6.3	Streamflow simulations in ACRU.....	73
4.3.7	Sediment yield generation in ACRU	74
4.4	Methodological approach to measuring total suspended solid (TSS) concentration 76	
4.5	Summary of methodology.....	77
5.	Results and Discussion	79
5.1	Introduction.....	79
5.2	Mfolozi catchment historical rainfall trends and extreme precipitation events	79
5.2.1	Rainfall trends within the Mfolozi – St Lucia System.....	79
5.2.2	Extreme rainfall within the Mfolozi – St Lucia system.....	82
5.2.3	Mean annual precipitation of the Mfolozi catchment.....	87
5.3	Modelling streamflow under present land-use conditions	88
5.3.1	Streamflow generation and verification under current land use conditions ..	88
5.3.1.1	Verification of streamflow output of White Mfolozi (W2H005) from ACRU model	90

5.3.1.2	Verification of streamflow output of Black Mfolozi (W2H006) from ACRU model	92
5.3.1.3	Verification of streamflow output of combined Mfolozi River (W2H010) from ACRU model.....	94
5.3.1.4	Verification of streamflow output of combined Mfolozi River (W2H032) from ACRU model.....	96
5.3.1.5	Summary of streamflow verification.....	98
5.3.2	Where in the Mfolozi catchment is streamflow generated	99
5.4	Modelling sediment yield under present land-use conditions.....	101
5.4.1	Where in the Mfolozi catchment is the soil prone to erosion	101
5.4.2	Mfolozi catchment present condition sediment yields	102
5.4.3	Validation of sediment yields	104
5.4.3.1	Validation of sediment yields using calibrated TSS vs. Turbidity relationship.....	104
5.4.3.2	Validation of simulated sediment yields against published reports	106
5.4.4	Discussion on long-term monthly variation in discharge and sediment concentration.....	109
5.5	Hydrological impacts of present land-uses on pristine streamflows and sediment yields	111
5.5.1	Evaluating impacts of present land uses on pristine streamflows	113
5.5.2	Evaluating impacts of present land uses on pristine sediment yields	115
5.5.3	Summary of hydrological responses due to land-use changes	118
5.6	Hydrological responses to projected climate change in the Mfolozi catchment.	122
5.6.1	GCM model performance assessment	122
5.6.1.1	Background to projected future climates.....	122
5.6.1.2	Summary of potential future climates of the Mfolozi catchment.....	123

5.6.2	Potential impacts of future climate on streamflows and sediment yields....	125
5.7	Streamflow and sediment yield responses to the combined effects of land-use and climate change	129
5.7.1	Summary of hydrological responses to land-use and climate change in the Mfolozi catchment	134
5.8	Discussion on the implications for the St. Lucia System.....	137
6.	Summary and conclusions	143
6.1	Evidence for regional climate change within the St. Lucia System using rainfall as an indicator	143
6.2	Evaluation of present land-uses on pristine streamflows and sediment yield.....	143
6.3	Hydrological responses to land-use and projected climate change.....	144
6.4	Summation	144
6.5	Recommendations for future research	145
7.	References.....	146
8.	APPENDICES	159
	Contents of appendices:.....	159
	Appendix A: Graphs of rainfall trends and peak over predefined thresholds	160
	Appendix B: National land cover classification.	166
	Appendix C: National land-cover classes aggregated into Agriculture, Degraded, Natural, Urban.	167
	Appendix D: Agro-hydrological modelling and validation of ACRU simulations ...	168
	Appendix E: Components of the SHETRAN model	178
	Appendix F: GCMs global climate change scenarios.....	180

LIST OF FIGURES

Figure 2-1: Catchments surrounding Lake St. Lucia	4
Figure 2-2: Basin elevations (in meters above mean sea level) and primary catchments within the Lake St. Lucia system	5
Figure 2-3: Predominant soil types within the Mfolozi-St. Lucia catchments	6
Figure 3.1-1: Annual precipitation from 1900 to 1999, showing increases at temperate latitudes and decreases at subtropical latitudes.....	9
Figure 3.1-2: Global trend in annual precipitation amounts, 1901-2005 (upper percentage per country) and 1979-2005 (lower percentage per decade), as a percentage of the 1961-1990 average from GHCN stations.....	12
Figure 3.1-3: Regions where analyses of heavy precipitation have been completed.	14
Figure 3.1-4: An increase in variance without a change in mean implying an increase in probability of extremes, as well as increases in absolute values of extremes.	15
Figure 3.1-5: Linear trends (%/decade) of heavy precipitation (above the 90th percentile) and total precipitation during the rainy season over various regions of the globe	17
Figure 3.1-6: 1950 – 1999 trend of change per decade in mean monthly number of rain-days with rainfall greater than 2mm	19
Figure 3.1-7: 1950 - 1999 trend of change per decade in mean monthly dry spell duration (days).	20
Figure 3.1-8: Percentage changes in the intensity of 10-year high rainfall events over South Africa from 1931-1990.	21
Figure 3.1-9: Trend (1950 – 1999) of change per decade in mean monthly 90 th percentile magnitude rainfall event (mm)	22
Figure 3.2-1: Raindrop impact potential: 5mm raindrop having 500 times more destructive potential than 1mm raindrop.....	26
Figure 3.2-2: Raindrop impact potential based on velocities for erosion, sedimentation & transportation vs. raindrop diameter.	27
Figure 3.2-3: Interaction between flow velocity, particle erosion, transport and deposition	28

Figure 3.2-4: Schematic of watershed illustrating the basic forms of sediment movement..	29
Figure 3.2-5: Suspended sediment in suspended turbulent flow	33
Figure 3.2-6: Vertical distribution of sediment concentration and fluid velocity	33
Figure 3.2-7: Theory controlling sediment transport rates, considering the relationship between sediment supply and sediment availability.....	36
Figure 3.2-8: The ACRU agro-hydrological modelling system: Concepts.	40
Figure 3.2-9: The ACRU agrohydrological modelling system: General Structure	41
Figure 3.2-10: Information flows and components of SHETRAN.....	43
Figure 3.2-11: Comparison of the SHETRAN, WEPP, and ACRU models based on erosion and sediment yield components.....	45
Figure 3.2-12: Percentage contributions of equally sized land-use units to the mean annual streamflow of a hypothetical subcatchment within the Mgeni catchment that experiences a MAP equal to the median MAP of the Mgeni catchment.....	47
Figure 3.2-13: Mean monthly ratios of stormflow to total runoff for commercial forestry, sugarcane plantation, urban areas, degraded areas, and natural vegetation for a hypothetical subcatchment in the Mgeni catchment.....	48
Figure 3.2-14: One year simulated daily evaporation (left) and accumulated monthly evaporation (right) of a typical subcatchment in the Upper Breede catchment under commercial irrigated agriculture and natural vegetation.	49
Figure 3.2-15: Lake St. Lucia catchments rainfall index.....	52
Figure 3.2-16: Comparison of the drainage area and sediment yield for various rivers.....	53
Figure 4-1: Flow chart showing main stages in statistical analysis of change	56
Figure 4-2: Mfolozi Quaternary Catchments: W21, W22, and W23 prefixes represent the White Mfolozi, Black Mfolozi, and Mfolozi Rivers respectively.	63
Figure 4-3: Quinary Catchments and major river systems of the Mfolozi River representing inter-catchment flow paths.....	64
Figure 4-4: An example of quaternary catchment flow routing between veld-units.	65
Figure 4-5: Mean Annual Precipitation for Northern KZN catchments.....	66
Figure 4-6: Mean annual A-Pan equivalent reference potential evaporation for South Africa	67

Figure 4-7: Soil types of the Mfolozi – St. Lucia catchments	69
Figure 4-8: Acocks Veld types for Mfolozi River	70
Figure 4-9: Mfolozi catchment current land-use	71
Figure 4-10: C-factor for permanent pasture, veld and woodland.....	76
Figure 4-11: Set-up of TSS filtration apparatus and vacuum pump.....	77
Figure 5-1: Mfolozi quaternary catchment mean annual precipitation (MAP) 1950-2010.	87
Figure 5-2: Verification flows of White Mfolozi River, 1964-2010 (weir: W2H005).....	90
Figure 5-3: Comparison of accumulated monthly streamflows of White Mfolozi: (a). from 1964 – 1999 and (b). 2000 – 2010	91
Figure 5-4: Verification flows of Black Mfolozi River, 1970-2010 (weir: W2H006).....	92
Figure 5-5: Comparison of accumulated monthly streamflows of Black Mfolozi: (a). from 1970 – 1999 and (b). 2000 – 2010	93
Figure 5-6: Verification flows of Mfolozi River, 1972-2010 (weir: W2H010).	94
Figure 5-7: Comparison of accumulated monthly streamflows of combined Mfolozi River (Weir W2H010): (a). from 1972 – 1984 and (b). 2000 – 2010	95
Figure 5-8: Verification flows of Mfolozi River, 1994-2010 (weir: W2H032).	96
Figure 5-9: Comparison of accumulated monthly streamflows of combined Mfolozi River (Weir W2H032): (a). from 1994 – 1999 and (b). 2000 – 2010	97
Figure 5-10: Comparison of mean monthly flows for weirs W2H005 (left) and W2H006 (right)	98
Figure 5-11: Mfolozi quaternary catchment mean annual runoff (MAR) under current land-use conditions.	100
Figure 5-12: Soil erosion index by quaternary catchment - Mfolozi catchment outlined in blue.....	101
Figure 5-13: Time series showing the Mfolozi catchment average annual sediment yield (1950-2010) under current land use conditions.	103
Figure 5-14: Quaternary catchment average sediment yield (1950-2010) for current land-use conditions.	104
Figure 5-15: Observed relationship between TSS (g/L) and turbidity (NTU).	105
Figure 5-16: Accumulated monthly simulated and observed sediment loads (2000 – 2010).	106

Figure 5-17: Correlation between simulated and measured sediment loads.	106
Figure 5-18: Comparison of quaternary catchment sediment yield (ACRU vs. WR2005)107	
Figure 5-19: Correlation between simulated ACRU quaternary sediment yields and WR2005 sediment yields.	107
Figure 5-20: Monthly averaged flows and suspended sediment loads in the Mfolozi based on measured suspended sediment concentrations.....	108
Figure 5-21: Comparison of Mfolozi catchment annual sediment loads (ACRU simulations vs. modified Pitman model by Stretch <i>et al.</i> , 2012).	109
Figure 5-22: Monthly time series of discharge and suspended sediment concentrations for the period 1950-1979 for the Mfolozi catchment.	110
Figure 5-23: Monthly time series of discharge and suspended sediment concentrations for the period 1980-2010 for the Mfolozi catchment.	110
Figure 5-24: Lake St. Lucia catchments rainfall index.....	111
Figure 5-25: Mfolozi Catchment land-cover characteristics.	112
Figure 5-26: Mfolozi Quaternary Catchment land-use distribution.	112
Figure 5-27: (a) Mfolozi quaternary catchment mean annual runoff (MAR) under pristine conditions; (b) changes in quaternary catchment MAR as a percentage change.....	114
Figure 5-28: Comparison of present and pristine quaternary water yields of the Mfolozi catchment.	115
Figure 5-29: Time series of average annual sediment yields (1950-2010) for the Mfolozi catchment.	116
Figure 5-30: (a) Mfolozi quaternary catchment average annual sediment yield under pristine conditions; (b) changes in quaternary catchment sediment yield as a multiplicative factor from pristine to current conditions.	117
Figure 5-31: Distribution of erosion gullies in the Lake St. Lucia catchments.	118
Figure 5-32: Mfolozi quaternary catchment 50-year (a) and 100-year (b) MAP projection.	124
Figure 5-33: Downscaled rainfall predictions for South Africa from various GCMs, for the next century to 2100	125
Figure 5-34: Potential impacts of near future (2046 – 2065) climate change on (a) streamflows and (b) sediment yields.	127

Figure 5-35: Potential impacts of future (2081 – 2100) climate change on (a) streamflows and (b) sediment yields. 128

Figure 5-36: Potential impacts on (a) streamflow and (b) sediment yield from combined land-use and climate change for near future (2046 – 2065). 130

Figure 5-37: Overall impact of combined land-use and climate change on sediment yield (2046-2065), showing a 20% net increase in catchment sediment yield from current conditions. 131

Figure 5-38: Potential impacts on (a) streamflow and (b) sediment yield from combined land-use and climate change for future (2081 – 2100). 132

Figure 5-39: Overall impact of combined land-use and climate change on sediment yield (2081-2100), showing a 54% net increase in catchment sediment yield from current conditions. 133

Figure 5-40: Percentage changes in Mfolozi quaternary catchment (a) MAR and (b) multiplication factors of sediment yield under projections of land-use change, potential climate change, and combined land-use and climate change (2046 – 2065). 135

Figure 5-41: Percentage changes in Mfolozi quaternary catchment (a) MAR and (b) multiplication factors of sediment yield under projections of land-use change, potential climate change, and combined land-use and climate change (2081 – 2100). 136

Figure 5-42: (a) Pristine (Acocks, 1988) and (b) current (NLC, 2005) land-uses for the Lake St. Lucia catchments, relative to the Mfolozi catchment. 138

Figure 5-43: Current (left column), 50 year projection (centre column), and 100 year projection (right column) of MAP, MAR, and sediment yield for the Lake St. Lucia catchments. 139

Figure 5-44: Past, recorded, and projected sea level rise. 141

Figure 5-45: Location of Lake St. Lucia Estuary in South Africa, and schematic of separate & combined Mfolozi inlets. 142

LIST OF TABLES

Table 3.1-1: Regions/seasons/periods where the linear trends of the number of days with heavy precipitation are amplified relative to mean precipitation totals and frequency.....	16
Table 3.1-2: Regional averages of precipitation projections for Southern Africa from 21 global models in the MMD for the A1B scenario.	24
Table 5-1: Mfolozi Catchment selected rainfall stations showing MAP, observed change in precipitation (%), and statistical significance.	80
Table 5-2: Results from stations t-test on approx. 20 year sub-periods	81
Table 5-3: St. Lucia Wetland quantile thresholds, regression gradient and statistical significance (p-value)	83
Table 5-4: Stations average number of wet days, and change in rainfall intensity above predefined thresholds of 10mm, 20mm, 30mm, and 50mm.....	83
Table 5-5: Selected stations mean, variance, and gamma distribution parameters fitted to daily rainfall data over 20-year periods.	85
Table 5-6: MAR, runoff coefficient, contributing catchment area, MAP and mean annual potential evaporation for weir W2H005	98
Table 5-7: MAR, runoff coefficient, contributing catchment area, MAP and mean annual potential evaporation for weir W2H006	99
Table 5-8: MAR, runoff coefficient, contributing catchment area, MAP and mean annual potential evaporation for weir W2H010	99
Table 5-9: MAR, runoff coefficient, contributing catchment area, MAP and mean annual potential evaporation for weir W2H032	99
Table 5-10: Hydrological characteristics of the White Mfolozi Catchment.....	119
Table 5-11: Hydrological characteristics of the Black Mfolozi Catchment	120
Table 5-12: Hydrological characteristics of the Mfolozi Catchment	121
Table 5-13: 50 and 100-year future climate projections from empirically downscaled GCMs.....	123
Table 5-14: Sea level rise rates for South Africa.....	141

ABBREVIATIONS

ACRU	Agricultural Catchments Research Unit
AOGCM	Atmosphere-Ocean Global Climate Model
DBN	Durban
DJF	December, January February
EDA	Exploratory Data Analysis
ENSO	El Nino Southern Oscillation
GCM	Global Climate Model
GIS	Geographical Information System
GHCN	Global Historical Climatology Network
IPCC	Intergovernmental Panel on Climate Change
ITCZ	Inter-Tropical Convergence Zone
JJA	June, July, August
KZN	KwaZulu-Natal
MAM	March April May
MMD	Multi-Model Data
MUSLE	Modified Universal Soil Loss Equation
NTU	Nephelometric Turbidity Unit
POT	Peak Over Threshold
PUT	Peak Under Threshold
RUSLE	Revised Universal Soil Loss Equation

SA	South Africa
SHETRAN	A 3-dimensional physically based model with coupled water and sediment transport multi-fractions
UKZN	University of KwaZulu-Natal
USLE	Universal Soil Loss Equation
UNFCCC	United Nations Framework Convention on Climate Change
WEPP	Water Erosion Prediction Project, National Soil Erosion Research Laboratory, USA
WMO	World Metrological Organisation

1. INTRODUCTION

1.1 BACKGROUND AND MOTIVATION

St. Lucia is South Africa's largest and most important estuarine system. The Mfolozi is the largest catchment within the St. Lucia Wetland Park and provides an important source of water to the system. Climate change affects the hydrological cycle by not only changing streamflow in catchments, but by altering the transformation and transport characteristics of water pollutants (Tu, 2009). On a regional scale, climate change may prove to be a significant factor which influences prospective water and sediment yields within the Mfolozi catchment. Other factors include land-use changes as a direct result of degradation, as well as human activities in the form of deforestation, urbanization, and/or unsustainable agricultural practices. It is important to note that the combination of land-use and climate change creates a complex interactive system by combining human action and environmental reactions, which in turn influence human responses (Schulze, 2000).

Lindsay *et al.* (1996) suggested that poor catchment management from the 1920s, particularly the extensive clearing of natural vegetation for sugarcane and commercial forest plantations has led to widespread erosion and high levels of suspended sediment loads. Due to fears of increased sediment loads as a direct threat to the Lake St Lucia system, the Mfolozi mouth was separated from the lake system in 1952 (Taylor, 2006; Cyrus *et al.*, 2010). Watson & Ramokgopa (1996), on the other hand, have attributed poor land-use practices and increased land degradation by native farmers in the former KwaZulu region to be responsible for a significant amount of sediment generated from the Mfolozi catchment.

During flood events the two systems may share the same mouth, allowing a sediment transfer between them. Increased suspended sediment concentrations into the lake may lead to light extinction, and lower dissolved oxygen levels thus inhibiting breeding patterns of certain species. Conversely during drought events without Mfolozi flows, the St. Lucia mouth may close stressing certain species in the estuary as a result of hyper-saline conditions (Lindsay *et al.*, 1996). It has become clear that the option of a combined

Mfolozi – St. Lucia mouth needs to be revisited in order to rejuvenate water levels in the lake as close as possible to natural conditions without sedimentation, salinity, and/or siltation issues.

The focus of the investigation is to determine hydrological responses to land-use and climate change within the Mfolozi catchment in order to provide quantitative guidelines for effective management of the St. Lucia estuary under different land-use and climatic scenarios. The work undertaken in this study primarily focuses on rainfall, runoff, and sediment yield.

1.2 RESEARCH QUESTIONS

- Is there evidence for regional climate change in the St Lucia system?
- What is the extent and effect of land-use change in the Mfolozi catchment?
- What are the likely effects of climate change on the Mfolozi-St Lucia system?

1.3 AIM

To develop a distributed hydrological modelling system to assist with current and future water quantity and quality management in the Mfolozi – St. Lucia System.

1.4 OBJECTIVES

- Assess the evidence of regional climate change in the Mfolozi – St. Lucia System using rainfall as an indicator.
- To set up an operating model for simulations of water quantity and quality under current land-use and climate conditions.
- Assess the goodness to performance of the model in relation to hydrological observations as well as other cited models.
- Evaluate the impacts of present land-uses on natural streamflows and sediment yields.
- Predict hydrological responses to regional climate change within the Mfolozi – St. Lucia system.
- Assess the environmental impact of re-establishing the Mfolozi – Lake St Lucia link.

1.5 DISSERTATION OUTLINE

The following describes the chapters included in this dissertation:

Following this introductory section, *Chapter 2* presents a general overview of the Mfolozi – St. Lucia Catchments, which includes catchment area, topography, predominant soil types, land-uses, and the hydrological characteristics of rainfall and runoff.

Chapter 3 contains a two-part critical literature review on:

- Climate change, variability, trends, and predictions from a global perspective to downscaled regional rainfall projections for Southern Africa.
- The processes of erosion and sediment dynamics, an overview of sediment transport formulae, and the mathematical modelling of sediment yield. The chapter concludes with an assessment of Mfolozi Catchment sediment yields in a global and regional perspective.

Chapter 4 contains the methodology used in this study. This includes the statistical methods used to evaluate the evidence of climate change using rainfall as an indicator, as well as the methodological approach to hydrological modelling with ACURU.

Chapter 5 presents and discusses key results obtained from the study. These include:

- Mfolozi catchment historical rainfall trends and precipitation events.
- Streamflow and sediment yield simulations under present land-use conditions.
- Hydrological impacts of present land-uses on pristine streamflows and sediment yields.
- Hydrological responses to projected regional climate change within the Mfolozi Catchment.
- A discussion on the implications of the results obtained for the Mfolozi-St. Lucia system.

Chapter 6 discusses the conclusions reached from this study and recommendations for further research.

2. GENERAL OVERVIEW OF MFOLOZI-ST LUCIA CATCHMENTS

With a catchment area of approximately 10 000 Km², the Mfolozi is the second largest drainage basin in KwaZulu-Natal (Orme, 1974; Pitman *et al.*, 1981; Perry, 1989; Grenfell & Ellery, 2009). The confluence point of the two main tributaries (The Black and White Mfolozi) is located 72 Km upstream of the mouth, east of the Hluhluwe – Mfolozi Game Reserve, as shown in Figure 2-1.

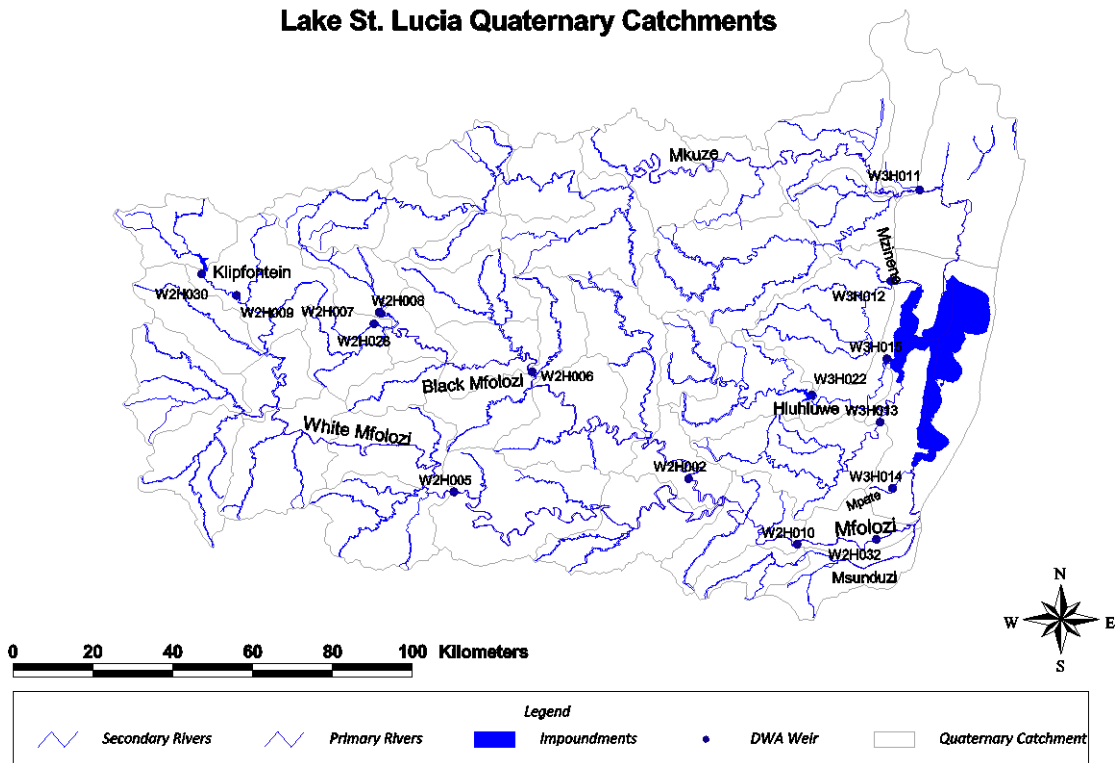


Figure 2-1: Catchments surrounding Lake St. Lucia.

The Black and White Mfolozi Rivers rise to altitudes of 1 524m and 1 600m, respectively. Figure 2-2 shows basin elevations which indicate an overall average catchment gradient of approximately 1:240. However, the bottom 100 km of the Mfolozi coastal flood plain maintains an average gradient of 1:1725 (Lindsay *et al.*, 1996).

Elevations of Lake St. Lucia Catchments

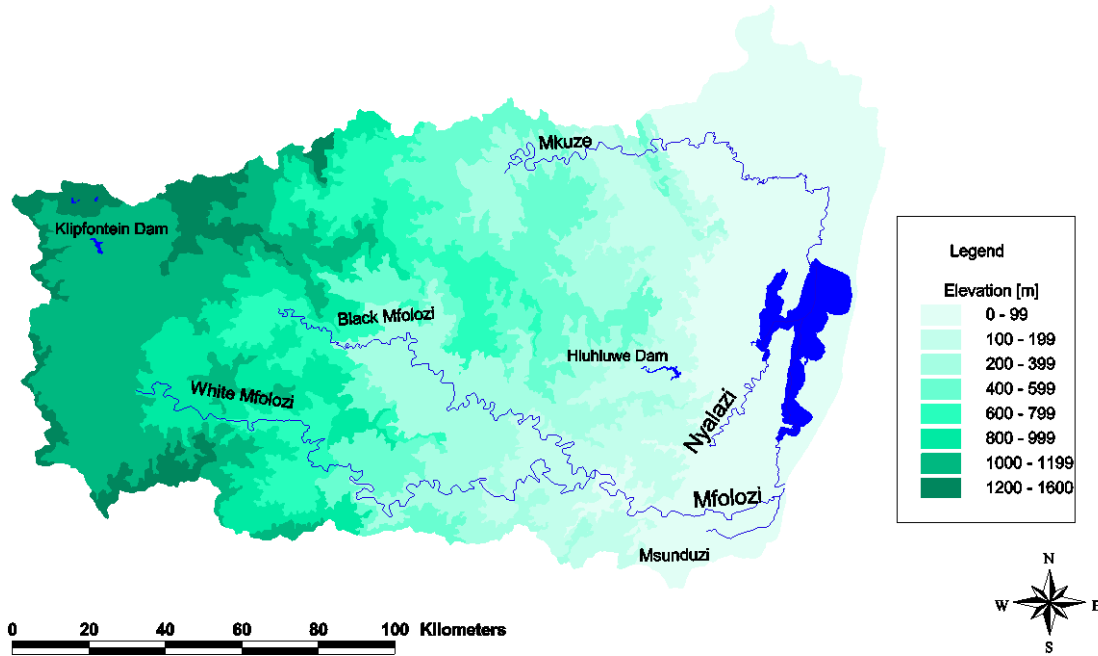


Figure 2-2: Basin elevations (in meters above mean sea level) and primary catchments within the Lake St. Lucia system.

Predominant soil types vary from loamy soils in the high elevations of the western catchments, to loamy sands in the bottom third of the catchment, and sandy clay loam in the low lying regions of the eastern catchments.

Predominant soil types of Lake St. Lucia Catchments

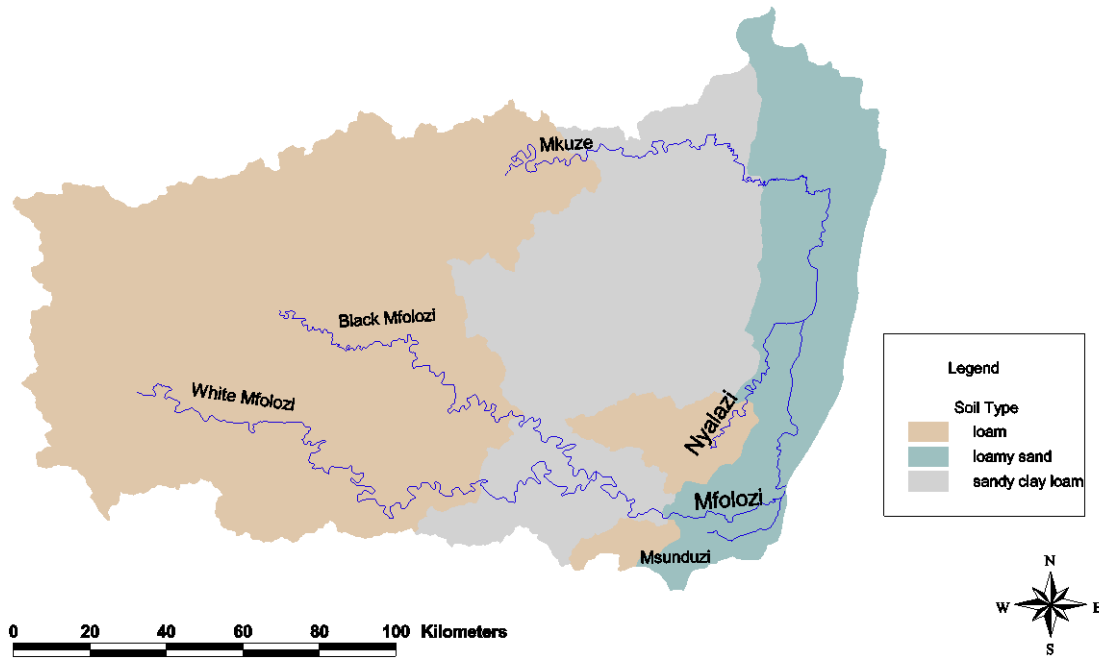


Figure 2-3: Predominant soil types within the Mfolozi-St. Lucia catchments (Source: ISWC, 2005).

The extent of land-use change is moderate and limited by Game Reserve preservation. These comprise of 23% subsistence agriculture and forestry, 13% degraded bushland and forestry, less than 1% urban, and 64% natural state vegetation (Harrison *et al.*, 2001).

Approximately 80% of rainfall in the region occurs between the summer months from November to April (Tyson, 1986; Grenfell & Ellery, 2009). Middleton & Bailey (2008) reported mean annual precipitation (MAP) within the 45 Mfolozi – St Lucia quaternary catchments ranging from 643mm to 1136mm. Furthermore, associated runoff coefficients (MAR/MAP) varying from 3% to 18% have been derived for these quaternaries. Inter-annual variability within the region is very high (Mason & Jury, 1997; Grenfell & Ellery, 2009) with semi-periodic flood/drought periods that can be linked to the southward migration of the Inter-Tropical Convergence Zone (ITCZ) and the El Nino Southern Oscillation (ENSO) (Nicholson, 2000; Toulmin, 2009).

3. LITERATURE REVIEW

3.1 CLIMATE CHANGE, VARIABILITY, TRENDS AND PREDICTIONS: A CRITICAL REVIEW

3.1.1 AN INTRODUCTION TO CLIMATE CHANGE

The Earth's climate is essentially determined by the physical and chemical nature of its atmosphere (Lockwood, 1979: cited in Hardy, 2003). The definition of climate change has evolved over time, and is given below in Box 1. Also highlighted in Box 1 is the definition of climate *variability*. The key difference in the two definitions, as interpreted by Burroughs (2010) is in the persistence of irregular conditions, i.e. the increasing frequency of rare events (such as record high summertime temperature, or record high rainfall intensities); or vice-versa, the decreasing frequency of rare events (such as record low rainfall amounts).

Climate Change

Climate change defines the difference between long-term mean values of a climate parameter or statistic, where the mean is taken over a specified interval of time, usually a number of decades.

WMO, 1988

Climate change as referred to in the observational record of climate occurs because of internal changes within the climate system or the interactions between its components, or because of changes in external forces either for natural reasons or because of human activities. It is generally not possible to make clear attribution between these causes. Projections of future climate change reported by IPCC generally consider only the influence on climate of anthropogenic increases in greenhouse gases and other human-related factors.

IPCC, 1996

Climate change encompasses all forms of climatic inconstancy (that is, any differences between long-term statistics of the meteorological elements calculated for different periods but relating to the same area) regardless of their statistical nature or physical causes.

NSIDC, 2010

A change of climate which is attributed directly or indirectly to human activity that alters the composition of the global atmosphere and which is in addition to natural climate variability over comparable time periods.

UNFCCC, 2010

Climate Variability

The extremes and differences of monthly, seasonal and annual values from the climatically expected value (temporal means). The differences are usually termed anomalies...Climate variability can be regarded as the variability inherent in the stationary stochastic process approximating the climate on a scale of a few decades, while climate change can be regarded as the differences between the stationary processes representing climate in successive periods of a few decades.

WMO, 1988

Box 1: Definitions of Climate Change and Climate Variability

Variability in climate has been preceded by variability in greenhouse gases, where warmer periods have been associated with higher concentrations of greenhouse gases, and cooler periods with lower concentrations (Hardy, 2003). The main greenhouse gases responsible for the greenhouse effect are carbon dioxide, methane, nitrogen oxides, chlorofluorocarbons, and ozone. Human activities such as the burning of fossil fuels or the change in land use patterns, such as deforestation and desertification, are results of urbanisation and/or unsustainable agricultural activities, all of which influence regional climate change (Karl & Trenberth, 2003; Bily, 2007).

With regards to water vapour and precipitation, a warmer troposphere results in increased evaporation of oceanic waters leading to a global increase in average water vapour and precipitation as rainfall (Hardy, 2003). As a result of the additional heat due to global warming, models foretell that evaporated oceanic water in tropical latitudes will be carried further pole-ward before precipitating as rain. The predicted result of this increased greenhouse effect is an increase in precipitation pole-ward of 30° latitude, and a decrease in precipitation between 5° and 30° latitude (Mason, 1999; Hardy, 2003; Toulim, 2009). Figure 3.1-1 depicts research carried out by Folland & Karl (2001), which illustrates this trend in rainfall data between 1900 and 1999.

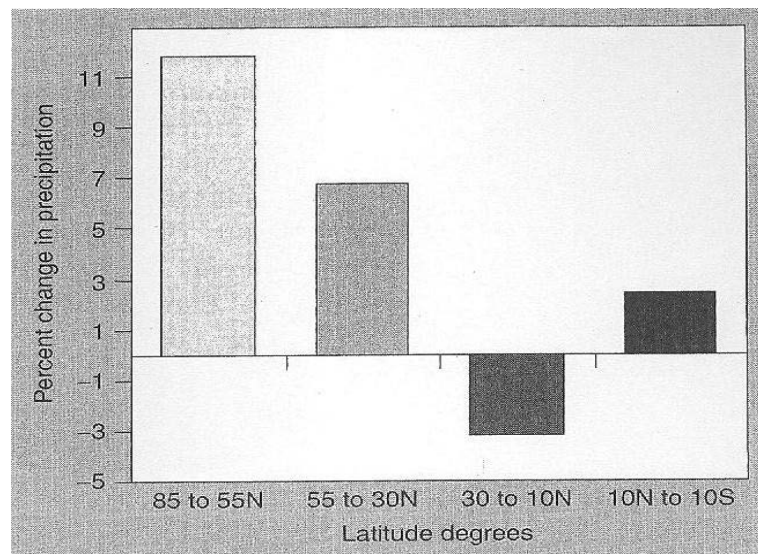


Figure 3.1-1: Annual precipitation from 1900 to 1999, showing increases at temperate latitudes and decreases at subtropical latitudes (Source: Folland and Karl, 2001: cited in Hardy, 2003).

As seen in Figure 3.1-1, rainfall has some latitude-dependent features, where the majority of the African continent is tropical/subtropical and experiences clear seasonal shifts of the tropical rainfall belts (Nicholson, 2000; Toulmin, 2009). One of these belts, the Inter-tropical Convergence Zone (ITCZ) spans the continent and its back and forth movement is responsible for seasonal rainfall. The ITCZ (see Box 2) usually follows a predictable seasonal pattern, bringing with it reliable rainfall. The exception to this occurs every three to eight years when the *El Nino Southern Oscillation* (ENSO) creates warmer than normal sea surface temperatures in the tropical Pacific and causes a shift in movement on the ITCZ (Nicholson, 2000; Toulmin, 2009). In Africa, the El Nino prevents the ITCZ from moving as far south as it normally would particularly over the eastern half of the continent, resulting in the deprivation of rain in parts of southern Africa.

The Inter-tropical Convergence Zone (ITCZ)

The ITCZ is formed near the equator, as a result of north-east and south-east trade winds. These winds force moist air upwards, resulting in the condensation of water vapour. In Africa, the ITCZ is located south of the Sahel, but can shift 40-45 degrees latitude north or south of the equator within a year. In southern Africa, annual rainfall is mainly distributed over two rainy seasons – spring and autumn. Small shifts of the ITCZ belt can result in large local changes in rainfall, bringing severe flooding or drought.

Box 2: Inter-tropical Convergence Zone (ITCZ) [Source: Adapted from Toulmin, 2009]

The *Climate Change* aspect of the critical review will now focus solely on hydrological evidence for climate change, variability, trends, and predictions, specifically using rainfall as an indicator. Climate change indicators are defined in Box 3

Climate change indicators present critical information regarding trends in climate variation that may also be used to identify potential environmental problems by acting as early warning systems (Sweeney *et al.*, 2004). Climate change indicators include, but are not limited to, air temperature, rainfall seasonality, annual rainfall, snow days, and sea level rise.

Box 3: Definition of climate change indicator (Source: Sweeney *et al.*, 2004)

3.1.2 OBSERVED CHANGES IN RAINFALL TRENDS INCLUDING EXTREME EVENTS: A GLOBAL OVERVIEW

3.1.2.1 OBSERVED RAINFALL TRENDS

During last 100 years, overland precipitation has generally increased between 30° north and 85° north, with significant decreases within the last 40 years from 10° South to 30° north (Bates *et al.*, 2008). Furthermore, from 1900 to the 1950s, precipitation increased significantly from 10° north to 30° north, but then declined after 1970. Figure 3.1-2 illustrates spatial patterns of annual precipitation trends, extracted from the Global Historical Climatology Network (GHCN).

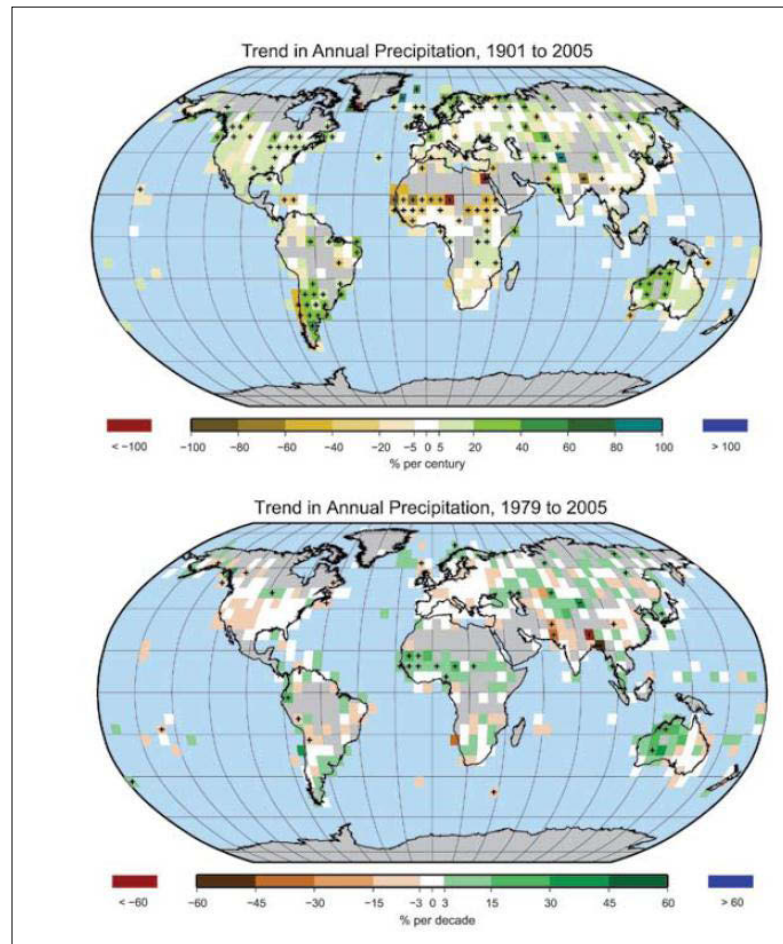


Figure 3.1-2: Global trend in annual precipitation amounts, 1901-2005 (upper percentage per country) and 1979-2005 (lower percentage per decade), as a percentage of the 1961-1990 average from GHCN stations (Source: Bates *et al.*, 2008).

From Figure 3.1-2, and with reference to the trend in annual precipitation from 1979 to 2005, there is evidence for regional drying, most visibly in south-west North America (Bates *et al.*, 2008). However, increasingly wet conditions are evident across South America, specifically over the Amazon Basin and the south-eastern part of the continent. This is in agreement with Lucero & Rozas (2002), who undertook a study within central Argentina, in the southern-mid latitudes. Their results indicated a strong positive trend in both annual and seasonal rainfall amounts produced by an increase in the number of rainy days, which occurred within the three month periods from January to March (summer), and April to June (autumn). Additionally, distribution of the annual average number of rainy days was found to have increased by 50% over a 36 year period (Lucero & Rozas, 2002).

In contrast, decreasing trends in annual precipitation were observed over Chile and the western parts of South America. Bates *et al.* (2008) suggested variations across North and South America are indicative of latitudinal changes in monsoon features.

3.1.2.2 EXTREME PRECIPITATION

There is a greater increase in extreme precipitation relative to the mean in a climate that is warming due to increased green house gas emissions (Bates *et al.*, 2008). Extreme precipitation is affected by the availability of water vapour, as discussed earlier in Section 3.1.1. In contrast, mean precipitation is influenced by the atmosphere's ability to radiate long-wave energy that is released as latent heat of condensation into space, which is restricted by increasing green house gases. Elaborating further on climate variability being preceded by variability in greenhouse gases (Section 3.1.1) a link can be established between climate change indicators of global mean temperature and global precipitation. In doing this, Nicholls *et al.* (1996) and Easterling *et al.*, (2000) identified that there has been an increase in *both* global temperature (+0.6°C) and global precipitation since the beginning of the twentieth century. This has been associated with anthropogenic activities that favour the argument of mankind being responsible for climate change.

Figure 3.1-3 illustrates regions of the world where large time series data is available for the analysis of extreme precipitation events. Regions where statistically significant changes in heavy precipitation have occurred within the past decades are indicated by positive or negative signs.

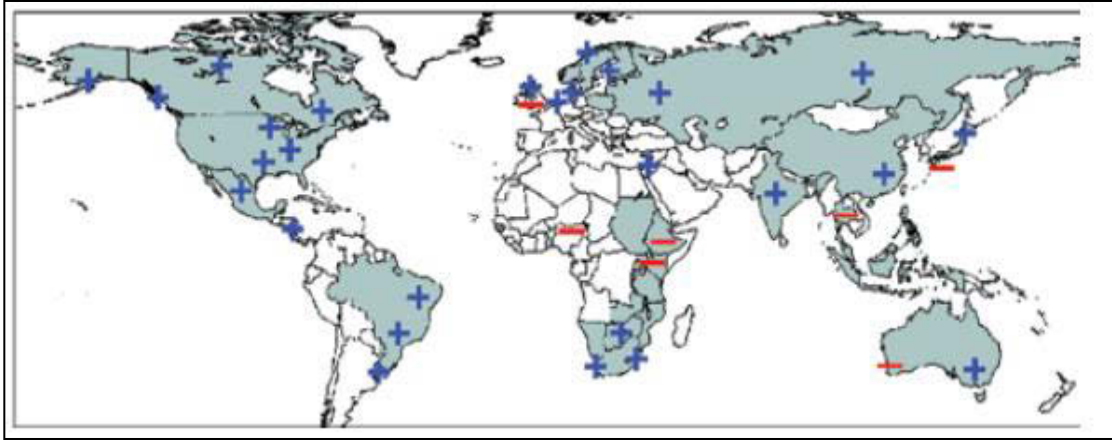


Figure 3.1-3: Regions where analyses of heavy precipitation have been completed (Source: updated from Groisman *et al.*, 2005: earlier depiction in Easterling *et al.*, 2000 and current depiction in Bates *et al.*, 2008).

In a majority of regions that have experienced a statistically significant increase (or decrease) in seasonal or monthly precipitation, there has been a propensity for this change to be directly associated with a change of the same sign in the amount of precipitation falling during extreme events (Easterling *et al.*, 2000). Additionally, there are regions where there has not been a change in total precipitation or the mean, that still displayed increases in the frequency and magnitude of heavy precipitation events, as was found in Japan (Iwashima & Yamamoto, 1993: cited in Easterling *et al.*, 2000; Manton *et al.*, 2001: cited in Folland & Karl, 2001). This can be demonstrated statistically (and qualitatively) by idealising and analysing a time-series plot into a Gaussian distribution. A constant mean with an increase in variance results in an increase in probability of both extremes (cold and hot; or wet and dry), and absolute values of extremes, as shown in Figure 3.1-4.

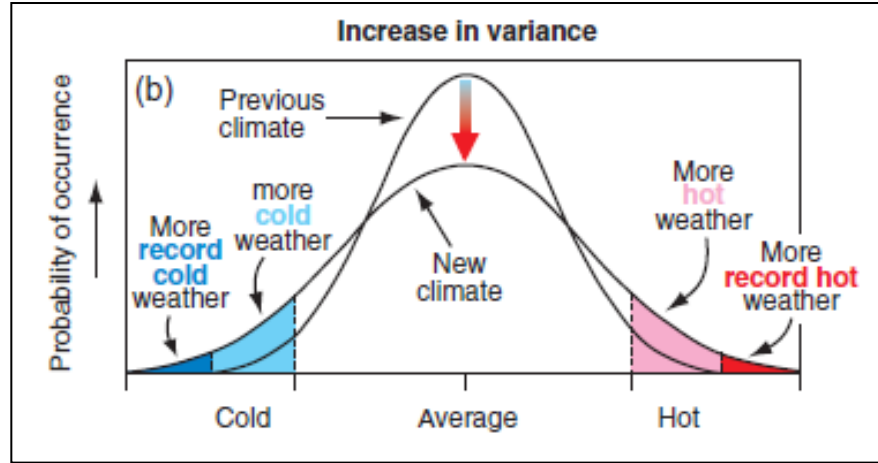


Figure 3.1-4: An increase in variance without a change in mean implying an increase in probability of extremes, as well as increases in absolute values of extremes (Source: Folland & Karl, 2001).

Although Figure 3.1-4 refers specifically to temperature extremes, its applicability to precipitation variables can be both qualitative and quantitative. In order to quantitatively apply this principle to precipitation variables, one of two approaches should be considered. The first requires the application of a transformation to the precipitation data resulting in a series that is Gaussian distributed, for which tests suited to Gaussian data can then be applied (Robson *et al.*, 2000). The second approach requires fitting an appropriate distribution to the precipitation data. The World Meteorological Organisation (WMO) recommends a gamma distribution (Neyers, 1990; Nastos & Zerefos, 2007) due to its skewed profile, which has the advantage of not under/over-estimating the frequency distribution, as other statistical methods tend to do (Nastos & Zerefos, 2007). This method of fitting a distribution is discussed further in section 4.2.2.5.

Linear trends in total and heavy precipitation have been defined (Sun & Groisman, 1999; Easterling *et al.*, 2000) for various countries, and are given in Table 3.1-1:

Table 3.1-1: Regions/seasons/periods where the linear trends of the number of days with heavy precipitation are amplified relative to mean precipitation totals and frequency. Single asterisks donates statistical significance at 95% confidence level, double asterisks donates disproportionately significant increases in extreme rainfall with constant mean (Source: Sun & Groisman, 1999).

Country	Period	Threshold used to define heavy rain (mm)	Season	Average number of days with heavy rain	Linear trend, % per 10 yr
Eastern two-thirds of the contiguous United States	1910–96	50.8	JJA	0.6	1.7*
European part of the former USSR	1936–94	20	JJA	1.8	3.9*
Asian part of Russia**	1936–94	20	JJA	2.3	1.9*
Southern Canada	1944–95	20	JJA	2.9	1.9*
Coastal regions of New South Wales and Victoria, Australia	1900–96	50.8	DJF	0.4	4.6*
Norway	1901–96	25.4	JJA	2.0	1.9
Southern Japan	1951–89	100	JJA	1.0	-6.1
Northern Japan**	1951–89	100	JJA	0.3	3.4*
Northeastern China	1951–97	50	JJA	1.0	-3.1
Southeastern China	1951–97	100	JJA	0.5	1.3
Ethiopia and Eritrea	1951–87	25.4	JJA	5.5	-11.6*
Equatorial east Africa	1950–97	50.8	MAM	1.1	-11.2*
Southwestern South Africa	1926–97	25.4	JJA	0.7	5.5*
Natal, South Africa**	1901–97	50.8	DJF	0.6	4.1*
Nord-Este, Brazil**	1935–83	50.8 100	MAM MAM	1.0 0.1	3.6 16.1*
Thailand	1951–85	50.8 100	SON SON	2.2 0.4	-8.4* -20.9*

Sun & Groisman (1999) constructed Table 3.1-1 using seasons with maximum precipitation. This is represented graphically in Figure 3.1-5:

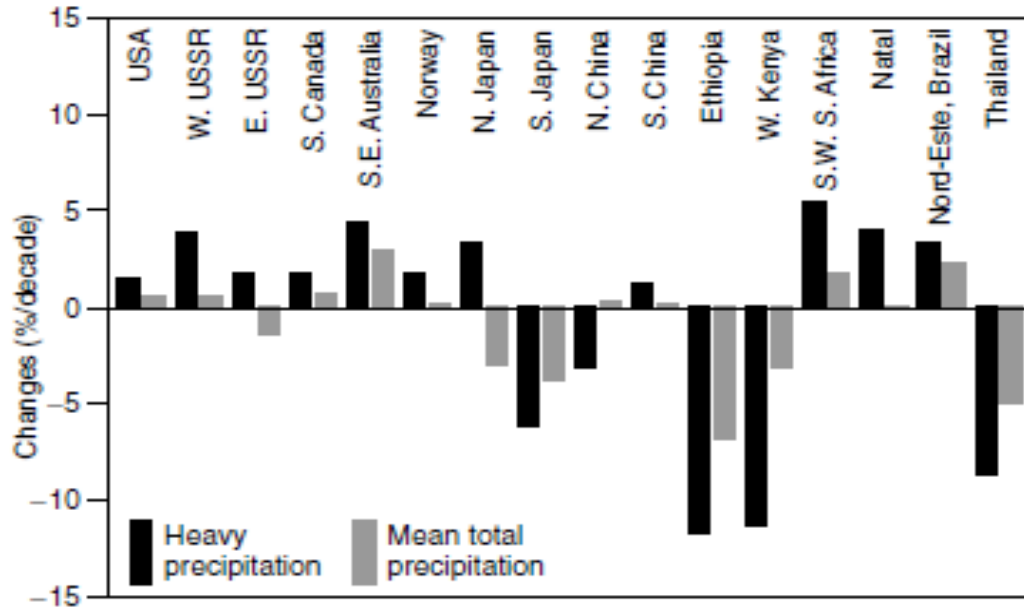


Figure 3.1-5: Linear trends (%/decade) of heavy precipitation (above the 90th percentile) and total precipitation during the rainy season over various regions of the globe (Source: Easterling *et al.*, 2000).

Two interesting observations arise when comparing Figure 3.1-5 with Figure 3.1-2. The first is that both figures concur with the work cited by Easterling *et al.* (2000) that indicates non-variation in mean precipitation as seen in Natal (Figure 3.1-5) and the eastern regions of South Africa (Figure 3.1-1 and Figure 3.1-2). The second is that the increases in both mean and extreme precipitation for south-western South Africa, shown in Figure 3.1-5, contradict both Hardy (2003) and those shown in Figure 3.1-1, that indicated an up to 3% decrease in mean precipitation.

Having established the global changes in precipitation trends, and the frequency and magnitude of extreme events above, this critical analysis will now focus on the mean trends and variations in extreme precipitation within the context of South Africa.

3.1.3 OBSERVED AND PROJECTED TRENDS INCLUDING EXTREME PRECIPITATION EVENTS IN SOUTH AFRICA.

3.1.3.1 CLIMATE CONTEXT

Climatic conditions in South Africa range from Mediterranean in the south-western corner of the country to temperate in the interior plateau, with sub-tropical climatic conditions occurring in the north-east. A small area in the north-west that borders Botswana and Namibia also experiences desert climate. The majority of rainfall generally occurs during the summer months of December, January, and February, with winter rainfall occurring in the south-western regions during June, July, and August.

Precipitation amounts vary considerably from east to west. Much of the eastern Highveld receives between 500mm and 900mm annual rainfall, and sporadically in some areas, up to 2000mm has been recorded (Middleton & Bailey, 2008). In contrast, the north-western regions of the country receive less than 200mm annual rainfall. The average annual rainfall across South Africa is 464mm compared to a world average of 857mm (Turpie *et al.*, 2008), implying that South Africa is a water-stressed country.

Inter-annual climate variability is high (Mason & Jury, 1997; Hewitson *et al.*, 2005) with occasional flood and drought events, which are in part influenced by the southern extension of the ITCZ, as discussed in Box 2. The coastal regions of the east are particularly vulnerable to tropical cyclones, which have had disastrous consequences in the past (Hewitson *et al.*, 2005).

3.1.3.2 OBSERVED TRENDS

South African trends in annual rainfall totals assessed in the 50-year period from 1950 to 1999 were not found to be significant (Hewitson *et al.*, 2005). However, stronger trends within this period were observed when sub-annual and seasonal scale investigations were conducted. Figure 3.1-6 illustrates the historical trend of change per decade in mean monthly number of rain-days with rainfall greater than 2mm.

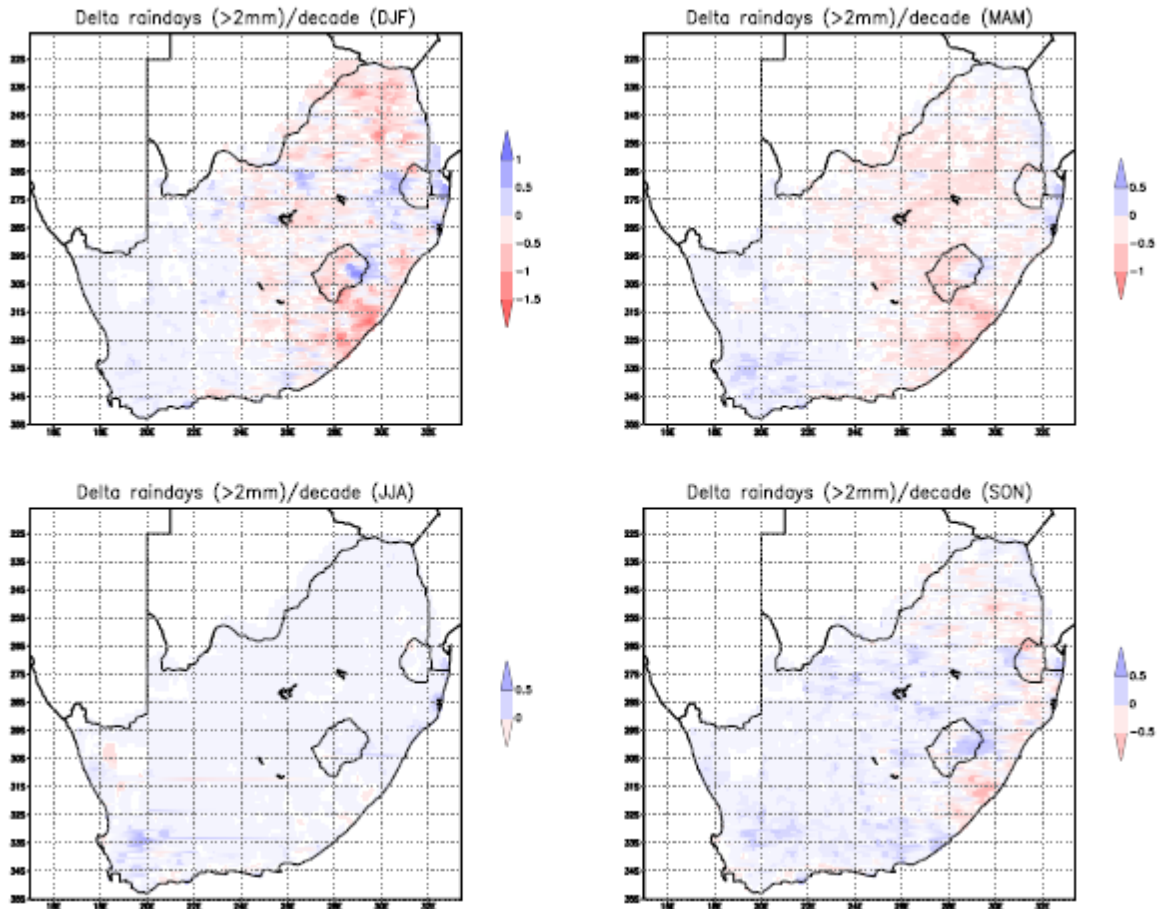


Figure 3.1-6: 1950 – 1999 trend of change per decade in mean monthly number of rain-days with rainfall greater than 2mm (Source: Hewitson *et al.* (2005)).

In order to gain a clear understanding of Hewitson *et al.* (2005), it is important to consider it alongside the trend of change per decade in mean monthly dry spell duration (Figure 3.1-7).

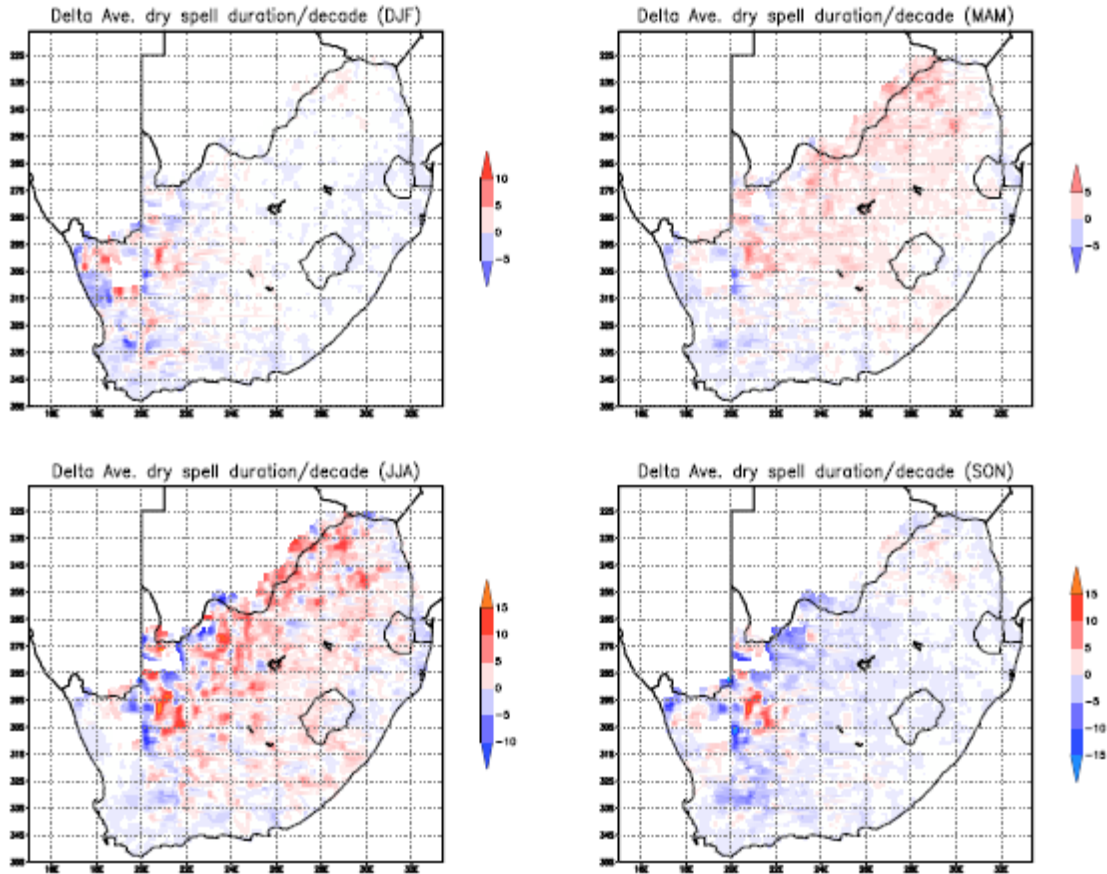


Figure 3.1-7: 1950 - 1999 trend of change per decade in mean monthly dry spell duration (days) (Source: Hewitson *et al.* (2005)).

From Hewitson *et al.* (2005), and with reference to the eastern part of the country (considering summer rainfall, i.e. the months of December, January, and February), it is evident that there is an increase in the number of rain-days accompanied by a decrease in dry day duration spells. Though the magnitude of this trend is not proportionally large (but still statistically significant), it does confirm that the eastern regions of the country have in actual fact become wetter, (as discussed in Section 3.1.3.2 which is consistent with Hardy, 2003; Bates *et al.*, 2008; Toulim, 2009).

An analysis of the western regions of the country that experience winter rainfall (i.e. during the months of June, July, and August) drew two opposing conclusions. The first was that the mountainous regions/areas received more rain-days per month, and the second being a decrease in rain-days per month in neighbouring coastal plains (Hewitson *et al.*, 2005).

3.1.3.3 OBSERVED EXTREME EVENTS

Mason *et al.* (1999) highlighted significant changes in extreme precipitation events over much of South Africa during two 30 year periods, specifically from 1931 to 1960 and 1961 to 1990, as shown in Figure 3.1-8.

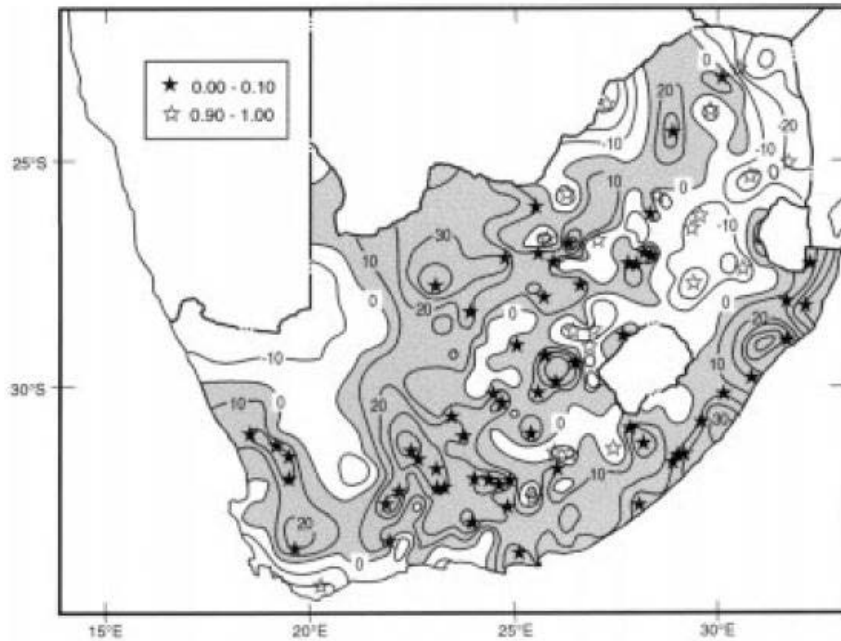


Figure 3.1-8: Percentage changes in the intensity of 10-year high rainfall events over South Africa from 1931-1990. Solid and hollow stars indicate stations where increases and decreases, respectively, in intensity occurred at the 90% significance level. The contours represent the magnitude (%) change (Source: Mason, 1999).

Mason (1999) observed increases in intensities of the high annual maxima over a significant portion of central South Africa, and along the east coast. Decreases in intensities of high rainfall have been experienced in the eastern part of the country over an area ranging from eastern Swaziland to northern Lesotho, the northwest, and southwest. This is in agreement with the work carried out by Hewitson *et al.* (2005) from the period 1950 – 1999 (Figure 3.1-9), and Easterling *et al.*, 2000 (Figure 3.1-5).

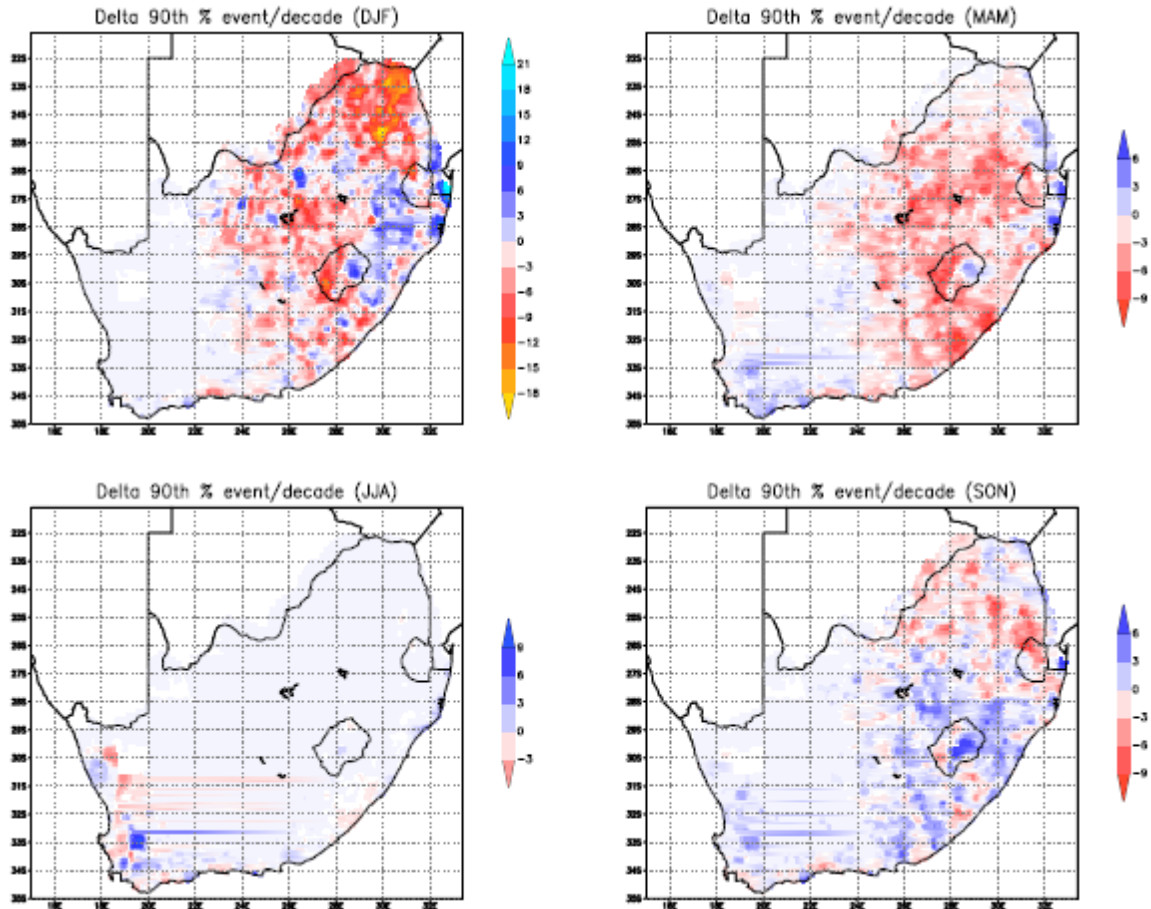


Figure 3.1-9: Trend (1950 – 1999) of change per decade in mean monthly 90th percentile magnitude rainfall event (mm) (Source: Hewitson *et al.* (2005)).

Along the east coast, an increase of over 50% in the intensity of 10-year high rainfall has been experienced (period 1980-1989). This increase may have been significantly influenced by the 1984 cyclone that hit north of Durban and precipitated over 800mm in one day (Mason, 1999). However, it should be noted that, excluding the 1984 event, there have been statistically significant increases in high rainfall events within eastern South Africa in the 1961-1990 period (Mason, 1999).

Furthermore, in parts of the northeast and northwest, and in the winter rainfall regions of the Western Cape, decreases in extreme rainfall events have been observed, which are consistent with a decline in observed rainfall totals since the late 1970s (Mason, 1999).

3.1.4 SUMMARY OF PAST RAINFALL TRENDS ACROSS SOUTH AFRICA

The most recent study of rainfall trends from the period 1900 – 2004 involving 138 stations found no significant change in precipitation over South Africa (Kruger, 2006). However, there were stations that recorded statistically significant increases in annual precipitation (in the provinces of the Eastern Cape, Western Cape, Northern Cape and Northwest), whilst other provinces experienced statistically significant decreases in annual precipitation during the wet seasons (in the provinces of northern Limpopo, western KwaZulu-Natal, north-eastern Free State, and south eastern regions of the Eastern Cape).

Although the majority of stations showed no significant change in mean annual precipitation, the evidence for increasing frequency and magnitude of extreme precipitation events has been presented by Mason (1999), Easterling *et al.* (2000), and Van Wageningen & du Plessis, (2007).

3.1.5 PROJECTED TRENDS

The large scale perspective on projected trends is that of drying in many sub-tropic areas, with slight changes (or increases) in precipitation in the tropics, accompanied by an increasing rainfall gradient (Christensen *et al.*, 2007). This is likely due to a warmer atmosphere and increased water vapour transportation (Mason & Joubert, 1997; Mason, 1999; Hardy, 2003; Toulim, 2009) as discussed in Section 3.1.1.

Mason & Joubert (1997) utilized the Commonwealth Scientific and Industrial Research Organisation nine-level model (CSIRO-9) to examine possible variability in daily rainfall over southern Africa. The CSIRO-9 model simulated small (between 10 and 20%) but widespread increases in rainfall intensity (expressed as amount of rain per rain-day) over much of South Africa, with slightly larger increases in parts of the south-western regions of the country, that is, south of 20° south (Mason & Joubert, 1997). This pattern was evident even in areas that simulated a decrease in mean annual rainfall.

In contrast, Christensen *et al.* (2007) anticipate robust drying (that is, 20% drying in the annual mean by the end of the 21st century) in the extreme southwest of the country due to a process involving increased moisture divergence and a systematic pole-ward shift of storm tracks that affect winter rains. However, the drying (or rather, the trend identified

above) is dependent on characteristic topographic features which may result in locally different changes such as large changes in intensity along both the west and east coasts where local maxima and minima are less pronounced (Mason & Joubert, 1997).

Table 3.1-2 illustrates regional average precipitation projection for southern Africa from a set of 21 global models in the Multi-Model Data (MMD) for the IPCC A1B scenario. The minimum, maximum, 25th, 50th, and 75th percentile values among the 21 global models are given. The middle half (25th to 75th percentile values) that showed all the same sign are coloured in red. The western regions of South Africa that experience winter rainfall (JJA) are expected to undergo a net decrease in rainfall, which is consistent with the findings of Mason & Joubert (1997), Folland & Karl (2001), and Hardy (2003).

Table 3.1-2: Regional averages of precipitation projections for Southern Africa from 21 global models in the MMD for the A1B scenario (Source: Christensen *et al.*, 2007).

	Precipitation Response (%)				
	min	25	50	75	max
D J F	-6	-3	0	5	10
M A M	-25	-8	0	4	12
J J A	-43	-27	-23	-7	-3
S O N	-43	-20	-13	-8	3
ANNUAL	-12	-9	-4	2	6

In closing, regional models predict drying over much of the western South Africa, with wetter conditions over eastern South Africa during the summer rainfall season when most of the rain falls (December, January, and February). Senior *et al.* (2002) anticipate an increase in the intensity (rather than an increase in the number of wet days) of the 1-in-20 year flood event over eastern South Africa, extending through to Mozambique and as far north as the Democratic Republic of Congo. Less extreme precipitation is predicted over the western regions of South Africa, which is associated with a reduction in both rainfall intensity and the number of wet days.

3.2 EROSION AND SEDIMENT DYNAMICS: A CRITICAL REVIEW

3.2.1 SOIL EROSION: CONCEPTS, PROCESSES AND PRINCIPLES

Soil erosion as described by Jones (2007) is “the wearing away of land surface by physical forces such as rainfall, flowing water, wind, ice, temperature, gravity or other anthropogenic agents that abrade, detach and remove soil or geological material from one point on the earth’s surface to be deposited elsewhere.” The characteristics of soil erosion are variable in intensity (scale and nature), and are usually event driven (by natural or human influenced processes) resulting in the conversion of soil into sediment.

3.2.2 EROSION DUE TO RAIN DROP IMPACT AND LEAF DRIP

Water erosion is the most common form of erosion, and is a resultant of poor drainage and/or rainfall (Anthoni, 2000; Jones, 2007). Specific consideration should be given to rainfall intensity, as it affects the erosion process that contributes to sediment generation by firstly, providing and maintaining the large amount of water needed in the water-to-sand ratio within the sediment flow, and secondly, maintaining the high hydraulic pressure in the sediment flow by delivering high frequency drop impact (Jungerius & ten Harkel, 1994). As presented earlier in Section 3.1.3.2, the increasing nature of extreme precipitation (both frequency and intensity) warrants an investigation into the contribution, or rather, the impact of raindrops towards the process of soil particle displacement.

The magnitude of the force of raindrops impacting the land surface affects the amount and size of soil particles displaced. The mass of a raindrop is directly proportional to the cube of its diameter. This infers that a 5mm raindrop has 125 times more mass than a 1mm raindrop. Furthermore, the terminal velocity of a 5mm raindrop is twice that of a 1mm raindrop (Anthoni, 2000). This substantiates the destructive potential of rain increases as the drop size increases; approximately 500 times increase in potential from a 5 fold increase in rain drop diameter, as shown in Figure 3.2-1:

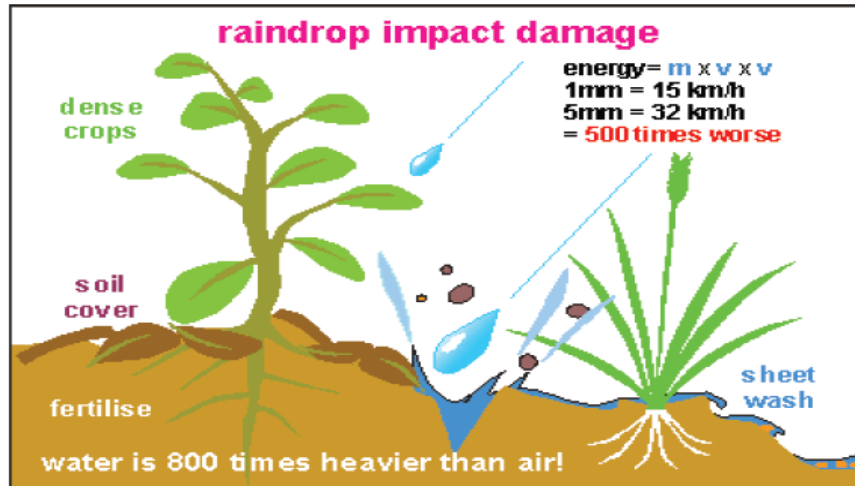


Figure 3.2-1: Raindrop impact potential: 5mm raindrop having 500 times more destructive potential than 1mm raindrop (Source: Anthoni, 2000).

Also shown in Figure 3.2-1 is how vegetative cover determines whether rain falls as direct raindrop impact or leaf drip, both of which affect the amount of sediment generated. The effect of a vegetative canopy diminishes the amount of rainfall impact energy on the soil due to the majority of rainfall being intercepted by vegetation (Smithers & Schulze, 2002; Msadala, 2009). Furthermore, the intercepted rainfall either disperses into smaller drops with less impact energy, drips from leaf edges, or flows down crop stems to the ground. The factors influencing the amount of erosion by raindrop or leaf drip include, but are not limited to the percentage of land surface covered by canopy, and the height of the vegetative canopy. All of these have a limited effect on the variation of annual sediment production.

3.2.3 PHYSICAL PROCESS OF RAINDROP EROSION AND SEDIMENT DEPOSITION

The physical process of raindrop erosion begins with the impact of the raindrop on the soil, which loosens the soil structure and releases the binding clay particles transporting them downhill (Anthoni, 2000). This process is illustrated in Figure 3.2-2.

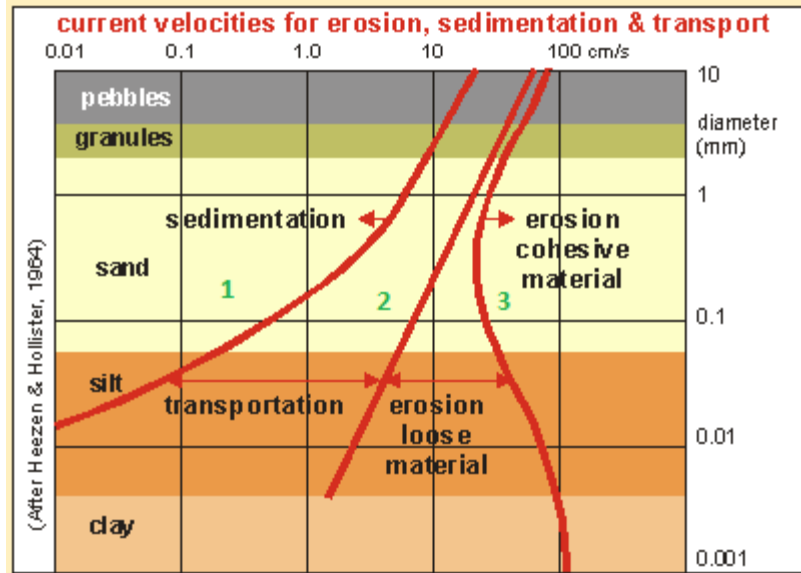


Figure 3.2-2: Raindrop impact potential based on velocities for erosion, sedimentation & transportation vs. raindrop diameter (Source: Heezen & Hollister, 1964).

Figure 3.2-2 also applies to wind, dunes, beaches, coasts, rivers & estuaries, and further illustrates how the actual transportation process of sediment particles takes place. Anthony (2000) rationalizes this from a study undertaken by Stokes which explains the different frictional forces experienced as the particle travels through a different medium (air or water). An analysis of the above curves yielded the following velocities:

- Curve 1: The velocity at which the particles settle out.
- Curve 2: The velocity needed to erode loose material.
- Curve 3: The velocity needed to erode cohesive material.

The transportation gap between erosion and sedimentation widens as the particle size decreases, and hence explains why clay particles aversely settle, but rather extend into the lower reaches of fresh water and eventually into the sea. By extension, as the river slows down further downstream, the pebble and sand particles settle rarely reaching the sea during normal flow conditions.

The deposition process begins with the reduction of particle flow velocity. Pidwirny & Sidney (2008); Msadala (2009) illustrate this in Figure 3.2-3, whereby the erosion velocity defines the velocity required to relocate particles from the surface and goes on to explain that the relocation process of clays and silts requires greater velocities than larger sand

particles. This is due to the cohesive ability of silts and clays to form inter-particle links, and therefore require increased velocities to break the inter-particle bond.

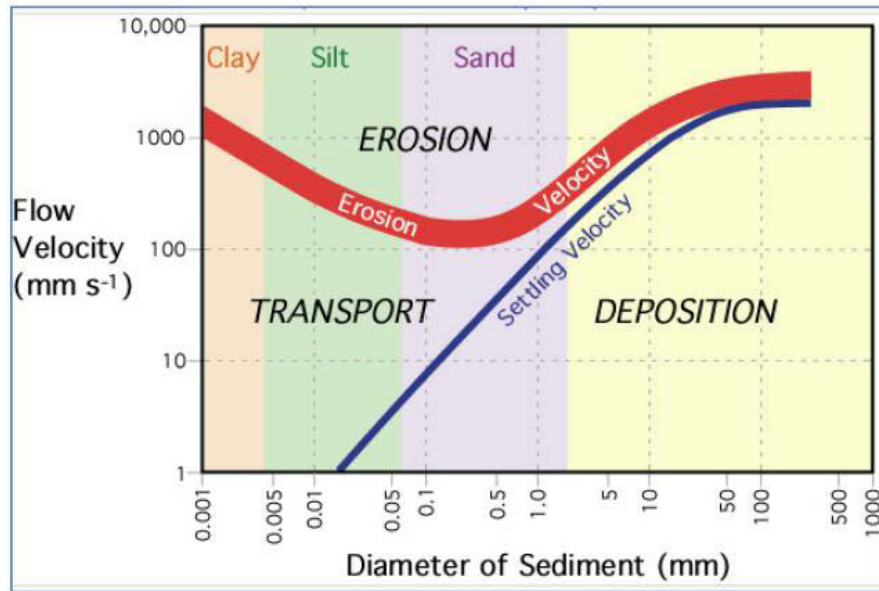


Figure 3.2-3: Interaction between flow velocity, particle erosion, transport and deposition (Source Pidwirny & Sidney, 2008).

Figure 3.2-3 shows the *settling velocity* of particles, which Harris (2003) describes as the rate at which particles settle in still fluid. The characteristic features of which depend on particle size, sensitivity to shape (both roundness and sphericity), particle density, as well as the density and viscosity of the fluid medium. Settling velocity integrates all of these into a key transport parameter (Harris, 2003).

The relationship between settling velocity and erosion velocity is demarcated by the shaded area in Figure 3.2-3 marked *deposition*, and illustrates that greater flow velocities are required not only to suspend and mobilize larger sized particles from river beds/banks, but to also drop particles out of transport and hence be deposited.

3.2.4 SEDIMENT TRANSPORT AND SEDIMENT YIELD

The science associated with sediment transport deals with the interaction between sediment particles and flowing water (Yang, 1996). Although the removal of sediment particles (erosion) and their concomitant movement involves a range of processes, the action of water (as direct rainfall and/or surface runoff) delivers sediment downstream of the water

shed. Furthermore, as described by Di Silvio (2008) sediment motion adopts three basic forms: mass, surface, and linear (Figure 3.2-4). These respectively correspond to:

1. Landslides: infrequently produced in the steepest of slopes within the watershed.
2. Distributed soil erosion: located in undulated, poorly vegetated surfaces.
3. Bed-load and suspended movement due to water flow in the catchment.

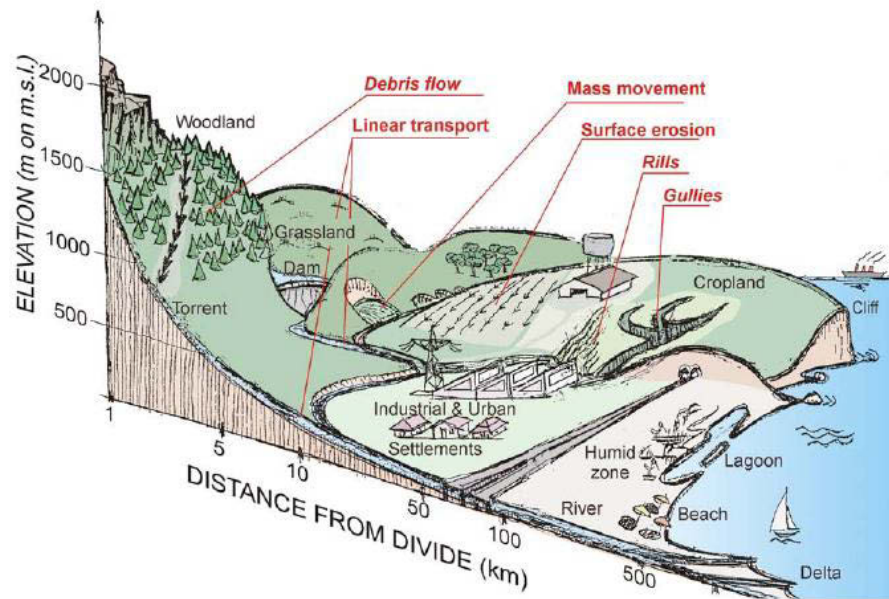


Figure 3.2-4: Schematic of watershed illustrating the basic forms of sediment movement (Source: Di Silvio, 2008).

Specific consideration will be given to linear sediment transport, as it is mainly responsible for river hydrological river processes and typically takes place longitudinally resulting in the motion of sediments produced by continuous channelized flow (Di Silvio, 2008).

3.3 BRIEF OVERVIEW OF SEDIMENT TRANSPORT FORMULAE

Sediment is transported through two main mechanisms, namely bed-load and suspended load. Bed-load is in constant contact with the river bed, and therefore must be estimated with relation to the effective shear stress acting directly on the surface grains. Suspended load, on the other hand moves without continuous contact with the bed as a result of fluid agitation due to turbulence, and can therefore be related to the total bed shear stress (Lui, 2001). Einstein (1950) proposed that the boundary between bed-load and suspended load

is a grain diameter equal to $2d_{50}$ above the bed. This typically is not the case due to the rippled characteristics of the bed. In which case, Bijker (1971) suggested that the transportation of bed-load takes place within a layer with an effective thickness equal to the bed roughness, or height of the ripples.

3.3.1 BED-LOAD TRANSPORT FORMULAE

3.3.1.1 DuBOY'S APPROACH

DuBoy (1879): cited in Yang (1996) assumed that the motion of sediment particles is in layers along the bed. The layers move due to tractive forces acting along the bed. Under equilibrium conditions, the tractive forces should be equal to the total resistive force between layers, and assuming a linearly varying velocity between the first and the m^{th} layers, the total bed-load discharge by volume per unit channel width (q_b) is:

$$q_b = \frac{0.173}{d^{\frac{3}{4}}} \tau (\tau - \tau_c) \quad (3-1)$$

where d = particle size
 τ = tractive force
 τ_c = critical tractive force.

DuBoy's equation was criticized in that all his data was obtained from small laboratory flumes with a small variation in particle size, and doubts to whether it is applicable to field conditions (Yang, 1996).

3.3.1.2 MEYER-PETER APPROACH

Meyer-Peter *et al.* (1934): cited in Yang (1996) and Lui (2001) conducted extensive laboratory investigations and derived the following relationship:

$$\frac{0.4q_b^{\frac{2}{3}}}{d} = \frac{q^{\frac{2}{3}}S}{d} - 17 \quad (3-2)$$

Where q_b = bed-load [(Kg/s)/m]
 q = water discharge [(Kg/s)/m]

S = slope

d = particle size (mm)

It should be noted that the equation is only valid for sands with $G_s = 2.65$ and coarser materials with particle sizes of up to 3mm.

3.3.1.3 EINSTEIN-BROWN APPROACH

Einstein (1942) considered two concepts that differed from DuBoy (1879). During equilibrium conditions, the first concept avoided initial motion conditions. The second assumed that bed-load transport is related to turbulent flow fluctuations rather than to average forces exerted by the flow on the sediment particles. Furthermore, Einstein (1942) inferred that the starting and stopping of sediment motion be expressed in terms of probability. From experimental methods, he determined the following:

- A steady and intensive exchange of particles between bed material and bed-load occurs.
- Bed-load movement occurs in a series of steps, of which the average step length is 1000 times the particle diameter.
- The deposition rate per unit bed-area is dependent of the transport rate past a specified section, as well as the probability that the hydrodynamic forces permitting the particle to deposit. The erosion rate on the other hand, depends on the number and properties of particles within the given section and the probability that the instantaneous hydrodynamic lift force on the particle is sufficient to move it. This infers that for a stable bed condition, the deposition rate must equal the rate of erosion.

Brown (1950) built on Einstein's findings and developed the following bed-load transport formula from curve fitting of experimental data:

$$\varphi = \frac{q_{bw}}{K[g(\frac{\gamma_s}{\gamma}-1)d^3]^{\frac{1}{2}}} \quad (3-3)$$

$$\text{where, } K = \left[\frac{2}{3} + \frac{36\nu^2}{gd^3\left(\frac{\gamma_s}{\gamma} - 1\right)} \right]^{\frac{1}{2}} - \left[\frac{36\nu^2}{gd^3\left(\frac{\gamma_s}{\gamma} - 1\right)} \right]^{\frac{1}{2}} \quad (3-4)$$

and:

φ = dimensionless sediment discharge

q_{bw} = bed-load discharge by weight per unit channel width

γ_s, γ = specific weights of sediment and water, respectively

ν = kinematic viscosity

3.3.1.4 SUMMARY OF BED-LOAD SEDIMENT TRANSPORT FORMULAE

A comparison of the Meyer-Peter *et al.* (1934) and Brown (1950) formulae, Lui (2001) reported more or less equal results. The total bed-load sediment transport in rivers was found to be dependent of river width. The consistency of the two formulae is indicative of similar methods used in the determination, i.e. curve fitting of experimental results. The DuBoy (1879) approach: cited in Yang (1996) was reported to overestimate bed-load, with the reason being attributed to the fact that bed-load is always less than or equal to the total bed-material load.

3.3.2 GENERAL APPROACH TO SUSPENDED LOAD TRANSPORT

In steady current, suspended sediment load is supported by the upward components of turbulent currents, and stays in suspension for considerable durations. Most sediment transport in rivers takes place in this manner (Yang, 1996). The vertical distribution of sediment concentration c , measured as the volume of sediments per cubic meter of water (m^3/m^3) is considered using mixing theory, as shown in Figure 3.2-5:

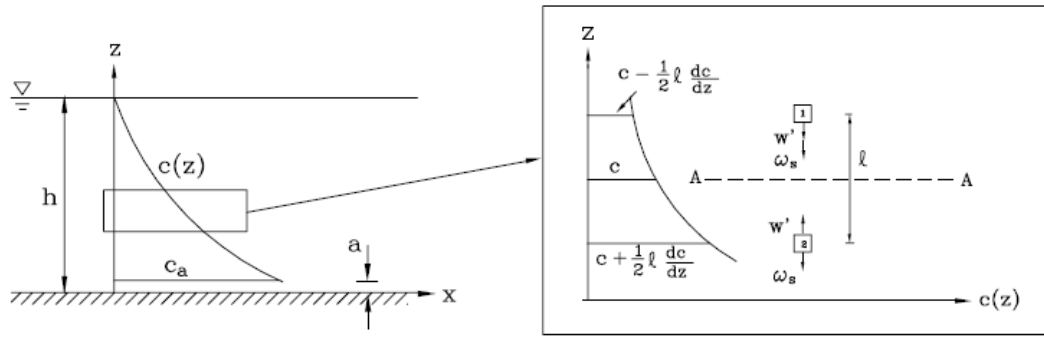


Figure 3.2-5: Suspended sediment in suspended turbulent flow (Source: Lui, 2001).

By superimposing the vertical distribution of fluid velocity, Figure 3.2-6 shows the combined vertical distribution profile of sediment concentration and fluid velocity.

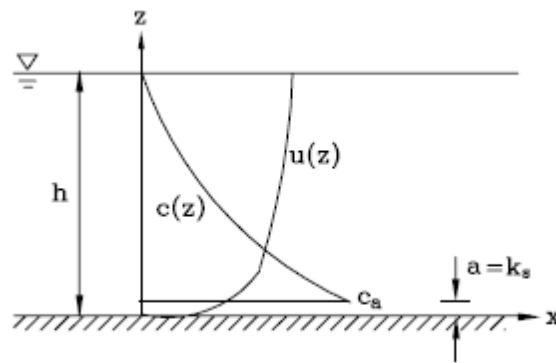


Figure 3.2-6: Vertical distribution of sediment concentration and fluid velocity (Source: Lui, 2001).

Interchanging y for z , and D for h , Yang (1996) mathematically defined the sediment transport load as:

$$q_{sv} = \int_a^D \bar{u} \bar{c} dy \quad (3-5)$$

or,

$$q_{sw} = \gamma_s \int_s^D \bar{u} \bar{c} dy \quad (3-6)$$

where:

q_{sv} and q_{sw}	=	suspended load transport rates in terms of volume and weight, respectively
\bar{u} and \bar{c}	=	time-averaged velocity and sediment concentration by volume at a distance y above the bed, respectively
a	=	thickness of bed-load transport
D	=	water depth
γ_s	=	specific weight of sediment

Before integrating the above expressions, \bar{u} and \bar{c} must be expressed mathematically as functions of y . The reader is referred to extensive analytical and experimental determinations of these functional relationships as defined by Lane & Kalinske (1941), Einstein (1950), Brooks (1963), and Yang (1996).

3.3.3 SUMMARY OF SEDIMENT TRANSPORT FORMULAE

Although many more sediment transport formulae exist, basic approaches and theories for non-cohesive sediment transport rates have been reviewed and evaluated. The evolution of sediment transport formulae has been towards the concept that sediment transport should be directly related to the rate of energy dissipation in transporting sediment particles. The choice in selecting a specific formula to predict sediment transport rates for a particular study should be based on a pilot investigation involving actual field data as different formulae respond differently to sediment characteristics, as well as hydraulic and geographic conditions.

3.4 SEDIMENT TRANSPORT CAPACITY, SEDIMENT LOAD, AND SEDIMENT YIELD

River channel characteristics predominately affect the sediment transport capacity, furthermore each sediment particle must satisfy the following two conditions, as outlined by Julien (1998):

1. The particle must be eroded above the cross section, somewhere in the catchment.

2. The particle must be transported by river flow from the erosion origin to the cross section.

This infers that the sediment transport capacity depends on both stream flow and the availability of sediment. Julien (1998) elaborates further by stating that the actual amount of sediment transported depends on two groups of variables:

1. *Characteristic*: catchment topography, geology, rainfall magnitude & intensity, weathering, vegetation cover, surface erosion, and land use.
2. *Defining*: channel geometry (width, depth, and shape), slope, vegetation, turbulence, and discharge uniformity.

Sediment yield is the amount of sediment mobilised from a known catchment size, passing through a river catchment's reference point per unit time (Msadala, 2009), and is usually expressed in tonnes per square kilometre per year ($t/Km^2/a$).

It is possible to hydraulically determine the sediment yield in regions where the sediment transported by the river is coarse (sand and/or gravel). Basson (2008) rationalizes that during certain flow conditions, when the upstream reach takes on depositional characteristics, the transport capacity can be achieved by bed-load re-suspension, which can only happen if the critical condition for re-suspension is exceeded. Therefore in a quasi-equilibrium river with coarse sediment, the observed sediment transport and the sediment transport capacity should be more or less equal. However, when considering fine sediment, this relationship falls apart, in that the sediment transport capacity and sediment transport are not in agreement. This is concept as illustrated by Shen (1971) is given in Figure 3.2-7:

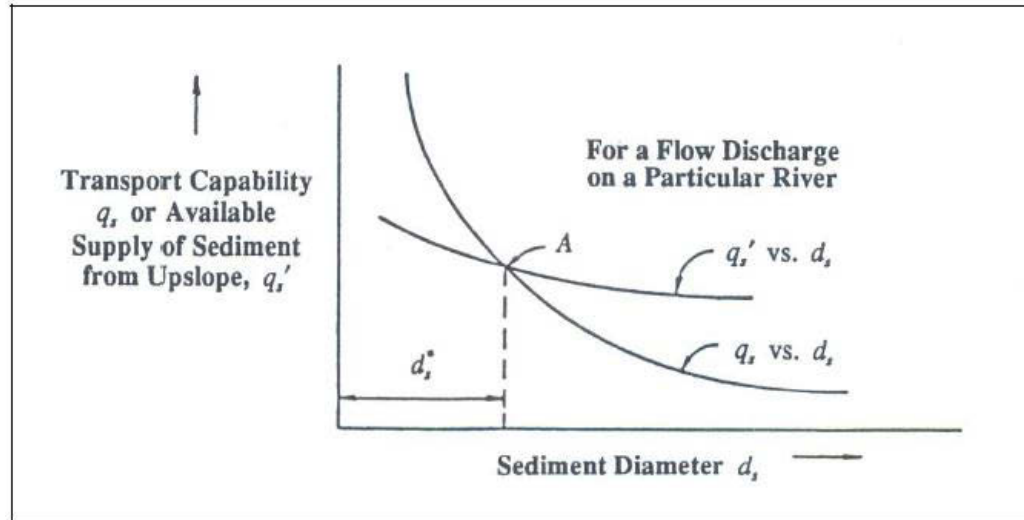


Figure 3.2-7: Theory controlling sediment transport rates, considering the relationship between sediment supply and sediment availability (Source: Shen, 1971).

Having introduced sediment yield and presented the theories that govern sediment transport, the section following examines the different methods developed and used to mathematically estimate sediment yield.

3.4.1 MATHEMATICAL MODELLING OF SEDIMENT YIELD

The ability to numerically model sediment yield can prove crucial for engineering design, and in terms of conservation management, can effectively aid water quality control by considering sediment control strategies for different scenarios (Msadala *et al.*, 2010). This is achieved through the use of spatially distributed models that have the ability to simulate spatially distributed evidence for changes in erosion and sediment yield. Additionally, this spatial data is either presented as individual grid squares that make up the catchment, or as sub-catchments that can be calculated as single computational units.

3.4.1.1 PHYSICAL AND EMPIRICAL BASED MODELS

Randle *et al.* (2006) classified the different types of models under the following sets:

- *Fully physically based:* These models are based on theoretical and physical interrelationships between erosion and sediment yield processes, simulating these processes in both time and space. Examples of this type of model include, but are not limited to the SHETRAN (Ewen *et al.*, 2000) and the Water Erosion Prediction Project (WEPP) (Nearing *et al.*, 1989).

➤ *Empirically based:* These models use empirical equations that are derived from, and rely on what occurs, rather than the theoretical principles of erosion and sediment processes. The development of the empirical equations that govern erosion and deposition usually involve both regression and statistical analyses, and are dependent on the following factors:

- Rainfall intensity and amount
- Soil type and topography
- Land cover and land use
- Upland erosion rates, drainage slope, shape, size, and alignment
- Runoff
- Grain size and mineralogy

The [Revised] Universal Soil Loss Equation (USLE/RUSLE) has been the pillar of success for the majority of empirically based models, which is discussed later in Section 3.4.1.2.

➤ *Mixed empirical and physically based.*

The following section leads into a further discussion on the Revised Universal Soil Loss Equation.

3.4.1.2 THE REVISED UNIVERSAL SOIL LOSS EQUATION (RUSLE)

The Universal Soil Loss Equation (Wischmeier & Smith, 1978) was empirically developed from “a large database and the component factors of the equation, while being physical determinants of soil loss, represent multiplicative statistical, and not strictly physical interrelationships” (Kienzle *et al.*, 1997). This method has also been used to identify sources of potential erosion problems that would develop over a period of years. The RUSLE is as follows:

$$A_{SY} = R K L S C P \quad (3-7)$$

where:

A _{SY}	=	long-term average soil loss per unit area (tonne/ha/a)
R	=	index of annual rainfall erosivity (MJ.mm/ha/hr/a)
K	=	soil erodibility factor (tonne.hr/MJ/mm)
LS	=	slope length and gradient factor (dimensionless)
C	=	cover and management factor (dimensionless)
P	=	support practice factor (dimensionless).

The provision of each of the RUSLE factors are based on datasets and information gathered and represented for each grid cell/subcatchment, and include:

- *Rainfall erosivity factor (monthly):*
 - Mean monthly rainfall (month-by month)
 - elevation.
- *Soil erodibility factor:*
 - Percentage silt and very fine sand
 - Percentage sand
 - Percentage clay
 - Soil permeability
 - Percentage organic matter
 - Soil structure
 - Slope
 - Surface curvature
 - Slow accumulation in the catchment
- *Slope length and gradient factor:*
 - Slope (percentage and degree)
 - Land cover class
 - Flow accumulation in the catchment
- *Cover and management factor:*
 - Percentage covered by canopy (month-by month)
 - Percentage covered by ground cover (month-by-month)

- Mass of buried residue and roots (month-by-month)
- *Support practice factor:*
 - Land cover class
 - Slope
 - Management practice, or land use.

[Adapted from: Kienzle *et al.*, 1997]

For further descriptions, and the fundamental principles in the determination of the RUSLE factors, refer to Wischmeier & Smith, (1978) and Schulze (1995).

The following section highlights and compares several sediment yield models, some of which incorporate the use of the RUSLE.

3.4.1.3 THE AGRICULTURAL CATCHMENTS RESEARCH UNIT (ACRU) MODEL

The ACRU model has been developed since the 1970s at the University of KwaZulu-Natal within the School of Bio-Resources Engineering and Environmental Hydrology (BEEH). The concepts of the ACRU agro-hydrological modelling system are represented in Figure 3.2-8, with the general structure of the system shown in Figure 3.2-9. The ACRU modelling system has been designed according to the following notions (after Schulze, 1995; Kienzle *et al.*, 1997):

- A physical conceptual model in which important hydrological processes and combinations are idealised.
- A multi-purpose model (Figure 3.2-8) incorporating various water budgeting and runoff producing components of the terrestrial hydrological system with risk analysis, and can be applied in design hydrology, crop yield modelling, reservoir yield simulation and irrigation supply/demand.
- The model operates on daily time steps employing daily rainfall input. Less sensitive variables (temperature or potential evaporation) may be inputted monthly, but will be internally transformed into daily values using a Fourier analysis.
- The ACRU model centres on daily multi-layered soil water budgeting, and is highly sensitive to changes in climate, land cover and land use.

- A multi-level model with multiple options or alternative pathways, depending on the level of input data available, or the specifics of the output required.
- ACRU is able to operate a point or lumped catchment model. In areas where the complexity of land use increases, ACRU may operate as a disturbed cell-type model, where sub-catchments are identified and each sub-catchment able to generate individually requested outputs.
- The model includes a dynamic input option that aids in the modelling of hydrological responses to climate, land use or management changes in a time series.
- Using the RUSLE, ACRU combines monthly soil loss potential with daily total runoff volume, peak daily discharge and soil water content to determine the daily sediment yield from a sub-catchment.

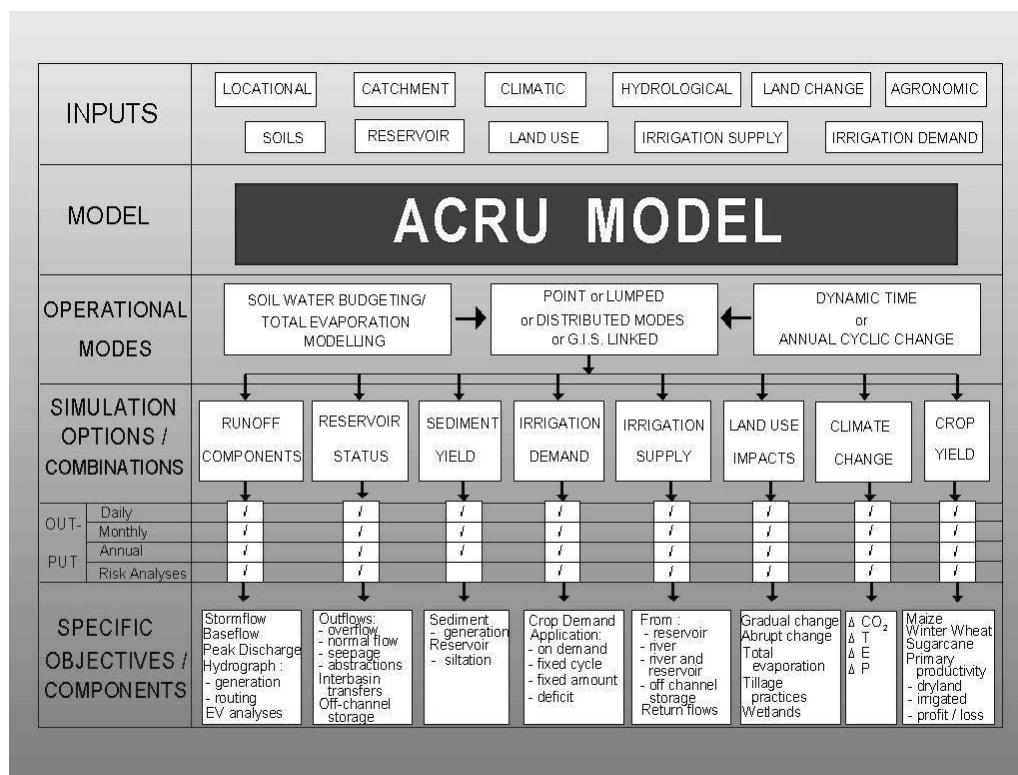


Figure 3.2-8: The ACRU agro-hydrological modelling system: Concepts (Source: Schulze, 1995).

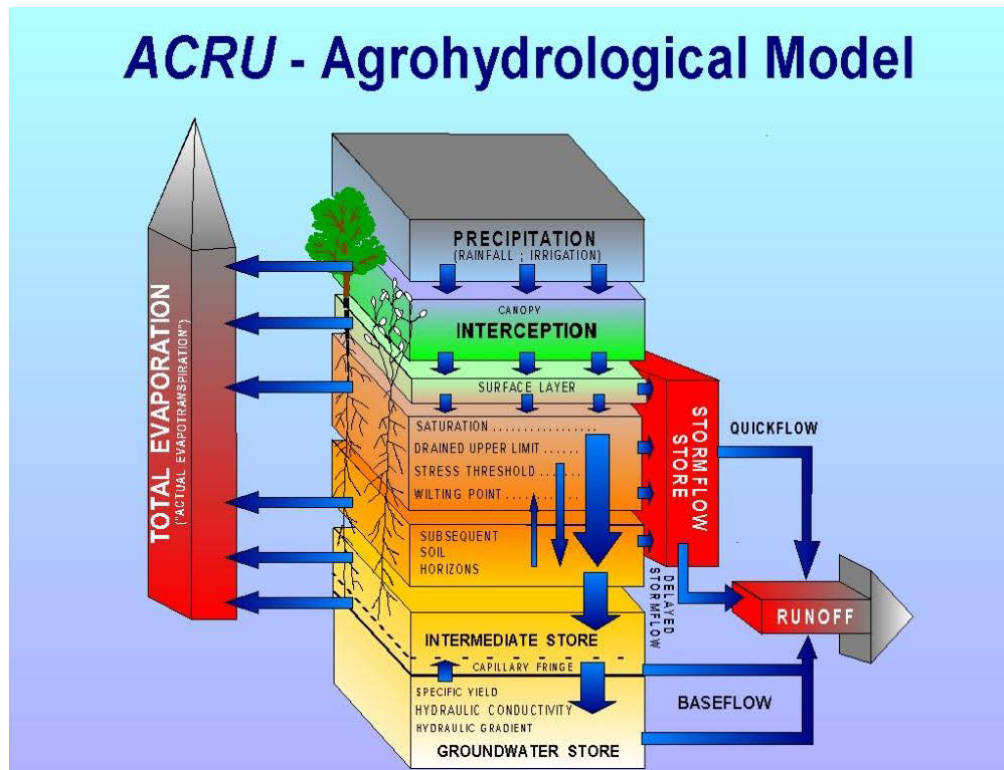


Figure 3.2-9: The ACRU agrohydrological modelling system: General Structure (Source: Schulze, 1995).

3.4.1.4 THE WATER EROSION PREDICTION PROJECT (WEPP) MODEL

The WEPP model is a continuous simulation distributed parameter erosion prediction model. Distributed input parameters that drive the runoff and erosion process include, but are not limited to rainfall amount and intensity, soil properties, plant growth parameters, slope steepness and orientation, and soil erodibility parameter (Falanagan & Livingstone, 1995). Critical components of model comprise of infiltration and runoff estimations. Peak runoff is a critical parameter in the model, as it is used to generate flow depth and flow shear stress. Other components comprise of a soil component to account for roughness, erodibility parameters, plant growth component to provide daily values for canopy cover, biomass, and plant water use, as well as a daily water balance accounting for soil evaporation, transpiration, infiltration, and percolation.

The sediment transport capacity is determined using a simplified shear stress function raised to the power $3/2$ multiplied by a coefficient that is determined through the application of the Yalin (1963); Foster *et al.* (1995) equation at the end of a sloped profile.

Sediment load down a hill-slope profile is predicted using a steady-state sediment continuity equation (Basson, 2008):

$$\frac{dG}{dx} = D_f + D_i \quad (3-8)$$

where G = sediment load ($\text{kg.s}^{-1}.\text{m}^{-1}$),
 x = distance down the hill-slope (in meters),
 D_f = rill erosion rate ($\text{kg.s}^{-1}.\text{m}^{-2}$), and
 D_i = inter-rill sediment delivery rate ($\text{kg.s}^{-1}.\text{m}^{-2}$).

Inter-rill sediment delivery is determined within the model using the following:

$$D_i = K_{iadj} I_e O_{ir} SDR_{RR} F_{nozzle} \frac{R_s}{w} \quad (3-9)$$

where K_{iadj} = adjusted rill erodibility factor (kg.s.m^{-4}),
 I_e = effective rainfall intensity (m.s^{-1}),
 O_{ir} = inter-rill runoff rate (m.s^{-1}),
 SDR_{RR} = Sediment delivery ratio as a function for random roughness, row side-slope, and particle size distribution,
 F_{nozzle} = adjustment factor to account for irrigation sprinkler nozzle impact energy,
 R_s = Rill spacing (meters), and
 w = rill width (meters)

A positive sign is given to rill erosion, and a negative sign to deposition. The model predicts rill detachment when the flow sediment load does not exceed transport capacity, and the flow shear stress acting on the soil exceeds critical shear stress. For this condition, the rill erosion rate is given as:

$$D_f = K_{radj}(\tau - \tau_{cadj})\left(1 - \frac{G}{T_c}\right) \quad (3-10)$$

where K_{radj} = adjusted rill erodibility factor ($s.m^{-1}$)
 τ and τ_{cadj} = flow shear stress and adjusted shear stress, respectively (Pa), and
 T_c = flow sediment transport ($kg.s^{-1}.m^{-1}$).

The two main drawbacks of the model as outlined by Basson (2008) are:

- Its neglecting of soil saturation at the foot of a hill-slope as a result of overland flow, which in-turn ignore important features of water erosion within the catchment.
- Its inability to simulate gully erosion, which could prove to be a critical result in semi-arid regions.

3.4.1.5 THE SHETRAN MODEL

The SHETRAN modelling system consists of three main components as outlined in Figure 3.2-10, namely: water flow, sediment transport, and solute/contaminant transport.

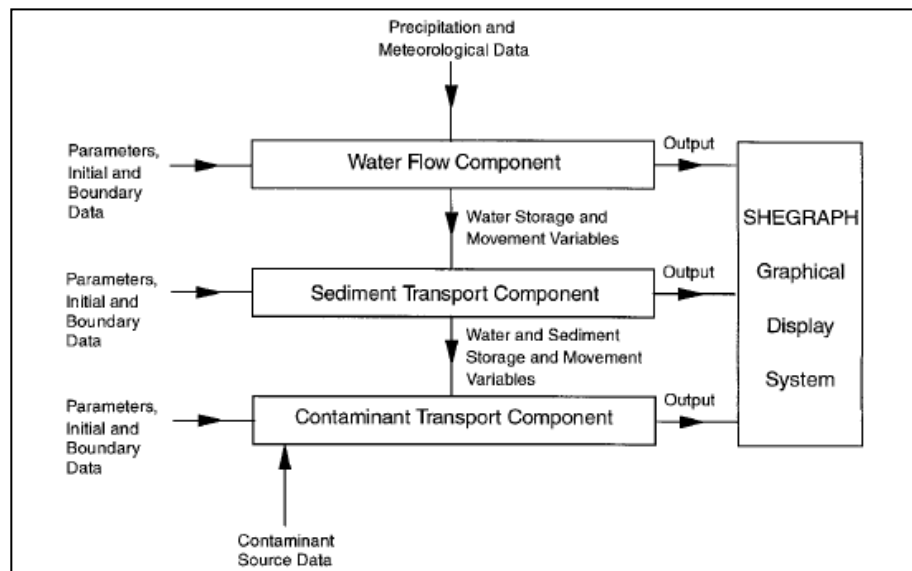


Figure 3.2-10: Information flows and components of SHETRAN (Source: Ewen *et al.*, 2000).

The typical hydrological processes modelled and equations used by the SHETRAN model include (Basson, 2008):

- Rainfall interception by canopy cover (Rutter storage model)
- Evaporation of intercepted rainfall, ground surface and channel water; water drawn transpiration from the root zone (Penman-Monteith equation)
- Snow accumulation and snowmelt (temperature based energy budget techniques)
- 1-Dimensional flow within the unsaturated zone (Richards equation)
- 2-Dimensional overland flow; 1-Dimensional channel flow (Saint Venant equations)
- Channel interaction/saturated zone, accounting for an allowance for an unsaturated zone below the channel
- Surface water/saturated zone interaction.

For erosion and sediment yield, sub-components allowing for erosion by raindrop impact, leaf-drip impact and overland flow (Section 3.2.2), channel bank & bed erosion as well as sediment transport from channel flow/overland flow.

Full details of the main components, processes, and the data for physical properties & initial boundary conditions are summarised in *Appendix E*.

The one notable advantage of the SHETRAN model over both the ACRU and WEPP models is its ability to model and account for sediment generated from gully erosion. The following section highlights the main features and limitations of the three models described above.

3.4.1.6 SUMMARY AND GENERAL COMPARISON OF THE ACRU, WEPP, AND SHETRAN MODELS

The features of the models reviewed above are summarised in Figure 3.2-11, with specific consideration given to each model's capability of predicting erosion and sediment yield.

Model Feature	SHETRAN	WEPP	ACRU
Simulation type:			
Continuous	Y	Y	Y
Single event	Y	Y	Y
Basin size	<2500 km ²	<2.6 km ²	<10000 km ²
Spatial distribution	Grid	grid	GIS raster
Overland flow:			
Rainfall excess	Y	Y	Y
Upward saturation	Y	N	Y
Erosion process:			
Raindrop impact/ Overland flow	Y	Y	Y
Rilling	N	Y	Y
Crusting	N	N	Y
Channel banks	Y	N	N
Gullying	Y	N	N
Landsliding	Y	N	N
Output:			
Time-varying sedigraph	Y	N	Y (daily)
Time-integrated yield	Y	Y	Y
Erosion map	Y	Y	Y
Land use	Most vegetation covers	Wide range of land use	Mainly agricultural
Y = yes; N = no			

Figure 3.2-11: Comparison of the SHETRAN, WEPP, and ACRU models based on erosion and sediment yield components (Adapted from: Basson, 2008)

In addition to this, it is worthy to note that the SHETRAN model differs from the other two in that it has ability to route channel sediment, including an estimate of the proportion of sediment originating from channel erosion. Additionally, SHETRAN is the only model that outputs the proportion of sediments predicted according to sediment particle sizes allowing for a particle size distribution analysis. The major drawback of the SHETRAN model is that catchment size analysis is limited to 2 500 km², where as ACRU can accurately model catchments of up to 10 000 km² (recall Mfolozi catchment size of 10 137 km²).

3.5 OVERVIEW ON HYDROLOGICAL IMPACTS OF LAND-USE CHANGE WITHIN SOUTH AFRICAN CATCHMENTS

The extent to which land-uses determine hydrological responses of a catchment depend on the extent of change of the natural land cover, the location of the land-use within a catchment, and the intensity of the changes (Warburton *et al.*, 2012). At catchment scale, as opposed to local scale, it becomes difficult to distinguish the effects that individual land-

use alterations have on hydrological responses. Schulze (2003) highlights that certain land-uses do not immediately affect the catchment's hydrological response, as they may be a time delay between the actual land-use change and its resulting effect on the water balance. Factors such as land-use practices (ploughing, for example), as opposed to land-use change may have greater impacts on the rationing of rainfall into stormflow and baseflow.

In order to evaluate the impacts of land-use change on hydrological responses, an initial condition (or baseline land cover) is required for which changes are assessed against. The Department of Water Affairs (DWA) recognises the land cover maps produced by Acocks (1988) as the generally accepted baseline maps of natural vegetation within South African catchments.

The following section reviews studies on hydrological impacts of land-use change on streamflow from five catchments with distinct characteristics and size. The first begins with a small rural catchment (263 km²) within the Mochlapetsi River (a tributary of the Olifants River). Troy *et al.* (2007) investigated land-use changes using satellite imagery analysis and field surveys, leading to an assessment of the Ga Mampa valley. In doing so they observed that land-use on the slopes of the catchment remained unchanged while significant changes occurred in the valley, particularly the wetlands area between 1996 and 2004. These changes were summarised as follows:

- 43 and 38% increases in residential area/bare soil and agricultural areas, respectively.
- 44% reduction in natural vegetation and a progressive disappearance (totalling 52%) of the wetlands into agricultural land.

From this, a small increase in streamflow was observed. To investigate if the change in land-use was responsible for the hydrological change, Troy *et al.* (2007) estimated the water transfer process in the different land-use units. They found that the process related to land-use change within the wetlands area only accounted for a small proportion of the observed increases in streamflow.

Using ACURU as a modelling tool, Warburton *et al.* (2012) reported that the Mgeni (4349 km²), the Luvuvhu (5940 km²), and the Upper Breede (2046 km²) catchments had

undergone changes of 40%, 38%, and 25% from natural conditions, respectively. Due to the complex nature of the hydrological responses on catchments, these changes from natural vegetations did not provide detailed insights into the resultant impact on hydrological responses. Contributions of specific land-uses, as well as their respective locations to generated streamflows within catchments, are not proportional to the relative area of that land-use (Warburton *et al.*, 2012). Furthermore, some land-use changes have greater impact on different components of the hydrological response than others. Urban areas have greater impact on stormflow response than commercial agriculture, sugarcane plantations, or degraded areas within a given catchment. This is presented in Figure 3.2-12 for a hypothetical scenario in a subcatchment within the Mgeni catchment where simulated rainfall was equivalent to the median MAP of the Mgeni catchment.

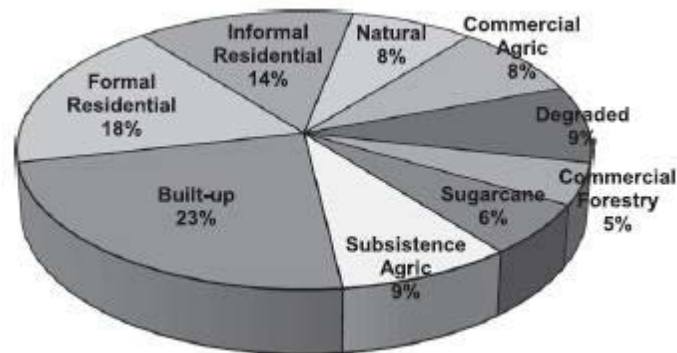


Figure 3.2-12: Percentage contributions of equally sized land-use units to the mean annual streamflow of a hypothetical subcatchment within the Mgeni catchment that experiences a MAP equal to the median MAP of the Mgeni catchment (Source: Warburton *et al.*, 2012).

In this incident, the contribution of degraded areas to streamflow is comparable to natural vegetation and was similar to the percentage area of the catchment it occupied. However, closer examination into the stormflow component of streamflow resulted in it being significantly altered by degraded areas (more than 80% of streamflow in the summer months). Similar results were observed in the Upper Thukela catchment where degraded areas were found to significantly increase stream flow (Blignaut *et al.*, 2010).

To further put this into perspective and evaluate the extent to which different land-uses impact different components of the hydrological response of a catchment, the following important land-uses (natural, urban areas, commercial forestry, and sugarcane plantations)

have been compared against degraded areas with respect to the ratio of stormflow to total runoff (Figure 3.2-13).

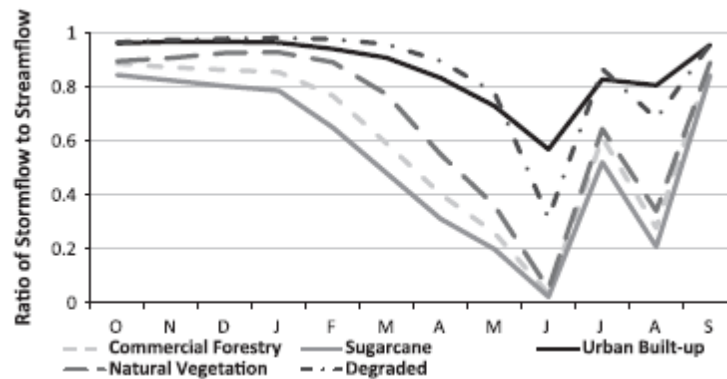


Figure 3.2-13: Mean monthly ratios of stormflow to total runoff for commercial forestry, sugarcane plantation, urban areas, degraded areas, and natural vegetation for a hypothetical subcatchment in the Mgeni catchment (Source: Warburton *et al.*, 2012).

Compounding this are anthropogenic interferences such the building of reservoirs or other hard water engineered structures. The Mgeni catchment has four large reservoirs which dampen flow variability and in some cases cause a reversal of the flows between the dry and wet months for both low and median flows.

The effects on total evaporation from commercial permanent irrigated agriculture in the Upper Breede catchment were found to have significant effects when compared against natural vegetation (Warburton *et al.*, 2012). During the growing months (October to March), the total evaporation from commercial irrigated agriculture is significantly higher than that of the natural vegetation it replaced. This has been attributed to the additional water inputs from the reservoir which increases the availability of soil moisture during the evaporation process, whereas natural vegetation relies exclusively on summer rainfall within the catchment (Figure 3.2-14).

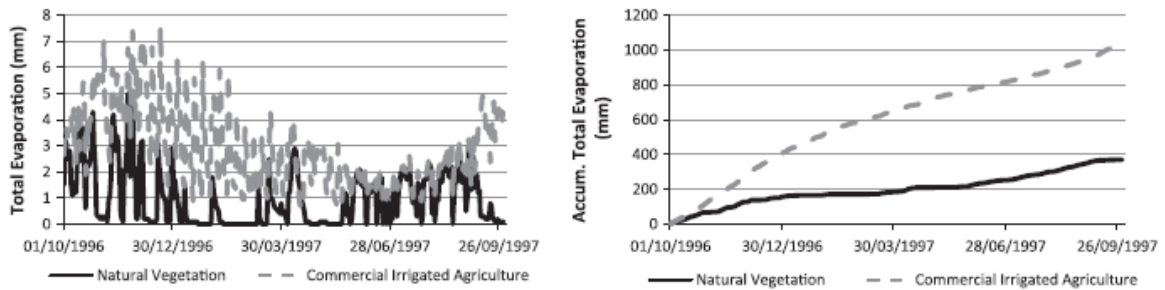


Figure 3.2-14: One year simulated daily evaporation (left) and accumulated monthly evaporation (right) of a typical subcatchment in the Upper Breede catchment under commercial irrigated agriculture and natural vegetation (Source: Warburton *et al.*, 2012).

In closing, both the Mgeni and the Upper Breede catchments showed significant changes in catchment runoff due to land-use change, specifically commercial irrigated agriculture (Warburton *et al.*, 2012). The Luvuvhu catchment, on the other hand, did not show any significant changes in streamflow. This was attributed to significantly large areas of natural vegetation in the middle to lower reaches of the catchment. The resultant of which was a self correcting effect on accumulated streamflows. Implications of this on future planning/management involve crucial assessments of the threshold beyond which the extent, type, and location of land-use changes become hydrologically significant. Although the extent of land-use change in Troy *et al.* (2007) study was extensive, it did not result in significant increases in streamflow mainly due to the size of the investigated catchment.

The above demonstrated that each catchment is unique relative to its respective feedbacks and feed-forwards, and hence will have a unique threshold where the extent of land-use change becomes significant in affecting an individual catchment's hydrological response. Warburton *et al.* (2012) have further demonstrated that the application of a spatial and temporal land-use sensitive, daily time-step model yielded confident, realistic results that aid in the better understanding of the complex interactions of land-use change. In doing so, they have provided a sound basis for similar studies in which the magnitude of land-use and climate change are to be measured in world heritage sites such as the Mfolozi – St Lucia system.

3.6 CRITERIA FOR THE SELECTION OF AN APPROPRIATE HYDROLOGICAL MODEL FOR LAND-USE CHANGE IN THE MFOLOZI CATCHMENT

Water quantity and quality modelling have traditionally been performed using one, or a combination of four modelling approaches (Kienzle *et al.*, 1997):

- *Stochastic models.* Also known as *black box* models where by inputs (rainfall) are transformed into outputs (runoff) with minimum understanding of the process involved in the transformation. This type of model relies heavily on historical records of both inputs and output variables being a representative sample over time.
- *Calibration and parameter optimising models.* These models utilise parameter adjustment to enable the model output to match observations as closely as possible. These models require extensive data for calibration, which is usually limited to a particular subcatchment making transfers to ungauged catchments problematic.
- *Parametric models.* Also referred to as *grey box* models that rely on partial understanding of the hydrological process. However, the system's spatial homogeneity (soils, vegetation, topography, etc) is not taken into account because inputs are spatially averaged or lumped. As a result, variability of hydrological processes are integrated such that their parameter expressions become indices rather than having strictly physically meaningful values.
- *Deterministic, physical conceptually based models.* Also known as *white box* models where the behaviour of the hydrological system is described with respect to mathematical relationships that outline the interactions and linkages of the various temporally or spatially varying catchment hydrological process.

Although calibration of deterministic, physically based models is often tedious and to some extent subjective (Midgley *et al.*, 1994), these models do hold advantages over the other aforementioned models:

- The generalisation and mapping of parameters to provide estimates for ungauged areas, and
- Hydrological responses to land-use changes such as irrigation and afforestation can be incorporated into the structure of the model.

Validation of resulting simulated streamflows usually involves comparing outputted MAR and statistics with those of the *monthly* streamflow at weir locations. Furthermore, parameter values would be adjusted until agreement was deemed satisfactory, i.e. the observed and simulated hydrographs coalesce within reason.

A model's capability of incorporating land-use change is of particular importance. Pitman (1973), Hutchinson & Pitman (1973), Midgley *et al.* (1994), and Middleton & Bailey (2008) accounted for the anthropogenic influences of historical land-use change and estimated unaffected streamflows using the Pitman (1973) model. In doing so, re-simulation is required with all land-use components being set to *virgin* conditions (Acocks, 1988) veld types. The virgin simulation yields an estimate of the natural hydrology at weir locations (Midgley *et al.*, 1994). The difference between the simulated virgin and the historical series (after calibration) results in an estimate of the overall effect of all land-use developments within a catchment, or *naturalised* streamflow and is calculated as follows:

$$O_n = O_h + (S_v - S_h) \quad (3-11)$$

where:

- S_h = Simulated historical flow
- S_v = Simulated virgin/natural flow
- O_h = Observed historical flow
- O_n = Observed natural flow.

The above expression merely adds back to the observed record the net effect of all upstream land-use changes. It should be noted that this method limits land-uses to irrigation, exotic forests, urbanised areas, reservoirs, and water transfer schemes.

Given the high spatial variability of rainfall, soil types, land covers/land-uses, and altitudes within the Mfolozi catchment it is vital to consider unique water quantity and quality characteristics of smaller homogenous areas of the subsystem, i.e. subcatchments. This confirms the need for a distributed, physical conceptually based model.

It has been accepted (Turner *et al.*, 1995; Samaniego & Bardossy, 2006; Choi & Deal, 2008) that the use of a hydrological model that is conceptualised to sufficiently represent

hydrological processes, and which is sensitive to land-use changes is an appropriate method to assess the impacts of land-use on catchment hydrology. The ACRU model satisfies all the required criteria. The advantages of ACRU are that it operates on a daily time step and can interface with *GIS*. This interface may prove vital when overlaying actual changed land-use features onto natural land covers to accurately investigate the resulting hydrological responses.

3.7 CATCHMENT SEDIMENT YIELDS: THE MFOLOZI CATCHMENT IN A GLOBAL AND SOUTHERN AFRICAN PERSPECTIVE

There are four published studies on sediment yields within the Mfolozi catchment that are reviewed in this section. The most recent of which was undertaken by Grenfell & Ellery (2009). In their study, and based on turbidity observations undertaken from 2000 to 2006, they estimated a suspended load of $6.8 \times 10^5 t/a$ (or $67 t/Km^2/a$, assuming a catchment area of $10\,137 Km^2$). Based on suspended sediment measurements taken on one day in January, Lindsay *et al.*, (1996) estimated a suspended sediment load of $1.24 \times 10^6 t/a$ ($122 t/Km^2/a$). Fleming & Hay (1983) estimated the Mfolozi catchment sediment yield at $2.75 \times 10^6 t/a$ ($272 t/Km^2/a$). Rooseboom (1975) estimated a suspended sediment load of $2.36 \times 10^6 t/a$ ($233 t/Km^2/a$).

These estimates differ significantly, and seem to be highly dependent on episodic events driven by rainfall, i.e. periods of flood and drought. This is clearly demonstrated in Figure 3.2-15, which shows the annual rainfall index, as the normalised deviation from the annual mean. Positive indices indicate relatively wet years, while a dry year is indicated by a negative index (Lawrie & Stretch, 2011).

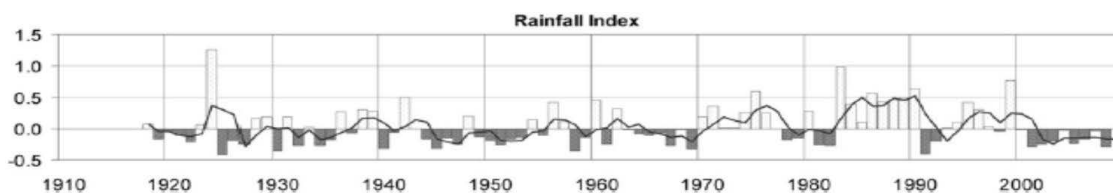


Figure 3.2-15: Lake St. Lucia catchments rainfall index (Source: Lawrie & Stretch, 2011).

From this, it becomes clear that the Grenfell & Ellery (2009) sediment yield estimate was undertaken during periods of drought, and is hence an underestimation. Conversely,

approximations from Rooseboom (1975) and Fleming & Hay (1983) were based during flood periods and hence the higher yields. Ideally, in order to accurately estimate a catchment average annual sediment yield, and its associated variability, one should look to simulate and validate annual sediment yields to include periods of both flood and drought. Robson (2000) recommends at least 50 years, for hydrological records.

According to Grenfell & Ellery (2009), the sediment load discharged from the Mfolozi catchment is small when compared to Orange ($1 \times 10^6 \text{Km}^2$) and Zambezi ($1.39 \times 10^6 \text{Km}^2$) catchments ($17 \times 10^6 \text{t/a}$ and $20 \times 10^6 \text{t/a}$, respectively). However, it should be noted that sediment yield is highly dependent on a combination of factors- the most significant of which include climate, topography and human activities, and is imperceptibly dependent on catchment size. That said, it becomes evident that comparing catchment sediment yields should be done according to the extent of land-use within catchments. Wolanski (2007) has classified these into minimal, moderate, and extensive land-uses, as presented in Figure 3.2-16. The catchments of Cimanuk and La Sa Fua rivers are small and strongly modified by human activities.

River	Area (10^6km^2)	Yield (tonne $\text{km}^{-2} \text{year}^{-1}$)
<i>Minimal land use</i>		
Ngerdoch (Palau)	39×10^{-6}	2
King Sound (Australia)	0.12	50
<i>Moderate land use</i>		
Yangtze (China)	1.9	252
Amazon (Brazil)	6.1	190
Mississippi (U.S.A.)	3.3	120
Mekong	0.79	215
<i>Extensive land use</i>		
La Sa Fua (Guam)	5×10^{-6}	480
Ganges/Brahmaputra (India)	1.48	1670
Cimanuk (Indonesia)	0.0036	6350

Figure 3.2-16: Comparison of the drainage area and sediment yield for various rivers (Source: Wolanski, 2007).

By extension, sediment yield within the Wolanski (2007) classes (minimal, moderate, and extensive) can be interpreted as low ($0-99 \text{ t/Km}^2/\text{a}$), medium ($100-399 \text{ t/Km}^2/\text{a}$), and high yields ($>400 \text{ t/Km}^2/\text{a}$), respectively. According to Harrison *et al.*, (2001), 23% of the Mfolozi comprised of subsistence agriculture and commercial forestry, 13% degraded bushland and forestry, less than 1% urban, and 64% in its natural state, indicating moderate land-use. This current state of land-use along side estimates provided by Grenfell & Ellery

(2009), Lindsay *et al.*, (1996), Fleming & Hay (1983), Milliman & Meade (1983), and Rooseboom (1975), classify the Mfolozi catchment as a medium yielding catchment in a regional and global perspective.

4. METHODOLOGY

4.1 INTRODUCTION

This chapter explores research methodology, definitions and statistical methods used to investigate the evidence of climate change using rainfall as an indicator. This is followed a discussion on the methods applied with the ACRU model to simulate water and sediment yields incorporating land use changes. Furthermore, the chapter attempts to delineate limitations associated with the chosen methods.

For the purpose of this study, a quantitative research approach was undertaken as it is contended that quantification allows more precision in analysing, summarising and drawing conclusions from numerical data. Additionally, quantitative research attempts to be very controlled and objective (Abawi, 2008).

4.1.1 LITERATURE REVIEW

The two-part critical review undertaken in Chapter 3 presented an in depth analysis from existing literature on:

- i. Climate change, variability, and trends. The focus of which utilised rainfall as an indicator to provide historical evidence of climate change, and future projections.
- ii. Erosion, sediment dynamics, and sediment yield of the Mfolozi catchment.

4.2 METHODOLOGICAL APPROACH TO ANALYSIS OF HYDROLOGICAL DATA

4.2.1 ANALYSIS OF HYDROLOGICAL DATA

The main steps to hydrological data analysis as described by Robson (2000) are:

- Obtaining and preparing a suitable dataset
- Exploratory analysis of the data
- Application of statistical tests
- Interpretation of results

These iterative steps are best represented in the flow chart shown in Figure 4-1

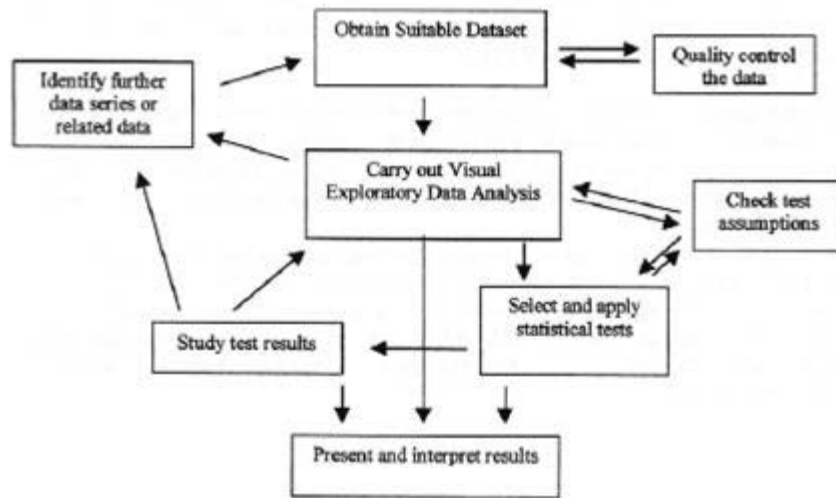


Figure 4-1: Flow chart showing main stages in statistical analysis of change (Source: Robson, 2000).

4.2.1.1 SUITABLE DATA SET

There are several important aspects that need to be considered when acquiring, analysing and preparing a suitable dataset. These include, but are not limited to quality of data, length of rainfall data record, and the extent of missing values or gaps.

A common problem with long time series hydrological data is the change of measurement methods over time, and it is often advisable to examine possible changes in data collection methods (Robson, 2000). Another aspect of data quality to be considered with specific regard to rainfall is that of relocated rain stations that still kept their original name and station reference number. It was therefore important to identify rainfall gauge stations with long data set records that were still in their established original locations.

With regard to length of rainfall data required to investigate variations, Robson (2000) recommends a minimum data record of 50 years, but follows on by advocating that this length may not be sufficient. It was therefore decided to identify rainfall gauge stations across South Africa that had record data dating as far back as 100 years.

It is not possible to record every rainfall event, therefore it is not only expected, but accepted to have a certain degree of missing raw data. Before any analysis was conducted,

the extent of missing data for each station was determined. Rainfall data gaps in the study were patched in accordance with Lynch (2004).

4.2.1.2 EXPLORATORY DATA ANALYSIS

Exploratory data analysis (EDA) involves using graphs to explore, understand and present data and is an essential component of any statistical analysis (Grubb & Robson, 2000). As described earlier this is an iterative process that involves plotting, interpreting and refining graphs to highlight important trends and features. The application of EDA to time-series hydrological data is useful in that they allow a visual assessment of any variation or step-change whilst indicating the magnitude of that variation relative to the overall variation (Grubb & Robson, 2000). Interpretation of the time series plot more often is aided by the addition of a smoothing curve and/or regression line that follows the general trend of the data.

The time-series rainfall graphs in this study are to be presented with both linear (Section 4.2.2.2) and locally weighted regression (Section 4.2.1.3) trend lines. The method of fitting a smoothing curve using LOESS fitting is described below.

4.2.1.3 LOCALLY WEIGHTED REGRESSION

LOESS builds on linear and non linear least squares regression models by fitting simple models to localised subsets of the data in order to build up a function that best describes the point by point deterministic part of the variation within the data (Fox, 2002). Given this, the main advantage of this method of smoothing fitting becomes apparently clear in that it is not required to define a global function of any form to fit a model to the data, but rather to segments of the data.

The LOESS procedure as described by Fox (2002) aims at fitting the model

$y_i = f(x_i) + \varepsilon_i$. The regression function is evaluated at a particular x -value, x_0 . The model will be fitted at representative ranges of x -values or at n observations, x_i . The p^{th} order weighted least-squares polynomial regression of y on x is performed as follows:

$$y_i = a + b_1(x_i - x_0) + b_2(x_i - x_0)^2 + \dots + b_p(x_i - x_0)^p + e_i \quad (4-1)$$

Using a tri-cube function, the observation is then weighted in relation to the proximity to the focal value x_0 :

$$W(z) = \begin{cases} (1 - |z|^3)^3 & \text{for } |z| < 1 \\ 0 & \text{for } |z| \geq 1 \end{cases} \quad (4-2)$$

Where $z_i = (x_i - x_0)/h$, and h is the half-width of a window enclosing the observations for the local regression. The fitted value at x_0 , that is, the estimated height of the regression curve, is $\widehat{y}_0 = a$ (produced conveniently by having centred the predictor x at the focal value x_0). It is typical to adjust h so that each local regression includes a fixed proportion s of the data; then, s is called the span of the local-regression smoother. The larger the span, the smoother the result; conversely, the larger the order of the local regressions p , the more flexible the smooth (Fox, 2002).

4.2.2 APPLICATION OF STATISTICAL TESTS

4.2.2.1 MOVING AVERAGES

The method of moving averages offers a simple procedure for smoothing erratic behaviour in time-series plots, allowing graphical representation of a trend (Warburton & Schulze, 2005). Similar to the method of LOESS fitting, moving averages do not provide the magnitude of a trend, or whether the trend is of any statistical significance, and therefore are only used as a starting point for further trend analyses. The study therefore uses the LOESS method of fitting smoothing curves through time series plots.

4.2.2.2 LINEAR REGRESSION

The basic form of a regression analysis is that of linear regression, which is an approach used to model the relationship between a dependent variable (y) and an independent variable (x). The model aims to utilize the independent variable to describe and predict the dependent variable (Warburton & Schulze, 2005). The relationship between x and y is assumed to be linear and described as follows:

$$y_i = \beta_0 + \beta_1 x_1 + \varepsilon_i \quad (4-3)$$

where:

y_i = response value of the i^{th} variable observation

β_0 = intercept of the regression line

β_1 = gradient of the regression line

x_i = value of the explanatory variable of the i^{th} observation

ε_i = i^{th} observation error term

In the study a linear regression line will be fitted to both annual rainfall trends, and observational data associated with peak over threshold plots (discussed in Section 4.2.3).

4.2.2.3 HYPOTHESIS TESTING

The study utilizes hypothesis testing at significant levels of $\alpha = 0.01$ and $\alpha = 0.05$, with the following hypothesis:

Null hypothesis, H_0 = There is no change in the mean of the time series

Alternative hypothesis, H_1 = There is a change in the mean of the time series (increasing or decreasing depending on sign of regression gradient).

4.2.2.4 USING THE T-TEST TO TEST FOR HOMOGENEITY

The T-test is a standard parametric test for testing whether two samples have different means. In its basic form it assumes normally distributed data and a known change- point time (Robson *et al.*, 2000). The study utilises the t-test in order to investigate shorter term (20 year periods) variations in trends, particularly when no statistically significant change in mean annual rainfall is observed over the entire 100-year period (or longest length of available data). The test hypotheses for the t-test were as follows:

Null hypothesis, H_0 = There is no change in the 20 – year mean of non-overlapping time series

Alternative hypothesis, H_1 = There is a change in the mean of non-overlapping time series (increasing or decreasing depending on sign of regression gradient).

4.2.2.5 GAMMA DISTRIBUTION

Due to its skewed profile, the gamma distribution has been recommended by the WMO with regards to fitting precipitation related distributions (Neyers, 1990; Nastos & Zerefos, 2007). Another advantage of the Gamma distribution is in fitting the distribution where the scale parameter is to be selected. Increasing the scale parameter results in stretching the probability density function, which can therefore be used to estimate the probability of extreme events (Nastos & Zerefos, 2007). The general equation of the probability density function is given below:

$$f(x) = \frac{\left(\frac{x-\mu}{\beta}\right)^{\gamma-1} \exp\left(-\frac{x-\mu}{\beta}\right)}{\beta T(\gamma)} \quad x \geq \mu, \gamma, \beta > 0 \quad (4-4)$$

Where γ is the shape parameter, μ the location parameter, β the scale parameter that can be used to describe the intensity of rainfall (where an increasing scale parameter describes increasing rainfall intensity).

Given that Gamma function is:

$$T(a) = \int_0^{\infty} t^{a-1} e^{-t} dt \quad (4-5)$$

The equation of the gamma distribution can hence be reduced to:

$$f(x) = \frac{x^{\gamma-1} e^{-x}}{T(\gamma)} \quad x \geq 0; \gamma > 0 \quad (4-6)$$

(Adapted from Nastos & Zerefos, 2007)

The study uses the Gamma distribution alongside the T-test (Section 4.2.2.4) to determine the change of distribution patterns of the rainfall data extracted from the various rain gauge stations, including changes to mean, frequency and intensity of rainfall events.

4.2.3 DEFINITION OF HEAVY RAINFALL EVENT

The definition of a heavy rainfall event varies across regions. The method adapted by Zhang *et al.* (2001) identifies an exceedance threshold of three heavy rainfall events per year for a study conducted in Canada.

A threshold of 50 mm rainfall per day was defined by Wang *et al.* (2008) in a study conducted in Taiwan. Furthermore, the South African Weather Service issues warnings and advisories for heavy precipitation greater than 50 mm per day is expected (Dyson, 2009).

The parameters used in this study are therefore defined as follows:

Monthly rainfall data: Peak over thresholds at the 92nd and 75th percentile (interpreted as an expected exceedance of 1 and 3 events per year, respectively)

Peak under thresholds of 25th and 8th percentile are defined for lower order rainfall.

Daily rainfall data: Predefined thresholds of 10 mm, 20 mm, 30 mm, and 50 mm, where any rainfall event exceeding 30 mm per day being classified as a heavy precipitation event.

It should be noted here that the definition of a *wet-day* used in this study denotes any daily rainfall event that is greater than, or equal to 1mm.

4.2.4 SUMMARY OF RAINFALL DATA COLLECTION AND ANALYSIS PROCEDURE

- Rainfall data was selected from representative stations within the Mfolozi catchment. Double-mass plots were then used to validate consistency of regional rainfall gauge stations.
- Annual maxima precipitation was plotted for each station, along with linear and LOESS fitting.
- Monthly rainfall data was then plotted at different percentile plots to investigate frequency of extreme rainfall events (with linear and LOESS fitting).
- Daily rainfall data was then plotted for different pre-defined thresholds (as described in section 4.2.3) as a percentage of the wet days, with linear and LOESS fitting.
- The t-test was used to investigate shorter duration (20 year) statistically significant variations of monthly rainfall data means.

- A gamma distribution was fitted to daily precipitation data over 20 year periods.

4.2.5 LIMITATIONS OF RAINFALL DATA ANALYSIS

The data analysed was collected as secondary data, and hence the collection process remains unknown (Boslaugh, 2007). One major limitation with specific regard to rainfall data is that it is not possible to acquire a precise measurement due to the occurrence of random and systematic errors during measurement (Warburton & Schulze, 2005). Furthermore, Boughton (1981) believes that deficiencies of up to 20% exist in rain gauge measurements. The sources systematic prejudices that exist in measuring rainfall include, but are not limited to:

- The effects of wind- being the largest source of a deficiency in rain gauge measurement (between 8% and 20 %)
- Wetting losses
- Evaporation losses from rain gauge
- Splashing effects out of the rain gauge
- Treatment of trace precipitation events (fog)

[Adapted from Warburton & Schulze, 2005]

Other aspects that may limit the accuracy of the results from this study include:

- The use of 10 rain gauge stations to represent the entire study area. The results from which may not be an accurate enough assessment of existing regional trends.
- Errors in the patching of missing rainfall data.

4.3 METHODOLOGICAL APPROACH TO HYDROLOGICAL MODELLING WITH ACRU

As described in section 3.4.1.3 and represented by Figure 3.2-9 the ACRU model is a four tier modelling tool requiring the user to configure the following: *inputs, model, operational modes, simulation options, and specific objectives*. The remainder of this section elaborates in detail ACRU model inputs used in the simulations.

4.3.1 CATCHMENT CONFIGURATION

The Mfolozi catchment was delineated into the 26 quaternary catchments (QC) as spatially represented by the Department of Water Affairs (DWA). This is shown in Figure 4-2.

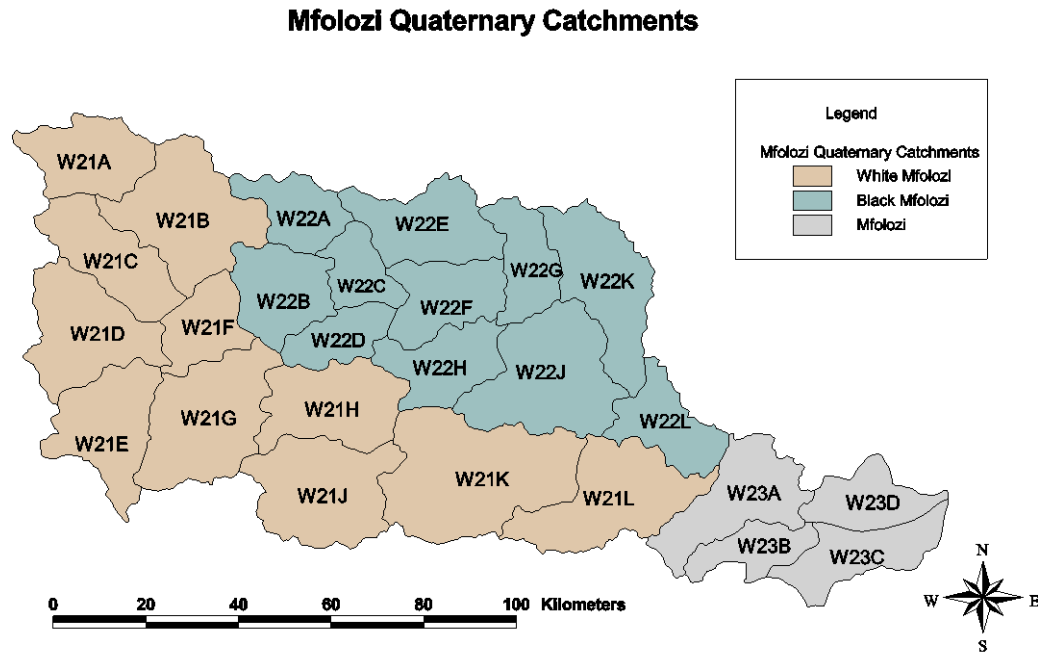


Figure 4-2: Mfolozi Quaternary Catchments: W21, W22, and W23 prefixes represent the White Mfolozi, Black Mfolozi, and Mfolozi Rivers respectively.

The 26 QCs were further subdivided into three interlinked cascading quinary catchments (or homogenous hydrological response units), i.e. upper, middle and lower Quinary catchments of similar topography but unequal area, allowing for more detailed assessments with regards to hydrological responses (Schulze & Horan, 2010).

Figure 4-3 represents a schematic of the river systems and inter-catchment flow paths of the Mfolozi River used in the study. This was based on the National Land Cover [NLC] (2005) digital land cover database. Each circled number indicates a particular land use or *veld unit* number such that each QC consists of 3 quinary catchments, and each quinary catchment comprised a number of individual veld units (Schulze, Horan & Knoesen, 2009). Veld units were allocated based on each unique veld type present within the quinary catchment, and were each considered distinctive “response zone” (Schulze, Horan &

Knoesen, 2009). Finally, each *response zone* was hydrologically linked to its respective upstream and downstream supply. Depending on the land cover, each quinary catchment encompassed between 1 and 18 *response zones*.

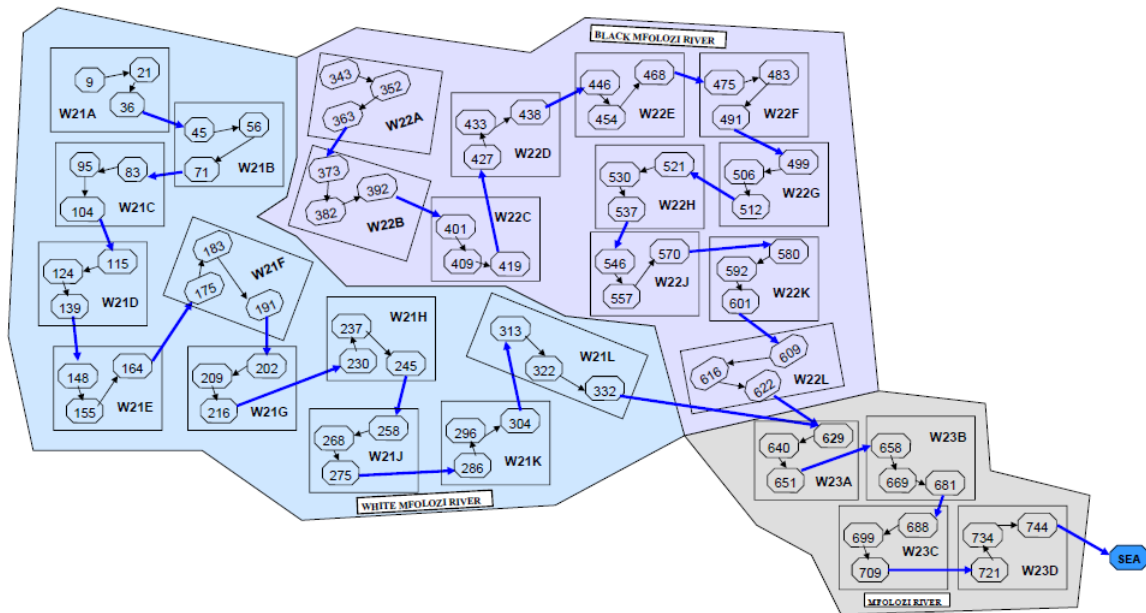


Figure 4-3: Quinary Catchments and major river systems of the Mfolozi River representing inter-catchment flow paths

Inter-quaternary flow paths were configured such that their streamflows were routed into each other in a consistent sequence representative of river flow, an example of which is shown in Figure 4-4.

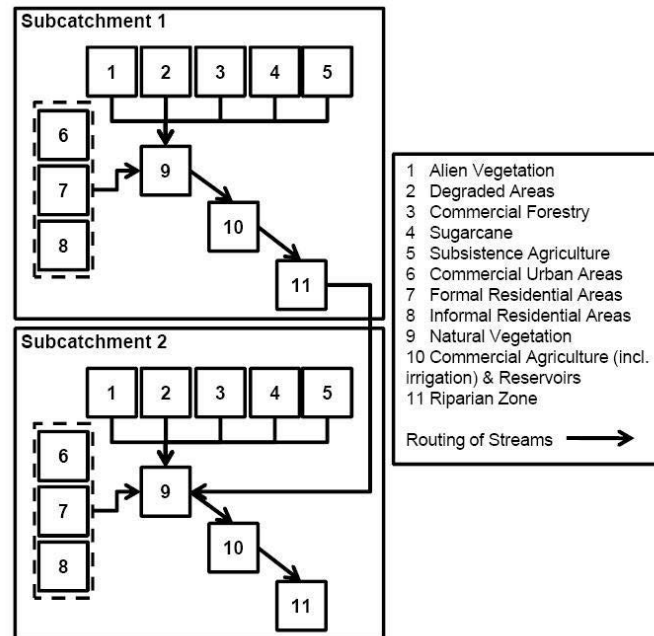


Figure 4-4: An example of quaternary catchment flow routing between veld-units (Source: Warburton *et al.*, 2010).

4.3.2 DAILY RAINFALL

Verified daily rainfall data for South African quaternary catchments has been compiled by Lynch (2004) and used in simulations for the period 1950-1999. The method of quaternary catchment driver station selection is outlined in Lynch (2004).

For the latter period of 2000-2010, daily rainfall data for the quaternary catchment driver stations as identified previously were sourced from the South African Weather Service (SAWS). Some quaternary driver stations have since been closed by SAWS, and new driver stations within the proximity of the respective Quaternary centroids were selected and checked by producing double-mass plots using overlapping periods to determine their consistency and usability.

The next phase in rainfall data verification (for the period 2000-2010) involved a statistical comparison of Mean Annual Precipitation (MAP) to the WR2005 Quaternary database (Figure 4-5), as well as a comparison to the Median Monthly Precipitation (MMP) from soil surface readings in the BEEH database. This additional MMP check as outlined in Smithers and Schulze (2005) is preferred over the sole MAP check where observed rainfall data is available for data records shorter than 20 years. This is due to the high inter-annual

variability of rainfall and secular trends in cycles of consecutive wet and dry years, which has a periodicity of approximately 18 years and may be present in rainfall data of regions that experience summer rainfall in DJF (Schulze, 1995). Daily rainfall correction (PPTCOR) factors for each quaternary catchment were hence adjusted based on MMP on a month-by-month basis where necessary.

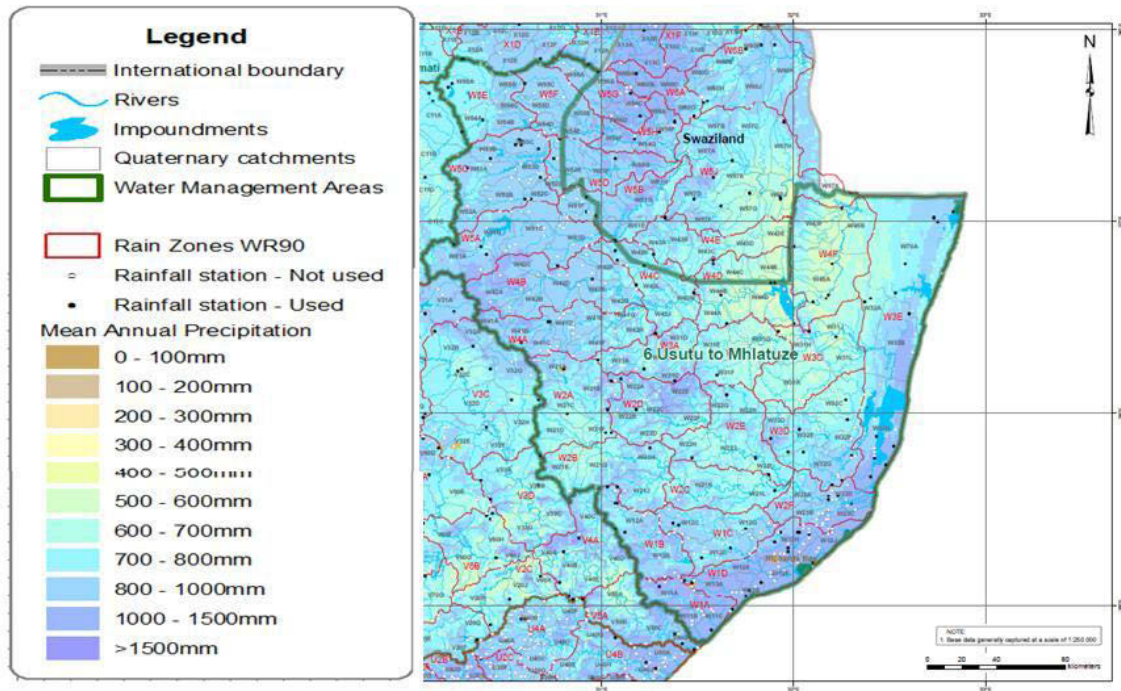


Figure 4-5: Mean Annual Precipitation for Northern KZN catchments (Source: Middleton & Bailey, 2008).

4.3.3 DAILY TEMPERATURE AND DAILY POTENTIAL EVAPORATION

Daily maximum and minimum temperatures were required for the estimation of vapour pressure, solar radiation, potential evaporation, and consequently soil moisture runoff generation (Schulze, Horan & Knoesen, 2009).

Daily maximum and minimum temperatures for quaternary catchments for the period 1950 to 1999 generated from quality controlled records were used and are given in Schulze & Maharaj (2004). For the latter period (2000 to 2010) daily maximum and minimum temperatures were sourced from SAWS. However due to the presence of only 4 temperature stations (Charters Creek, Mtunzini, Ulundi, and Vryheid), within the Mfolozi Catchment, it was necessary to apply an adiabatic lapse rate correction for monthly means of both daily and maximum and minimum temperatures. The method and recommended

adiabatic lapse rates for monthly means of daily (maximum and minimum) temperatures is presented in Schulze & Maharaj (1994). These are based on the 12 delineated temperature regions across South Africa. It was observed that some of the quaternary catchments crossed temperature regions. It was therefore decided to apply an average adiabatic lapse rate correction of -7°C (applied to daily maximum temperatures) and -5.5°C (applied to daily minimum temperatures) per 1000m difference in elevation from the reference stations to the centroids of the veld type unit. The daily temperature series was then used to generate daily estimates of reference potential evaporation since there were no measured daily A-Pan or A-Pan equivalent observations for quaternary catchments within the study area. These were then compared to mean annual A-Pan equivalent reference potential evaporation after Schulze (1997). The values for South Africa are presented in Figure 4-6.

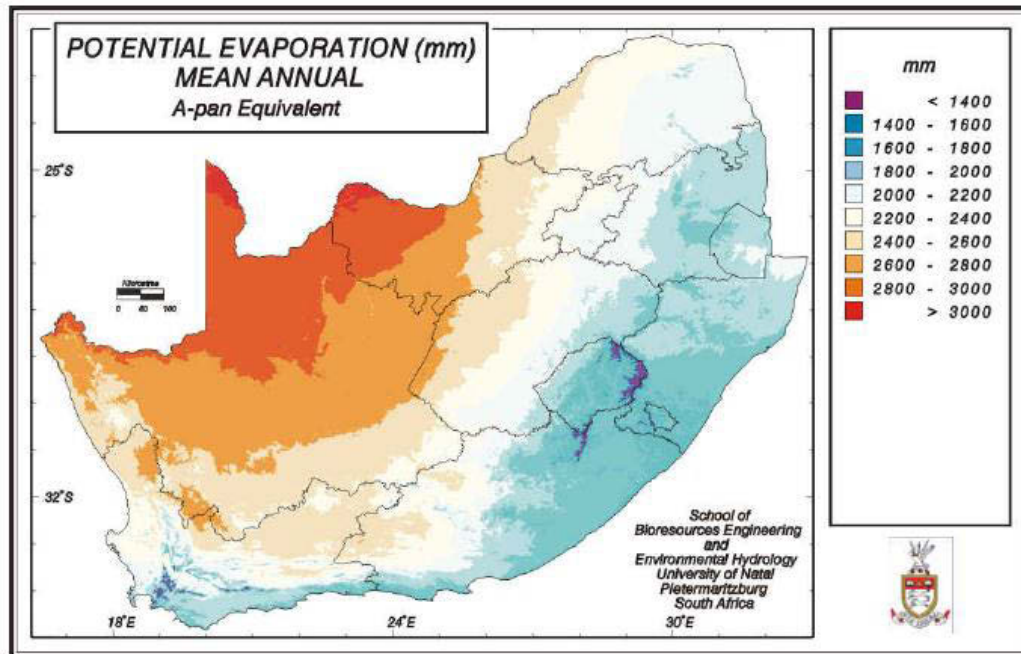


Figure 4-6: Mean annual A-Pan equivalent reference potential evaporation for South Africa (Source: Schulze, 1997).

The Hargreaves & Samani (1985) method was chosen to estimate reference potential evaporation as it satisfied its objective of being a simple and practical method of estimating crop water requirements using a minimum of climatological data i.e. daily minimum and maximum temperature data. This method is incorporated as an ACRU option and was used

to estimate daily A-Pan equivalent evaporation for the entire simulation period (1950-2010). This method is based on the following empirical equation:

$$E_{apan} = 1.25 \times 0.0023 \times R_a T_r^{0.5} (T_a + 17.8) \quad (4-7)$$

where:

- E_{apan} = A-Pan equivalent reference potential evaporation (mm.day⁻¹)
- K_{HS} = Regional calibration coefficient for Hargreaves-Samani equation
- R_a = Extra-terrestrial solar radiation (mm equivalent.day⁻¹)
- T_r = Range of daily air temperature (°C)
- T_a = daily mean air temperature (°C).

[Adapted from Hargreaves & Samani, 1985]

4.3.4 SOILS INFORMATION

For the purpose of simulating the impacts of changes in land use, Schulze, Horan & Knoesen (2009) outline the necessary soils information required by ACRU, which are:

- Thicknesses of identified soil horizons
- Soil surface properties affecting infiltration such as cracking, tillage, sealing and/or crusting
- The percentage distribution of clay, sand, or silt within in the soil horizon profiles and how these relate to permeability and hydraulic conductivity
- Water retention properties of the soil, i.e. permanent wilting point, field capacity, and total porosity, and
- Soil erodibility

Soil properties database per quinary catchment was sourced from the Institute of Soil, Climate and Water [ISCW] (2005). This database identified nine broad categories of soil land types in South Africa, of which three are present in the Mfolozi Catchment with soil horizon depths from 0.2m to 0.8m, and erodibility factors from 0.2 to 0.6 (refer to Figure 4-7):

- Loam
- Loamy sand
- Sandy clay loam

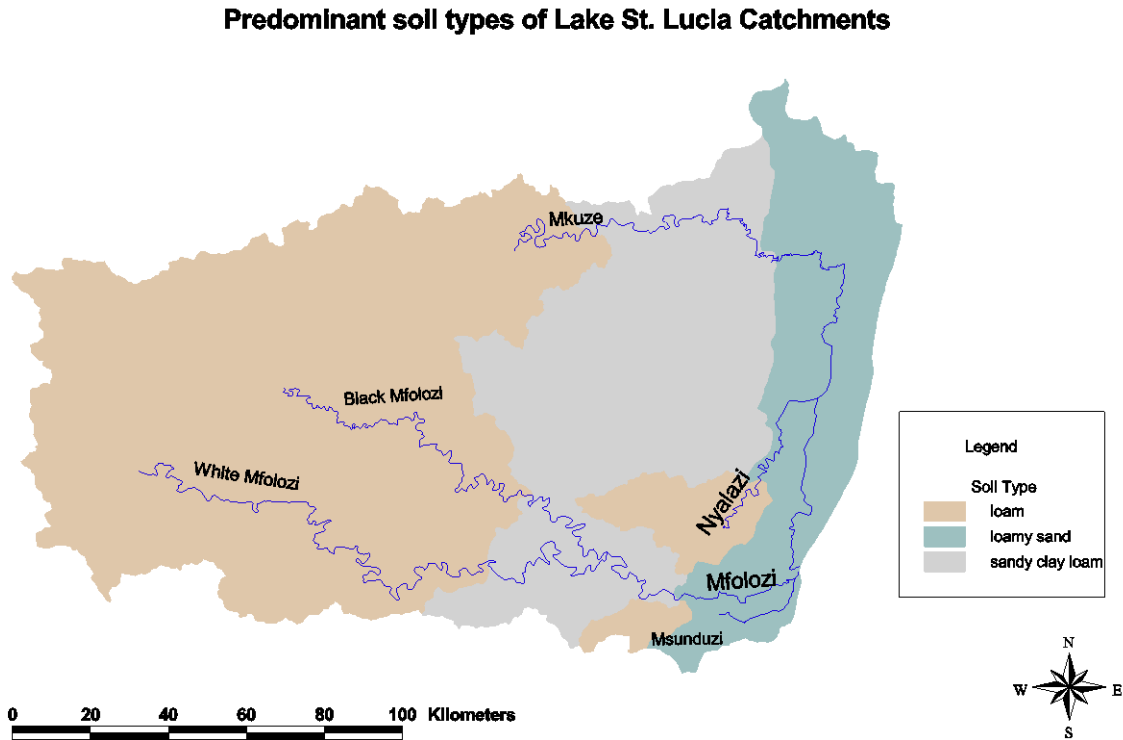


Figure 4-7: Soil types of the Mfolozi – St. Lucia catchments (Source: ISWC, 2005)

4.3.5 BASELINE LAND COVER AND CURRENT LAND USE SCENARIOS

Schulze (2000) highlighted the essential differences between land cover and land use, where *land cover* is indicative of natural vegetative cover, whilst *land use* implies anthropogenic influences through infrastructure development, cropping, plantations and agricultural practices such as irrigation. These factors contribute to the significant dynamic functioning within the plant and soil water evaporative process and influence runoff generation mechanisms. The remainder of this sub-section therefore describes the baseline land cover and current land use scenarios.

4.3.5.1 BASELINE (PRISTINE) LAND COVER

Acocks (1988) veld types have been frequently used in hydrological studies, namely Taylor (1997); Tefera *et al.* (2008), and have been accepted as the *benchmark* land cover with respect to modelling hydrological responses due to changes in land use and management practices. Schulze *et al.* (2011) generated streamflow and sediment yields assuming natural land-cover (Acocks, 1988) for South African quinary catchments from 1950-1999. The simulations were administered at quinary level utilizing one veld unit (typically the predominate land use) within each quinary catchment. It was necessary to setup and extend simulations for the latter period from 2000 to 2010. The Acocks veld types within the study area are given in Figure 4-8.

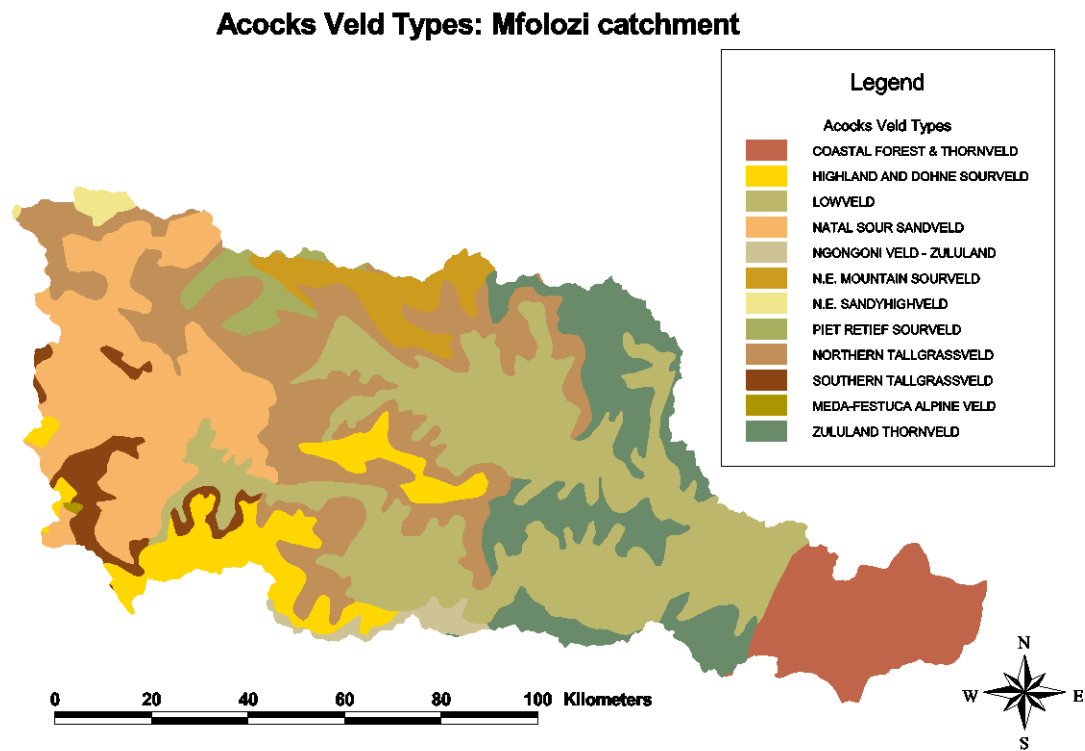


Figure 4-8: Acocks Veld types for Mfolozi River (Source: Acocks, 1988)

The simulations take into account wetlands and natural water-bodies, but do not include impervious areas, and assume an irrigated area of one hectare per quinary catchment.

4.3.5.2 PRESENT DAY LAND-USE

As previously mentioned in Section 4.3.1, the South African NLC (2005) database which comprised of 42 distinct land use classes (within the study area) was established from satellite imagery. This is graphically represented in Figure 4-9. Using *ArcView GIS*, land use classes were overlaid onto the Mfolozi Quinary Catchments. Each Quinary Catchment was then delineated into distinct land use classes, and each land use class was allocated as a unique veld unit. Moreover, each veld unit was hydrologically linked maintaining inter-quinary flow paths, as shown in Figure 4-4.

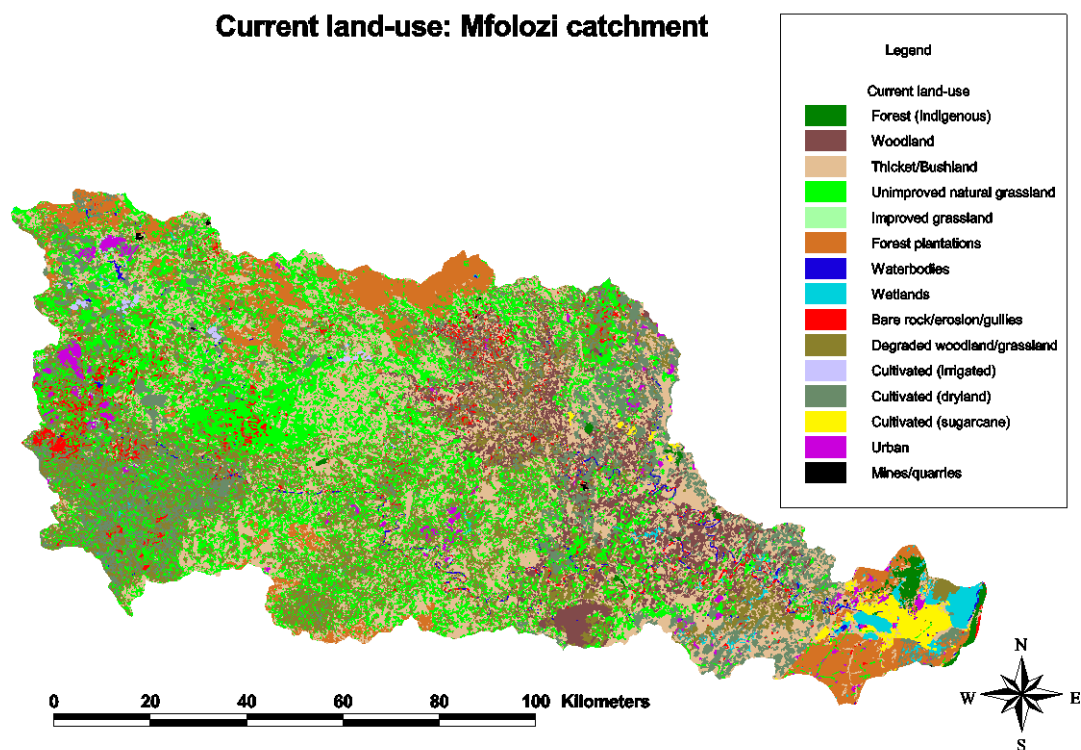


Figure 4-9: Mfolozi catchment current land-use (Source: NLC, 2005).

4.3.6 STREAMFLOW SIMULATION CONTROL VARIABLES

Information required for streamflow generation for each subcatchment is comprised of a coefficient representing a fraction of total stormflow generated from rainfall occurring on a particular day that will exit the subcatchment on the same day as the rainfall event (Kienzie, Lorentz & Schulze, 1997). Furthermore, factors that affect streamflow include, but are not limited to baseflow, effective soil depth from which stormflow generation occurs, the extent of impervious areas both directly and indirectly in contact with the

watercourse, and the coefficient of initial abstraction used to approximate the amount of abstracted rainfall through interception, surface storage and infiltration prior to the commencement of stormflow.

4.3.6.1 STORMFLOW GENERATION IN ACRU

Stormflow generation in ACRU is outputted as a mm depth equivalent, and depends on how wet or dry the catchment is before a rainfall event (Schulze, Horan & Knoesen, 2009).

The ACRU computational method of stormflow is given by the following equation:

$$Q_s = (P_n - I_a)^2 / (P + I_a + S) \text{ for } P_n > I_a \text{ and } Q_s = 0 \text{ for } P_n < I_a \quad (4-8)$$

where:

Q_s = stormflow

P_n = net rainfall (mm) (excluding canopy interception)

I_a = initial abstractions (mm) before stormflow commences

S = the soil's potential maximum retention (mm), i.e. the extent of wetness of the soil or soil water deficit.

[Adapted from Schulze, 1995]

Soil water deficit within ACRU is determined through the multi-layer soil water budget after defining a critical soil depth. The critical soil depth takes into account different runoff generating mechanisms as resultants of different land use or climate conditions. For simulations within this study, this critical soil depth was limited to the thickness of the top horizon soil.

Due to catchment characteristics such as slope and size, not all stormflow generated from a rainfall event exits the catchment on the same day as the rainfall event (Schulze, 1995). This is taken into account in ACRU and is incorporated by a stormflow response coefficient and described by Schulze, Horan & Knoesen (2009) as an index of interflow and is typically approximated to 0.3. It should, however be noted here that due to high

inter-variability nature of the Mfolozi River, this coefficient was taken as 0.4 for simulations within this study.

4.3.6.2 BASEFLOW GENERATION IN ACRU

Baseflow is the fraction of streamflow that originates from accumulated deep subsurface flow or intermediate/groundwater store. This is computed in ACRU exclusively from recharged soil water stored in the intermediate/groundwater zone (Schulze, 1995). This recharging effect is a result of rainfall events that have been redistributed through soil horizons into the intermediate/groundwater store when the deepest soil horizon's water containment exceeds field capacity. A release coefficient, *COFRU* determines the rate of release of groundwater into the stream. This coefficient is also dependent on catchment characteristics such as slope, area and geology; and operates as a decay function. A release coefficient of 0.009 was applied to all quaternary and quinary Catchments within the study area.

4.3.6.3 STREAMFLOW SIMULATIONS IN ACRU

Monthly input parameter values for the land-uses considered in this study are given in *Appendix D* (Tables D-1 and D-2). These include:

- The proportion of water consumed by plants under conditions of maximum evaporation in relation to that evaporated by an A-Pan (*CAY*).
- Interception loss by vegetation (*VEGINT*).
- The fraction of effective root system in the topsoil horizon (*ROOTA*).
- The coefficient of initial abstraction used to estimate the rainfall abstracted by interception, surface storage, and infiltration before stormflow commences (*COIAM*).

Having described in detail factors that influence and affect streamflow modelling in ACRU, streamflow was simulated and accumulated on monthly time steps and verified against DWA flow gauges (shown in Figure 2-1). The calibration process followed steps outlined by Smithers & Schulze (2005).

4.3.7 SEDIMENT YIELD GENERATION IN ACRU

Sediment yield modelling in ACRU utilizes the *Revised Universal Soil Loss Equation*, discussed earlier in Section 3.4.1.2. The equation as it appears in ACRU is given below:

$$A_{SY} = \alpha_{SY} (Q_v \times q_p)^{\beta_{SY}} K LS C P \quad (4-9)$$

where:

- Y_{sd} = sediment yield (t) from an individual stormflow event,
- Q_v = stormflow volume for the event (m^3),
- q_p = peak discharge for the event (m^3/s),
- K = soil erodibility factor (t h/N/ha),
- LS = slope length and gradient factor,
- C = cover and management factor
- P = support practice factor

The coefficients α_{SY} and β_{SY} are location specific and usually determined for specific catchments within specific climate zones, however values of 8.934 and 0.56 (respectively) calibrated by Williams (1975) have been accepted in Williams & Berndt (1977); Williams, Menzel & Coleman (1984); Williams (1991): cited in Schulze (1995) and used in this study.

In order to simulate sediment yield, the peak discharge per stormflow event is required for each Quaternary Catchment or, in the case veld unit. ACRU uses the modified SCS peak discharge equation after Schulze & Schmidt (1995):

$$q_p = 0.2083 Q_s A / 1.83 L \quad (4-10)$$

where:

- q_p = peak discharge (m^3/s)
- Q_s = stormflow depth (mm)

$$A = \text{catchment area (Km}^2\text{)}$$
$$L = (A^{0.35} \text{MAP}^{1.1}) / (41.67 S_{\%}^{0.3} f_{30}^{0.87})$$

i.e. the catchment lag (response) time (h)

and

$$\text{MAP} = \text{mean annual precipitation (mm),}$$
$$S_{\%} = \text{average catchment slope (\%), and}$$
$$f_{30} = \text{30 minute rainfall intensity (mm/h) for the 2 year return period.}$$

Upon successful calibration and validation of stormflow, the required input data for the sediment yield module in ACRU are discussed below:

1. The average catchment slope per Quinary Catchment, derived from 20m Digital Elevation Model.
2. Stormflow volume per land use management scenario.
3. Soil erodibility factor, K , ascertained from the Institute of Soil, Climate and Water.
4. Slope length and gradient function, internally calculated in ACRU using catchment slope input information.
5. Soil erodibility cover and management, C (Schulze, 1995).

It should be noted here that K -factor has been predetermined by the ISCW (1995) for the different soil types within South Africa, and was therefore not adjusted. The C -factor, on the other hand is dependent on a combination of surface and canopy cover, and was hence adjusted to account for crop rotation and/or tree planting rotation where in one given year an area that had trees planted would be clearveld the next year, and so on.

In order to account for this, Wischmeier & Smith (1978) determined C -factors for permanent, veld, and woodland. These are represented in Figure 4-10.

Vegetative Canopy ²	Canopy Cover (per cent) ³	Cover that Contacts the Soil Surface						
		Type ⁴	Per cent Ground Cover					
			0	20	40	60	80	95+
No appreciable canopy	25	G	0.45	0.20	0.10	0.042	0.013	0.003
		W	0.45	0.24	0.15	0.091	0.043	0.011
Grassland or short brush with average drop height of 0.5 m	25	G	0.36	0.17	0.09	0.038	0.013	0.003
		W	0.36	0.20	0.13	0.083	0.041	0.011
	50	G	0.26	0.13	0.07	0.035	0.012	0.003
		W	0.26	0.16	0.11	0.076	0.039	0.011
	75	G	0.17	0.10	0.06	0.032	0.011	0.003
		W	0.17	0.12	0.09	0.068	0.038	0.011
Appreciable brush or bushes, with average drop fall height of 2m	25	G	0.40	0.18	0.09	0.040	0.013	0.003
		W	0.40	0.22	0.14	0.087	0.042	0.011
	50	G	0.34	0.16	0.08	0.038	0.012	0.003
		W	0.34	0.19	0.13	0.082	0.041	0.011
	75	G	0.28	0.14	0.08	0.036	0.012	0.003
		W	0.28	0.17	0.12	0.078	0.040	0.011
Trees, but no appreciable low brush. Average drop fall height of 4m	25	G	0.42	0.19	0.10	0.041	0.013	0.003
		W	0.42	0.23	0.14	0.089	0.042	0.011
	50	G	0.39	0.18	0.09	0.040	0.013	0.003
		W	0.39	0.21	0.14	0.087	0.042	0.011
	75	G	0.36	0.17	0.09	0.039	0.012	0.003
		W	0.36	0.20	0.13	0.084	0.041	0.011

- ¹ The listed C-values assume that the vegetation and mulch are distributed randomly over the entire area.
- ² Canopy height is measured as the average fall height of water drops falling from the canopy to the ground. Canopy effect is inversely proportional to drop fall height and is negligible if fall height exceeds 10 m.
- ³ Portion of total-area surface that would be hidden from view by canopy in a vertical projection (a bird's-eye view).
- ⁴ G: cover at surface is grass, grasslike plants, decaying compacted duff, or litter at least 50 mm deep.
W: cover at surface is mostly broadleaf herbaceous plants (e.g. weeds with little lateral-root network near the surface) or undecayed residues or both.

Figure 4-10: C-factor for permanent pasture, veld and woodland (Wischmeier & Smith, 1978).

4.4 METHODOLOGICAL APPROACH TO MEASURING TOTAL SUSPENDED SOLID (TSS) CONCENTRATION

The equipment required to determine TSS comprised of the following:

- 0.7µm glass fibre filter (GF/F)
- 100ml measuring cylinder
- Filtration apparatus and vacuum pump (Figure 4-11)
- Vacuum pump



Figure 4-11: Set-up of TSS filtration apparatus and vacuum pump.

Subsequent to the collection of water samples on site at the Mtubatuba Water Works, the following procedure was undertaken:

- Filters were dried overnight in an oven at 110°C and then weighed.
- Field sample bottles were shaken to ensure no settling had occurred, and a 100ml sample was filtered.
- Each filtered sample was then placed overnight in an oven at 110°C and then weighed.
- TSS was then calculated using the following equation: $TSS (mg/L) = (A - B)/C$, where A = final dried weight of the filter in mg, B = initial dried weight of the filter in mg, and C = volume of water filtered in L.

4.5 SUMMARY OF METHODOLOGY

In closing, the methods undertaken in order to achieve the objectives in this study were as follows:

- A critical literature review on climate change, variability and trends, as well as the effects of land-use change on water yields, soil erosion, sediment dynamics, and modelling of catchment sediment yields.

- Statistical analyses of historical precipitation to determine rainfall trends within the past 100 years, including those of extreme rainfall events.
- Using the ACRU model, setup, calibrate and validate Mfolozi catchment streamflow for present day land-uses at weir locations (simulation period: 1950-2010). It should be mentioned here that irrigation has not been considered for the present day land-use scenario, as it only accounted for less than 2% of the Mfolozi MAR as estimated by Middleton & Bailey (2008).
- Calibrate sediment yield module in ACRU and validate against derived observations.
- Reverting from present day land-uses to natural land covers, streamflows and sediment yields were simulated for 1950-2010 at quinary level in order to establish a historical baseline for comparison purposes.
- Simulations for natural land covers as well as present day land-uses were repeated using empirically downscaled GCM projections of future climate for the simulation periods of 2046 – 2065 (~50 yr projection) and 2081 – 2100 (~100 yr projection).

5. RESULTS AND DISCUSSION

5.1 INTRODUCTION

This chapter presents and discusses results obtained from the study. This is presented in four main sections. The first section begins with a discussion on results pertaining to historical precipitation trends, followed by an examination of extreme rainfall events. The second section presents and validates monthly streamflow and sediment yield simulations for present day land-use conditions. The third section evaluates the impacts of present land-uses on natural streamflows and sediment yields. The final section assesses impacts of future climate change scenarios from empirically downscaled GCM projections.

5.2 MFOLOZI CATCHMENT HISTORICAL RAINFALL TRENDS AND EXTREME PRECIPITATION EVENTS

This section presents results from statistical analyses carried out on long records (82 year average across 10 rainfall stations) from monthly and daily rainfall datasets. Results pertaining to precipitation trends are discussed first, followed by a discussion on results concerning extreme rainfall events. Due to the large volume of analysis data, only key results and conclusions of statistical tests are given in this section. Full statistical results and representative plots/tables from rainfall data may be found in *Appendix A*. It should be noted here that, unless otherwise indicated, the level of statistical significance used was the 95% confidence band (i.e. $\alpha = 0.05$).

5.2.1 RAINFALL TRENDS WITHIN THE MFOLOZI – ST LUCIA SYSTEM

Table 5-1 lists and summarizes data range, mean annual precipitation, percentage change, and statistical significance of rainfall stations chosen within the Mfolozi – St. Lucia System. Only three stations showed any significant changes. The Cape St. Lucia and Hlobane stations showed increases in rainfall amounts, while the Utrecht station showed a decrease. From this, it can be concluded that there are no consistent statistically significant changes in mean annual precipitation within the region.

Table 5-1: Mfolozi Catchment selected rainfall stations showing MAP, observed change in precipitation (%), and statistical significance.

Station	Data Range	Station MAP (mm)	Reg. gradient	% Change
Cape St. Lucia	1919 - 2005	1211	1.88	+13.5%
Gluckstadt	1914 - 2008	883	-1.26	-13.6%
Hlabisa	1967 - 2002	1070	-4.48	-15.1%
Hlobane	1916 - 2010	691	2.40	+33.0% *
Mahlabatini	1916 - 2010	760	0.55	6.9%
Melmoth	1940 - 2010	846	-0.71	-6.0%
Mposa-Fairview	1920 - 2010	954	0.44	+4.2%
Nkandla	1917 - 1992	748	1.77	+18% **
Umbombo	1920 - 2005	850	-0.17	-1.7%
Utrecht	1921 - 2000	834	-2.54	-24% *

*Significant at 95% confidence level; **Significant at 90% confidence level

Furthermore, non-overlapping t-tests (20-year intervals) were used to investigate data record homogeneity, particularly in stations that were not characterized by a statistically significant change in mean annual rainfall within their respective data ranges. A summary of this is given in Table 5-2.

The overall results indicate homogenous mean annual precipitation within stations, with 7 (out of 32) sub-periods proving exceptions. From these, four were statistically significant ($p < 0.05$) and three were probable ($0.05 \leq p \leq 0.1$). The aforementioned discrepancies in mean annual rainfall can be attributed to major flooding events that occurred in March 1925, July 1963, January/February 1984, and September 1987.

Table 5-2: Results from stations t-test on approx. 20 year sub-periods

Cape St. Lucia				Gluckstadt				Utrecht			
Period	df	t(df)	p-value	Period	df	t(df)	p-value	Period	df	t(df)	p-value
1919-1938 and 1939-1958	38	-0.41	0.34	1914-1935 and 1936-1955	39	-1.58	0.06	1933-1949 and 1950-1966	26	1.67	0.05
1959-1978 and 1979-1998	38	1.43	0.08	1956-1975 and 1976-1995	32	0.58	0.28	1967-1983 and 1984-2000	31	-0.87	0.19
1979-1998 and 1999-2005	10	-0.14	0.44	1976-1995 and 1996-2008	30	0.89	0.19	1933-1949 and 1984-2000	29	2.48	0.01
1919-1938 and 1986-2005	36	-0.69	0.25	1914-1935 and 1989-2008	40	-1.17	0.13				

Melmoth				Mposa-Fairview				Nkandla			
Period	df	t(df)	p-value	Period	df	t(df)	p-value	Period	df	t(df)	p-value
1940-1962 and 1963-1986	45	-0.73	0.23	1920-1941 and 1942-1963	41	-0.28	0.39	1917-1935 and 1936-1954	34	-0.58	0.28
1963-1986 and 1987-2010	44	0.48	0.32	1964-1985 and 1986-2010	41	1.19	0.12	1955-1973 and 1974-1992	28	2.08	0.02
1940-1962 and 1987-2010	43	-0.15	0.44	1920-1941 and 1986-2010	42	0.10	0.46	1914-1935 and 1974-1992	34	-1.35	0.09

Hlobane				Mahlabatini				Umbombo			
Period	df	t(df)	p-value	Period	df	t(df)	p-value	Period	df	t(df)	p-value
1916-1935 and 1936-1955	34	0.95	0.18	1916-1935 and 1936-1955	33	0.14	0.45	1920-1940 and 1941-1961	34	0.49	0.31
1956-1975 and 1976-1995	38	-0.24	0.41	1956-1975 and 1976-1995	30	-0.38	0.35	1962-1982 and 1983-2005	42	-1.21	0.12
1976-1995 and 1996-2010	31	-0.56	0.29	1976-1995 and 1996-2010	30	0.00	0.50	1920-1940 and 1983-2005	42	-0.15	0.44
1916-1935 and 1989-2010	34	-2.61	0.01	1916-1935 and 1991-2010	38	-0.50	0.31				

Hlabisa			
Period	df	t(df)	p-value
1967-1984 and 1985-2002	33	0.44	0.33

5.2.2 EXTREME RAINFALL WITHIN THE MFOLOZI – ST LUCIA SYSTEM

Extreme rainfall events within the study area were analysed using quantile regressions of monthly data (Table 5-3), and peak over predefined thresholds of daily data (Table 5-4), allowing conclusions to be reached on the relative changes in the frequency and intensity of rainfall events. The majority of the stations examined showed consistent statistically significant reductions in the number of wet-days. This implies an increase in average intensity of rainfall events. Half of the stations analysed showed small but statistically significant increases in the occurrence of higher order rainfall intensities (>30mm/day and >50mm/day).

Furthermore, the statistics of each 20-year gamma distribution are presented in Table 5-5. While the shape parameter is relatively constant for each station, the increase in scale parameter, variance, as well as the migration of the mean towards higher values is indicative of extreme daily rainfall. This is in concurrence with Groisman *et al.* (1999) for various global studies including Canada, Norway, USA and Australia, as well as Nastos & Zerefos (2007) for a study in Greece. Both studies agreed that the precipitation shape parameter fitted to gamma distributions remains relatively unchanged or independent of total rainfall. However, the varying or increasing scale parameter is indicative of disproportionate increases in heavy precipitation as total rainfall increases in the future.

Table 5-3: St. Lucia Wetland quantile thresholds, regression gradient and statistical significance (p-value)

Quantile threshold	Cape St. Lucia		Gluckstadt		Hlabisa		Hlobane		Mahlabatini	
	Regr. Grad.	p-value	Regr. Grad.	p-value	Regr. Grad.	p-value	Regr. Grad.	p-value	Regr. Grad.	p-value
POT 92 nd percentile	0.0009	0.8355	-0.0023	0.5036	0.0130	0.4117	0.0100	0.0011	0.0103	0.0034
POT 75 th percentile	0.0039	0.6139	-0.0048	0.2891	-0.0108	0.5948	0.0098	0.0698	0.0102	0.0736
PUT 25 th percentile	-0.0077	0.2602	0.0137	0.0194	0.0501	0.0239	-0.0072	0.1065	0.0029	0.5624

Quantile threshold	Melmoth		Mposa-Fairview		Nkandla		Umbombo		Utrecht	
	Regr. Grad.	p-value	Regr. Grad.	p-value	Regr. Grad.	p-value	Regr. Grad.	p-value	Regr. Grad.	p-value
POT 92 nd percentile	-0.0019	0.7170	-0.0015	0.6841	0.0021	0.6547	0.0004	0.9178	-0.0083	0.0283
POT 75 th percentile	-0.0052	0.5113	0.0062	0.3052	0.0078	0.2834	-0.0017	0.7775	-0.0099	0.1427
PUT 25 th percentile	0.0020	0.7928	0.0016	0.7612	-0.0236	0.0004	-0.0012	0.8457	0.0131	0.0310

Table 5-4: Stations average number of wet days, and change in rainfall intensity above predefined thresholds of 10mm, 20mm, 30mm, and 50mm.

Station	no. days precipitation > 1mm			no. days precipitation > 10mm		
	av. No. wet days	change (days/yr)	total change(days)	av. No. >10mm days	change (days/yr)	total change(days)
Cape St. Lucia (87)	85	0.11	9.3	37	0.03	2.6
Gluckstadt (95)	68	-0.54	-51.3*	27	-0.04	-3.4
Hlabisa (36)	54	-1.76	-63.2*	29	-0.32	-11.4*
Hlobane (95)	66	-0.10	-9.9*	26	0.07	6.5*
Mahlabatini (95)	56	-0.52	-49.4*	24	0.01	1.3
Melmoth (71)	73	-0.90	-63.9*	26	0.10	7.0*
Mposa-Fairview (91)	80	-0.06	-5.6	29	0.00	-0.3
Nkandla (76)	64	-0.18	-13.6*	28	0.04	3.2
Umbombo (86)	53	-0.67	-57.9*	24	-0.01	-1.2
Utrecht (85)	53	-0.31	-26.0*	26	-0.06	-5.2*

*Significant at 95% confidence level; number in bracket indicates data record in years.

Station	no. days precipitation > 20mm			no. days precipitation > 30mm		
	av. No. >20mm days	change (days/yr)	total change(days)	av. No. >30mm days	change (days/yr)	total change(days)
Cape St. Lucia (87)	19	0.01	0.8	10	0.00	0.2
Gluckstadt (95)	12	0.03	3.2*	6	0.03	2.7
Hlabisa (36)	17	0.10	3.5*	9	0.08	2.8*
Hlobane (95)	12	0.05	4.9*	6	0.05	4.5*
Mahlabatini (95)	12	0.05	5.1*	6	0.04	3.6
Melmoth (71)	12	0.09	6.1*	6	0.05	3.4*
Mposa-Fairview (91)	13	0.01	0.9	7	0.01	0.5
Nkandla (76)	13	0.02	1.6*	7	0.01	0.8
Umbombo (86)	13	0.04	3.1*	8	0.03	3.0
Utrecht (85)	11	-0.01	-0.7*	5	-0.01	-0.8*

Station	no. days precipitation > 50mm		
	av. No. >50mm days	change (days/yr)	total change(days)
Cape St. Lucia (87)	4	0.00	0.2
Gluckstadt (95)	2	0.02	1.5*
Hlabisa (36)	4	0.07	2.6*
Hlobane (95)	2	0.02	2.2*
Mahlabatini (95)	2	0.03	3.0*
Melmoth (71)	2	0.02	1.1*
Mposa-Fairview (91)	3	0.00	0.0
Nkandla (76)	2	0.001	0.1*
Umbombo (86)	3	0.03	2.6*
Utrecht (85)	2	0.001	0.4*

*Significant at 95% confidence level; number in bracket indicates data record in years.

Table 5-5: Selected stations mean, variance, and gamma distribution parameters fitted to daily rainfall data over 20-year periods.

Cape St. Lucia (0 339 720)				
Period	Obs. Mean	Obs. Variance	Scale Par. (β)	Shape Par. (α)
1919-1938	11.44	287.08	25.09	0.46
1939-1958	11.51	319.59	27.75	0.41
1959-1978	10.44	312.22	17.24	0.52
1979-1998	10.30	399.79	38.82	0.27
1999-2005	11.68	470.23	40.25	0.29

Gluckstadt (0 373 058)				
Period	Obs. Mean	Obs. Variance	Scale Par. (β)	Shape Par. (α)
1914-1935	8.83	125.07	14.17	0.62
1936-1955	9.77	137.90	14.11	0.69
1956-1975	12.99	231.96	17.86	0.73
1976-1995	13.34	335.64	25.16	0.53
1996-2008	17.72	306.14	17.28	1.03

Hlabisa (0 338 668)				
Period	Obs. Mean	Obs. Variance	Scale Par. (β)	Shape Par. (α)
1967-1984	13.25	313.31	23.65	0.56
1985-2002	27.67	1015.41	36.70	0.75

Hlobane (0 372 852)				
Period	Obs. Mean	Obs. Variance	Scale Par. (β)	Shape Par. (α)
1916-1935	9.17	139.91	15.26	0.60
1936-1955	8.88	107.06	12.06	0.74
1956-1975	12.11	206.26	17.03	0.71
1976-1995	12.54	280.33	22.36	0.56
1996-2009	13.27	245.90	18.53	0.72

Mahlabatini (0337 795)				
Period	Obs. Mean	Obs. Variance	Scale Par. (β)	Shape Par. (α)
1916-1935	9.84	205.09	20.84	0.47
1936-1955	10.35	179.50	17.34	0.60
1956-1975	13.52	255.34	18.88	0.72
1976-1995	21.33	547.96	25.69	0.83
1996-2009	20.19	499.12	24.72	0.82

Melmoth (0 303 695)				
Period	Obs. Mean	Obs. Variance	Scale Par. (β)	Shape Par. (α)
1940-1962	6.32	101.86	16.11	0.39
1963-1986	12.81	280.17	21.86	0.59
1987-2009	13.91	302.08	21.72	0.64

Mposa-Fairview (0 305 037)				
Period	Obs. Mean	Obs. Variance	Scale Par. (β)	Shape Par. (α)
1920-1941	10.88	290.53	26.71	0.41
1942-1963	12.01	369.31	30.75	0.39
1964-1985	12.04	381.48	31.69	0.38
1986-2009	11.79	288.35	24.46	0.48

Nkandla (0 303 127)				
Period	Obs. Mean	Obs. Variance	Scale Par. (β)	Shape Par. (α)
1917-1935	10.51	178.44	16.98	0.62
1936-1954	13.65	254.35	18.49	0.74
1955-1973	13.61	217.49	15.98	0.85
1974-1992	14.07	215.09	15.28	0.92

Ubombo (0 375 124)				
Period	Obs. Mean	Obs. Variance	Scale Par. (β)	Shape Par. (α)
1920-1940	9.29	255.45	27.50	0.34
1941-1961	12.70	266.88	21.01	0.60
1962-1982	19.28	567.90	29.45	0.65
1983-2005	23.54	857.09	36.41	0.65

Utrecht (0 371 579)				
Period	Obs. Mean	Obs. Variance	Scale Par. (β)	Shape Par. (α)
1916-1932	9.70	141.63	14.60	0.66
1933-1949	12.10	216.70	17.91	0.68
1950-1966	12.29	166.91	13.58	0.90
1967-1983	13.33	181.52	13.62	0.98
1984-2000	13.25	226.68	17.11	0.77

5.2.3 MEAN ANNUAL PRECIPITATION OF THE MFOLOZI CATCHMENT

The mean annual precipitation (MAP) of the Mfolozi catchment ranges from 700mm to 1100mm, as shown in Figure 5-1.

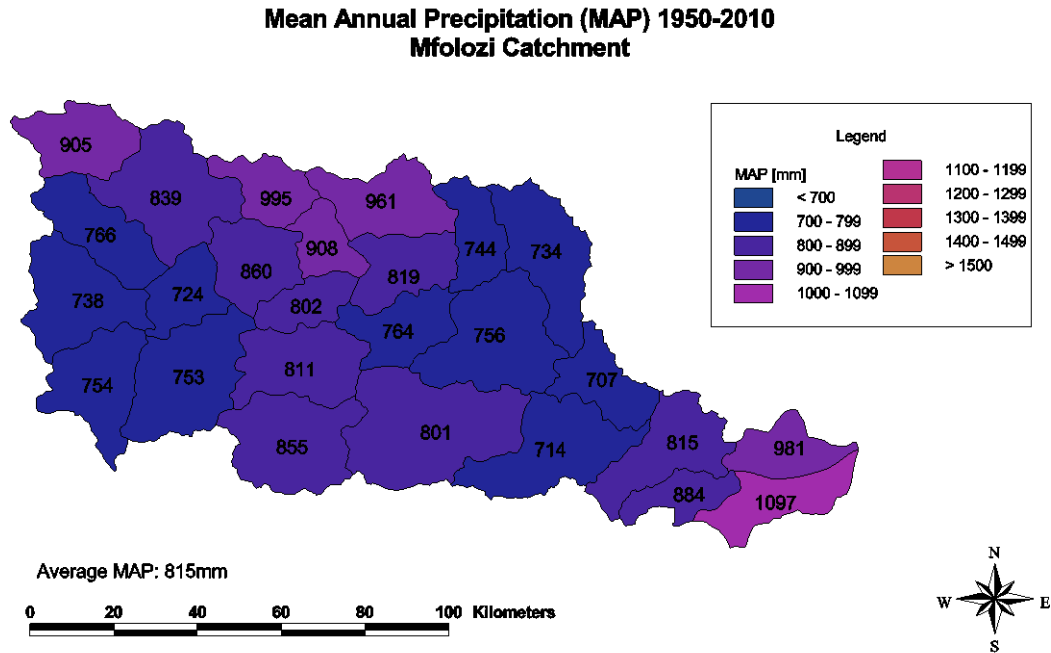


Figure 5-1: Mfolozi quaternary catchment mean annual precipitation (MAP) 1950-2010

When comparing Figure 5-1 with Figure 2-2 (basin elevations), it is evident that the high rainfall area in the mid-upper catchment can be attributed to orographic effects resulting in the accumulation of higher precipitation at higher altitudes, while the development of a rain-shadow develops downwind of the mountain. This results in the rain-shadow zone receiving significantly less rain than the elevated zone.

5.3 MODELLING STREAMFLOW UNDER PRESENT LAND-USE CONDITIONS

Daily streamflows were simulated for the period 1950-2010 using the ACRU model under subcatchment configurations discussed in Section 4.3. Simulated time series have been compared against observed time series. Tables and maps have also been produced to quantify and verify the following hydrological components on both a subcatchment and quaternary catchment basis:

- Streamflow and sediment yield generation under current land use and current climate conditions,
- Streamflow and sediment yield generation under pristine (Acocks veld types) and current climate conditions,
- The impact of current land use on streamflow and sediment yield generation, and
- The impacts of projected future climate conditions.

5.3.1 STREAMFLOW GENERATION AND VERIFICATION UNDER CURRENT LAND USE CONDITIONS

Although simulations were carried out from 1950-2010, the following section presents simulated monthly flows of the Mfolozi catchment for the indicated respective verification periods only. These were compared to observed flows recorded by the following DWA weir stations:

- W2H005 (White Mfolozi River),
- W2H006 (Black Mfolozi River), and
- W2H010 and W2H032 (Combined Mfolozi River).

It should be noted here that the aim of streamflow modelling in the Mfolozi catchment was not the perfect matching of daily observed streamflow, but rather to achieve reasonable estimates of monthly runoff in order to determine peak flows as required by the Universal Soil Loss Equation in order to simulate sediment yield.

The following subsections present:

- A time series plot of observed and simulated monthly totals of daily streamflow (Figure 5-2, Figure 5-4, Figure 5-6, and Figure 5-8).

- A comparison of accumulated monthly totals of daily streamflows for observed and simulated values for water budget verification (Figure 5-3, Figure 5-5, Figure 5-7, and Figure 5-9).
- Sub-catchment summaries at the four indicated weir locations.

5.3.1.1 VERIFICATION OF STREAMFLOW OUTPUT OF WHITE MFOLOZI (W2H005) FROM ACRU MODEL

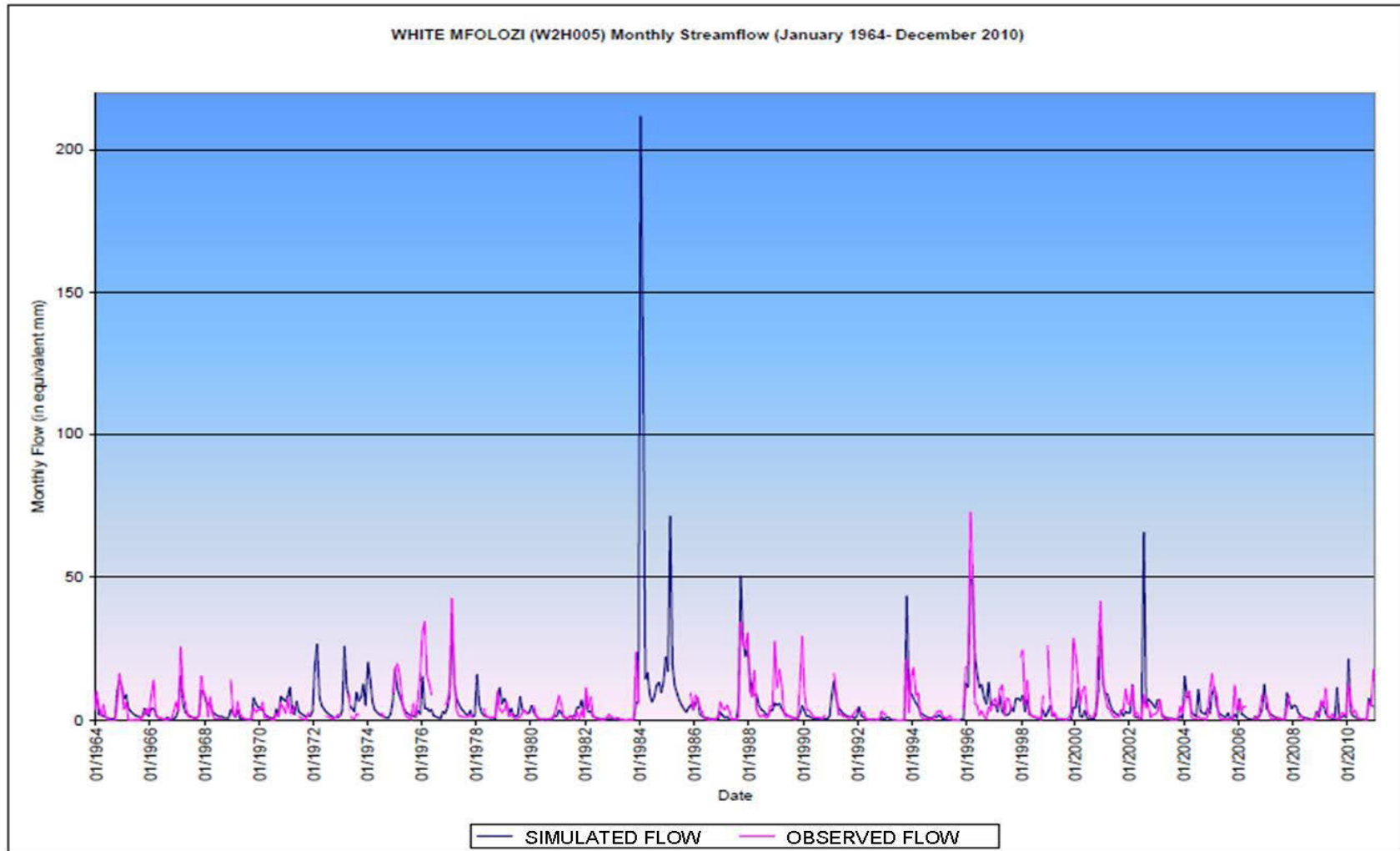


Figure 5-2: Verification flows of White Mfolozi River, 1964-2010 (weir: W2H005).

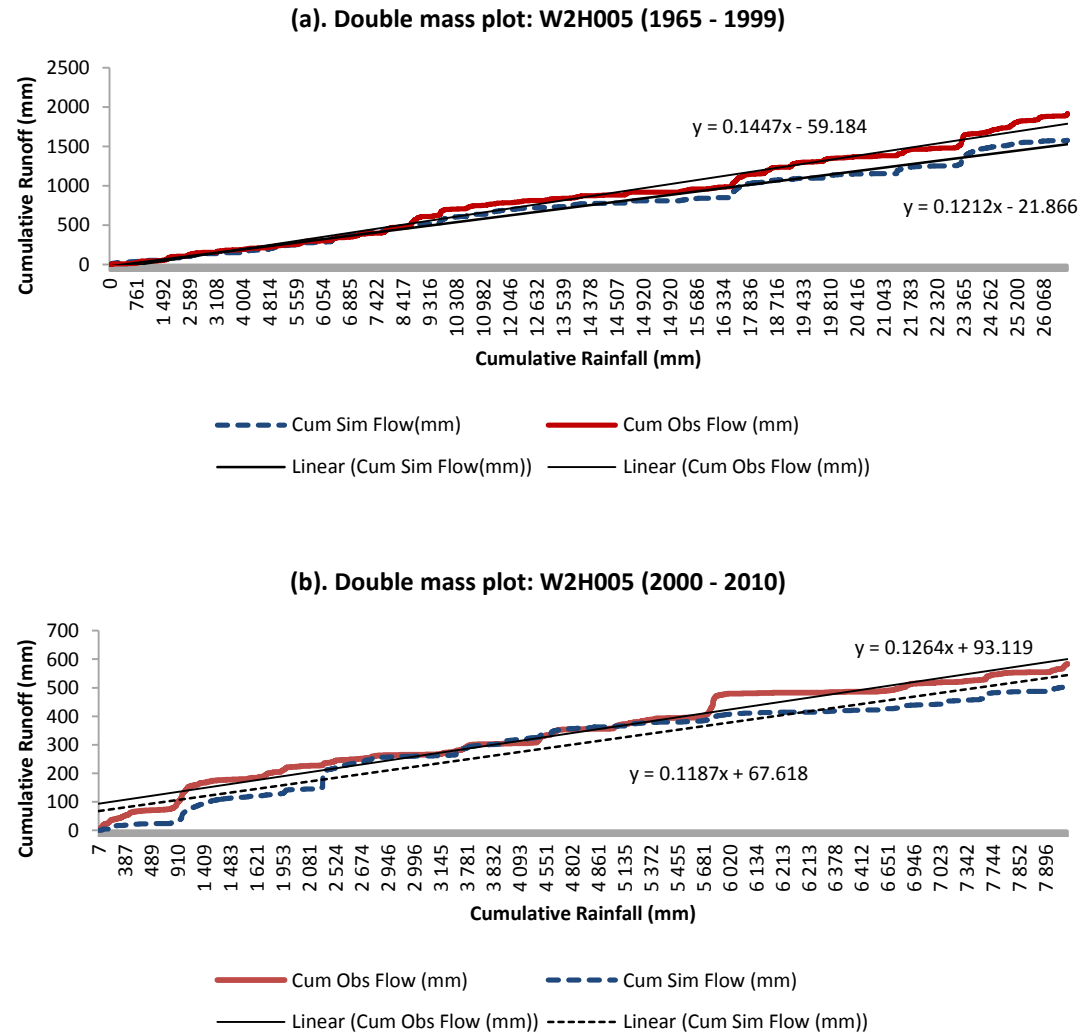


Figure 5-3: Comparison of accumulated monthly streamflows of White Mfolozi: (a). from 1964 – 1999 and (b). 2000 – 2010

5.3.1.2 VERIFICATION OF STREAMFLOW OUTPUT OF BLACK MFOLOZI (W2H006) FROM ACRU MODEL

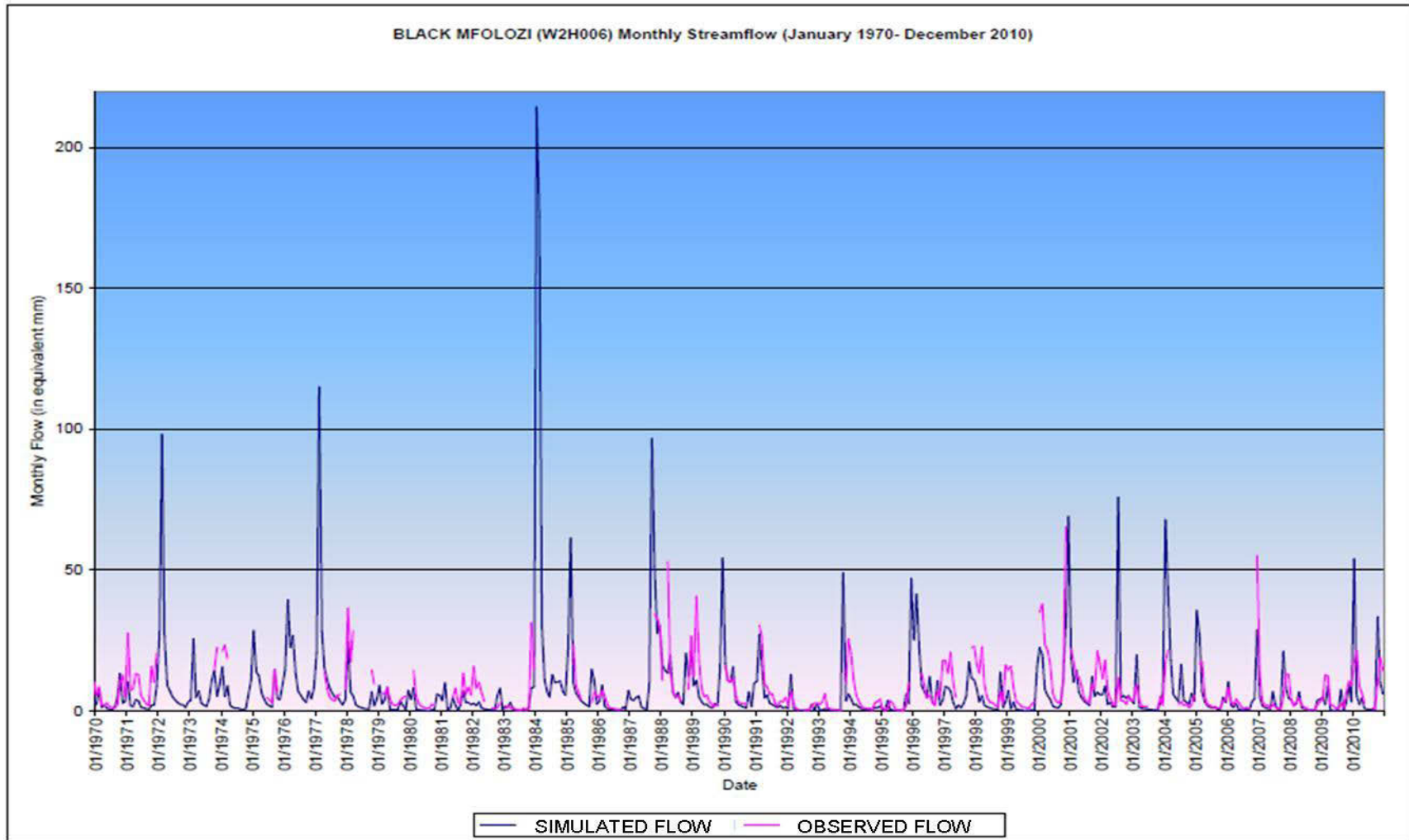


Figure 5-4: Verification flows of Black Mfolozi River, 1970-2010 (weir: W2H006).

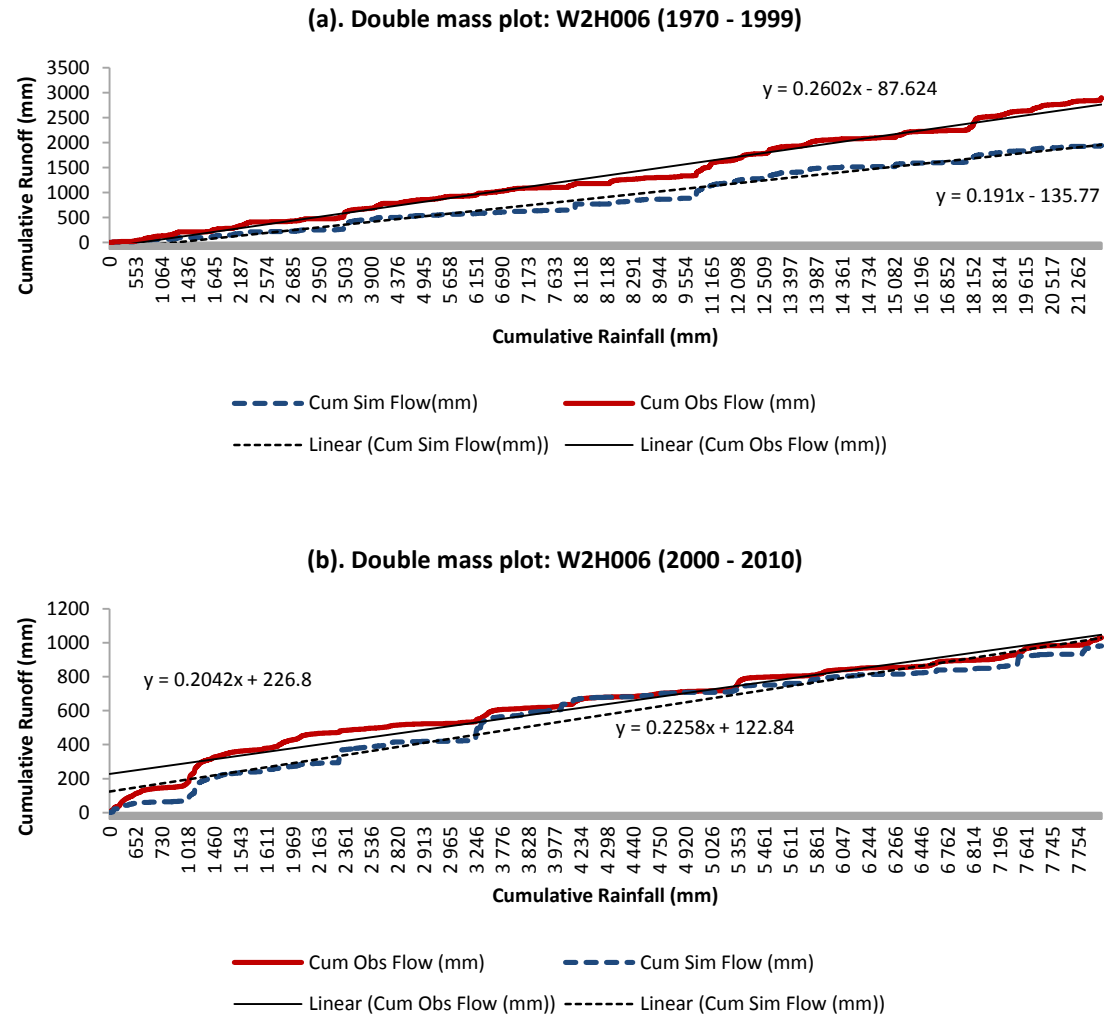


Figure 5-5: Comparison of accumulated monthly streamflows of Black Mfolozi: (a). from 1970 – 1999 and (b). 2000 – 2010

5.3.1.3 VERIFICATION OF STREAMFLOW OUTPUT OF COMBINED MFOLOZI RIVER (W2H010) FROM ACRU MODEL

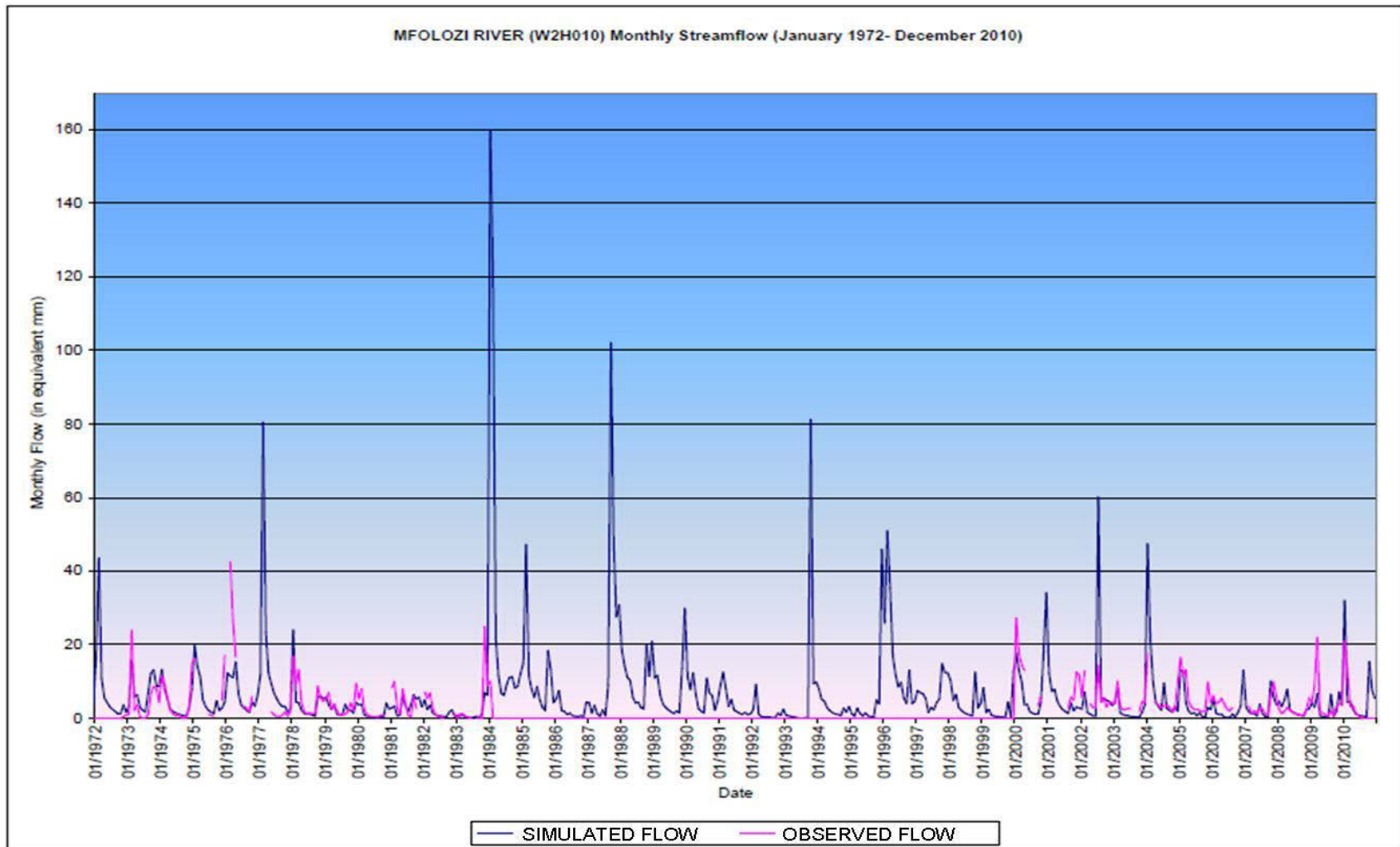


Figure 5-6: Verification flows of Mfolozi River, 1972-2010 (weir: W2H010).

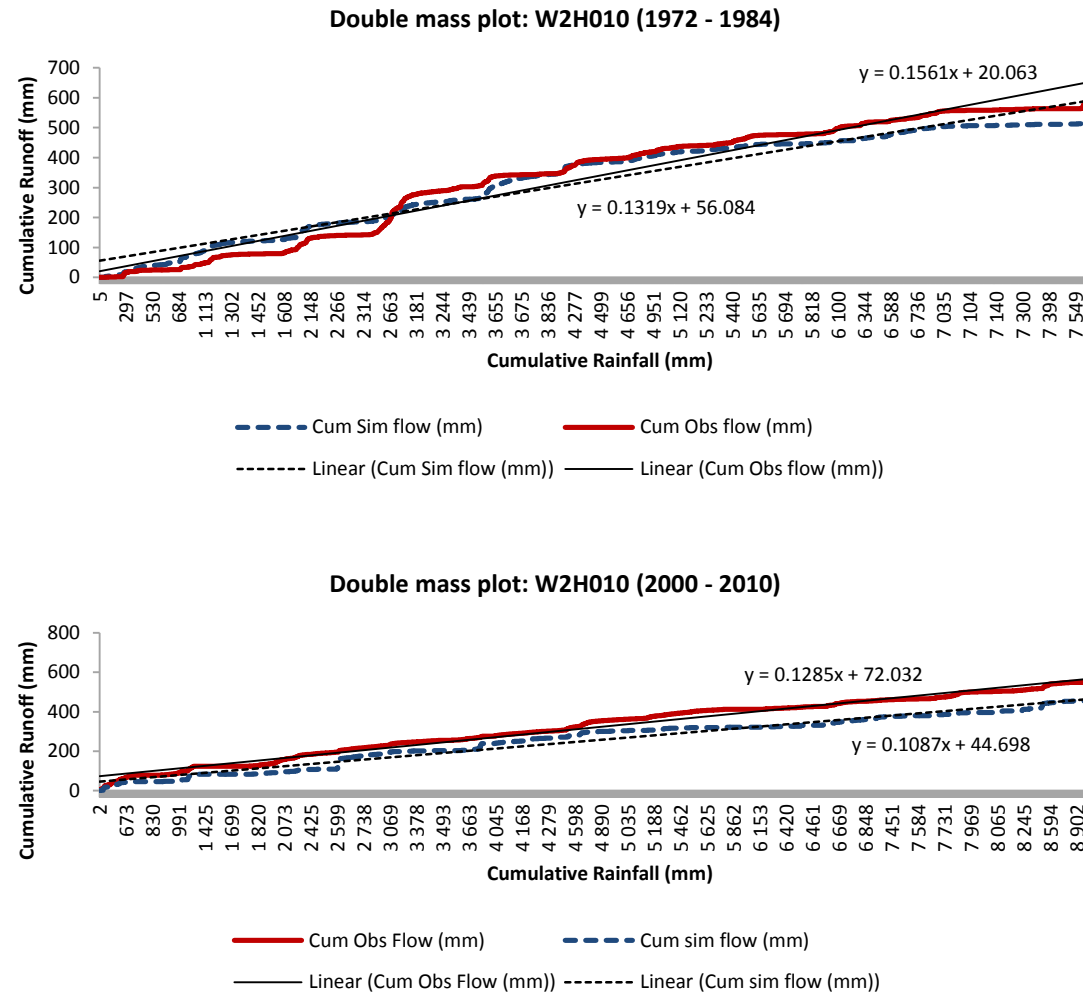


Figure 5-7: Comparison of accumulated monthly streamflows of combined Mfolozi River (Weir W2H010): (a). from 1972 – 1984 and (b). 2000 – 2010

5.3.1.4 VERIFICATION OF STREAMFLOW OUTPUT OF COMBINED MFOLOZI RIVER (W2H032) FROM ACRU MODEL

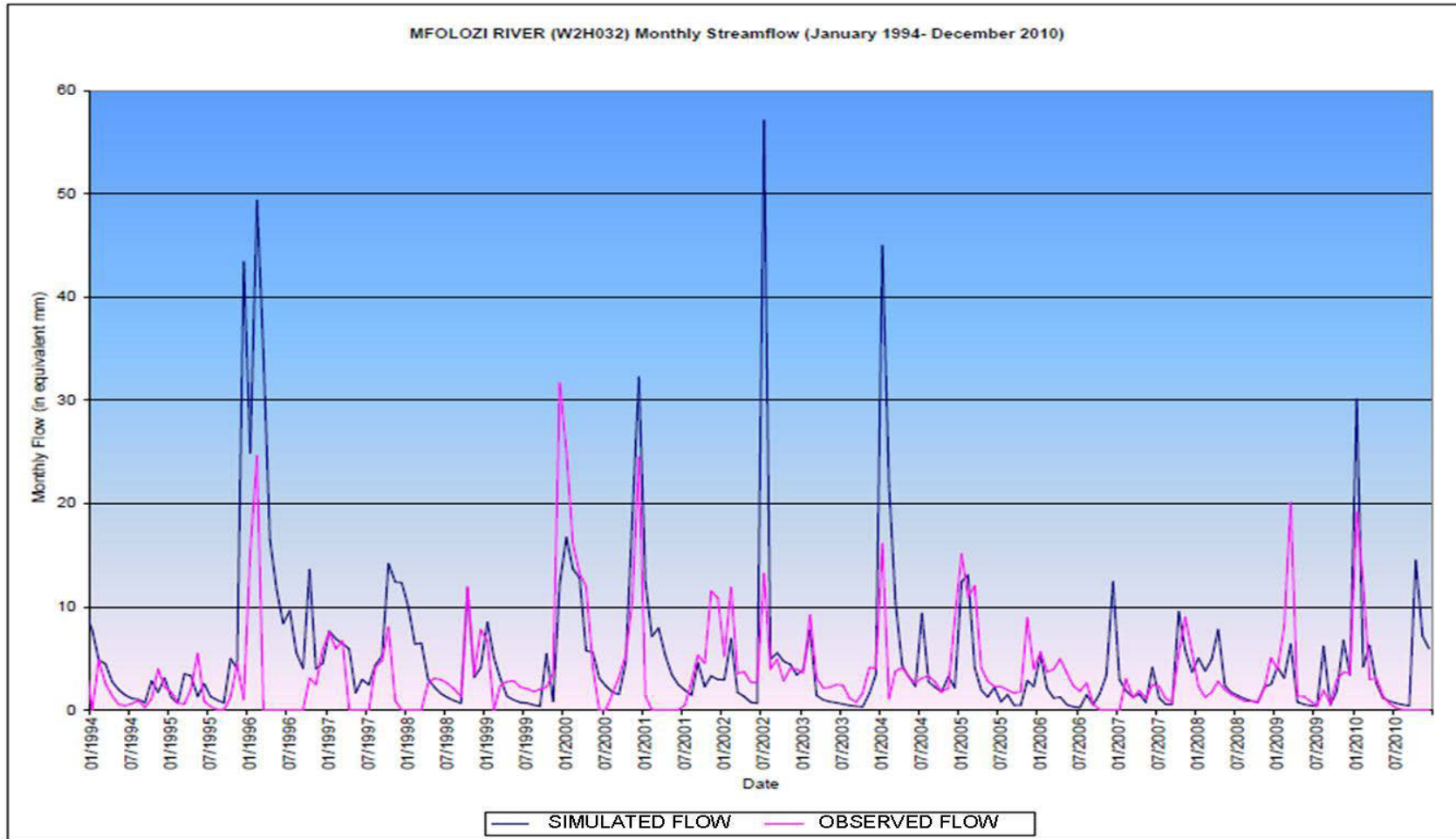


Figure 5-8: Verification flows of Mfolozi River, 1994-2010 (weir: W2H032).

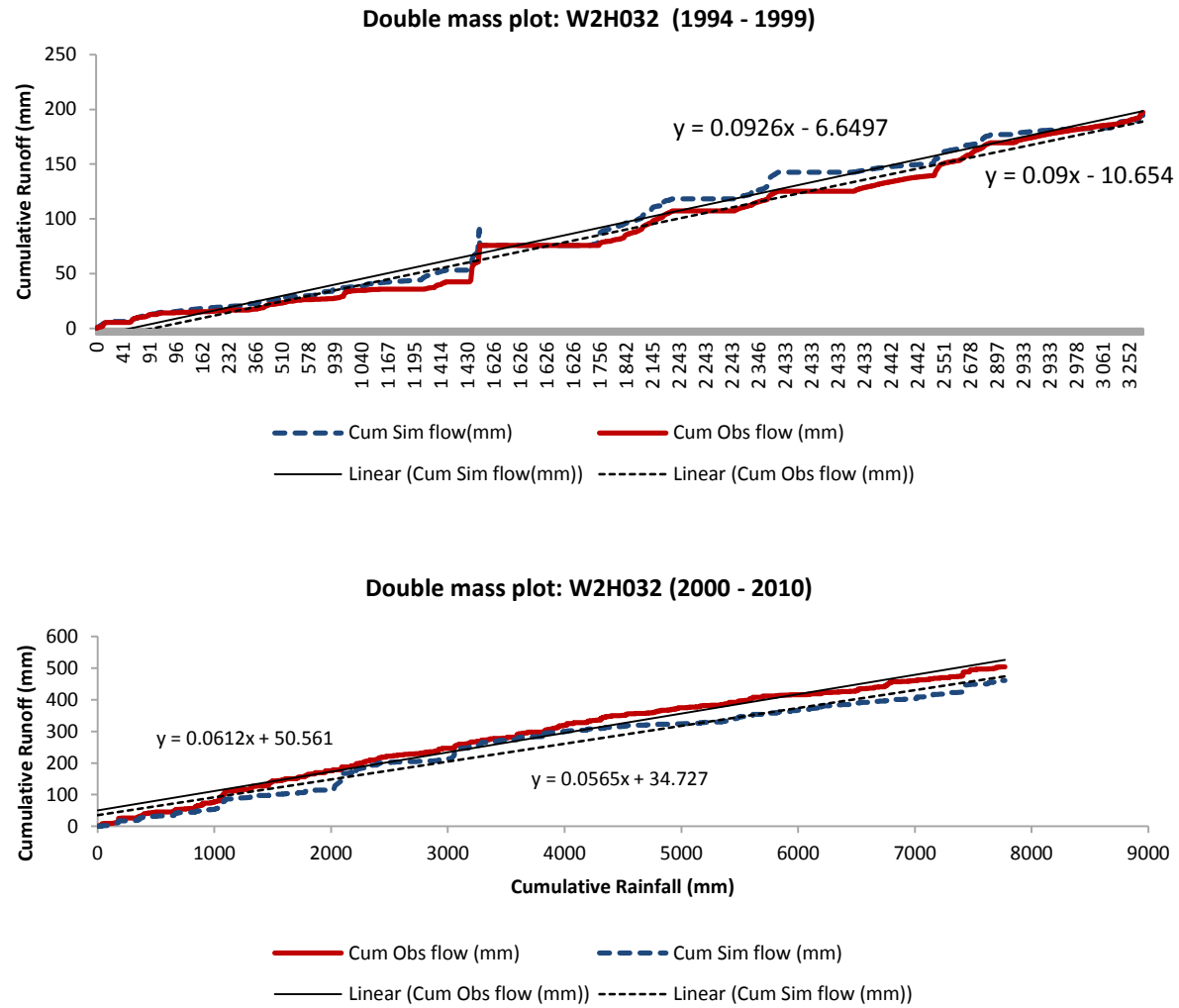


Figure 5-9: Comparison of accumulated monthly streamflows of combined Mfolozi River (Weir W2H032): (a). from 1994 – 1999 and (b). 2000 – 2010

5.3.1.5 SUMMARY OF STREAMFLOW VERIFICATION

From the above results, streamflow calibration presented simulations that reasonably fit observed flows. Further evidence of this is presented in Figure 5-10, which compares mean monthly flows from the W2H005 (White Mfolozi) and W2H006 (Black Mfolozi) weirs, as these retained the longest data record for comparison.

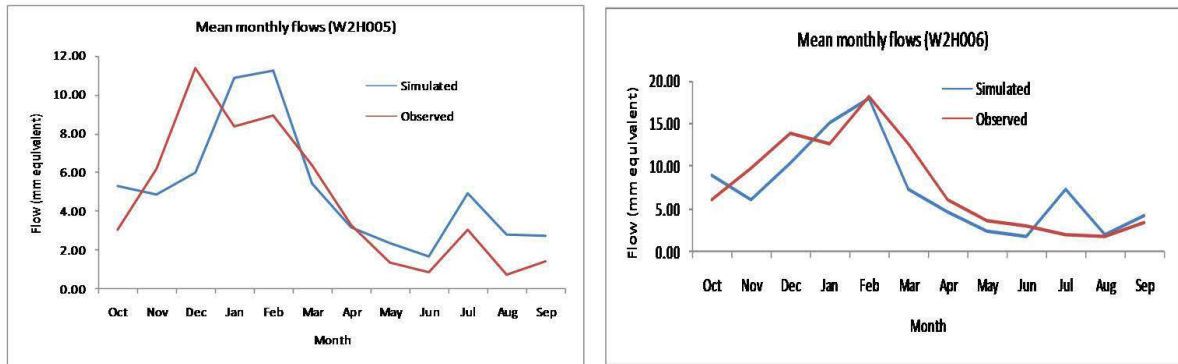


Figure 5-10: Comparison of mean monthly flows for weirs W2H005 (left) and W2H006 (right)

According to Kienzle et al. (1997) the conservation of streamflow variability is of great significance within the management of water resources and water quality simulations including those of sediment yield. Monthly comparisons of simulated against observed means generated good association, including those present during seasonal variations. Tables 5-6, 5-7, 5-8, and 5-9 summarize MAR, runoff coefficients, MAP, mean annual potential evaporation (in mm as A-Pan equivalent), as well as the land-use percentage class associated with sub-catchments upstream of their respective weir locations.

Table 5-6: MAR, runoff coefficient, contributing catchment area, MAP and mean annual potential evaporation for weir W2H005

WEIR: W2H005	observed	simulated	Land-use (%)	
			MAR (validation period)	49.4mm (195 Mm ³)
Runoff coeff. (validation period: 1965 - 2010)	13.6%	12.0%	Natural	63%
Upstream contributing catchment area	3942 km ²		Degraded	22%
Mean annual precipitation (MAP)	865mm		Agric	14%
Mean annual potential evaporation (A-Pan equivalent)	1677mm		Urban	0.95%

Table 5-7: MAR, runoff coefficient, contributing catchment area, MAP and mean annual potential evaporation for weir W2H006

WEIR: W2H006	observed	simulated	Land-use (%)	
MAR (validation period)	93.9mm (154Mm ³)	89.1mm (146Mm ³)		
Runoff coeff (validation period: 1970 - 2010)	23.2%	20.8%	Natural	77.7%
Upstream contributing catchment area	1642 km ²		Degraded	3.8%
Mean annual precipitation (MAP)	831mm		Agric	18.5%
Mean annual potential evaporation (A-Pan equivalent)	1823mm		Urban	0%

Table 5-8: MAR, runoff coefficient, contributing catchment area, MAP and mean annual potential evaporation for weir W2H010

WEIR: W2H010	observed	simulated	Land-use (%)	
MAR (validation period)	65mm (601Mm ³)	57.5mm (531Mm ³)		
Runoff coeff (validation period: 1972 - 2010)	14.2%	12.0%	Natural	70.33%
Upstream contributing catchment area	9242 km ²		Degraded	13.70%
Mean annual precipitation (MAP)	821mm		Agric	15.60%
Mean annual potential evaporation (A-Pan equivalent)	1729mm		Urban	0.37%

Table 5-9: MAR, runoff coefficient, contributing catchment area, MAP and mean annual potential evaporation for weir W2H032

WEIR: W2H032	observed	simulated	Land-use (%)	
MAR (validation period)	56.5mm (558Mm ³)	67.5mm (667Mm ³)		
Runoff coeff (validation period: 1994 - 2010)	7.7%	7.3%	Natural	66.90%
Upstream contributing catchment area	9882 km ²		Degrad.	14.40%
Mean annual precipitation (MAP)	984mm		Agric	18.40%
Mean annual potential evaporation (A-Pan equivalent)	1726mm		Urban	0.20%

5.3.2 WHERE IN THE MFOLOZI CATCHMENT IS STREAMFLOW GENERATED?

Upon successful verification of streamflow at weir locations, it is important to present mean annual runoff at both catchment and quaternary level in order to examine the distribution of variations associated with both land use and climate change. The mean annual runoff of the Mfolozi catchment (10 137 km²) for the simulation period (1950-2010) under current land-use conditions was ascertained to be 727 Mm³; compared to 729 Mm³ (Hutchinson & Pitman, 1973), 711 Mm³ (Middleton & Bailey, 2008), and 887 Mm³

(Cooper *et al.*, 1990). Under these conditions, Figure 5-11 represents the distribution of the Mfolozi MAR at quaternary level.

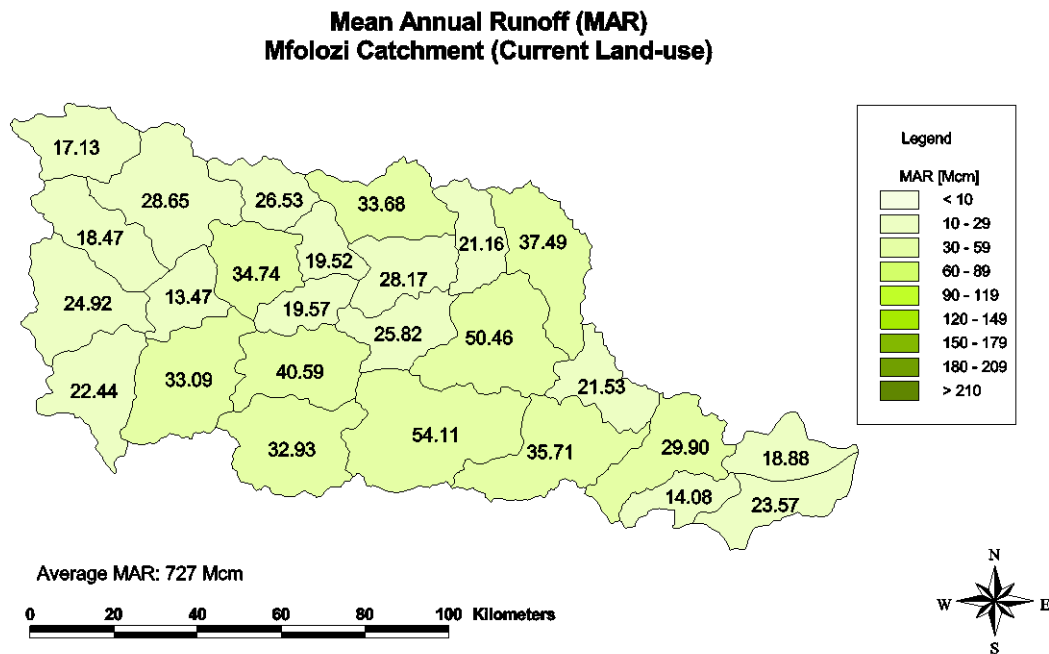


Figure 5-11: Mfolozi quaternary catchment mean annual runoff (MAR) under current land-use conditions.

Quaternary catchments with low MAR received relatively low rainfall (Figure 5-1), as is the case for quaternary catchments W21C, W21F, W21G, W21L, W22C and W22G. Quaternary catchments with low MAR and relatively high MAP were found to be under intensive agricultural or cultivation activities. These were mainly located in the floodplain of quaternaries W23B and W23D. Land-uses linked to high water demands include but are not limited to commercial plantations of pines, eucalypts, wattle, and sugarcane cultivations, most of which are present in the aforementioned quaternaries.

In contrast, quaternary catchments with high MAR and moderate or average MAP can attribute their increased flows to degraded land types. This trend emerges in W21H and W21K, as well as a combination of commercial agriculture and degraded land cover evident in W22J and W22K.

Assuming current climatic conditions, these trends within quaternary catchments raise significant concerns over the impact of changing land cover/land-use on water yields. This

is discussed in considerable detail in Section 5.5 which examines the effects of land-use change on water yields.

5.4 MODELLING SEDIMENT YIELD UNDER PRESENT LAND-USE CONDITIONS

Before proceeding into the discussion of sediment yield results, it is important to first identify quaternary catchments within the study area that are susceptible to soil erosion.

5.4.1 WHERE IN THE MFOLOZI CATCHMENT IS THE SOIL PRONE TO EROSION?

Impacts on water quality in the Mfolozi catchment begin with the detachment of soil particles from parent material. The process of soil particle detachment by raindrop impact has been reviewed in Section 3.2.1. The potential of these detached particles (soil loss potential) reaching and impacting a recipient river is reliant on the amount of detached soil and the energy of the overland flow. Although the Mfolozi catchment soil loss potential was not explicitly modelled using ACRU, the identification of areas prone to soil loss was dependent on the work carried out by Msadala *et al.* (2010), and is reproduced in Figure 5-12.

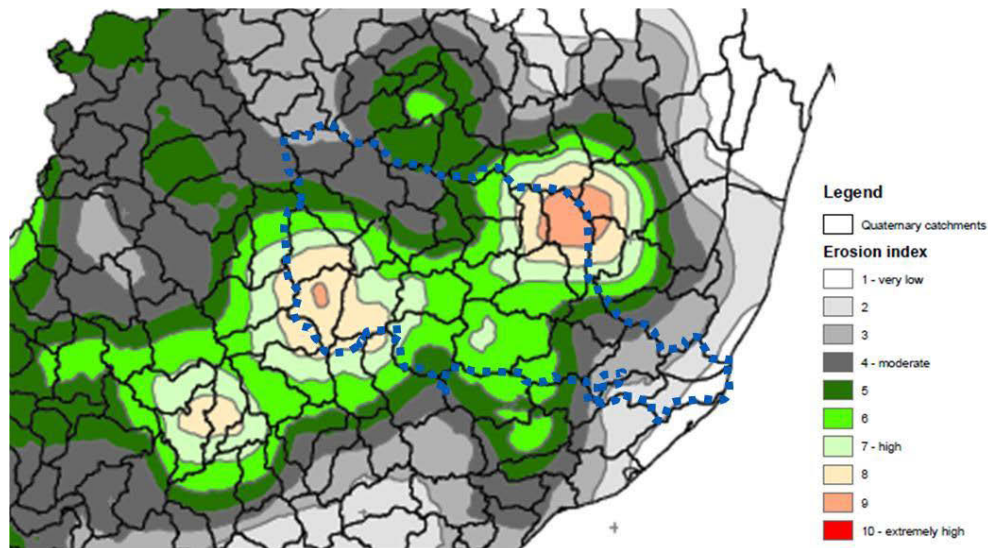


Figure 5-12: Soil erosion index by quaternary catchment - Mfolozi catchment outlined in blue (Source: Msadala *et al.*, 2010).

The St Lucia catchments lie within the two main sediment producing zones within the northern KZN region. The main distribution of moderate to extremely high sediment source areas varies centrally from the east to the west of the Mfolozi catchment covering 12 out of the 26 quaternary catchments (W21C/D/E/F/H/J/K; W22F/G/H/J/K).

It should be noted that not all of the soil particles detached from the parent material reach the river network as progressive re-entrainment and deposition of sediments may occur. Therefore, the identified quaternaries of moderate to high soil loss potential may not necessarily be the areas which yield the highest sediment loads. The ACRU model therefore estimates the daily amount of stormflow derived sediment reaching the outlet of the subcatchment allowing for the identification quaternaries with large sediment yields.

5.4.2 MFOLOZI CATCHMENT PRESENT CONDITION SEDIMENT YIELDS

The average annual simulated sediment yield (1950-2010) for the Mfolozi catchment was estimated at 156 t/km²/a; compared to 122 t/km²/a (Lindsay *et al.*, 1996), 233 t/km²/a (Rooseboom, 1975), 161 t/km²/a (Middleton & Bailey, 2008), and 61 t/km²/a (Grenfell & Ellery, 2009). The annual sediment yield time series is shown Figure 5-13. It should be noted that 28% of the total sediment yield during the simulation period was from three major flood events, namely:

- July 1963:

Between the 3rd and 4th of July 1963, large sections of the contributing catchments received exceptionally high 24 hour rainfall during which recorded rainfall exceeded 100mm. Moderate rain was measured on the days before and after the event. In some areas the daily rainfall was estimated to exceed 500mm in 24 hours.

- Jan/Feb 1984:

Cyclone Domoina at end of Jan 1984, followed by Cyclone Imboa 11 – 20 Feb, 1984. Most sub-catchment's rainfall exceeded 100mm for more than 2 or 3 days consecutively, with consecutive rainfall for 4-5 days in places. The lower reaches of the Black Mfolozi experienced relatively moderate rainfall (< 100mm/day).

- Sep 1987:

About 600mm of rainfall measured in the town of Mtubatuba.

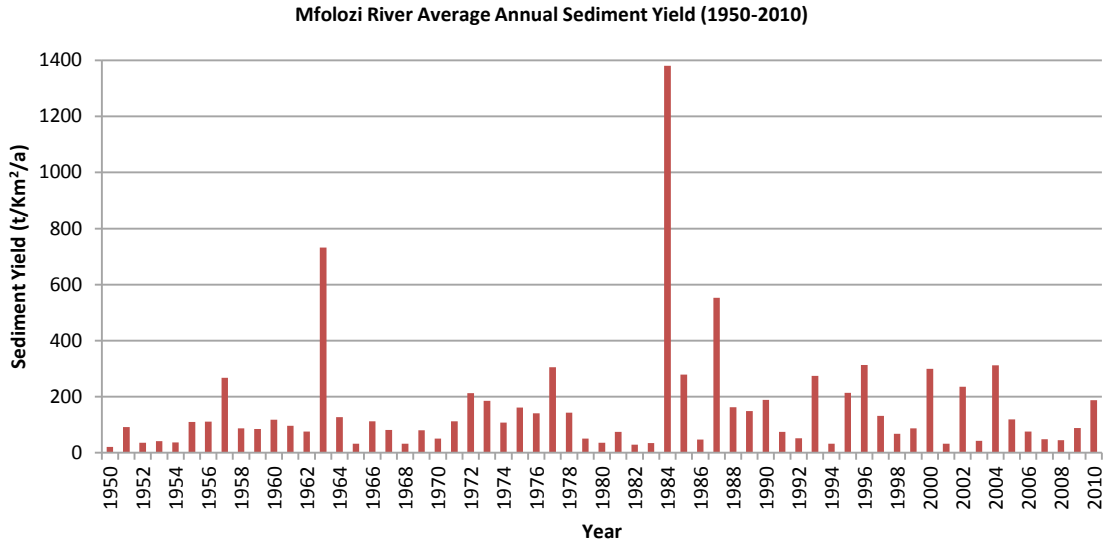


Figure 5-13: Time series showing the Mfolozi catchment average annual sediment yield (1950-2010) under current land use conditions.

Furthermore, the accumulation of the top ten annual sediment contributions accounted for 50% of the total sediment yields within the simulation period. This not only confirms the highly variable nature of Mfolozi catchment rainfall but also validates the theory that sediment yields within this catchment are highly episodic in nature.

For management of sediment loads to be effective, it is imperative that sediment yields be examined and compared at quaternary level against areas within the catchment that are prone to soil loss. Figure 5-14 presents simulated quaternary catchment average sediment yields. From this, it can be confirmed that the highest sediment yields in Mfolozi catchment do in fact occur within the same areas of potentially high sediment generation. The distribution of high sediment yields follows that outlined in Section 5.4.1, i.e. centrally from the east to the west of the catchment within the previously mentioned quaternaries.

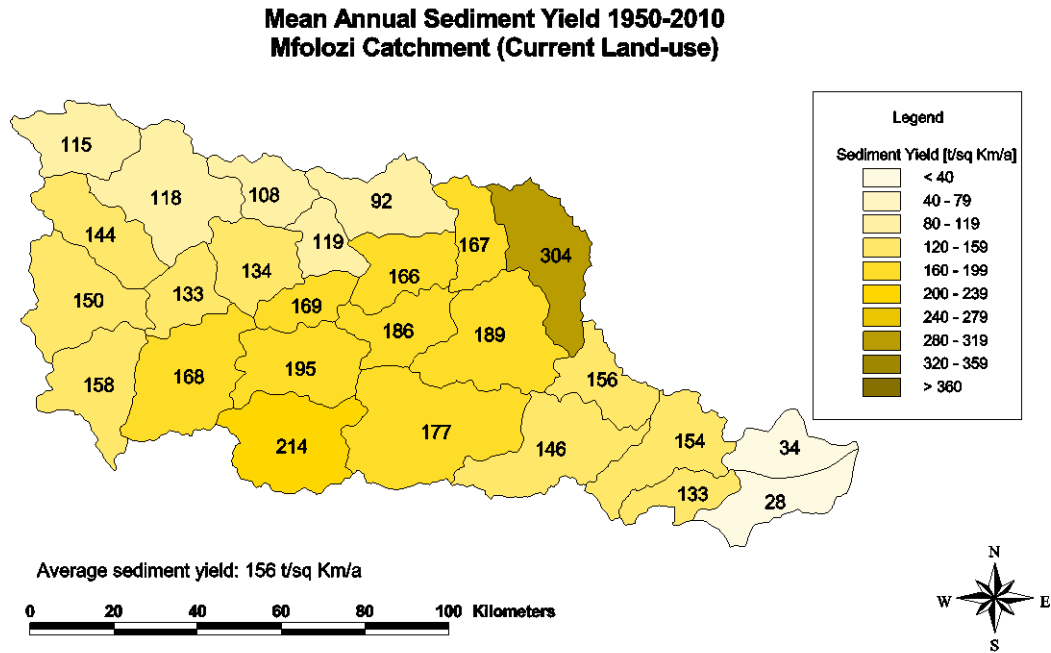


Figure 5-14: Quaternary catchment average sediment yield (1950-2010) for current land-use conditions.

5.4.3 VALIDATION OF SEDIMENT YIELDS

The main verification method used in this study involved establishing a relationship between TSS and Turbidity by directly taking field measurements between the months of March and June of 2011.

5.4.3.1 VALIDATION OF SEDIMENT YIELDS USING CALIBRATED TSS VS. TURBIDITY RELATIONSHIP

Figure 5-15 shows the strongly correlated relationship ($r^2 = 0.99$) between TSS and turbidity. Using this relationship, TSS has been indirectly derived from monitored turbidity measurements collected at the Mtubatuba water treatment works for the period 2000 – 2010.

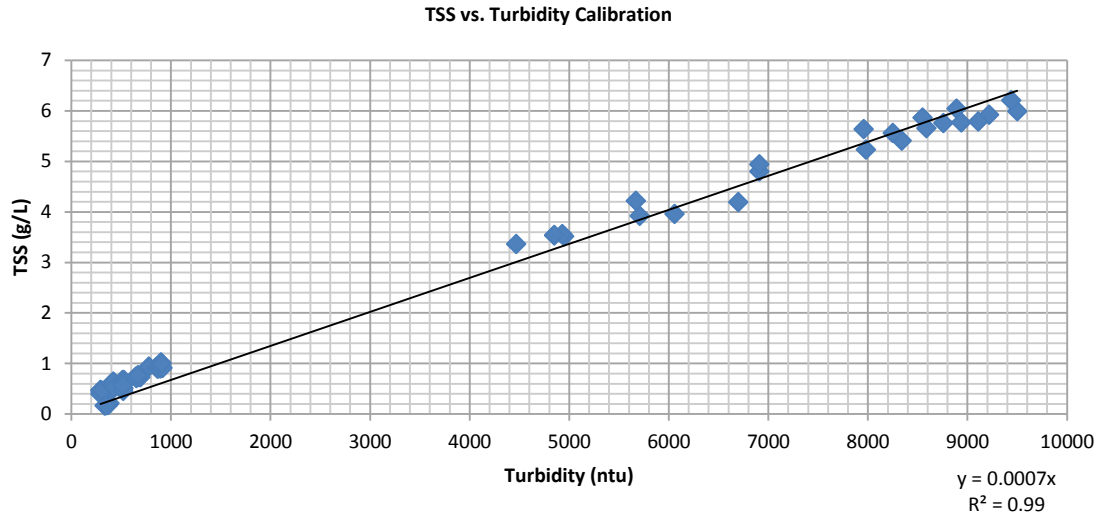


Figure 5-15: Observed relationship between TSS (g/L) and turbidity (NTU).

Using these TSS concentrations and the product of daily average streamflow measurements from weir W2H032, daily suspended sediment loads were estimated. Accumulated monthly suspended solids were increased by 20% to account for bed-load. This factor was determined by averaging measured ratios of suspended load to bed-load obtained by Grenfell & Ellery (2009). This factor is consistent with Yang (1996) who cites a river's bed-load transport rate between 5-25% of that in suspension. Sedimentary and hydrological data summary results from the Grenfell & Ellery (2009) study are given in *Appendix D*.

Figure 5-16 shows accumulated monthly simulated and observed sediment loads from 2000-2010. From Figure 5-17, it is clear that simulated and observed sediment loads within the validation period are strongly correlated ($r^2 = 0.96$).

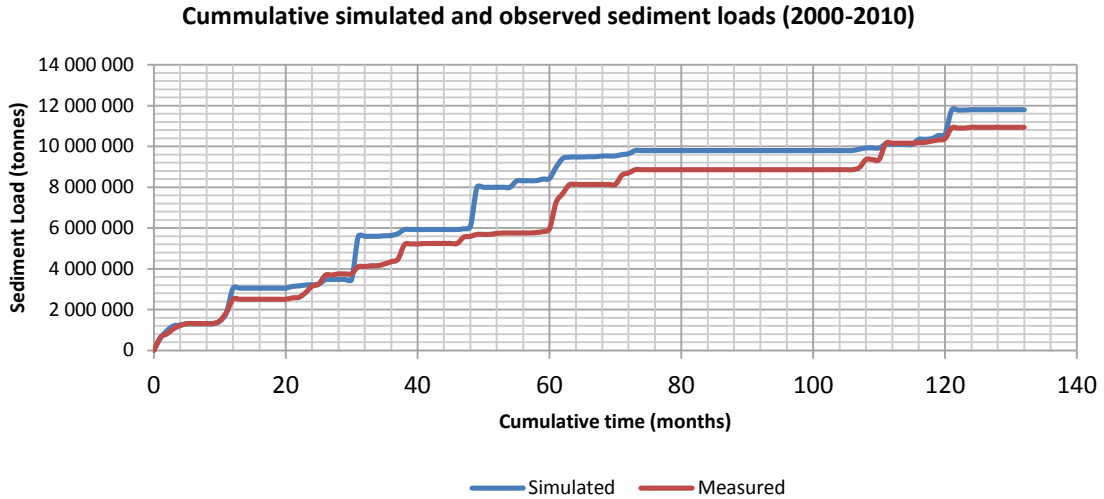


Figure 5-16: Accumulated monthly simulated and observed sediment loads (2000 – 2010).

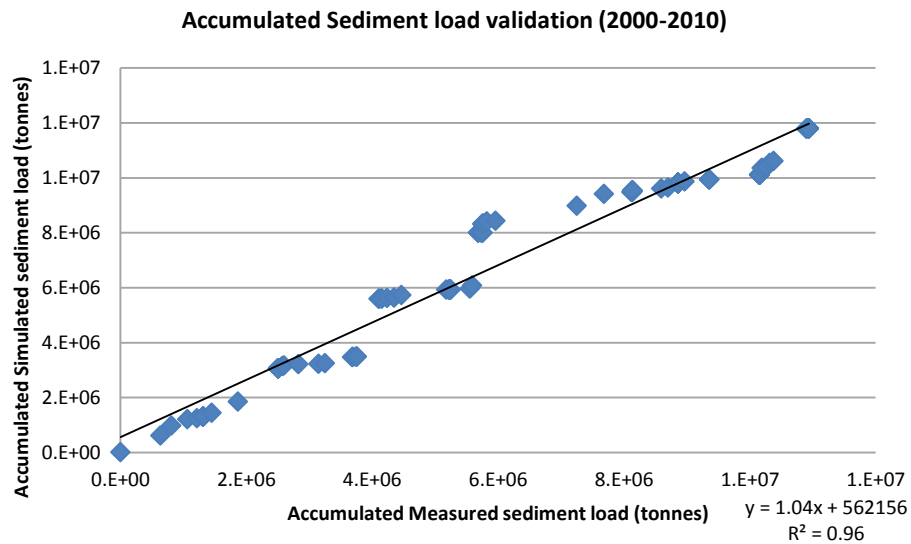


Figure 5-17: Correlation between simulated and measured sediment loads.

5.4.3.2 VALIDATION OF SIMULATED SEDIMENT YIELDS AGAINST PUBLISHED REPORTS

The WR2005 database is one of the most comprehensive hydrological databases within South Africa. Sediment yield results from this database are based on the Rooseboom *et al.* (1992) study. Figure 5-18 compares quaternary catchment sediment yields from the ACRU simulation with the sediment yields estimated by Rooseboom (1992) in the *WR90/2005* studies (Midgley *et al.*, 1994; Middleton & Bailey, 2008).

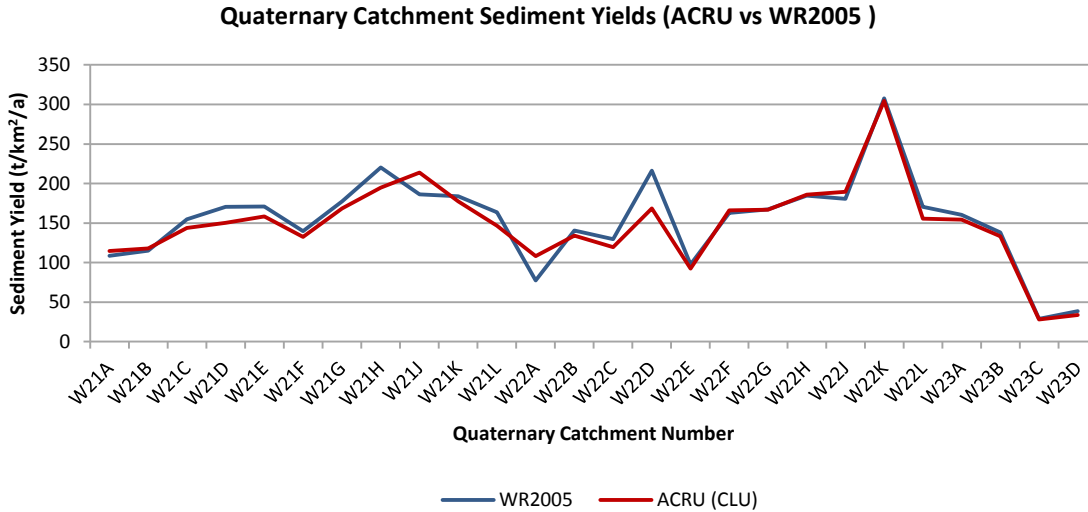


Figure 5-18: Comparison of quaternary catchment sediment yield (ACRU vs. WR2005)

From Figure 5-19, the results are strongly correlated ($r^2 = 0.93$) with simulated annual average sediment yields for each quaternary agreeing within 20%. The accumulated sediment yield from the whole catchment agreed to within 5%.

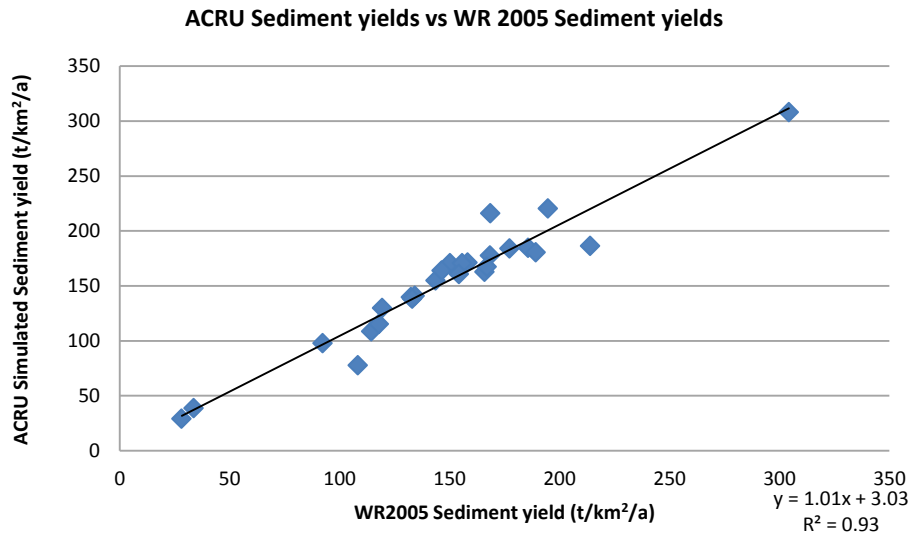


Figure 5-19: Correlation between simulated ACRU quaternary sediment yields and WR2005 sediment yields.

Measuring reservoir sedimentation is another way of validating sediment yields. The Klipfontein Dam is the only reservoir within the study area located at the bottom of quaternary catchment W21A. The dam has final adopted sediment yield of 121 t/km²/a (Msadala *et al.*, 2010). The ACRU simulation agrees within 5% of this at 115 t/km²/a,

confirming the accuracy of the model. The validation graph from the Msadala *et al.* (2010) study is given in *Appendix D*.

Monthly distribution of average flows and suspended sediment loads for the Mfolozi derived from direct turbidity measurements (2000-2010) by the Mtubatuba water works are shown in Figure 5-20. For typical runoff conditions, sediment concentrations are highest during the months from November to April, with much lower values during the dry season from May to October.

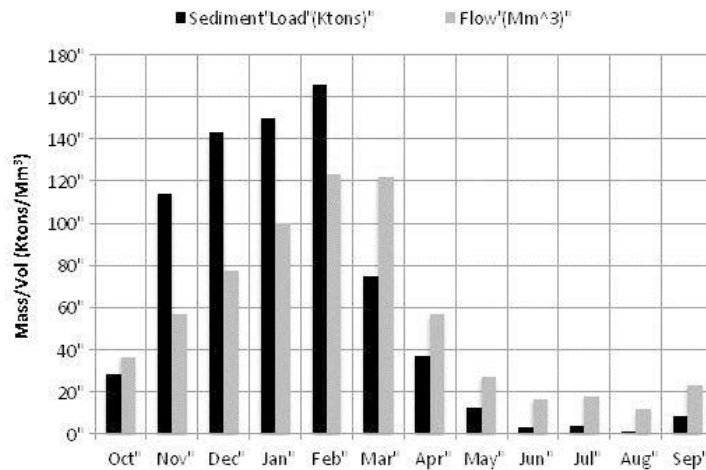


Figure 5-20: Monthly averaged flows and suspended sediment loads in the Mfolozi based on measured suspended sediment concentrations

By applying these average sediment concentrations with the modified Pitman model by Stretch *et al.* (2012) calibrated for the period 2000-2010, average annual sediment loads of the ACRU model and modified Pitman model (1950-2010) are compared in Figure 5-21. The models were found to reasonably agree, with the exception of the large sediment load for 1963 that was not picked up by the Stretch *et al.*, (2012) model. This can be attributed to the fact that the flooding event of 1963 occurred during out of season rainfall (July) and the modified Pitman model used the monthly averaged value of sediment concentration shown in Figure 5-20.

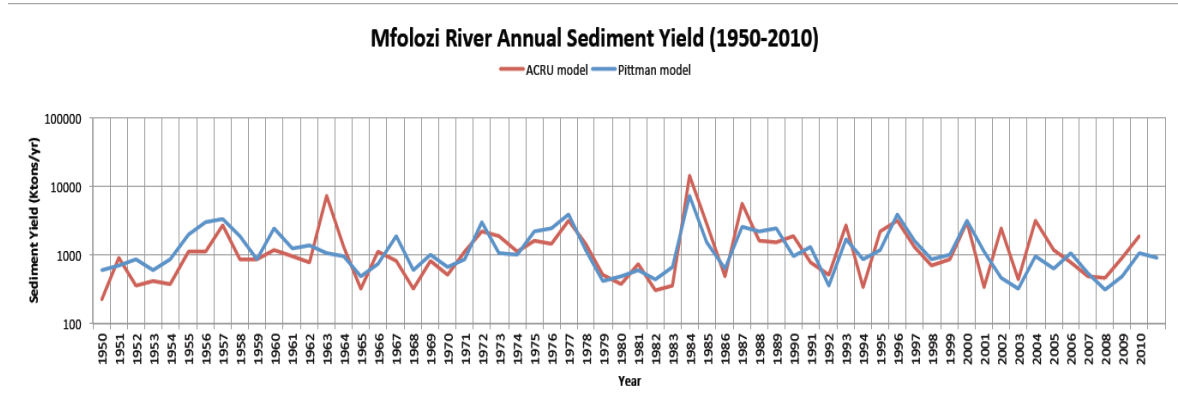


Figure 5-21: Comparison of Mfolozi catchment annual sediment loads (ACRU simulations vs. modified Pitman model by Stretch *et al.*, 2012).

5.4.4 DISCUSSION ON LONG-TERM MONTHLY VARIATION IN DISCHARGE AND SEDIMENT CONCENTRATION

The Mfolozi catchment illustrated highly variable and seasonal characteristics of suspended sediment loads and discharge. Further evidence of this is presented in Figure 5-22 and Figure 5-23, which show the simulated time series of monthly suspended concentrations together with discharge. Suspended sediment concentrations were highest following flood events mentioned in Section 5.4.2, further exemplifying the episodic occurrence of high sediment concentrations/yields. Simulation results further suggest that peak monthly averaged sediment concentrations during flood events exceed 7 kg/m^3 (7 g/L) or 10 000 NTU, as outlined in Figure 5-22 and Figure 5-23.

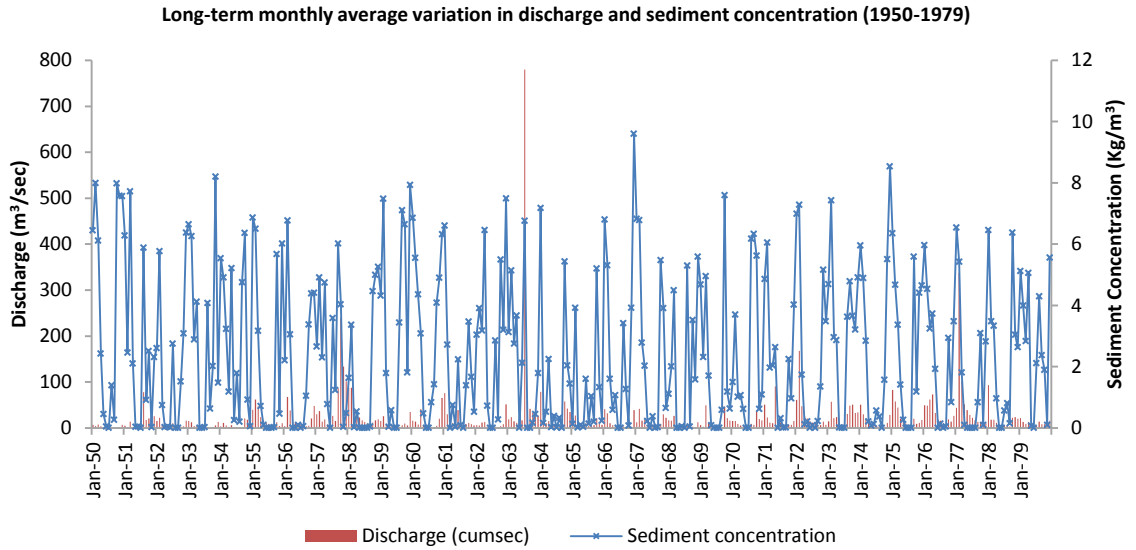


Figure 5-22: Monthly time series of discharge and suspended sediment concentrations for the period 1950-1979 for the Mfolozi catchment.

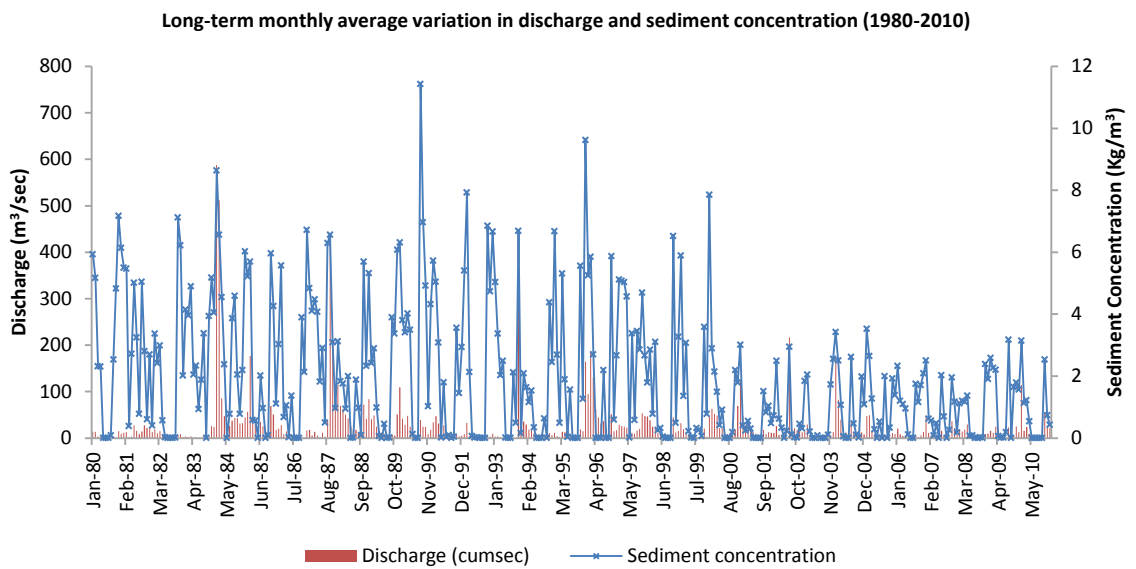


Figure 5-23: Monthly time series of discharge and suspended sediment concentrations for the period 1980-2010 for the Mfolozi catchment.

The reduction in both sediment concentration and discharge from the year 2000 can be attributed to the onset of drought, as shown in Figure 5-24.

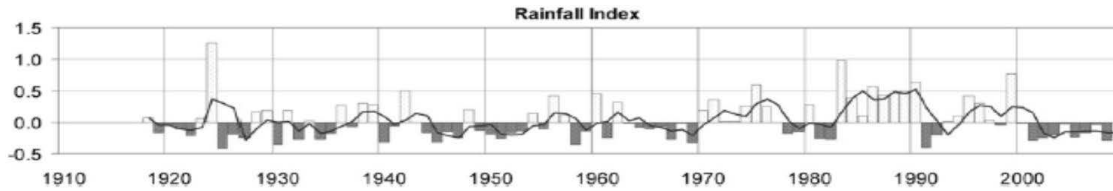


Figure 5-24: Lake St. Lucia catchments rainfall index (Source: Lawrie & Stretch, 2011).

From the above discussion, it is clear that Grenfell & Ellery (2009) have significantly underestimated the Mfolozi catchment sediment yield ($61 \text{ t/km}^2/\text{a}$). Their study was confined within the drought period (2000-2006) and did not take into account any significant flood events, and hence has not considered or analyzed the episodic nature of sediment yield within the Mfolozi catchment.

5.5 HYDROLOGICAL IMPACTS OF PRESENT LAND-USES ON PRISTINE STREAMFLOWS AND SEDIMENT YIELDS

Before proceeding into evaluating impacts of present land-uses on pristine streamflows and sediment yields, it is imperative to categorize and identify how much of the study area has actually changed from natural or virgin conditions. At catchment level, the Mfolozi has undergone a 33% change from natural conditions. Of this, 18% is attributed to agricultural developments, 14% to land degradation, and 0.2% to urban developments (the town of Vryheid in W21A). Figure 5-25 illustrates land-use distribution for the Mfolozi Catchment into the following national land-cover classes aggregated into *Agriculture*, *Degraded*, *Natural* and *Urban* categories. Details of each land cover class are presented in *Appendix B* and *Appendix C*.

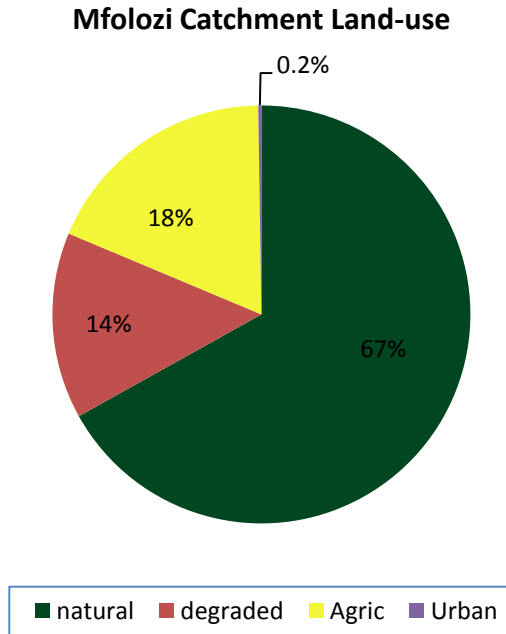


Figure 5-25: Mfolozi Catchment land-cover characteristics.

This can further be disaggregated by quaternary catchment in order to isolate areas of increased changes, given below in Figure 5-26.

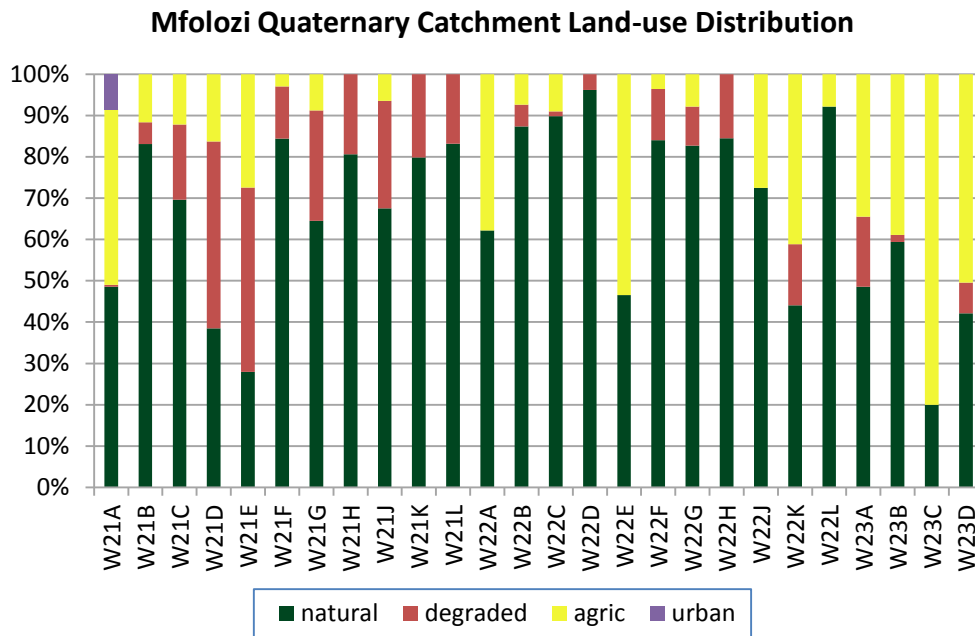


Figure 5-26: Mfolozi Quaternary Catchment land-use distribution.

5.5.1 EVALUATING IMPACTS OF PRESENT LAND USES ON PRISTINE STREAMFLOWS

Impacts of present land-use are considered by comparing streamflows generated under present land covers (NLC, 2005) and under natural (Acocks, 1988) veld types. For comparison purposes, Figure 5-27 presents the distribution of pristine MAR of the Mfolozi catchment at quaternary level (Figure 5-27a) and the impact of present land use as a percentage change (Figure 5-27b). Streamflow response to a 33% change in land-use from pristine to current conditions resulted in a 38% reduction in catchment MAR (i.e. from 1183 Mm³ to 727 Mm³).

There is no method involving experimental data to verify the result for pristine MAR. In this case it is presumed that the result achieved is reasonable when it is evaluated against the following: 1064 Mm³ (Midgley & Pitman, 1964), 1044 Mm³ (H.R.U., 1966), 746 Mm³ (Hutchison & Pitman, 1973), 972 Mm³ (Midgley *et al.*, 1994), and 911 Mm³ (Middleton & Bailey, 2008).

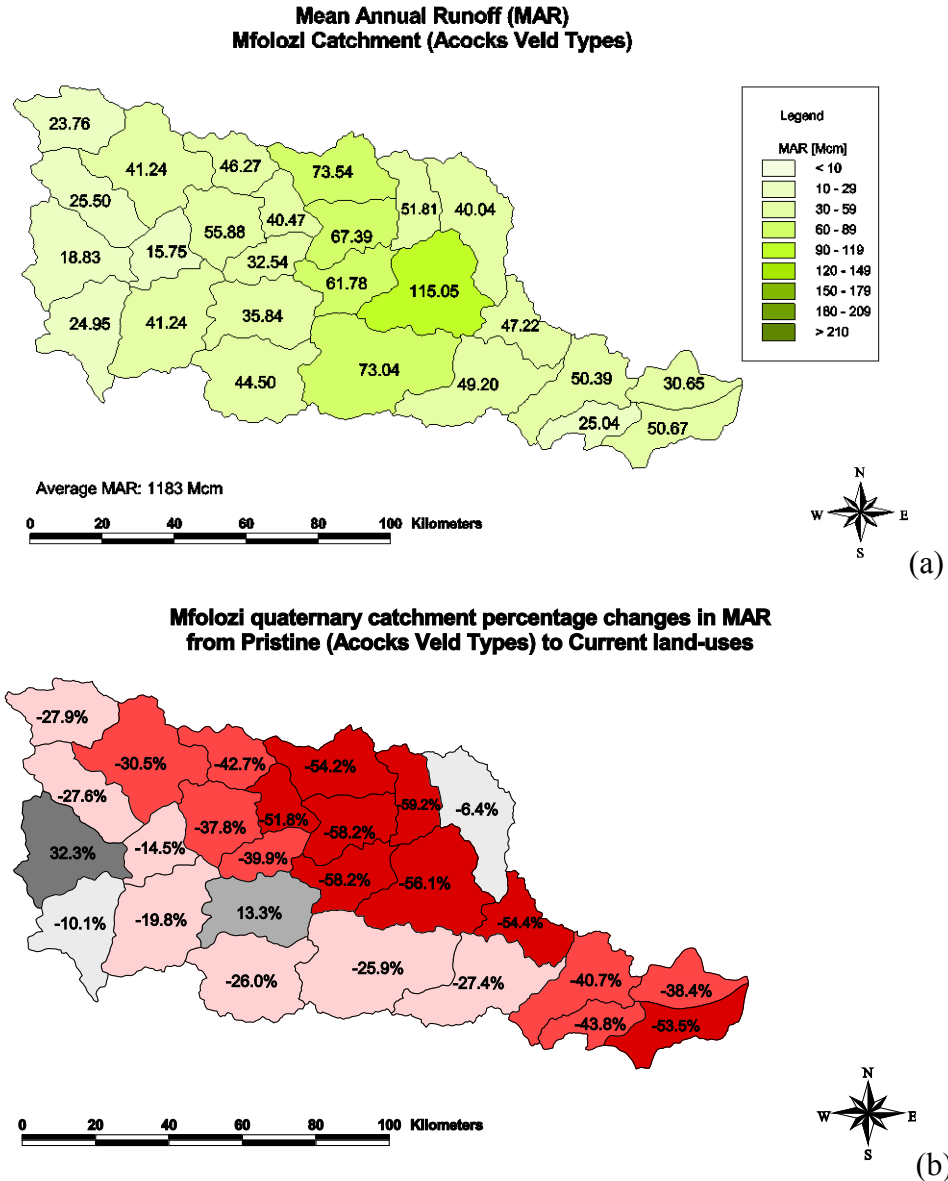


Figure 5-27: (a) Mfolozi quaternary catchment mean annual runoff (MAR) under pristine conditions; (b) changes in quaternary catchment MAR as a percentage change.

From this and Figure 5-28, it is clear that a comparison of current land-use with natural land-use streamflows can be significant within individual quaternary catchments, ranging from a 32% increase in streamflows to a 58% reduction. The highest streamflow reductions were found in quaternary catchments which were under intense agricultural use. Specifically, quaternary catchments with a high proportion of commercial forest or sugarcane plantations showed evidence of high reductions in water yields of about 60%. These included W21L, W22E, W22J, as well as the lower Mfolozi quaternary catchments

of W23A, W23B, W23C, and W23D. On the contrary, the quaternary catchments of W21D and W21H can attribute their water yield enhancements to large proportions of land degradation.

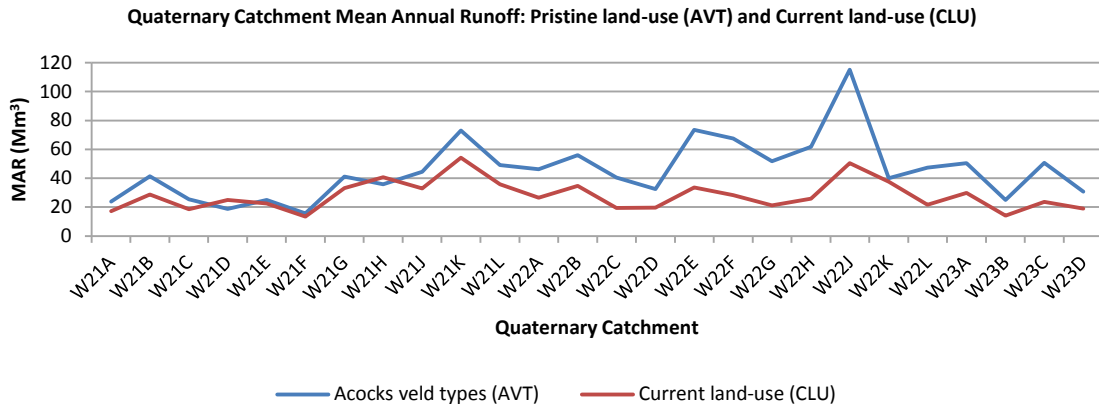


Figure 5-28: Comparison of present and pristine quaternary water yields of the Mfolozi catchment.

In a South African perspective, the performance the ACRU simulations discussed above were consistent with results obtained in Kienzle *et al.* (1997) on a study of the Mgeni catchment (4387 Km²). Re-plotting their results, an overall reduction in catchment MAR of 23% was noted from a 40% change in land-use from natural conditions. The highest sub-catchment (quaternary) MAR reductions were in the order of 60% and were mainly due to abstractions, commercial cultivations, and forest plantations.

5.5.2 EVALUATING IMPACTS OF PRESENT LAND USES ON PRISTINE SEDIMENT YIELDS

Long term records of suspended loads can provide key evidence for evaluating recent variations in the Mfolozi catchment sediment yield. However, these records are at times incomplete, and certainly do not date back to periods unaffected by human habitation. Acocks (1988) veld types have become the accepted standard when describing land-use in the unaffected state. Using these as a baseline the Mfolozi catchment average annual sediment yield in the unaffected state for the period 1950-2010 was simulated at 102 t/km²/a. Figure 5-29 compares the affected (current land-use) with the unaffected (natural land-covers) sediment yield annual time series of the Mfolozi catchment.

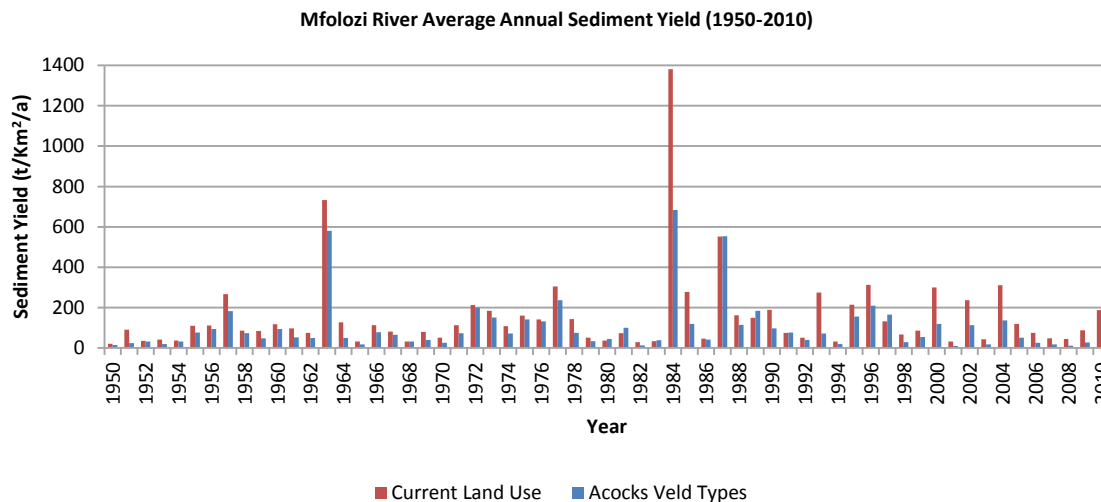


Figure 5-29: Time series of average annual sediment yields (1950-2010) for the Mfolozi catchment.

Simulations indicate a 53% increase in sediment yield from unaffected to affected catchment conditions. The sediment yield contribution from each quaternary catchment is shown in Figure 5-30.

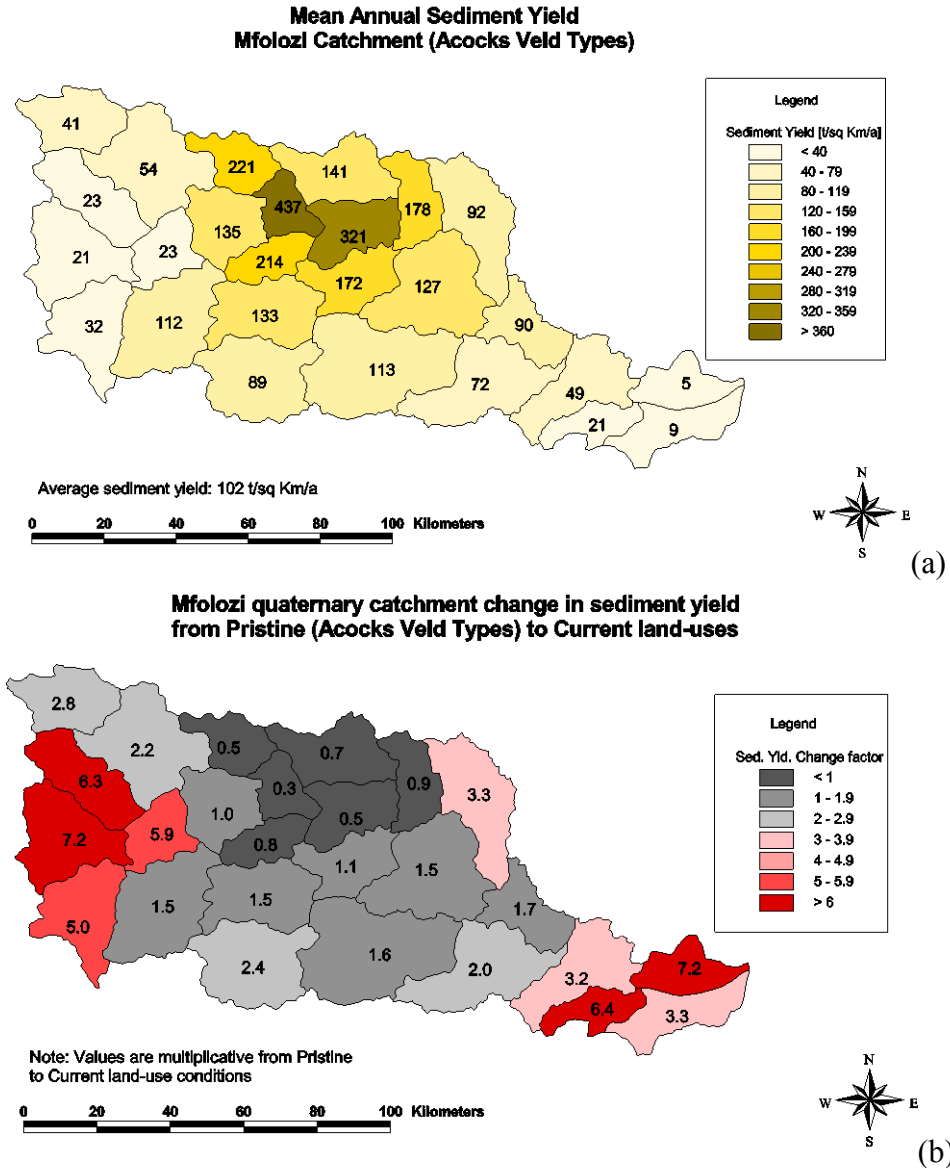


Figure 5-30: (a) Mfolozi quaternary catchment average annual sediment yield under pristine conditions; (b) changes in quaternary catchment sediment yield as a multiplicative factor from pristine to current conditions.

By examining Figure 5-30, the highest gains in sediment yield were found in the western quaternaries of W21C, W21D, W21E, & W21F, as well as the eastern quaternaries of W23B & W23D. Large areas of degraded land-uses within the western quaternaries are responsible for increased sediment yield. This is confirmed in Figure 5-31, which shows the distribution of erosion gullies as mapped by Le Roux *et al.* (2010). The highest concentration of erosion gullies is located in the quaternary catchment of W21D, which underwent an increase in sediment yield of over 600% (or multiplicative factor of 7.2) from unaffected conditions.

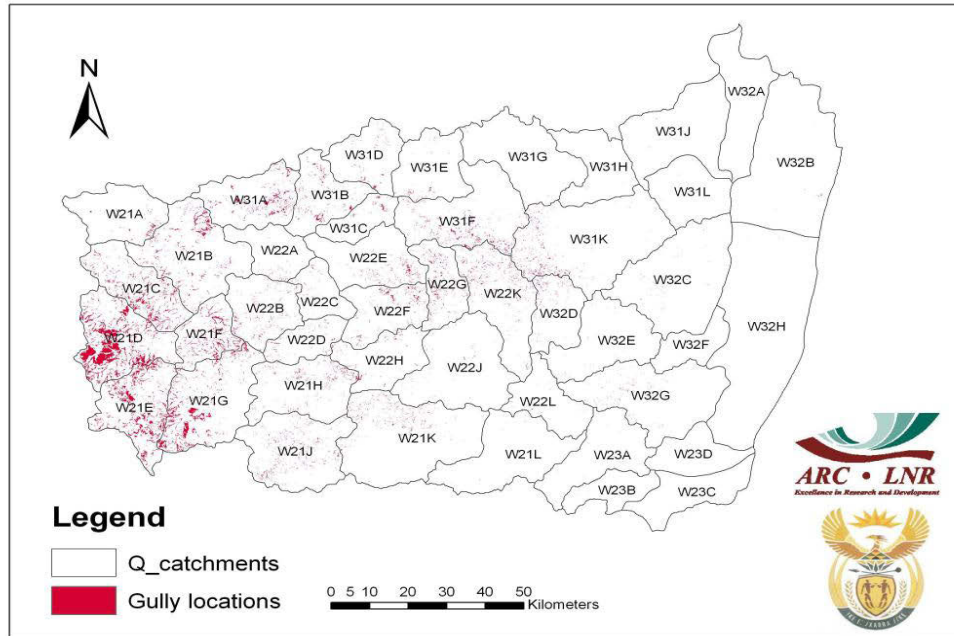


Figure 5-31: Distribution of erosion gullies in the Lake St. Lucia catchments (Source: Le Roux, *et al.*, 2010).

Conversely, increased commercial forest and sugarcane plantations are responsible for the increased sediment yield found in the eastern quaternary catchments located in the coastal flood plain of quaternaries W23B and W23D. The underlying cause of which is the exposure of soil surface due to reduced canopy cover.

5.5.3 SUMMARY OF HYDROLOGICAL RESPONSES DUE TO LAND-USE CHANGES

For the 26 quaternary catchments of the Mfolozi catchment, Table 5-10, Table 5-11, and Table 5-12 present mean annual runoff, runoff coefficients for both pristine and present land-use scenarios, together with streamflow changes, selected quaternary catchment information, and climatic variables.

Table 5-10: Hydrological characteristics of the White Mfolozi Catchment

White Mfolozi	W21A	W21B	W21C	W21D	W21E	W21F	W21G	W21H	W21J	W21K	W21L
ACRU Sub-catchments	1-38	39-73	74-106	107-141	142-166	167-193	194-218	219-247	248-276	277-306	307-334
AREA (km ²)	343.9	587.1	373.7	473.8	420.6	245.6	569.4	438.2	536.6	808.2	540.5
Mean Altitude (m)	1344	1243	1110	1151	1201	990	1070	886	897	561	310
MAP (mm)	905	839	766	738	754	724	753	811	855	801	714
MAPE ¹ (mm)	1717	1740	1762	1767	1652	1766	1685	1711	1725	1681	1711
MATE ² (mm)	739	697	648	624	643	587	614	620	650	621	508
Pristine MAR (Mm ³)	23.76	41.24	25.50	18.83	24.95	15.75	41.24	35.84	44.50	73.04	49.20
Present MAR (1950-2010) (Mm ³)	17.13	28.65	18.47	24.92	22.44	13.47	33.09	40.59	32.93	54.11	35.71
Pristine R-C ³ (MAR/MAP)	7.6%	8.4%	8.9%	5.4%	7.9%	8.9%	9.6%	10.1%	9.7%	11.3%	12.7%
Present R-C ³ (1950-2010) (MAR/MAP)	5.5%	5.8%	6.5%	7.1%	7.1%	7.6%	7.7%	11.4%	7.2%	8.4%	9.3%
Streamflow change (%)	-27.9%	-30.5%	-27.6%	32.3%	-10.1%	-14.5%	-19.8%	13.3%	-26.0%	-25.9%	-27.4%
Pristine Sediment Yield (t/Km ² /a)	41	54	23	21	32	23	112	133	89	113	72
Present Sediment Yield (t/Km ² /a)	115	118	144	150	158	133	168	195	214	177	146
Change in Sediment Yield (CLU/AVT)	2.8	2.2	6.3	7.1	4.9	5.8	1.5	1.5	2.4	1.6	2.0

¹ Mean annual potential evaporation (A-Pan equivalent)

² Mean annual total (actual) evaporation

³ Runoff coefficient

Table 5-11: Hydrological characteristics of the Black Mfolozi Catchment

Black Mfolozi	W22A	W22B	W22C	W22D	W22E	W22F	W22G	W22H	W22J	W22K	W22L
ACRU Sub-catchments	335-363	364-394	395-420	421-438	439-468	469-493	494-514	515-539	540-572	573-602	603-624
AREA (km ²)	241.7	335.7	188.0	200.0	390.5	316.2	252.8	310.2	613.4	482.4	283.5
Mean Altitude (m)	1132	911	870	832	852	633	550	596	415	449	274
MAP (mm)	995	860	908	802	961	819	744	764	756	734	707
MAPE ¹ (mm)	1618	1708	1653	1671	1675	1774	1785	1712	1732	1751	1718
MATE ² (mm)	787	685	702	612	612	644	594	603	600	578	504
Pristine MAR (Mm ³)	46.27	55.88	40.47	32.54	73.54	67.39	51.81	61.78	115.05	40.04	47.22
Present MAR (1950-2010) (Mm ³)	26.53	34.74	19.52	19.57	33.68	28.17	21.16	25.82	50.46	37.49	21.53
Pristine R-C ³ (MAR/MAP)	19.2%	19.4%	23.7%	20.3%	19.6%	26.0%	27.5%	26.1%	24.8%	11.3%	23.6%
Present R-C ³ (1950-2010) (MAR/MAP)	11.0%	12.0%	11.4%	12.2%	9.0%	10.9%	11.3%	10.9%	10.9%	10.6%	10.7%
Streamflow change (%)	-42.7%	-37.8%	-51.8%	-39.9%	-54.2%	-58.2%	-59.2%	-58.2%	-56.1%	-6.4%	-54.4%
Pristine Sediment Yield (t/Km ² /a)	221	135	437	214	141	321	178	172	127	92	90
Present Sediment Yield (t/Km ² /a)	108	134	119	169	92	166	167	186	189	304	156
Change in Sediment Yield (CLU/AVT)	0.5	1.0	0.3	0.8	0.7	0.5	0.9	1.1	1.5	3.3	1.7

Table 5-12: Hydrological characteristics of the Mfolozi Catchment

Combined Mfolozi	W23A	W23B	W23C	W23D
ACRU Sub-catchments	625-653	654-683	684-711	712-746
AREA (km ²)	420.1	195.8	317.6	252.0
Mean Altitude (m)	137	118	44	52
MAP (mm)	815	884	1097	981
MAPE ¹ (mm)	1676	1679	1656	1683
MATE ² (mm)	594	647	787	732
Pristine MAR (Mm ³)	50.39	25.04	50.67	30.65
Present MAR (1950-2010) (Mm ³)	29.90	14.08	23.57	18.88
Pristine R-C ³ (MAR/MAP)	14.7%	14.5%	14.5%	12.4%
Present R-C ³ (1950-2010) (MAR/MAP)	8.7%	8.1%	6.8%	7.6%
Streamflow change (%)	-40.7%	-43.7%	-53.5%	-38.4%
Pristine Sediment Yield (t/Km ² /a)	49	21	9	5
Present Sediment Yield (t/Km ² /a)	154	133	28	34
Change in Sediment Yield (CLU/AVT)	3.1	6.3	3.1	6.8

5.6 HYDROLOGICAL RESPONSES TO PROJECTED CLIMATE CHANGE IN THE MFOLOZI CATCHMENT

Having performed an analysis for the evidence of historical climate change (Section 5.2), the remainder of this section presents future estimates of hydrological variables for the Mfolozi catchment. Using the ACRU model and an assembly of empirically downscaled GCM projections (discussed in Section 5.6.1.1), the following hydrological variables are discussed herein: rainfall, runoff, and sediment yield.

5.6.1 GCM MODEL PERFORMANCE ASSESSMENT

The following section briefly introduces the Global Climate Models (GCMs) used in the research, followed by a concise summary of their projected changes with respect to rainfall.

5.6.1.1 BACKGROUND TO PROJECTED FUTURE CLIMATES

Future projections were empirically downscaled from coarse horizontal resolution (200-300 km) coupled atmosphere-ocean global climate models (AOGCMs). These were downscaled to a resolution of 50 km with the RCA3 regional climate model (Jones *et al.*, 2007 & Samuelsson *et al.*, 2011) over an area covering southern Africa. The regional climate model was then adjusted for southern African conditions with respect to land-surface physiography and atmospheric physics (Andersson & Samuelsson, 2010). Temperature and precipitation for the regional climate model projections were further adjusted using a distribution-based scaling (DBS) approach for bias correction (Yang *et al.*, 2010). Using this approach, correction factors were derived by comparing regional climate model outputs with observed climate variables (1961-1990), and then further applied to the regional climate model for future projections. Empirical downscaling techniques often involve the derivation of relationships between synoptic scale and local climates using observed data, followed by the application of these relationships to GCM outputs in order to generate higher resolution regional climate change scenarios (Hewitson *et al.*, 2005). Through empirical downscaling coupled AOGCM simulation outputs to point-scale, regional scenarios were developed. The names of the AOGCMs, the year of the first publication of the results, and the institutions responsible for them are given in *Appendix F*.

5.6.1.2 SUMMARY OF POTENTIAL FUTURE CLIMATES OF THE MFOLOZI CATCHMENT

A summary of projected near future (2046 – 2065) and future (2081 – 2100) climate changes for the downscaled GCMs are presented in Table 5-13.

Table 5-13: 50 and 100-year future climate projections from empirically downscaled GCMs

1950-2010	50-yr projection (2046-2065)				100-yr projection (2081-2100)		
Obs. Historical mean	CRM	ECH	IPS	CCC	CRM	ECH	IPS
815mm	+19%	+12%	+30%	+8%	+36%	+38%	+37%

Each GCM projection was ran using the calibrated ACRU model. The average results for 50-year and 100-year rainfall projections are given in Figure 5-32.

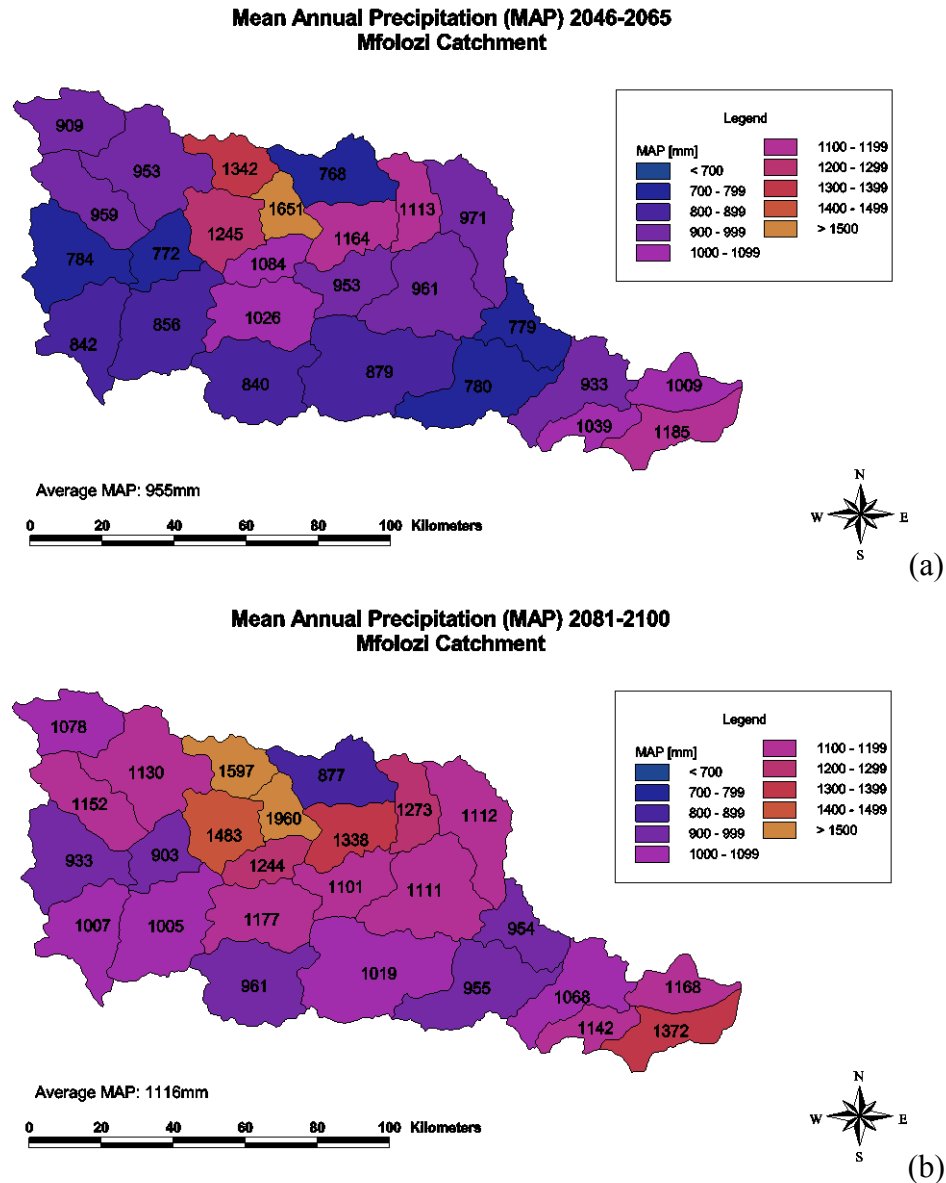


Figure 5-32: Mfolozi quaternary catchment 50-year (a) and 100-year (b) MAP projection.

Lumsden *et al.* (2009) reviewed predicted rainfall trends in South Africa for climate change scenarios based on the IPCC 3rd and 4th assessment reports. The predictions are from a suite of empirically downscaled GCMs. The magnitudes predicted by the different GCMs vary considerably but there is general agreement concerning the expected patterns of change. In particular, increased average rainfall (between 10 - 60% over 100 years) is predicted for the eastern part of the country, including the St Lucia region (Figure 5-33). The predicted increase is in the form of increased rainy days and more intense rainfall. Lumsden *et al.*

(2009) noted that the combination of wetter antecedent conditions and larger rainfall events would lead to significantly increased streamflow.

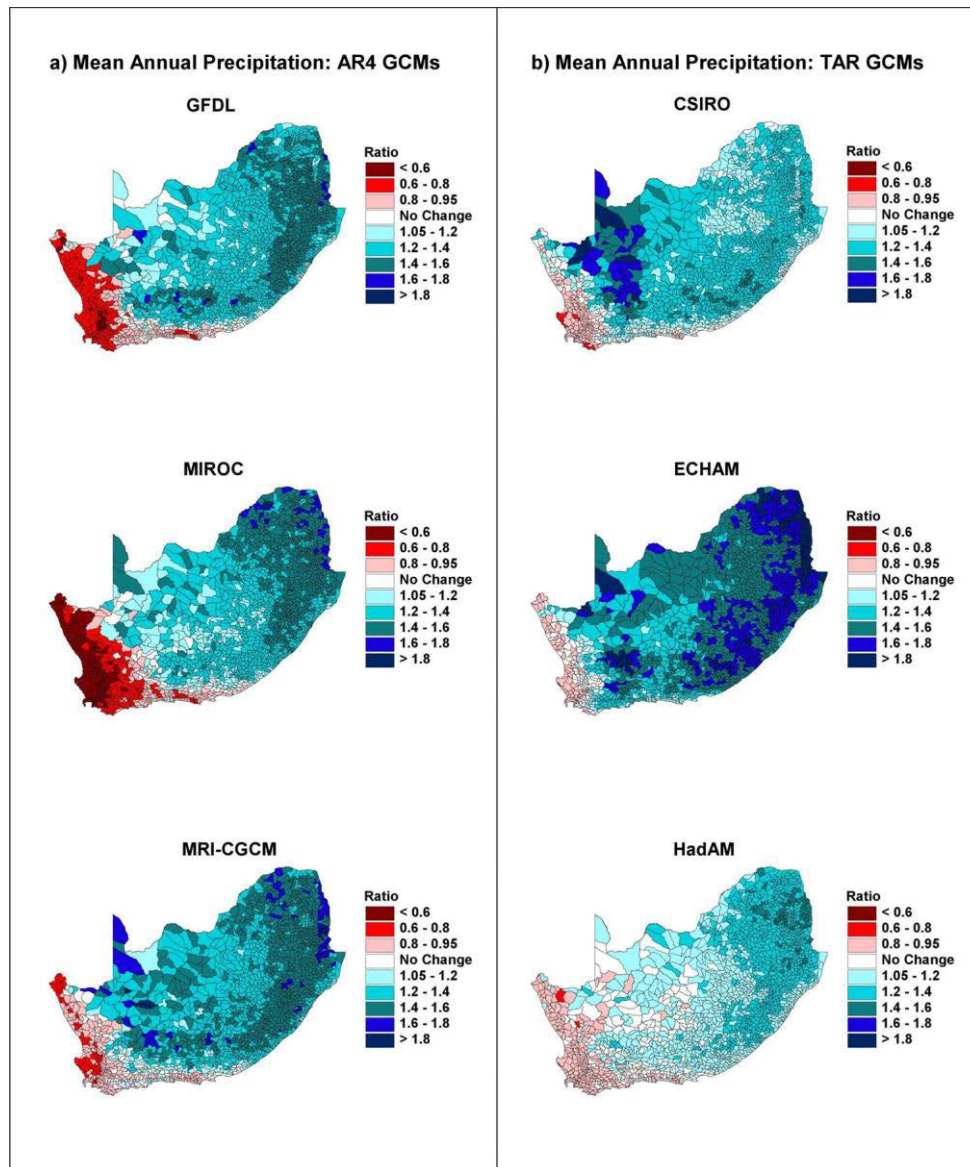


Figure 5-33: Downscaled rainfall predictions for South Africa from various GCMs, for the next century to 2100 (Source: Lumsden *et al.*, 2009).

5.6.2 POTENTIAL IMPACTS OF FUTURE CLIMATE ON STREAMFLOWS AND SEDIMENT YIELDS

The following section assesses the magnitude of impact of climate change on streamflow and sediment yield response of the Mfolozi catchment. This was achieved by firstly keeping catchment land-uses to Acocks (1988) veld types, and secondly by maintaining

streamflow response variables and soils constant, varying only climate. Streamflows and sediment yields outputted for potential future climates were then compared to those generated under (pristine) historical climate (Sections 5.5.1 and 5.5.2). Potential future climate scenarios were assessed from near future (2046 – 2065) and future (2081 – 2100) simulations.

The results obtained from near future simulations (2046 – 2065) for the Mfolozi catchment showed a 20% reduction in streamflow accompanied by a 10% reduction in sediment yield, as shown in Figure 5-34. This translates to a catchment MAR of 939 Mm³ and an average annual sediment yield of 93 t/km²/a.

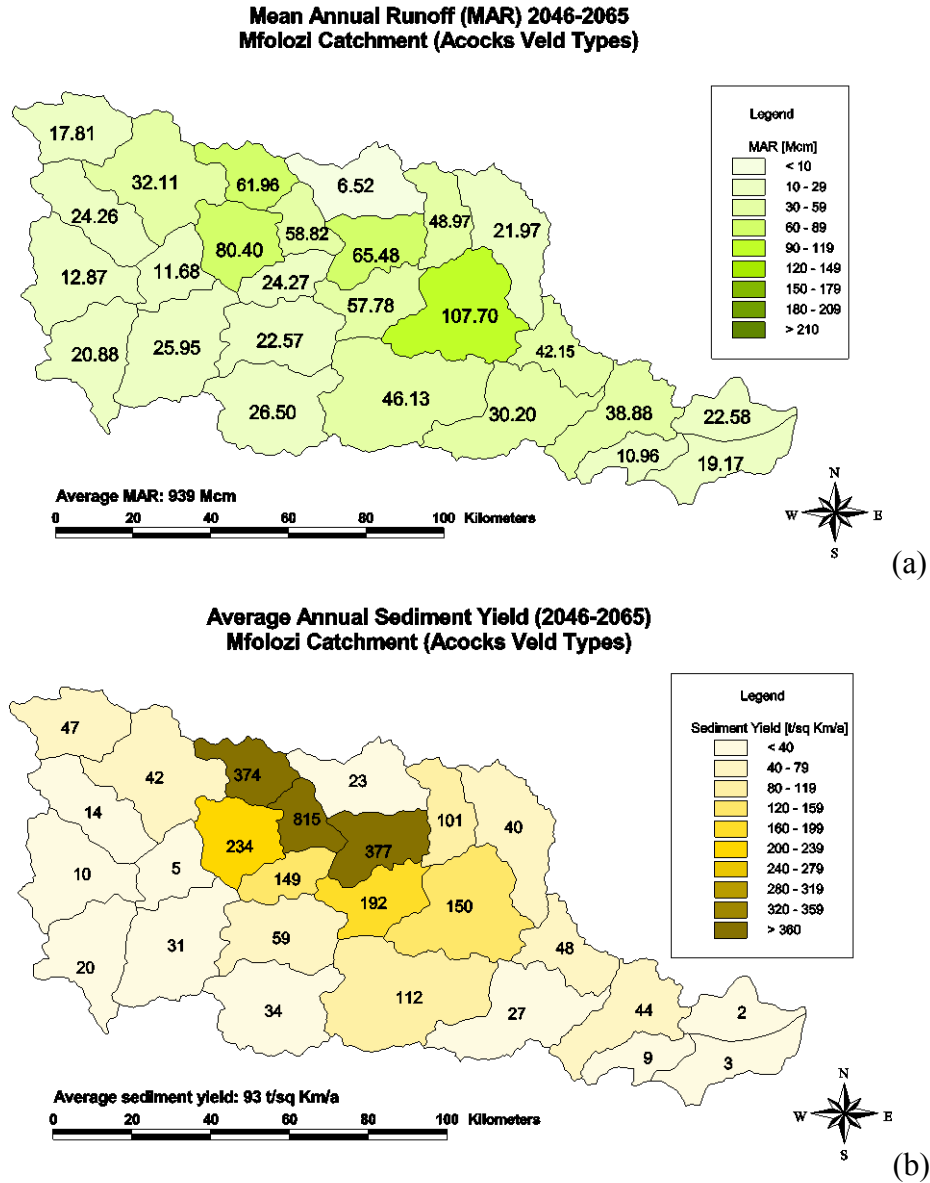


Figure 5-34: Potential impacts of near future (2046 – 2065) climate change on (a) streamflows and (b) sediment yields.

Figure 5-35 shows results obtained from future (2081 – 2100) simulations. These produced a MAR of 1299 Mm³ with a catchment average annual sediment yield of 102 t/Km²/a, translating to hydrological enhancements of 10% and 15%, respectively.

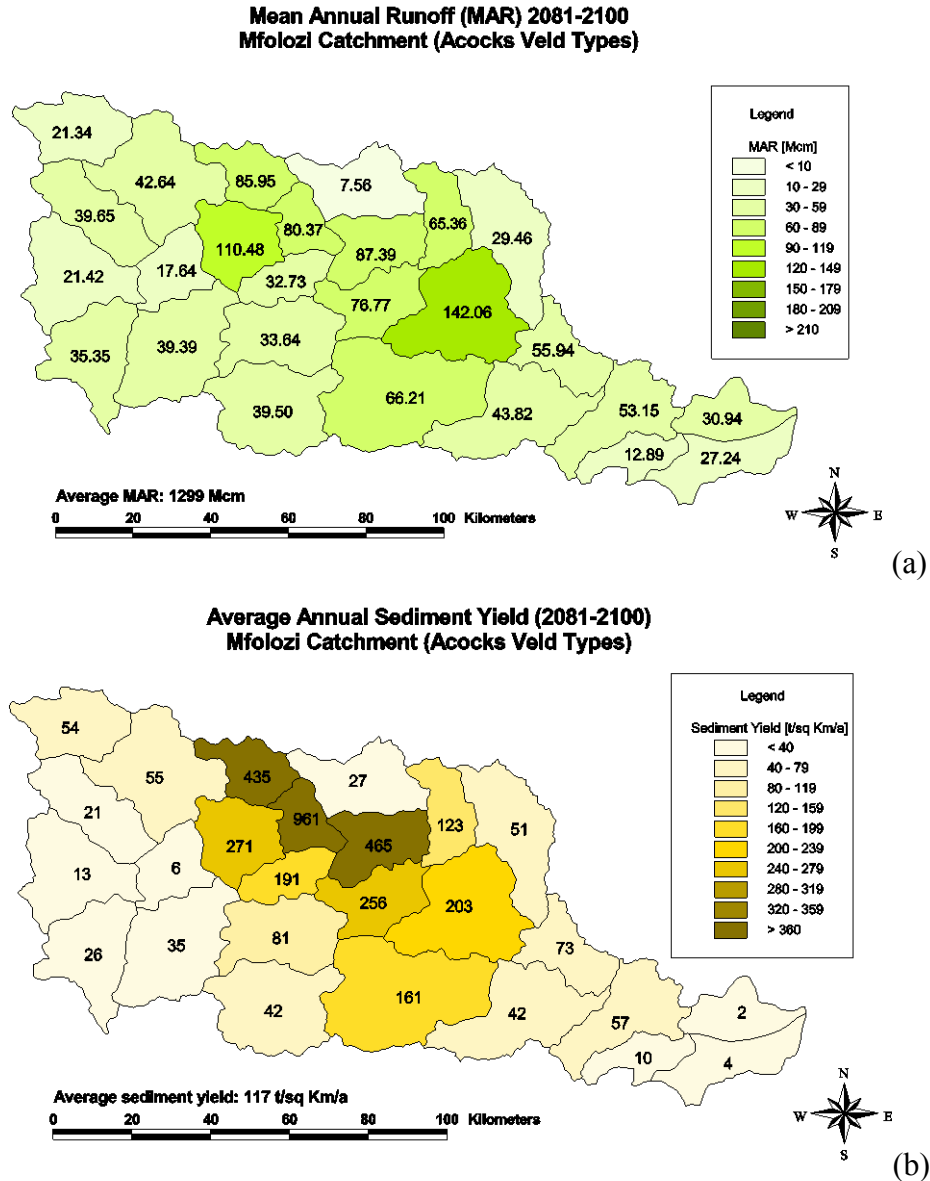


Figure 5-35: Potential impacts of future (2081 – 2100) climate change on (a) streamflows and (b) sediment yields.

Although the magnitude of variation due to climate change alone is very small, it is clear that a changing climate will certainly have implications on streamflow and sediment yield. The question of *how significant these results are* can only be addressed when the joint effects of land-use and climate change are taken into account. This in turn, will enable an assessment on whether land-use change, climate change, or a combination of both has the greatest impact on the Mfolozi catchment.

5.7 STREAMFLOW AND SEDIMENT YIELD RESPONSES TO THE COMBINED EFFECTS OF LAND-USE AND CLIMATE CHANGE

Considering pristine (historical) conditions as the baseline for initial measure, the combination of land-use and climate change for the 50 year projection (2046 – 2065) showed a 2% increase in streamflow and an 83% increase in sediment yield (Figure 5-36). The 100 year projection (2081 – 2100) showed a 37% increase in streamflow and a 135% increase in sediment yield (Figure 5-38). It should however, be noted that for future projections to have meaningful value, they should be compared against *current* conditions.

Therefore, comparing the effects of land-use and climate change against current conditions yielded a 65% increase in streamflow and a 20% increase in sediment yield (Figure 5-37) for the 50 year projection. The 100 year projection yielded a 120% increase in streamflow and a 54% increase in average annual sediment (Figure 5-39).

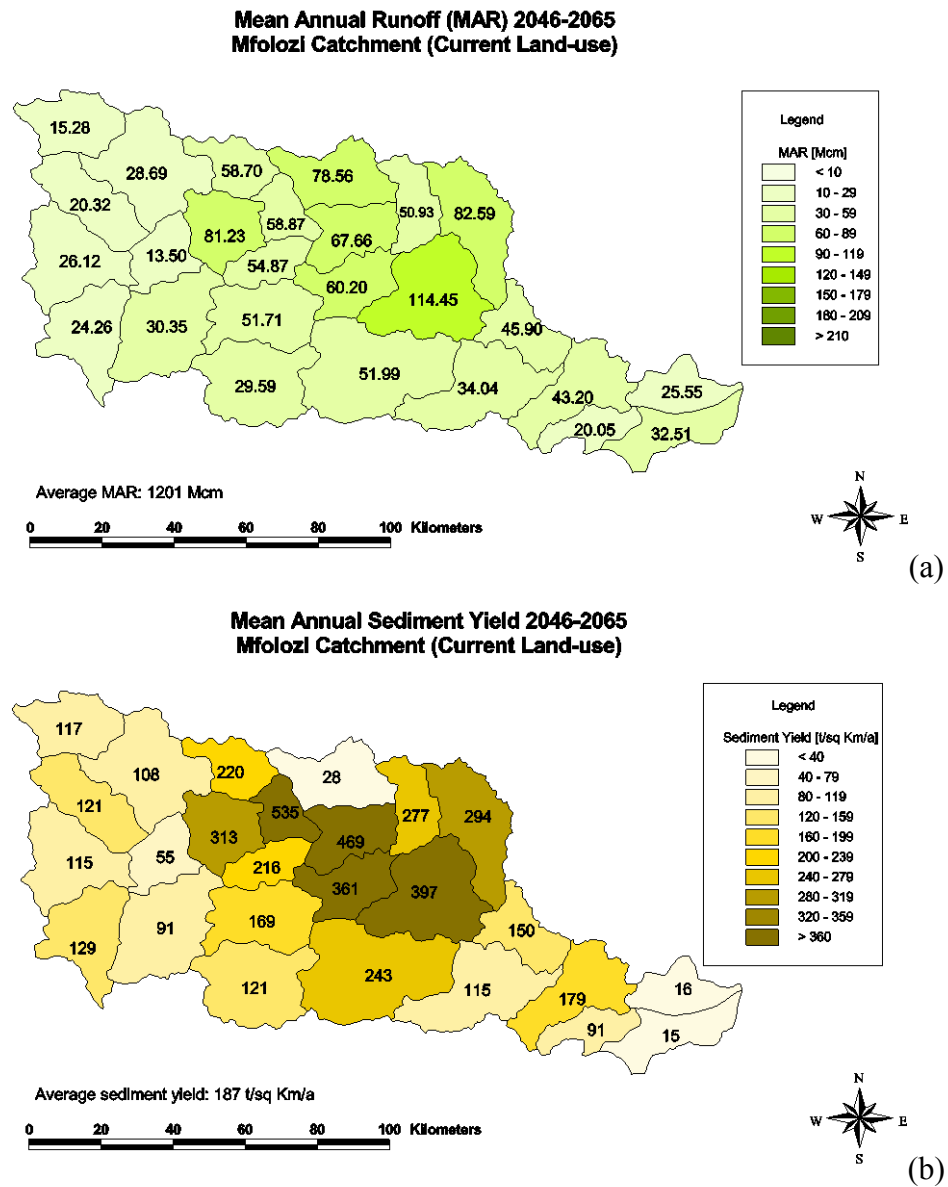


Figure 5-36: Potential impacts on (a) streamflow and (b) sediment yield from combined land-use and climate change for near future (2046 – 2065).

Mfolozi Quaternary Catchment Factor of Change in Sediment Yield from Present Land Use/Present Climate (1950-2010) to Present Land Use/Future Int. Climate (2046-2065)

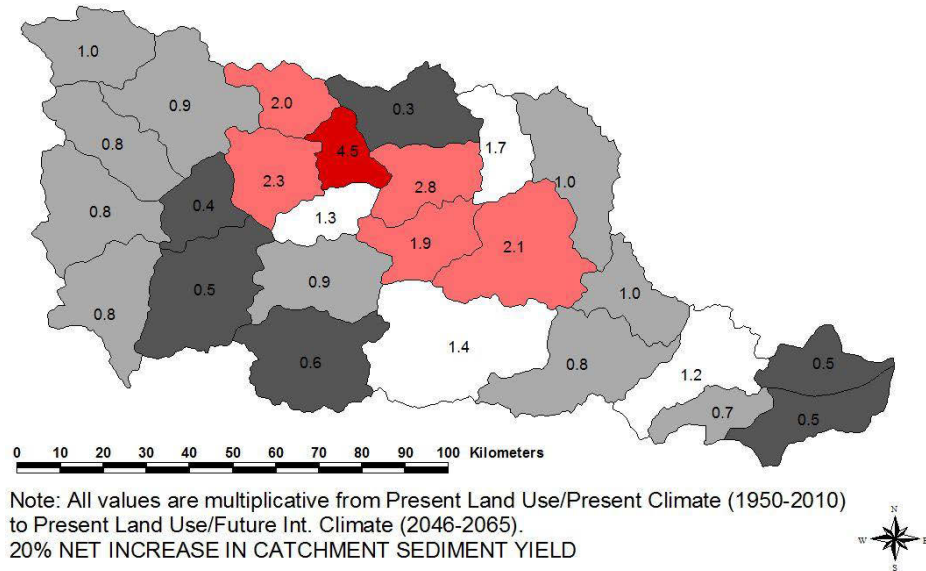


Figure 5-37: Overall impact of combined land-use and climate change on sediment yield (2046-2065), showing a 20% net increase in catchment sediment yield from current conditions.

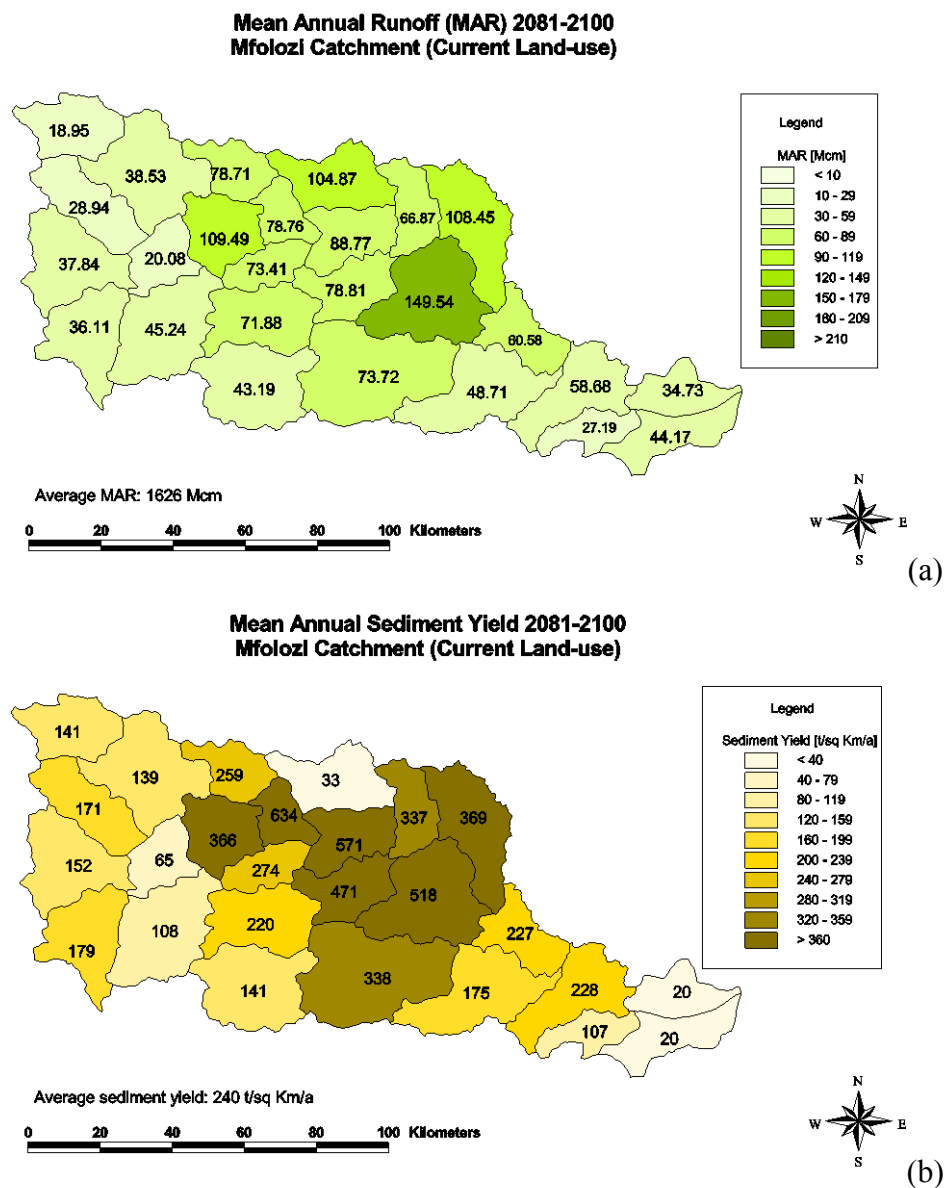


Figure 5-38: Potential impacts on (a) streamflow and (b) sediment yield from combined land-use and climate change for future (2081 – 2100).

Mfolozi Quaternary Catchment Factor of Change in Sediment Yield from Present Land Use/Present Climate (1950-2010) to Present Land Use/Future Climate (2081-2100)

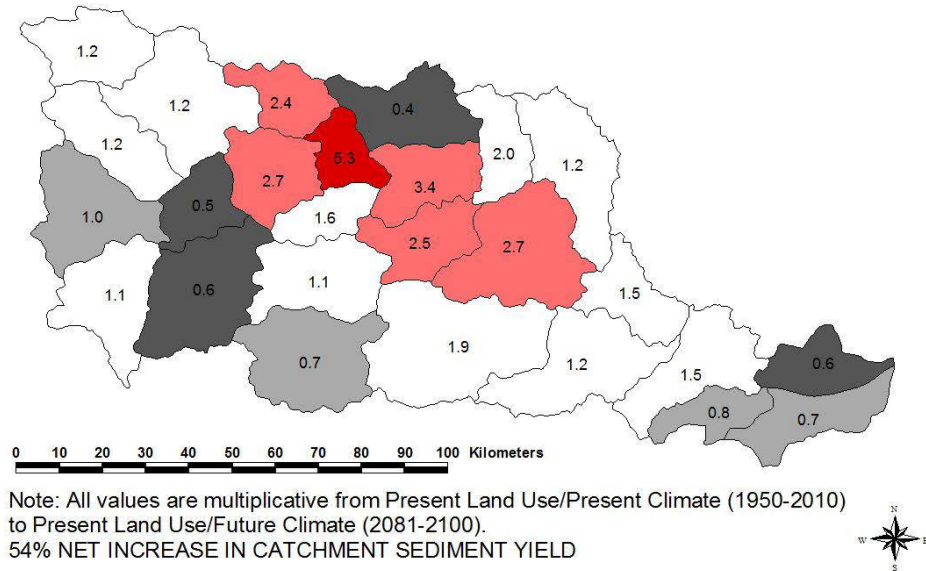


Figure 5-39: Overall impact of combined land-use and climate change on sediment yield (2081-2100), showing a 54% net increase in catchment sediment yield from current conditions.

5.7.1 SUMMARY OF HYDROLOGICAL RESPONSES TO LAND-USE AND CLIMATE CHANGE IN THE MFOLOZI CATCHMENT

It is evident from the above that both land-use and climate change have significant impacts on hydrological responses within the Mfolozi catchment. As mentioned in Section 1.1, the joint effects of land-use and climate change establish a complex interactive system through the combination of human action and environmental responses (Schulze, 2000). The results presented thus far on the effects of climate change indicate a non-linear impact effect with an amplification or attenuation response to runoff. Sediment generation, on the other hand, appears to be restricted by changes in land-use, with highly degraded areas yielding larger sediment loads. These responses are further illustrated in Figure 5-40 and Figure 5-41.

Having determined that land-use change is more dominant in influencing the hydrological cycle of the Mfolozi catchment, it becomes clear that further investigation is required in assessing specific land-use changes in order to aid in effective catchment management and gain further understanding of these intricate interactions. Since land-use can effectively be managed or controlled, one should investigate the effects of increasing commercial forest and sugarcane cultivation in the coastal flood plains of the Mfolozi, for example.

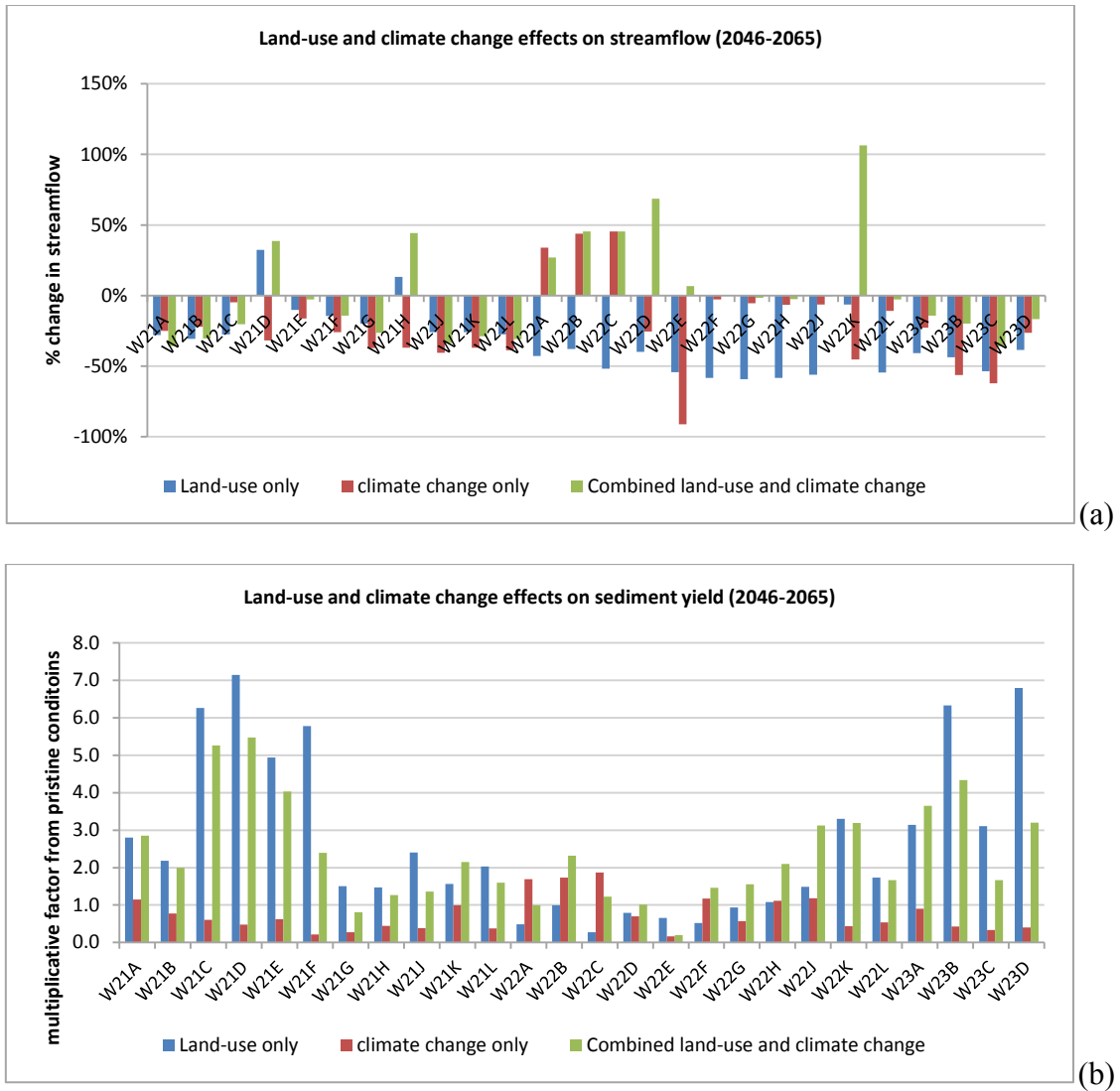


Figure 5-40: Percentage changes in Mfholzi quaternary catchment (a) MAR and (b) multiplication factors of sediment yield under projections of land-use change, potential climate change, and combined land-use and climate change (2046 – 2065).

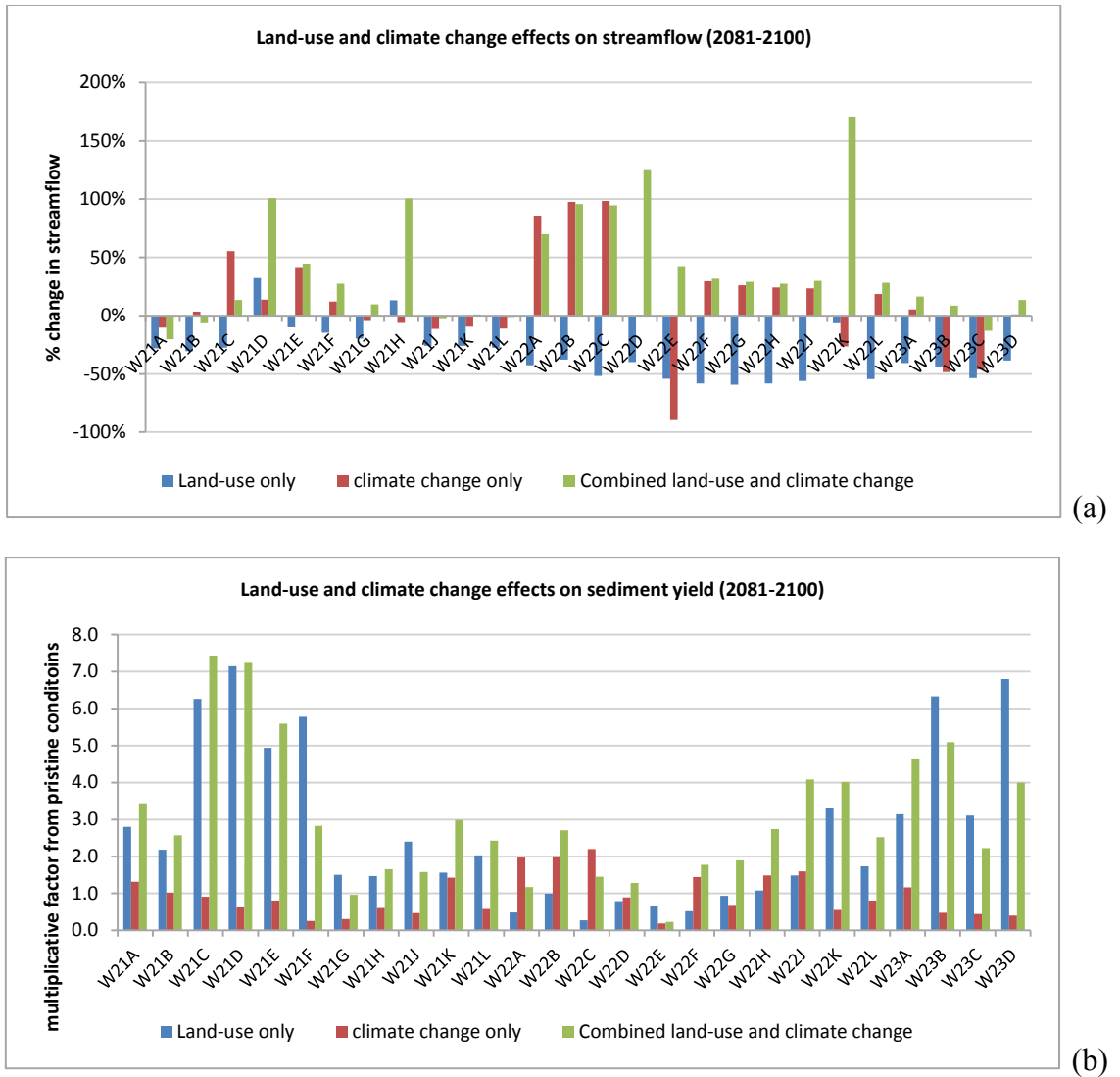


Figure 5-41: Percentage changes in Mfolozi quaternary catchment (a) MAR and (b) multiplication factors of sediment yield under projections of land-use change, potential climate change, and combined land-use and climate change (2081 – 2100).

5.8 DISCUSSION ON THE IMPLICATIONS FOR THE ST. LUCIA SYSTEM

The remainder of the Lake St. Lucia catchments, namely, the Mkuze, Nyalazi, Mzinene, and Mzimane catchments retain similar land-uses, or rather, land cover properties as the Mfolozi catchment, both at Pristine state and current state (Figure 5-42).

Applying net increases in rainfall, runoff and sediment yield obtained from the analysis of the Mfolozi catchment, and by considering data from *WR2005* (Middleton & Bailey, 2008) as a baseline, the hydrological responses as shown in Figure 5-43 were obtained for these catchments.

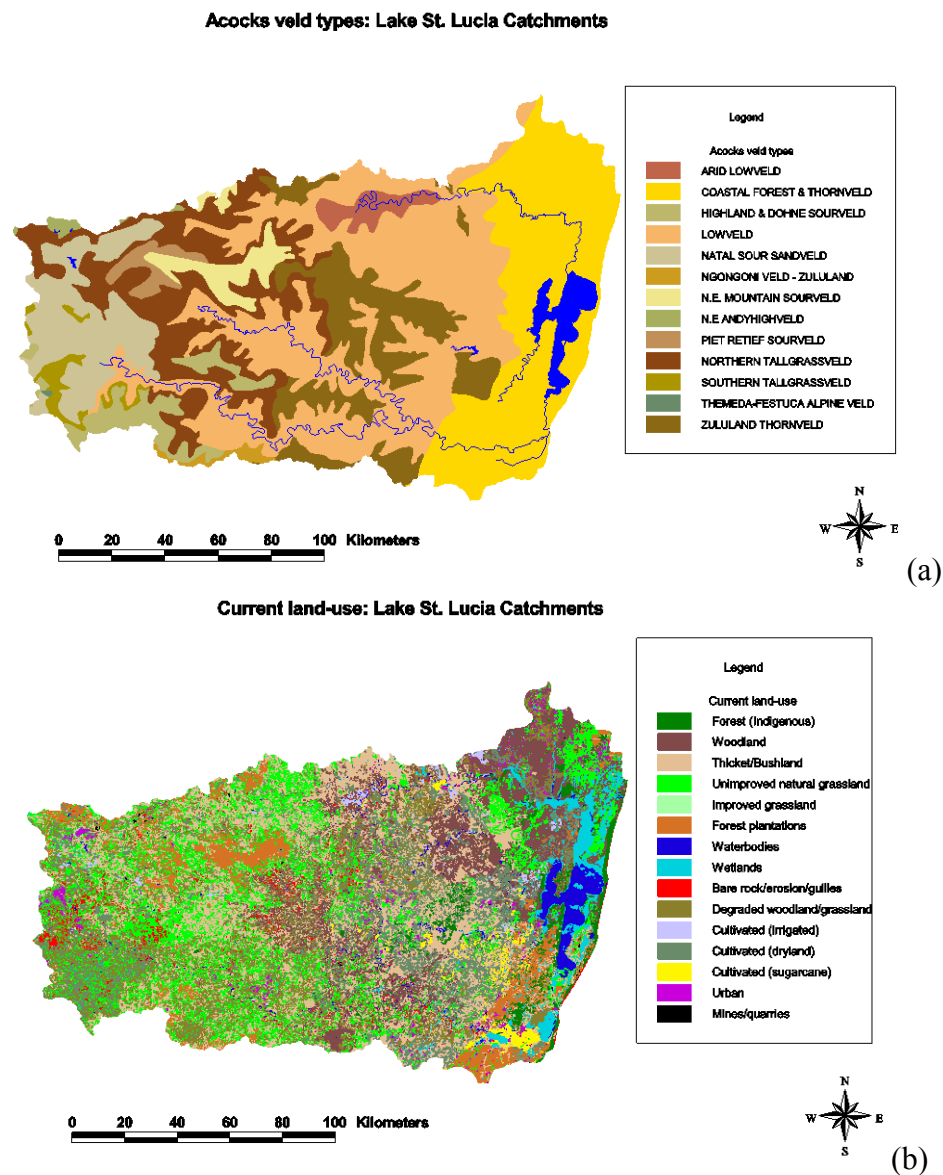


Figure 5-42: (a) Pristine (Acocks, 1988) and (b) current (NLC, 2005) land-uses for the Lake St. Lucia catchments, relative to the Mfolozi catchment

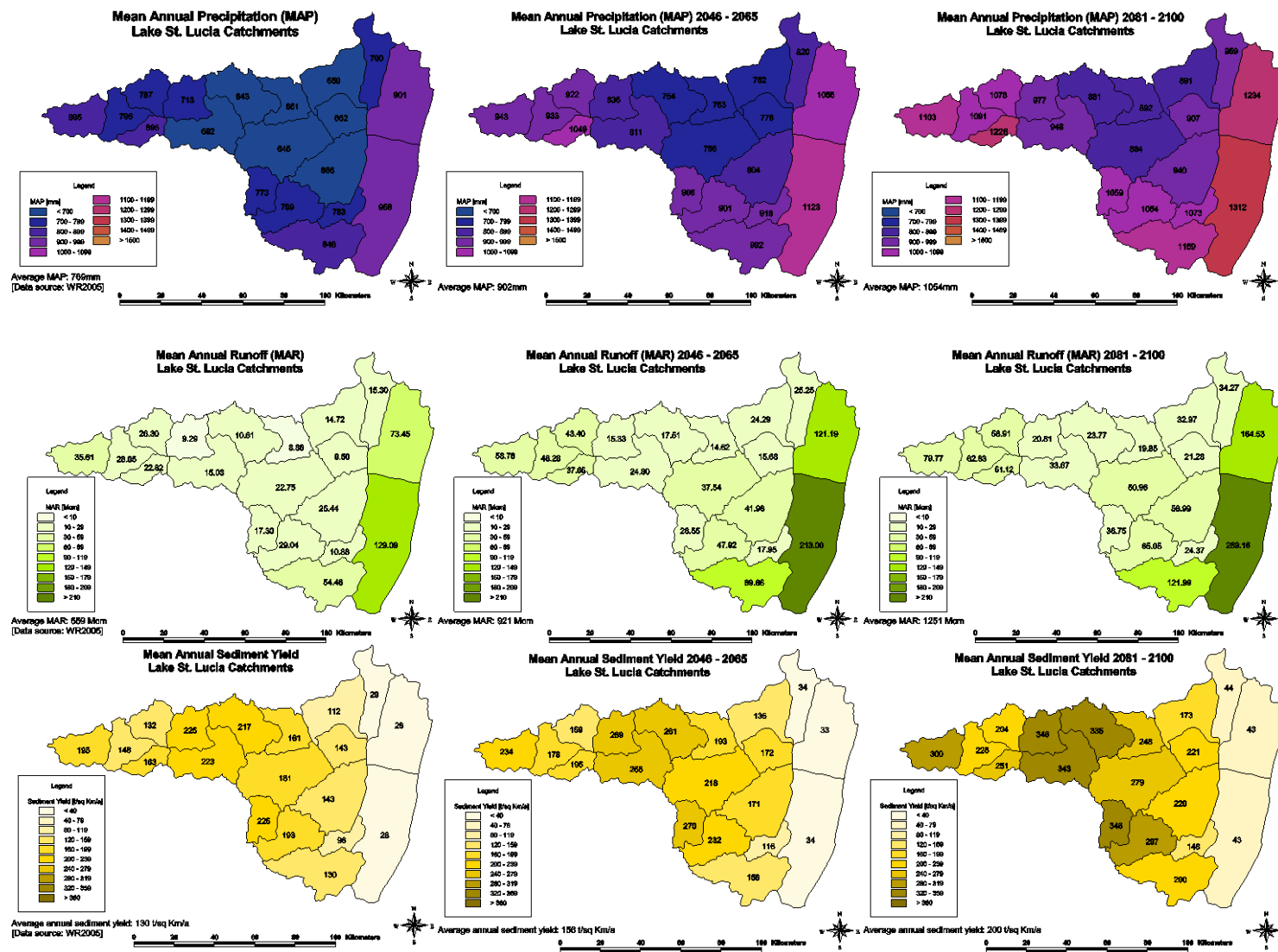


Figure 5-43: Current (left column), 50 year projection (centre column), and 100 year projection (right column) of MAP, MAR, and sediment yield for the Lake St. Lucia catchments.

The results indicate increases in mean annual precipitation of 20% (50 year projection) and 40% (100 year projection). These imply large increases in water and sediment supply to the Lake St. Lucia system. Sediment yield projections showed increases of 20% and 55% for the 50-year and 100-year projection, respectively.

To further investigate the overall effect of increased sediment supply into the lake, it is interesting to evaluate the projected sediment yields as annual millimetre depth inputs and compare them against projected sea level rise due to climate change. Neglecting the distribution of the generated sediments and assuming a lake area of 325 Km² with a specific gravity of submerged sediment (sand) of 1.6, depth increases in sediment of 2.9mm/yr (50-year projection⁴) and 3.7mm/yr (100-year projection) are to be expected.

Historical sea level rise rates as estimated by Mather *et al.* (2009) are given in Table 5-14. From these, and assuming the value of 2.7mm/yr for Durban, there appears to be a zero net effect of sea level rise as sediment inputs are enough to raise the basin level of the lake, essentially maintaining a constant lake volume. This infers little or no risk of increased salinities in the lake as a result of little or no inflow of saltwater from the sea. In addition to sediment input, increased streamflows from the Mfolozi catchment result in the mouth state being open more often therefore increasing freshwater input and reducing the risk of seawater influx.

⁴ $200t.km^{-2}.yr^{-1} \times 9545km^2 = 1489020 t.yr^{-1}$

$$\frac{1489020 t.yr^{-1}}{325km^2 \times 1.6 \times 10^3} = 2.9mm.yr^{-1}$$

Table 5-14: Sea level rise rates for South Africa (Source: Mather *et al.*, 2009)

Station	Years of record	Sea level change (mm/yr \pm 1 SD)
Simon's Town	1957-2007	+1.58 \pm 0.22
Mossel Bay	1958-2009	+0.33 \pm 0.35
Knysna	1960-2009	+1.81 \pm 0.54
Port Elizabeth	1978-2009	+2.52 \pm 0.77
East London	1967-2009	+2.30 \pm 0.93
Durban	1971-2009	+2.70 \pm 0.05

It should, however be noted that future projections of sea level rise as given by the IPCC (2007) estimate values between 220mm and 500mm by the year 2100 (or approximately 2.2 – 5 mm/yr), as shown in Figure 5-44.

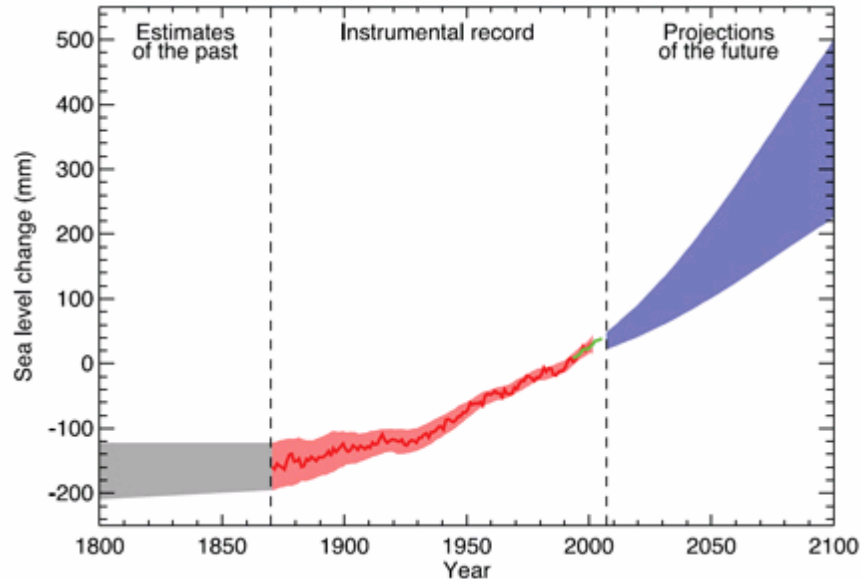


Figure 5-44: Past, recorded, and projected sea level rise (source: IPCC, 2007).

From this, and considering the medium value of the 100-year projection for sea level rise (approx. 3.6mm/yr) it becomes clear that sediment infilling will be sufficient to balance out the effects of sea level rise by the year 2100.

The question of whether the Mfolozi catchment can be a source of sediment to aid in minimizing the effects of sea level rise needs to be addressed. When the inlets are combined (Figure 5-45) and the mouth is closed, it is assumed that all the Mfolozi flows and suspended sediments are diverted through the Narrows. Kelbe & Taylor (2010) observed trapping efficiencies of more than 90% during periods when the Mfolozi closed and water was diverted through the Back Channel into St Lucia. It is therefore assumed that all Mfolozi sediments settle within the Narrows. Conversely, during an open mouth state, all sediments from the Mfolozi will be discharged into the sea. Therefore it can be concluded that sedimentation issues will be negligible when the Mfolozi link is re-established with the system to increase water levels of the lake.

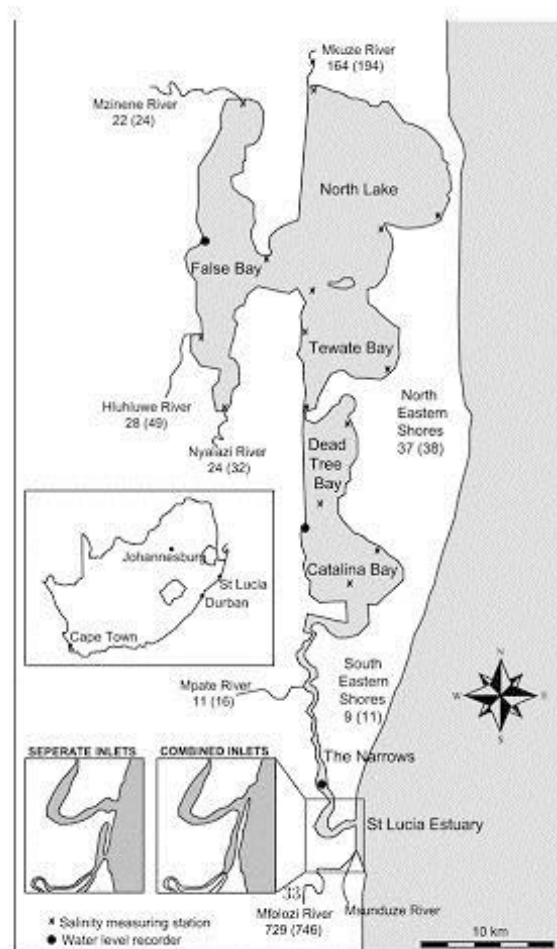


Figure 5-45: Location of Lake St. Lucia Estuary in South Africa, and schematic of separate & combined Mfolozi inlets (Source: Lawrie & Stretch, 2011).

6. SUMMARY AND CONCLUSIONS

Three questions were proposed at the inception of this study. The evidence of regional climate change using rainfall as an indicator within the study area was presented. The extent and effect of land-use changes have been investigated. Land-use changes have been identified as having greater impacts on the hydrological cycle than climate change. This chapter presents a summary of key results, conclusions and recommendations for further research.

6.1 EVIDENCE FOR REGIONAL CLIMATE CHANGE WITHIN THE ST. LUCIA SYSTEM USING RAINFALL AS AN INDICATOR

The analysis of ten of the longest available rain gauge data records (on average 82 years data) yielded no consistent evidence of statistically significant changes in the mean annual rainfall. An increase in the average intensity of rainfall events was supported by statistically significant reductions in the number of wet-days. Furthermore, evidence of small but statistically significant increases in the occurrence of high intensity rainfall (>30mm/day and >50mm/day) has been presented. This was further corroborated by increases in the variance and scale parameter of the fitted gamma distribution, as well as the shift of the mean towards increasing values thereby indicating an increase in extreme daily precipitation values within the last 40-50 years.

6.2 EFFECT OF PRESENT LAND-USES ON PRISTINE STREAMFLOWS AND SEDIMENT YIELD

Using hydrological modelling (from 1950-2010) the effects of land-use change on water and sediment yields from pristine conditions to current conditions were investigated. Streamflow simulations under unaffected conditions were consistent with WR2005 (Middleton & Bailey, 2008), in order of 20%. The results observed a decrease in catchment mean annual runoff of 38% as well as an increase in catchment average annual sediment yield of 50%, due to a 33% change in land-use. Insight into the nature of sediment dynamics of the Mfolozi catchment revealed that relatively large sediment contributions are made by episodic flood events. These amounted to 50% of the total sediment yield from the accumulation of the top ten annual sediment loads within the

simulation period, further confirming the highly variable nature of the Mfolozi catchment. Sugarcane and commercial forestry production were found to have significant impacts on both streamflows and sediment yields. Although these land-uses mainly dominate the lower reaches of the Mfolozi catchment, they still affect accumulated streamflow as it cascades through the catchment.

6.3 HYDROLOGICAL RESPONSES TO LAND-USE AND PROJECTED CLIMATE CHANGE

The impacts of climate change on streamflows and sediment yield, as well as their corresponding hydrological responses have been assessed at two levels: (i) where land-uses have assumed to be natural (Acocks, 1988); and (ii) using present land-uses (NLC, 2005). This was done so as to determine whether land-use change or climate change was the prevailing driver of hydrological response. For the Mfolozi catchment, it was determined that land-use change was the dominant driver, with climate change providing an amplification effect on the hydrological responses. Maintaining rainfall as the chosen indicator for climate change, increases in mean annual precipitation of 17% (~ 50-year projection) and 37% (~ 100-year projection) are to be expected. Increases in mean annual runoff are predicted to be 65% and 124% for the two scenarios. Sediment yield increases of 20% and 54% are expected for the 50-year and 100-year projection, respectively. All of which suggest relatively large increases in water and sediment supply to the Lake St Lucia system under these projected changes.

Simulations indicated that sediment inputs from the Mfolozi and other St Lucia catchments can be effectively managed with minimum impact. Furthermore, potential issues of increased sedimentation can be effectively managed by the restoration of the lower Mfolozi coastal flood plain to natural conditions. This in turn may reduce the risk of sedimentation by acting as a sediment trap for suspended sediments.

6.4 SUMMATION

Using a validated distributed hydrological model, the objectives of the study have been achieved. The model has been effectively setup and is capable of running simulations for the Mfolozi catchment to account for both land-use and climate change. This hence means that it can be effectively used to assess hydrological response to land-use change scenarios

that could be essential in catchment management including, but not limited to the effects of coastal flood plain restoration, or the impacts of increased commercial forestry.

6.5 RECOMMENDATIONS FOR FUTURE RESEARCH

In order to further the research, the model should be used to run simulation scenarios based on the restoration of land-uses to natural conditions, as well as hydrological responses to proposed land-use changes, specifically sugarcane and commercial forestry plantations.

Furthermore, a validated daily time step model for the remainder of the St Lucia catchments is required in order to investigate changes within specific areas of the system, such as the Mkuze Swamps and the effect of gum tree eradication on baseflow within that area.

7. REFERENCES

- Abawi, K., 2008. *Qualitative and Quantitative Research*, WHO, Geneva.
- Acocks, J.P.H., 1988. Veld types of South Africa. *Memoirs of the Botanical Survey of South Africa*. No. 57, 3rd ed. Botanical Research Institute, Dept. of Agriculture and Water Supply, South Africa.
- Andersson, L. & Samuelsson, P., 2010. Application of RCA for assessment of climate change impact on water resources in the Pungwe drainage basin, Mozambique/Zimbabwe. Available: <http://www.smhi.se/forskning/forskningsomraden/klimatforskning/1.8840> [10/07/2011].
- Anthoni,, 2000. *Soil Erosion and Conservation*. Available: <http://www.seafriends.org.nz/enviro/soil/erosion2.htm> [25/05/2011].
- Basson, G., 2008. *A Southern Perspective*; in Di Silvio, G. & Basson, G. 2008 “Erosion and Sediment Dynamics from catchment to coast” Technical documents in hydrology, no. 82. UNESCO, Paris, France.
- Bates, B.C., Kundzewicz, Z.W, Wu, S, & Palutikof, J.P., 2008. *Climate Change and Water. Technical Paper of the Intergovernmental Panel on Climate Change*, IPCC Secretariat, Geneva.
- Bijker, E.W., 1971. Longshore transport computation. *Journal of Waterways, Harbours and Coastal Engineering Division*, ASCE, Vol. 97, pp. 687-701.
- Bily, CA. (Ed), 2007. *Global Warming- Opposing viewpoints*. Greenhaven Press, New York, USA. Chapter 1 & Chapter 5.
- Blignaut, J., Mander, M., Schulze, R., Horan, M., Dickens, C., Pringle, C., Mavundla, K., Mahlangu, I., Wilson, A., McKenzie, M., McKean, S., 2010. Restoring and managing natural capital towards fostering economic development: evidence from the Drakensberg, *South Africa. Ecol. Econ*, vol. 69, pp. 1313–1323.

- Boslaugh, S., 2007. "An introduction to secondary data analysis" in *Secondary Data Sources for Public Health: A Practical Guide* Cambridge Univ Press, United Kingdom.
- Brooks, N. H., 1963. Calculation of Suspended Load Discharge from Velocity Concentration Parameters, *Proceedings of Federal Interagency Sedimentation Conference*, U.S. Department of Agriculture, no. 970.
- Brown, C. B., 1950. Sediment Transportation. *Engineering Hydraulics*, ed. Wiley, New York, USA.
- Burroughs, W., 2003. *Climate: into the 21st century* Cambridge, U.K. ; Cambridge University Press.
- Choi, W., Deal, B.M., 2008. Assessing hydrological impact of potential land use change through hydrological and land use change modelling for the Kishwaukee River Basin (USA). *J. Environ. Manage*, vol. 88, pp. 1119–1130.
- Christensen, J.H., B. Hewitson, A. Busuioc, A. Chen, X. Gao, I. Held, R. Jones, R.K. Kolli, W.-T. Kwon, R. Laprise, V. Magaña Rueda, L. Mearns, C.G. Menéndez, J. Räisänen, A. Rinke, A. Sarr and P. Whetton, 2007. "Climate change 2007: the physical science basis" in *Climate Change 2007: The Physical Science Basis. Contribution of Working Group I to the Fourth Assessment Report of the Intergovernmental Panel on Climate Change* Cambridge University Press, Cambridge, United Kingdom and New York, NY, USA.
- Cooper, J.A.G., Mason, T.R., Reddering, J.S.V., & Illenberger, W.I., 1990. Geomorphological effects of catastrophic fluvial flooding in a small subtropical estuary. *Earth Surf Proc* no. 15, pp. 24–41.
- Cyrus, D.P, Vivier, L., Jerling, H.L., 2010. Effect of hyper-saline and low lake conditions on ecological functioning of St. Lucia estuarine sytem, South Africa: an overview 2002-2008. *Estuarine, Coastal Shelf Science*, vol. 86, pp. 535-542.
- Di Silvio, G., 2008. *A Northern Perspective*; in Di Silvio, G. & Basson, G. 2008 "Erosion and Sediment Dynamics from catchment to coast" Technical documents in hydrology, no. 82. UNESCO, Paris, France.

- Dyson, L.L., 2009, Heavy daily-rainfall characteristics over the Gauteng Province, *Water SA*, vol. 35, no. 5.
- Easterling, D., Evans, J., Groisman, P.Y., Karl, T., Kunkel, K. & Ambenje, P., 2000. Observed variability and trends in extreme climate events: a brief review.
- Einstein, H. A., 1942. Formula for the Transportation of Bed-Load. *Transactions of the ASCE*, vol. 107.
- Einstein, H. A., 1950. The Bed-load function for Sediment Transportation in Open Channel Flows, U.S. Department of Agriculture, Soil Conservation Service, Technical Bulletin no. 1026.
- Ewen, J., Parkin, G. & O'Connell, P.E., 2000. SHETRAN: Distributed River Basin Flow and Transport Modelling System. *Journal of Hydrologic Engineering*, vol. 5, pp. 250-258.
- Foster, G.R., Flanagan, D.C., Nearing, M.A., Lane, L.J., Risse, L.M., Finker, S.C., 1995. Hillslope erosion component. In: USDA Water Erosion Prediction Project Hillslope Profile and Watershed Model Documentation. NSERL Report 10. NSERL, West Lafayette, Indiana, USA.
- Fox, J., 2002. *An R and S-Plus companion to applied regression*, 1st edition, Sage Publications, Inc, London, United Kingdom.
- Grenfell, S. E., & Ellery, W. N., 2009. Hydrology, sediment transport dynamics and geomorphology of a variable flow river: The Mfolozi River, South Africa. *Water SA Vol. 35 No.3* , 271-282.
- Groisman, P., Karl, T. R., Easterling, D. R., *et al.*, 1999. Changes in the probability of heavy precipitation: Important indicators of climatic change. *Climatic Change*. Vol. 42, pp. 243-283.
- Grubb, H. & Robson, A., 2000. Exploratory / Visual Analysis. In Kundzewicz & Robson *Detecting trend and other changes in hydrological data*. WMO, Geneva, Switzerland, WMO/TD-No. 1013, Chapter 4, 19-49.

- Hardy, J.T., 2003. *Climate change: causes, effects, and solutions*, Wiley, United Kingdom.
- Hargreaves, G.H. & Samani, Z.A., 1985. Reference crop evaporation from temperature. *Applied Engineering in Agriculture*, vol. 1, no. 2, pp. 96-99.
- Harris, C., 2003. *Sediment transport processes in coastal environments*.
- Harrison, T. D., Hohls, D. R., Meara, T. P. & Webster, M. S., 2001. South African Estuaries: Catchment Land-Cover, National Summary Report. CSIR, Congella, RSA.
- Heezen, B. C. & Hollister, C., 1964. Deep-sea current evidence from abyssal sediments, *Marine Geology*, vol. 1, pp. 141-174.
- Hewitson, B.C., Tadross, M. & Jack, C., 2005. Historical Precipitation Trends over Southern Africa: A Climatology Perspective. In: Schulze, R.E. (Ed) *Climate Change and Water Resources in Southern Africa: Studies on Scenarios, Impacts, Vulnerabilities and Adaptation*. Water Research Commission, Pretoria, RSA, WRC Report 1430/1/05. Chapter 18, 319-324.
- HRU., 1981. *Surface water resources of South Africa*. Hydrological Research Unit, University of the Witwatersrand, Johannesburg. HRU report nos. 8/81 to 13/81
- Hutchinson, I & Pitman, W.V., 1973. Hydrology and Climatology of the St Lucia Lake System. Hydrological Research Unit, University of Witwatersrand, Johannesburg, South Africa.
- Institute for Soil Climate and Water [ISCW], 2005. Land Type digital data. ISCW, Pretoria, RSA.
- [IPCC, 2007] Meehl, G.A., T.F. Stocker, W.D. Collins, P. Friedlingstein, A.T. Gaye, J.M. Gregory, A. Kitoh, R. Knutti, J.M. Murphy, A. Noda, S.C.B. Raper, I.G. Watterson, A.J. Weaver and Z.-C. Zhao, 2007: Global Climate Projections. In: *Climate Change 2007: The Physical Science Basis. Contribution of Working Group I to the Fourth Assessment Report of the Intergovernmental Panel on Climate Change* [Solomon, S., D. Qin, M. Manning, Z. Chen, M. Marquis, K.B. Averyt, M. Tignor and H.L. Miller (eds.)]. Cambridge University Press, Cambridge, United Kingdom and New York, NY, USA.

- Jones, C.G., Willén, U., Ullerstig, A. and Hansson, U., 2004. The Rossby Centre Regional Atmospheric Climate Model - Part I: Model climatology and performance for the present climate over Europe. *Ambio* vol. 33, 199-210.
- Julien, P., 1998. *Erosion and Sedimentation*. Cambridge University Press, Cambridge, United Kingdom.
- Jungerius, P. & ten Harkel, T., 1994. The effect of rainfall intensity on surface runoff and sediment yield in the Grey Dunes along the Dutch coast under conditions of limited rainfall acceptance. *Catena* vol. 23, pp. 269-279.
- Jones, B., 2007, *Soil Erosion: A workshop to support the Thematic Strategy for Soil Protection Common Criteria for Risk Area Identification in the Soil Framework Directive*. BGR, Hanover, Germany.
- Kelbe, B. & Taylor, R., 2010. *Analyses of the hydrological linkage between Mfolozi/Msunduzi estuary and lake St Lucia*. In: Bate, G.C., Whitfield, A.K., Forbes, A.T. (Eds.), "A review of studies on the Mfolozi estuary and associated flood plain, with emphasis on information required by management for future reconnection of the river to the St Lucia system", Water Research Commission report KV 255/10, pp. 276-315.
- Kienzle, S.W., Lorentz, S.A. and Schulze, R.E., 1997. *Hydrology and Water Quality of the Mgeni Catchment*. Water Research Commission, Pretoria, Report TT87/89. Pp88.
- Kruger, A., 2006. Observed trends in daily precipitation indices in South Africa: 1910–2004, *International Journal of Climatology*, vol. 26, no. 15, pp. 2275-2285.
- Lane, E. W. and Kalinske, A. A., 1941. Engineering Calculations of Suspended Sediment, *Transactions of the American Geophysical Union*, vol. 20, pt. 3, pp. 603-607.
- Lawrie, R. & Stretch, D., 2011. Anthropogenic impact on the water and salt budgets of the St Lucia estuarine lake in South Africa. *Estuarine, Coastal and Shelf Science*, vol. 93, pp 58-67.

- Le Roux, J.J., Nkambule, V.T., Mararakanye, N. and Pretorius, D.J., 2010. Provincial mapping of gully erosion at the field scale using high resolution satellite imagery (SPOT 5). *ARC-ISCW* report no. GW/A/2009/04.
- Lindsay, P., Mason, T.R., Pillay, S., Wright, C.I., 1996. Suspended particulate matter and dynamics of the Mfolozi estuary, north KwaZulu-Natal, South Africa. *Environmental Geology*. vol. 28, pp. 40–51.
- Lucero, O. A. & Rozas, D., 2002. Characteristics of aggregation of daily rainfall in a middle-latitudes region during a climate variability in annual rainfall amount. *Atmospheric Research* vol. 61, pp. 35-48.
- Lui, Z., 2001. Sediment Transport. Laboratoriet for Hydraulik og Havnebygning, Aalborg Universitet, Denmark.
- Lumsden, T.G., Schulze, R.E. & Hewitson, B.C., 2009. Evaluation of potential changes in hydrologically relevant statistics of rainfall in Southern Africa under conditions of climate change. *Water SA*, vol. 35, no. 5, pp. 649-656.
- Lynch, S.D., 2004. Development of a Raster Database of Annual, Monthly and Daily Rainfall for Southern Africa, *Water Research Commission*, Pretoria, South Africa.
- Ma, N., 2006. Mathematical Modelling of Water Soil Erosion and Sedimen Yield in Large Catchments. MSc Thesis. University of Stellenbosch, South Africa.
- Mason, S.J., Waylen, P.R., Mimmack, G.M., Rajaratnam, B. & Harrison, J.M., 1999. Changes in extreme rainfall events in South Africa, *Climatic Change*, vol. 41, no. 2, pp. 249-257.
- Mason, S. & Jury, M., 1997. Climatic variability and change over southern Africa: A reflection on underlying processes. *Progress in Physical Geography*, vol. 21, pp. 23-50.
- Mason, S. & Joubert, A., 1997. Simulated changes in extreme rainfall over southern Africa, *International Journal of Climatology*, vol. 17, no. 3, pp. 291-301.

- Mather, A.A., Stretch, D.D. and Garland, G.G., 2009. Southern African sea level: corrections, influences and trends. *African Journal of Marine Science*, vol. 31, no. 2, pp. 145-156.
- Middleton, B.J., Bailey, A.K., 2008, *Water Resources of South Africa, 2005 study (WR2005)*. Water Research Commission of South Africa, Report TT 380/08, South Africa.
- Midgley, D.C., Pitman, W.V. & Middleton, B.J., 1994, *Surface Water Resources of South Africa 1990*, Water Research Commission Report of South Africa No. 298/1/94, South Africa.
- Milliman, J.D., Meade, R.H., 1983. World-wide delivery of river sediment to the oceans. *The Journal of Geology*, vol. 91, no. 1, pp. 1-21.
- Msadala, V., 2009. Sediment Yield Predictions Based on Analytical Methods and Mathematical Modelling. MSc Thesis. University of Stellenbosch, South Africa.
- Msadala, V., Gibson, L., Le Roux, J., Rooseboom, A., Basson, G., 2010. Sediment Yield Prediction for South Africa: 2010 Edition. University of Stellenbosch & ARC/WRC Project K5/765.
- Nastos, P. & Zerefos, C, 2007. On extreme daily precipitation totals at Athens, Greece, *Advances in Geosciences*, vol. 10, pp. 59-66.
- Nearing, M.A., Foster, G.R., Lane, L.J. & Finker, S.C., 1989. A process-based soil erosion model for USDA, WEPP (Water Erosion Prediction Project technology. *Trans. Am. Soc. Agric. Engnrs.*, vol. 32, pp. 1587-1593.
- Neyers, S., 1990. The statistical analysis of meteorological observations, *WMO Techn Note*, No. 143.
- NLC, 2005. National Land Cover satellite imagery. CSIR and ARC Consortium, Pretoria, RSA.

Nicholls, N. N., and Coauthors, 1996. Observed climate variability and change. *Climate Change 1995: The Science of Climate Change*, J. T. Houghton et al., Eds., Cambridge University Press, pp. 135–192.

Nicholson, S.E., 2000. The nature of rainfall variability over Africa on time scales of decades to millenia, *Global and Planetary Change*, vol. 26, no. 1-3, pp. 137-158.

Orme, A.R., 1974. Estuarine sedimentation on the Natal coast, South Africa. Office of Naval Research Technical Report vol. 5, pp. 53.

Perry, 1989. The impact of the September 1987 floods on the estuaries of Natal/Kwazulu; a hydro-photographic perspective. Research Report CSIR vol. 640, pp. 46.

Pidwirny, M., Sidney D., 2008. Soil erosion and deposition. Encyclopaedia of Earth. Washington, D.C.: Environmental Information Coalition, National Council for science and the environment.

Pitman, W. V., 1973. Simulation of long-term runoff from South African catchments, Ph.D thesis.

Pitman, W. V., Middleton, B. J. and Midgley, D. C., 1981. Surface water resources of South Africa. Parts 1 and 2. *Dept. Water Affairs Rep.*, 9/81: VI Pretoria, SA.

Randle, T.J., Yang, C.T., and Daraio, J., 2006. Erosion and sedimentation manual. U.S. Department of the Interior, Bureau of Reclamation, Technical Service Centre. Sedimentation and River Hydraulics Group Denver, Colorado.

Robson, A., 2000. Guideline to Analysis. In Kundzewicz & Robson *Detecting trend and other changes in hydrological data*. WMO, Geneva, Switzerland, WMO/TD-No. 1013, Chapter 2, 11-15.

Robson, A., Bardossy, Jones, D. & Kundzewicz, Z., 2000. Statistical Methods For Testing For Change. In Kundzewicz & Robson *Detecting trend and other changes in hydrological data*. WMO, Geneva, Switzerland, WMO/TD-No. 1013, Chapter 4, 19-49.

- Rooseboom, A., 1992. Sediment transport in rivers and reservoirs- a southern African perspective. *Water Research Commission*, Report no. 297/1/92, Pretoria, South Africa.
- Rooseboom, A., Verster, E., Zietsman, H.L., and Lotriet, H.H., 1992. The development of the new sediment yield map of South Africa. WRC Report No. 297/2/92, *Water Research Commission*. Pretoria, South Africa.
- Rooseboom, A., 1975. Sediment yield for South Africa. Technical Report No. 61, *Department of Water Affairs*, Pretoria, SA. pp. 34.
- Samaniego, L., Bárdossy, A., 2006. Simulation of the impacts of land use/cover and climatic changes on the runoff characteristics at the mesoscale. *Ecol. Model*, vol. 196, pp. 45–61.
- Samuelsson, P., Jones, C.G., Willén, U., Ullerstig, A., Gollvik, S., Hansson, U., Kjellström, E. and Wyser, K., 2011. The Rossby Centre Regional Climate Model RCA3: Model description and performance. *Tellus*, vol. 63, pp. 4-23.
- Schulze, R.E., 1995. Hydrology and Agrohydrology: A Text to Accompany the ACRU 3.00 Agrohydrological Modelling System. *Water Research Commission*, Pretoria, RSA, Report TT 69/9/95. pp 552.
- Schulze, R.E., 1997. South African Atlas of Agrohydrology and -Climatology. *Water Research Commission*, Pretoria, RSA, TT 82/96. pp 276.
- Schulze, R.E., 2000. Modelling Hydrological Responses to Land Use and Climate Change: A Southern African Perspective. *Ambio*, vol. 29, no. 1, pp. 12-22.
- Schulze, R.E. & Horan, M.J.C., 2008. Soils: Hydrological Attributes. In: Schulze, R.E. (Ed). 2008. South African Atlas of Climatology and Agrohydrology. *Water Research Commission*, Pretoria, RSA, WRC Report 1489/1/08, Section 4.2.
- Schulze, R.E. & Maharaj,, M. 2004. Development of a Database of Gridded Daily Temperatures for Southern Africa. *Water Research Commission*, Pretoria, RSA, WRC Report 1156/2/04. pp 83.

Schulze, R.E. & Maharaj, M., 2007. A-Pan Equivalent Reference Potential Evaporation. In: Schulze, R.E. (Ed). 2007. South African Atlas of Climatology and Agrohydrology. *Water Research Commission*, Pretoria, RSA, WRC Report 1489/1/06, Section 13.2.

Schulze, R.E. (Ed.), 2003. Modelling as a Tool in Integrated Water Resources Management: Conceptual Issues and Case Study Applications. *Water Research Commission*, Pretoria, South Africa, Report 749/1/04, pp. 84–97.

Schulze, R.E., 2005. Climate Change and Water Resources in South Africa. WRC Report No 1430/1/05. *Water Research Commission*, Pretoria.

Schulze, R.E. & Horan, M.J.C., 2010. Methods 1: Delineation of South Africa, Lesotho and Swaziland into Quinary Catchments. In: Schulze, R.E., Hewitson, B.C., Barichievy, K.R., Tadross, M.A., Kunz, R.P., Lumsden, T.G. and Horan, M.J.C. (2010). Methods to Assess Eco-Hydrological Responses to Climate Change over South Africa. *Water Research Commission*, Pretoria, RSA, WRC Report 1562/1/10. Chapter 6.

Schulze, R.E., Horan, M.J.C. & Knoesen, D.M., 2009. An Ecosystem trading model for selected areas in the Baviaanskloof Mega Reserve: A Hydrological Perspective.

Schulze, R.E., Hewitson, B.C., Barichievy, K.R., Tadross, M.A., Kunz, R.P., Lumsden, T.G. & Horan, M.J.C., 2011. Methods to Assess Eco-Hydrological Responses to Climate Change over South Africa. *Water Research Commission*, Pretoria, RSA, WRC Report 1562/1/10. pp197.

Senior, C., Jones, R., Lowe, J., Durman, C. & Hudson, D., 2002, Predictions of extreme precipitation and sea-level rise under climate change, *Philosophical Transactions of the Royal Society of London. Series A: Mathematical, Physical and Engineering Sciences*, vol. 360, no. 1796, pp. 1301.

Shen, H.W., 1971. *River Mechanics*. Vol 1 and 2. Fort Collins, USA.

Smithers, J.C. and Schulze, R.E., 1995. ACRU Agrohydrological Modelling System: User Manual Version 3.00. *Water Research Commission*, Pretoria, RSA, Report TT70/95. AM6-1 to AM6-188.

- Smithers, J. & Schulze, R., 2002. ACRU Agrohydrological Modelling System User Manual Version 3. University of Natal, Pietermaritzburg, RSA.
- Smithers, J.C. & Schulze, R.E., 2005. *ACRU Agrohydrological Modelling System - User Manual Version 4.0*. University of KwaZulu-Natal, Pietermaritzburg, RSA, School of Bioresources Engineering and Environmental Hydrology. pp 302.
- Stretch, D.D., Chrystal, C.P., Chrystal, R., A., Maine, C.M., Pringle, J.P. & Maro, A.Z., 2012. Estuary and lake hydrodynamics. *In: Perissinotto, R., Stretch, D. & Taylor, R., (ed) 2012. Ecology and Conservation of Estuarine Ecosystems: Lake St. Lucia as a global model. Cambridge University Press. (in press).*
- Sun, B., & Groisman, P., 1999. Cloudiness variations over the former Soviet Union. *International Journal of Climatology*.
- Taylor, R.H., 2006. Ecological responses to changes in the physical environment of the St Lucia estuary. Unpublished PhD thesis 2006, Norwegian University of Life Sciences, Aas, Norway.
- Tefera, S., Dlamini, B., & Dlamini, A., 2008. Invasion of *Chromolaena odorata* in the Lowveld regions of Swaziland and its effect on Herbaceous Layer Productivity. *International Journal of Agricultural Research* 3, vol. 2, pp. 98-109.
- Toulmin, C., 2009. *Climate Change in Africa*, Zed Books Ltd, New York, USA.
- Troy, B., Sarron, C., Fritsch, J., Rollin, D., 2007. Assessment of the impacts of land use changes on the hydrological regime of a small rural catchment in South Africa. *Elsevier*, vol. 32, pp. 984-994.
- Tu, J., 2009. Combined impact of climate and land use changes on streamflow and water quality in eastern Massachusetts, USA, *Journal of Hydrology*, vol. 379, pp. 268–283.
- Turpie, J.K., Marais, C. & Blignaut, J.N., 2008. The Working for Water Programme: evolution of a payments for ecosystem services mechanism that addresses both poverty and ecosystem service delivery in South Africa. *Ecological Economics*, vol. 65, pp. 788-798.

- Turner, B.L., Skole, B., Sanderson, S., Fischer, G., Fresco, L., Leemans, R., 1995. Land-Use and Land-Cover Change: Science Research Plan. *IGBP Report*, 35, IGBP, Stockholm, Sweden.
- Tyson, P.D., 1986, *Climatic Change and Variability in Southern Africa*. Oxford University Press, Cape Town. pp. 220.
- UNFCCC 2006, *Impacts, vulnerability and adaptation to climate change in Africa*, UNFCCC, Geneva.
- Van Wageningen, A. & du Plessis, J., 2007. Are rainfall intensities changing, could climate change be blamed and what could be the impact for hydrologists? *Water S. A.*, vol. 33, no. 4, pp. 571-574.
- Wang, W., Chen X., Shi P., van Gelder P., 2008. Detecting changes in extreme precipitation and extreme streamflow in the East River Basin in southern China. *Hydrology and Earth System Sciences*, vol. 12, pp. 207-221.
- Warburton, M. & Schulze, R.E. 2005. Historical Precipitation Trends over Southern Africa: A Hydrology Perspective. In: Schulze, R.E. (Ed) *Climate Change and Water Resources in Southern Africa: Studies on Scenarios, Impacts, Vulnerabilities and Adaptation*. Water Research Commission, Pretoria, RSA, WRC Report 1430/1/05. Chapter 19, 325-338.
- Warburton, M.L., Schulze, R.E. and Jewitt, G.P.W., 2010. Confirmation of ACRU model results for applications in land use and climate change studies. *Hydrol. Earth Sys. Sci.*, vol. 14, pp. 2399-2414.
- Warburton, M.L., 2012. Projections of Future Climate for the Mgeni Catchment. In: Warburton, M., Lumsden, T., Mauck, B., Summerton, M., Ngcobo, S. & Lorentz, S. Projected Impacts Of Climate Change On Water Quantity And Quality In The Mgeni Catchment. *Water Research Commission Research Project K5/1961*, Second Annual Report, reporting period: April 2011 – March 2012 (in press).

- Warburton, M.L., Schulze, R. E., Jewitt, G. P, 2012. Hydrological impacts of land use change in three diverse South African catchments. *Journal of Hydrology*, vol. 414-415, pp. 118-135.
- Watson, H.K., Ramokgopa, R. & Looser, U., 1996. The distribution of erosion in the Mfolozi drainage basin-implications for sediment yield control. Erosion and Sediment Yield: Global and Regional Perspectives (Proceedings of the Exeter Symposium, July 1996). *IAHS*. Publication no. 236. Wallingford, UK. pp. 357-366.
- Wischmeier, W.H. & Smith, D.D., 1978. Predicting rainfall erosion losses: a guide to conservation planning. Agriculture handbook, US Dept of Agriculture, Washington DC. USA.
- Wolanski, E., 2007. Estuarine Ecohydrology, Elsevier, Amsterdam, The Netherlands.
- Yang, C., 1996, *Sediment Transport Theory and Practice*. McGraw-Hill Companies, USA.
- Zhang, X., Hogg, W. & Mekis, É. 2001, "Spatial and temporal characteristics of heavy precipitation events over Canada", *Journal of Climate*, vol. 14, pp. 1923-1936.

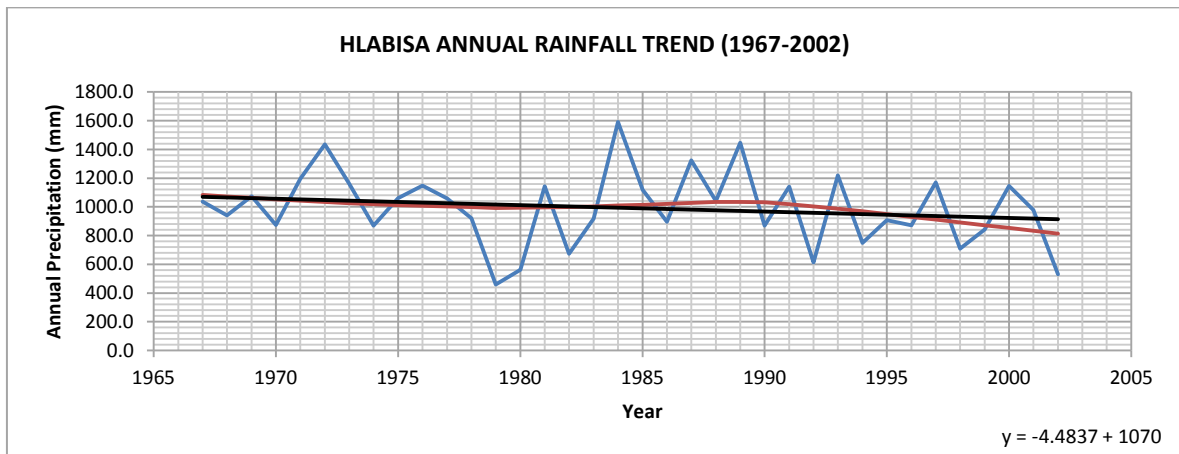
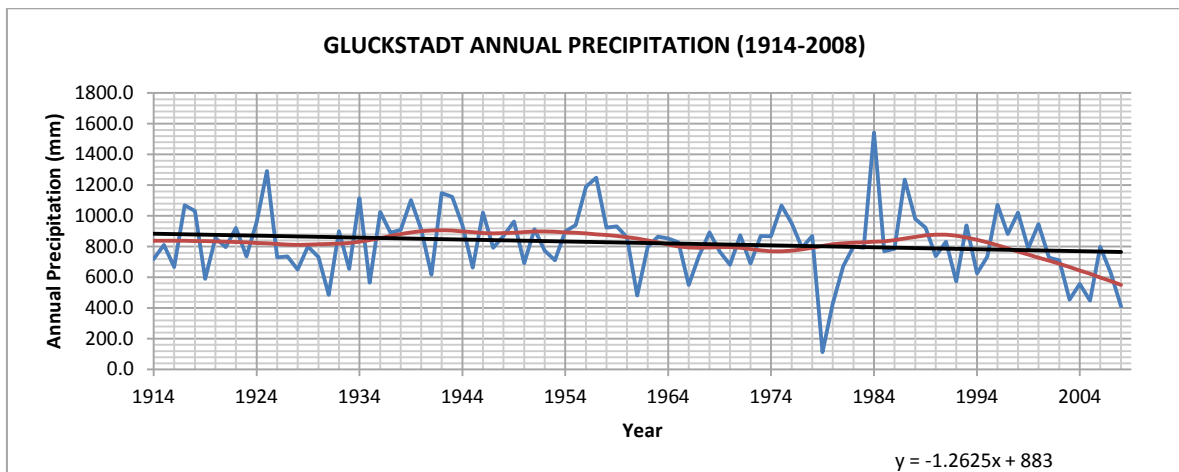
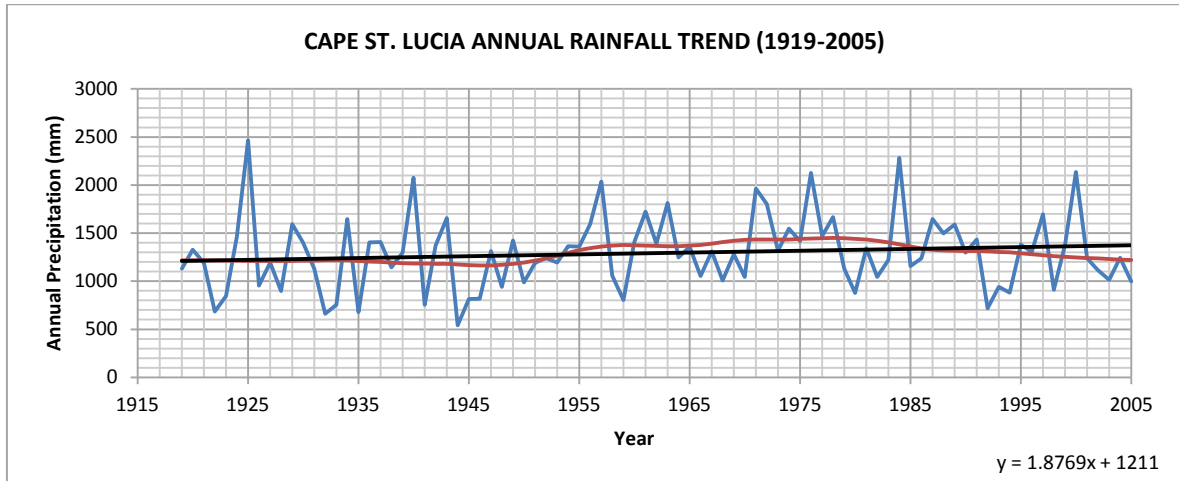
8. APPENDICES

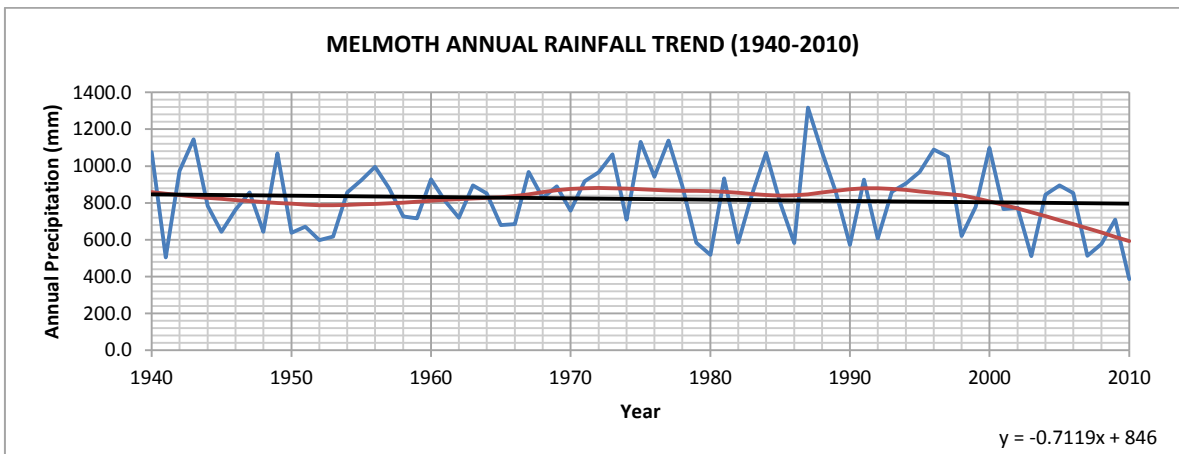
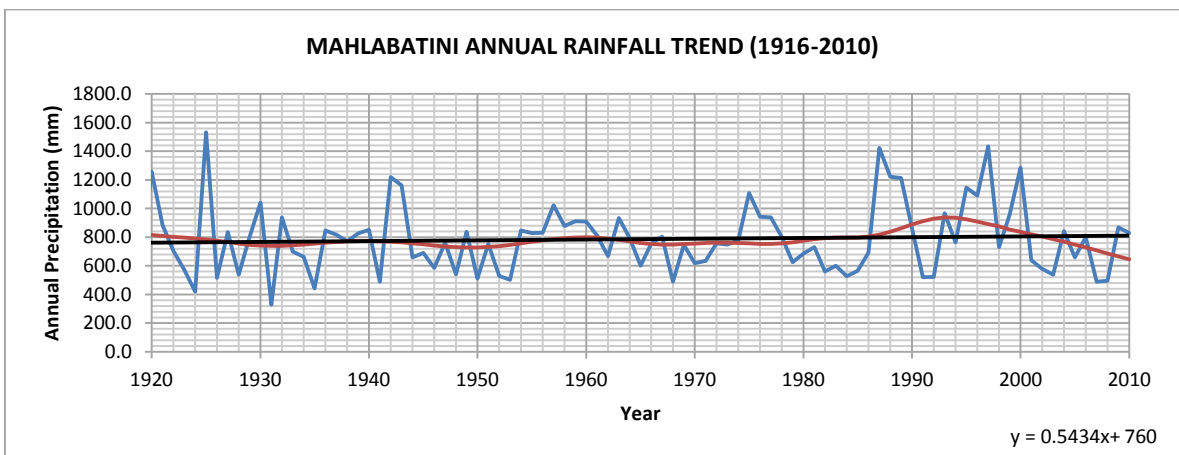
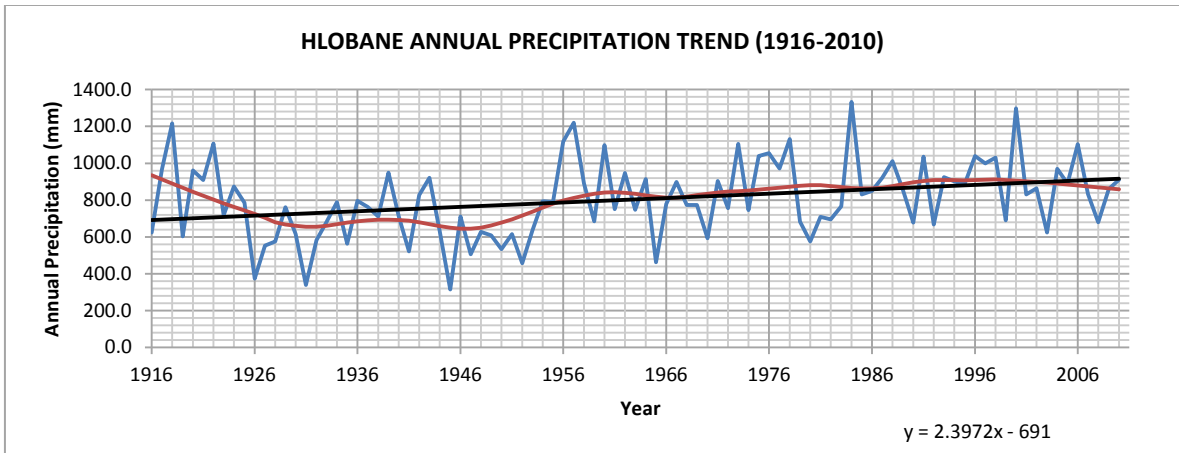
CONTENTS OF APPENDICES:

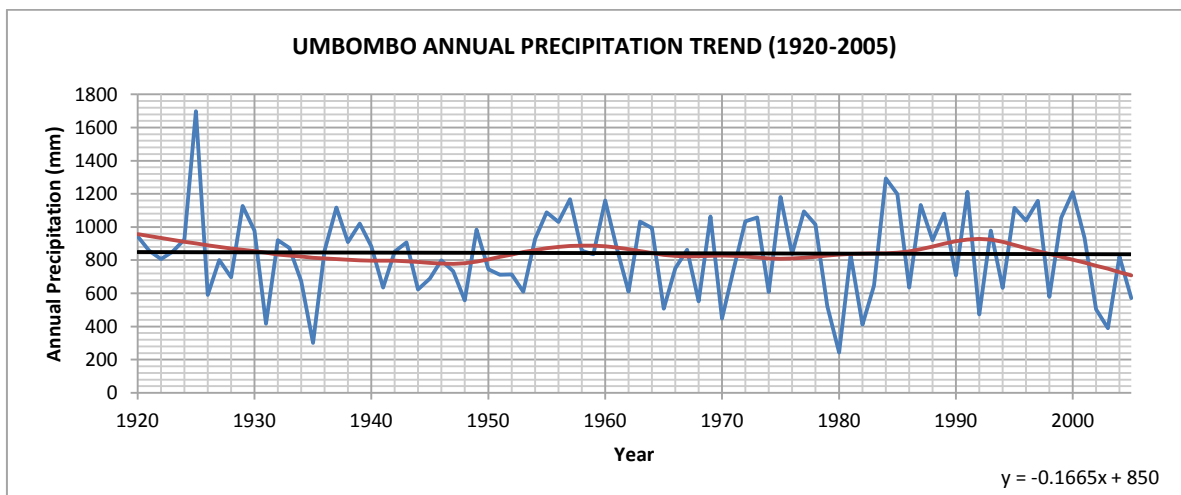
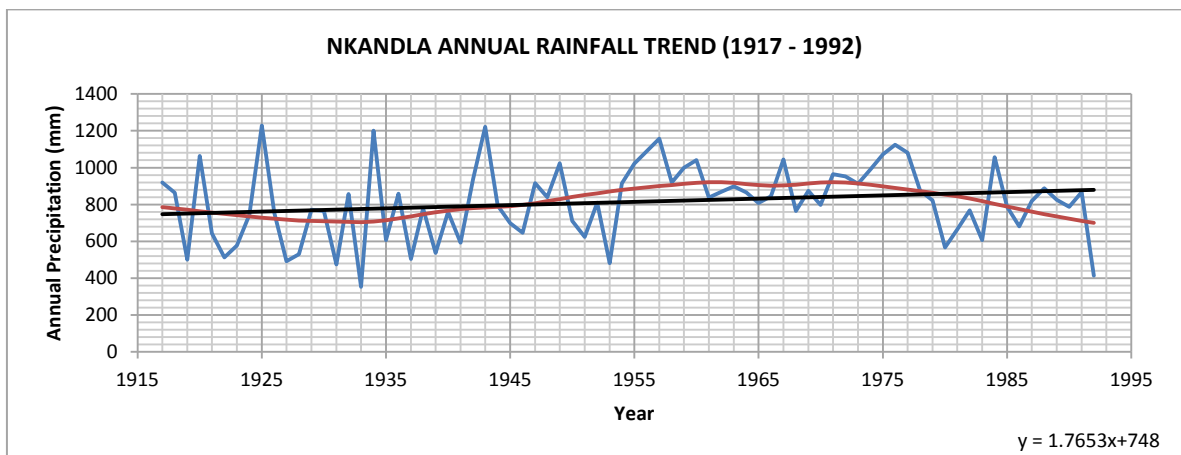
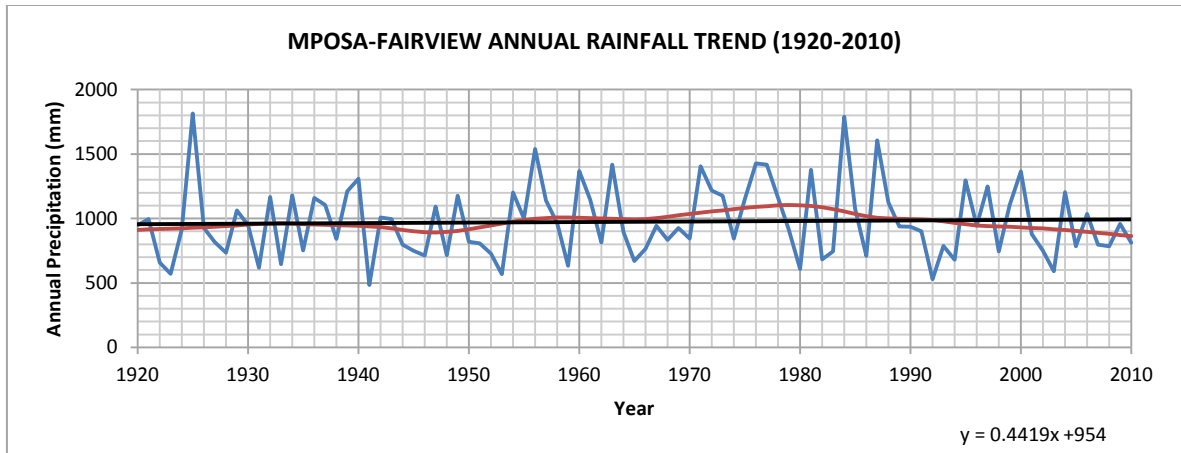
- Appendix A: Rainfall trends and extreme precipitation events for selected rainfall stations.
- Appendix B: National land-cover classification
- Appendix C: National land-cover classes aggregated into Agriculture, Degraded, Natural and Urban categories
- Appendix D: Agro-hydrological modelling with ACRU and validation of ACRU simulations
- Appendix E: Components of the SHETRAN model
- Appendix F: GCMs global climate change scenarios

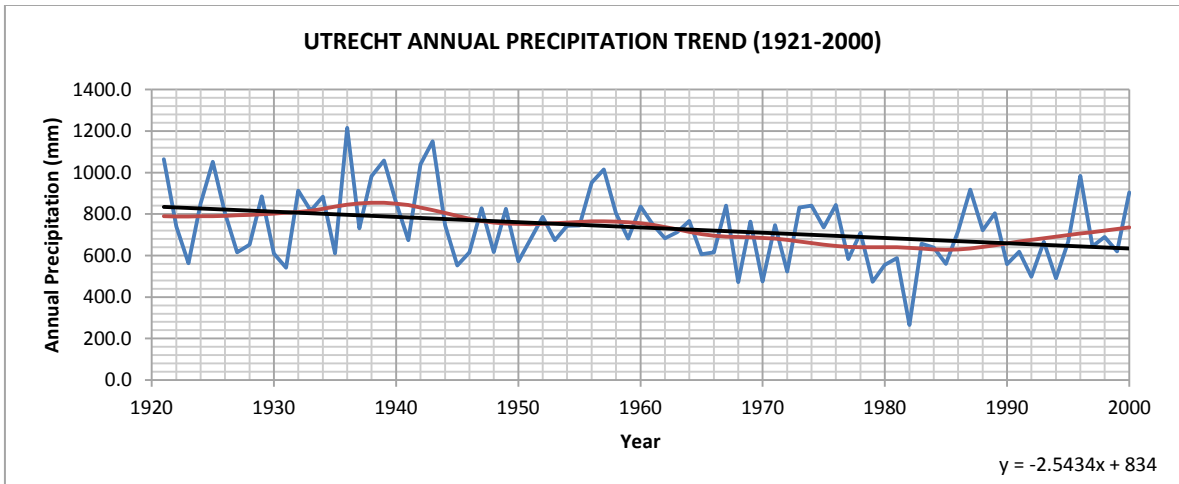
APPENDIX A: GRAPHS OF RAINFALL TRENDS AND PEAK OVER PREDEFINED THRESHOLDS

Annual rainfall trends with linear and loess fitting:

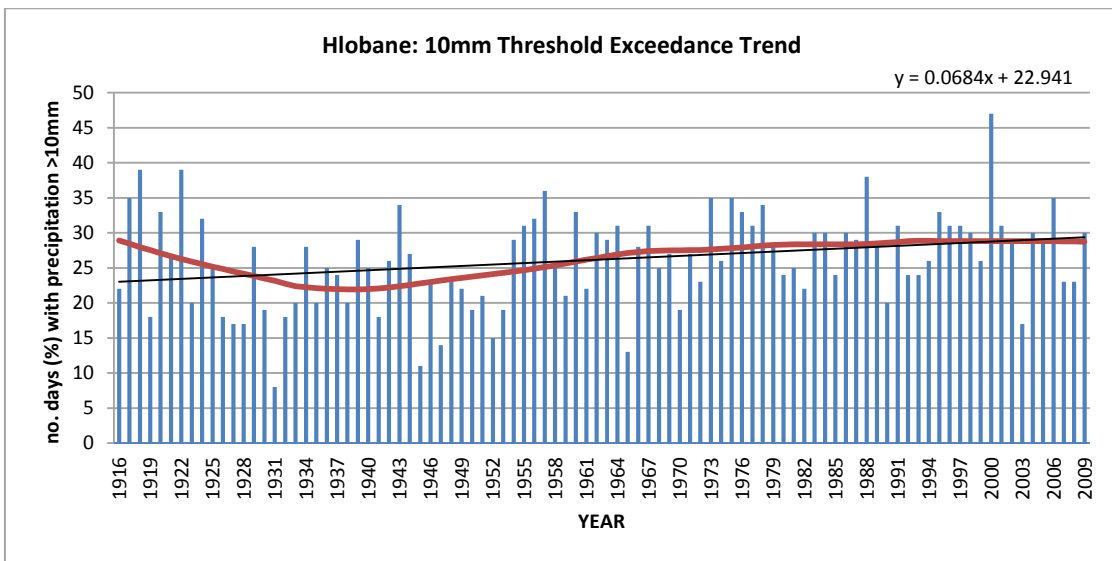
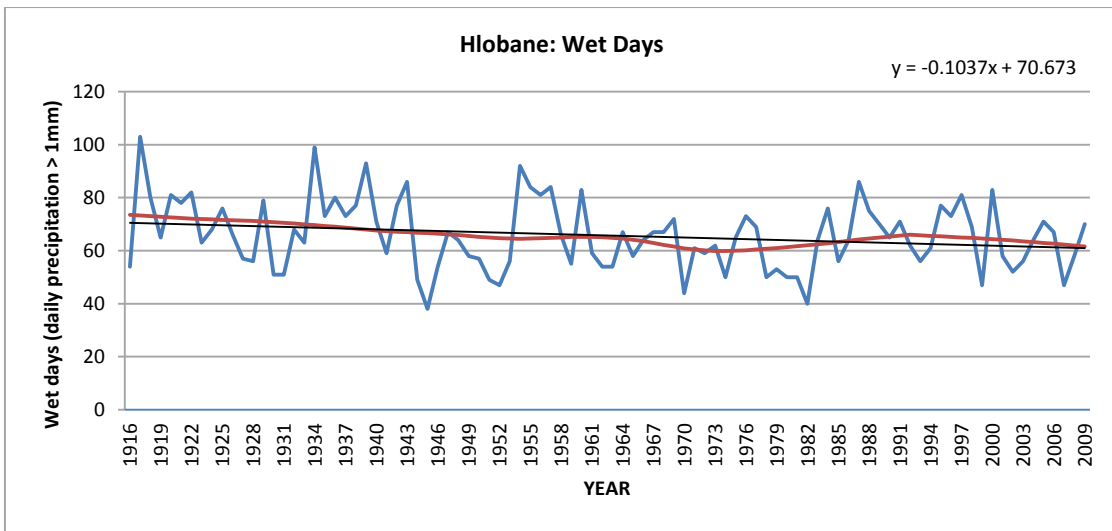


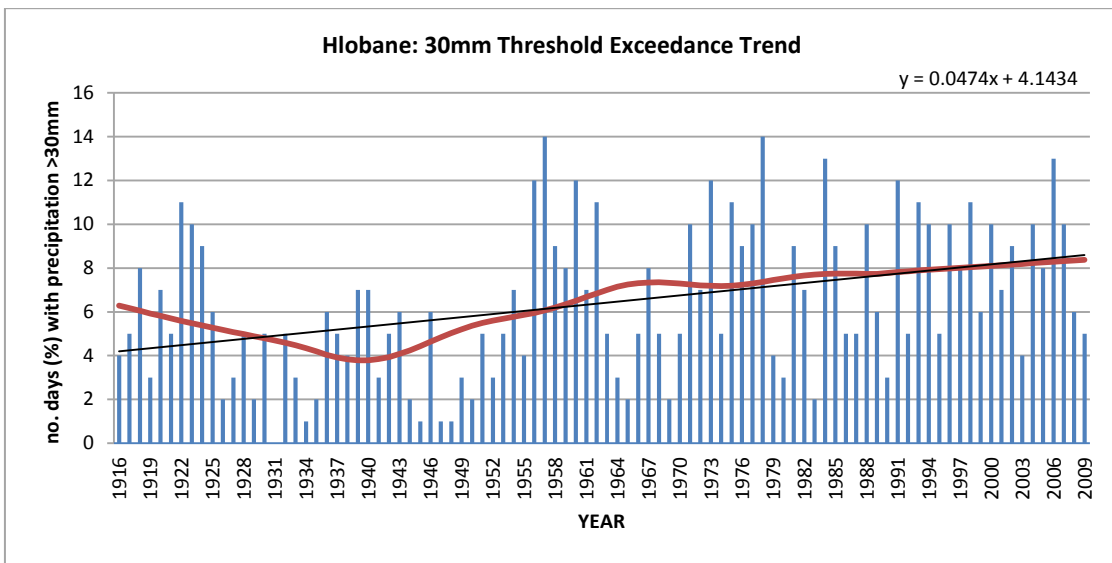
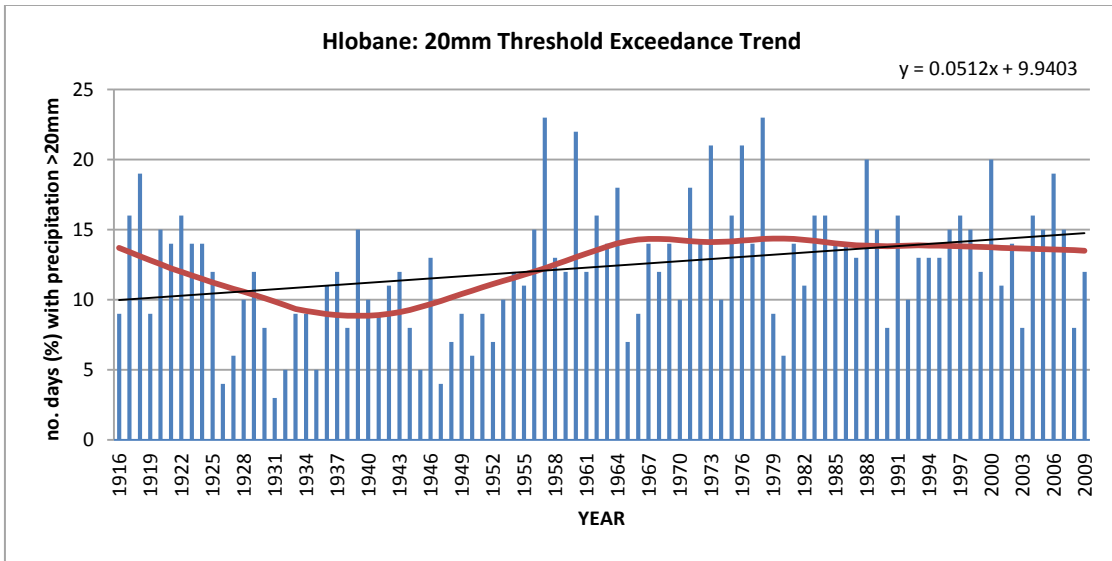


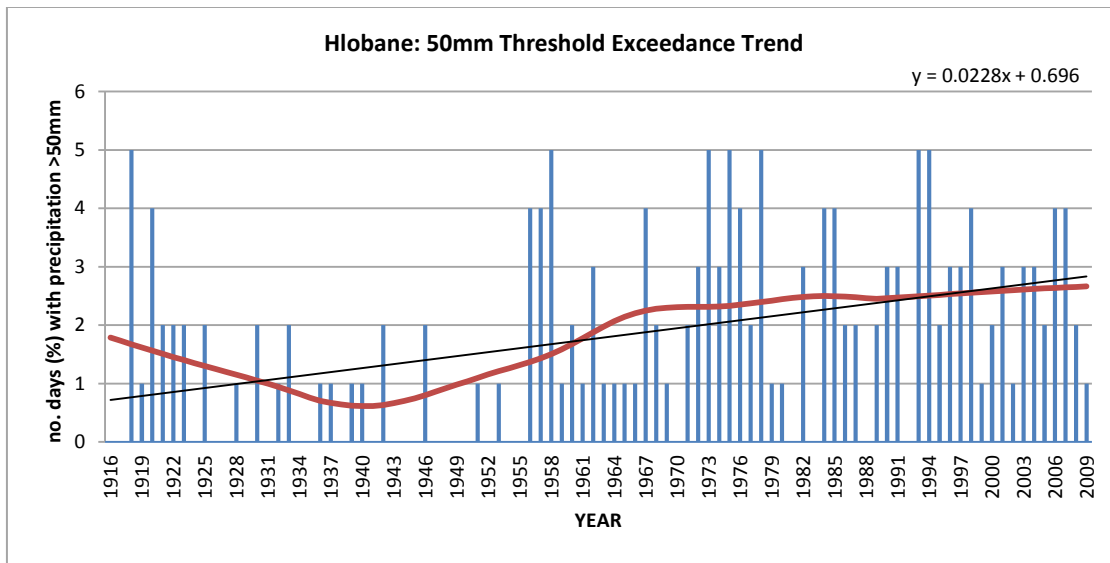




Peak over threshold graphs for Hlobane Station with linear and loess fitting:







APPENDIX B: NATIONAL LAND COVER CLASSIFICATION (THOMPSON, 1996: CITED IN HARRISON *ET AL.*, 2001).

NLC Code	Land-cover class	Description
1	Forest and Woodland	All wooded areas with greater than 10% tree canopy cover, where the canopy is composed of mainly self-supporting, single stemmed, woody plants >5 m in height. Essentially indigenous tree species growing under natural or semi-natural conditions.
2	Forest	
3	Thicket, scrub forest, bushland & high Fynbos	Communities typically composed of tall, woody, self-supporting, single and/or multi-stemmed plants (branching at or near the ground), generally with no clearly definable structure. Total canopy cover >10%, with canopy height between 2-5 m. Essentially indigenous species growing under natural or semi-natural conditions.
4	Shrubland & low Fynbos	Communities dominated by low, woody, self-supporting, multi-stemmed plants branching at or near the ground, between 0.2-2 m in height. Total tree cover <1.0%.
5	Herbland	Communities dominated by low, non-woody, self-supporting, non-grass like plants, between 0.2-2 m in height. Total tree cover <1.0%.
6	Unimproved grassland	Areas dominated by grass-like, non-woody, rooted herbaceous plants. Essentially indigenous species growing under natural or semi-natural conditions
7	Improved grassland	Planted grassland, containing either indigenous or exotic species, growing under man-managed conditions for grazing, hay or turf production, and recreation (e.g. golf courses).
8	Forest plantations	Areas of systematically planted, man-managed tree resources, composed of primarily exotic species (e.g. pine, eucalypt, wattle)
9	Waterbodies	Areas of open water including natural and man-made water bodies such as rivers, dams, permanent pans, lakes, lagoons and coastal waters.
10	Wetlands	Natural or artificial areas where the water level is at (or very near) the land surface on a permanent or temporary basis including saltmarsh, pans, reed-marsh, papyrus-swamp and peat bogs.
11	Barren rock	Natural areas of exposed sand, soil or rock with no, or very little, vegetation cover during any time of the year such as rock outcrops, dune and beach sand, dry river beds and gravel plains.
12	Dongas and sheet erosion scars	Permanent or seasonal, man-induced areas of very low vegetation cover (i.e. removal of tree, bush and/or herbaceous cover) in comparison with the surrounding natural vegetation cover. Typically associated with subsistence level farming and rural population centres, where overgrazing of livestock and/or wood-resource removal has been excessive. Often associated with severe soil erosion problems.
13	Degraded: forest and woodland	
14	Degraded: thicket & bushland etc.	
15	Degraded: unimproved grassland	
16	Degraded: shrubland and low Fynbos	
17	Degraded: herbland	
18	Cultivated: permanent - commercial irrigated	
19	Cultivated: permanent - commercial dryland	Lands cultivated with crops that occupy the area for long periods and are not replanted after harvest. Examples include tea plantations, vineyards, sugar cane, citrus orchards, hops and nuts.
20	Cultivated: permanent - commercial sugarcane	
21	Cultivated: temporary - commercial irrigated	Land under temporary crops that is harvested at the completion of the growing season, that remains idle until replanted. Examples include maize, wheat, legumes, potatoes, onions and Lucerne.
22	Cultivated: temporary - commercial dryland	
23	Cultivated: temporary - subsistence dryland	
24	Urban: residential	Areas in which people reside on a permanent or near-permanent basis including both formal and informal settlement areas, ranging from high to low building densities.
25	Urban: residential (smallholdings - forest & woodland)	
26	Urban: residential (smallholdings - thicket, bushland ...etc)	
27	Urban: residential (smallholdings - shrubland & low fynbos)	
28	Urban: residential (smallholdings - grassland)	
29	Urban: commercial	Non-residential areas used primarily for the conduct of commerce and other mercantile business, typically located in the central business district.
30	Urban: industrial/ transport	Non-residential areas with major industrial or transport related infrastructure. Examples include power stations, steel mills, dockyards and airports.
31	Mines and quarries	Areas in which mining activity has been done or is being done. Includes opencast mines and quarries as well as surface infrastructure (mine dumps etc.) associated with underground mining activities.

APPENDIX C: NATIONAL LAND-COVER CLASSES AGGREGATED INTO AGRICULTURE, DEGRADED, NATURAL, URBAN (SOURCE: HARRISON *ET AL.*, 2001).

NLC Code	Land-cover class	Aggregated categories
7	Improved grassland	Agriculture
8	Forest plantations	
18	Cultivated: permanent - commercial irrigated	
19	Cultivated: permanent - commercial dryland	
20	Cultivated: permanent - commercial sugar cane	
21	Cultivated: temporary - commercial irrigated	
22	Cultivated: temporary - commercial dryland	
23	Cultivated: temporary - subsistence dryland	
12	Dongas & sheet erosion scars	Degraded
13	Degraded: forest and woodland	
14	Degraded: thicket & bushland (etc)	
15	Degraded: unimproved grassland	
16	Degraded: shrubland and low Fynbos	
17	Degraded: hermland	
1	Forest and Woodland	Natural
2	Forest	
3	Thicket & bushland (etc)	
4	Shrubland and low Fynbos	
5	Hermland	
6	Unimproved grassland	
9	Waterbodies	
10	Wetlands	
11	Barren rock	
24	Urban: residential	Urban
25	Urban: residential (smallholdings: forest & woodland)	
26	Urban: residential (smallholdings: bushland)	
27	Urban: residential (smallholdings: shrubland)	
28	Urban: residential (smallholdings: grassland)	
29	Urban: commercial	
30	Urban: industrial/transport	
31	Mines & Quarries	

APPENDIX D: AGRO-HYDROLOGICAL MODELLING AND VALIDATION OF ACRU SIMULATIONS

Table D-1: Acocks veld types monthly values of water use coefficients, canopy interception per rain-day, root mass distribution in the topsoil, coefficient of initial abstractions and index of suppression of soil water evaporation by a litter/mulch layer, for natural land covers of the Mfolozi catchment.

Land-use (Acocks veld types)	Variable	Monthly values											
		Jan	Feb	Mar	Apr	May	Jun	Jul	Aug	Sep	Oct	Nov	Dec
Northern Tall Grassveld	CAY	0.75	0.75	0.75	0.5	0.4	0.3	0.2	0.2	0.55	0.7	0.75	0.75
	VEGINT	1.7	1.7	1.7	1.6	1.5	1.4	1.4	1.5	1.6	1.7	1.7	1.7
	ROOTA	0.9	0.9	0.9	0.95	0.95	1	1	1	0.95	0.9	0.9	0.9
	COIAM	0.15	0.15	0.2	0.3	0.3	0.3	0.3	0.3	0.3	0.3	0.3	0.25
Natal Sour Sandveld	CAY	0.75	0.75	0.7	0.5	0.35	0.2	0.2	0.2	0.5	0.65	0.7	0.75
	VEGINT	1.8	1.8	1.8	1.8	1.6	1.4	1.4	1.4	1.5	1.7	1.8	1.8
	ROOTA	0.9	0.9	0.9	0.95	0.95	1	1	1	0.95	0.9	0.9	0.9
	COIAM	0.15	0.15	0.2	0.3	0.3	0.3	0.3	0.3	0.3	0.3	0.3	0.25
Piet Retief Sourveld	CAY	0.7	0.7	0.7	0.55	0.45	0.2	0.2	0.2	0.5	0.6	0.7	0.7
	VEGINT	1.3	1.3	1.3	1.3	1.1	1	1	1	1.2	1.3	1.3	1.3
	ROOTA	0.9	0.9	0.9	0.9	0.95	1	1	1	0.95	0.9	0.9	0.9
	COIAM	0.15	0.15	0.25	0.3	0.3	0.3	0.3	0.3	0.3	0.3	0.3	0.2
Highland and Dohne Sourveld	CAY	0.7	0.7	0.7	0.5	0.3	0.2	0.2	0.2	0.5	0.65	0.7	0.7
	VEGINT	1.6	1.6	1.6	1.4	1.2	1	1	1	1.3	1.6	1.6	1.6
	ROOTA	0.9	0.9	0.9	0.95	1	1	1	1	0.95	0.9	0.9	0.9
	COIAM	0.15	0.15	0.25	0.3	0.3	0.3	0.3	0.3	0.3	0.3	0.3	0.2
Southern Tall Grassveld	CAY	0.75	0.75	0.75	0.5	0.4	0.2	0.2	0.2	0.55	0.7	0.75	0.75
	VEGINT	1.6	1.6	1.6	1.6	1.5	1.4	1.4	1.4	1.5	1.6	1.6	1.6
	ROOTA	0.9	0.9	0.9	0.95	0.95	1	1	1	0.95	0.9	0.9	0.9
	COIAM	0.15	0.15	0.2	0.3	0.3	0.3	0.3	0.3	0.3	0.3	0.3	0.2
Lowveld	CAY	0.8	0.8	0.8	0.65	0.55	0.4	0.4	0.4	0.6	0.75	0.75	0.8
	VEGINT	2.5	2.5	2.5	2.1	1.9	1.9	1.9	1.9	2.1	2.5	2.5	2.5
	ROOTA	0.8	0.8	0.8	0.85	0.9	0.9	0.9	0.9	0.85	0.8	0.8	0.8
	COIAM	0.2	0.2	0.25	0.3	0.3	0.3	0.3	0.3	0.3	0.3	0.3	0.25
Ngongoni Veld - Zululand	CAY	0.7	0.7	0.7	0.65	0.55	0.5	0.5	0.55	0.6	0.65	0.65	0.7
	VEGINT	1.4	1.4	1.4	1.4	1.3	1.2	1.2	1.3	1.4	1.4	1.4	1.4
	ROOTA	0.9	0.9	0.9	0.9	0.95	0.95	0.95	0.95	0.9	0.9	0.9	0.9
	COIAM	0.2	0.2	0.25	0.3	0.3	0.3	0.3	0.3	0.3	0.3	0.3	0.25

Appendices

Zululand Thornveld	CAY	0.8	0.8	0.8	0.7	0.65	0.5	0.5	0.6	0.75	0.8	0.8	0.8
	VEGINT	2.4	2.4	2.4	2.1	1.8	1.8	1.8	1.8	2.2	2.4	2.4	2.4
	ROOTA	0.8	0.8	0.8	0.8	0.9	0.9	0.9	0.9	0.8	0.8	0.8	0.8
	COIAM	0.2	0.2	0.25	0.3	0.3	0.3	0.3	0.3	0.3	0.3	0.3	0.25
N.E. Mountain Sourveld	CAY	0.75	0.75	0.75	0.6	0.5	0.25	0.25	0.25	0.5	0.7	0.7	0.75
	VEGINT	2.6	2.6	2.6	2.4	2.2	2	2	2	2.2	2.6	2.6	2.6
	ROOTA	0.8	0.8	0.8	0.85	0.9	1	1	1	0.87	0.8	0.8	0.8
	COIAM	0.2	0.2	0.25	0.3	0.3	0.3	0.3	0.3	0.3	0.3	0.3	0.25
Coastal Forest & Thornveld	CAY	0.85	0.85	0.85	0.85	0.75	0.65	0.65	0.75	0.85	0.85	0.85	0.85
	VEGINT	3.1	3.1	3.1	3.1	2.5	2	2	2.5	3.1	3.1	3.1	3.1
	ROOTA	0.75	0.75	0.75	0.75	0.75	0.75	0.75	0.75	0.75	0.75	0.75	0.75
	COIAM	0.3	0.3	0.3	0.3	0.3	0.3	0.3	0.3	0.3	0.3	0.3	0.3

Table D-2: Monthly values of water use coefficients, canopy interception per rain-day, root mass distribution in the topsoil, coefficient of initial abstractions and index of suppression of soil water evaporation by a litter/mulch layer, for current land-uses of the Mfolozi catchment.

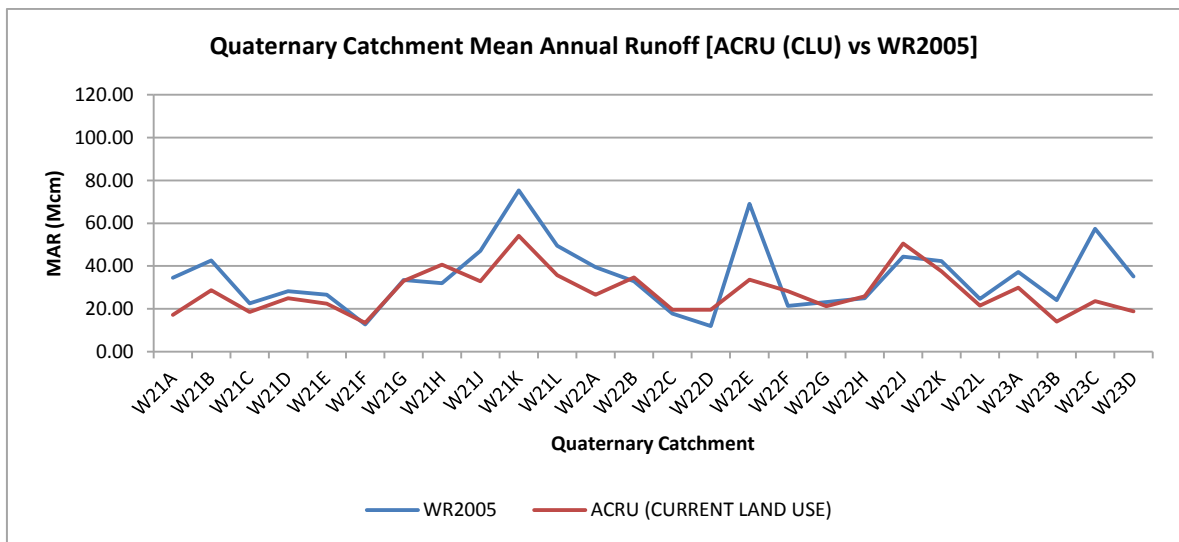
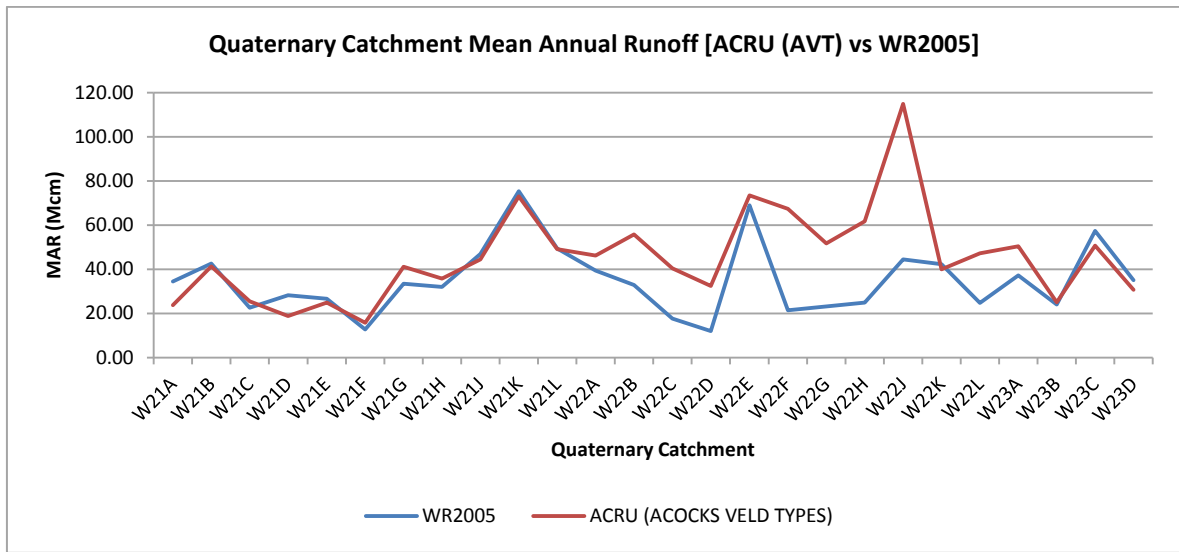
Land-use (Current land-use)	Variable	Monthly values											
		Jan	Feb	Mar	Apr	May	Jun	Jul	Aug	Sep	Oct	Nov	Dec
WOODLAND (Indigenous/Tree-bush savanna)	CAY	0.8	0.8	0.8	0.8	0.7	0.7	0.7	0.7	0.75	0.8	0.8	0.8
	VEGINT	2.5	2.5	2.5	2	2	2	2	2	2	2.5	2.5	2.5
	ROOTA	0.8	0.8	0.8	0.9	0.9	0.9	0.9	0.9	0.9	0.8	0.8	0.8
	COIAM	0.2	0.2	0.25	0.3	0.3	0.3	0.3	0.3	0.3	0.3	0.25	0.2
INDIGENOUS FOREST - ZULULAND	CAY	0.9	0.9	0.9	0.85	0.8	0.8	0.8	0.8	0.85	0.9	0.9	0.9
	VEGINT	3	3	3	3	3	3	3	3	3	3	3	3
	ROOTA	0.7	0.7	0.7	0.7	0.7	0.7	0.7	0.7	0.7	0.7	0.7	0.7
	COIAM	0.15	0.15	0.25	0.3	0.3	0.3	0.3	0.3	0.3	0.3	0.2	0.15
THICKET AND BUSHLAND	CAY	0.75	0.75	0.75	0.65	0.55	0.4	0.4	0.5	0.65	0.75	0.75	0.75
	VEGINT	2.5	2.5	2	2	2	2	2	2	2	2.5	2.5	2.5
	ROOTA	0.8	0.8	0.9	0.9	0.9	0.9	0.9	0.9	0.9	0.8	0.8	0.8
	COIAM	0.2	0.2	0.2	0.2	0.3	0.3	0.3	0.3	0.3	0.3	0.2	0.2
UNIMPROVED GRASSLAND	CAY	0.65	0.65	0.65	0.55	0.3	0.2	0.2	0.2	0.3	0.5	0.55	0.65
	VEGINT	1.5	1.5	1.5	1.5	1.5	1.5	1.5	1.5	1.5	1.5	1.5	1.5
	ROOTA	0.9	0.9	0.9	0.94	0.98	1	1	1	1	0.95	0.9	0.9
	COIAM	0.15	0.15	0.15	0.2	0.3	0.3	0.3	0.3	0.3	0.3	0.2	0.15
IMPROVED GRASS LAND (COASTAL)	CAY	0.55	0.55	0.55	0.55	0.55	0.55	0.55	0.55	0.55	0.55	0.55	0.55
	VEGINT	0.7	0.7	0.7	0.7	0.7	0.7	0.7	0.7	0.7	0.7	0.7	0.7
	ROOTA	0.95	0.95	0.95	0.95	0.95	0.95	0.95	0.95	0.95	0.95	0.95	0.95

	COIAM	0.2	0.2	0.2	0.3	0.3	0.3	0.3	0.3	0.3	0.3	0.2	0.2
FOREST PLANTATIONS EUCALYPTUS	CAY	0.95	0.95	0.95	0.95	0.95	0.95	0.95	0.95	0.95	0.95	0.95	0.95
	VEGINT	2.5	2.5	2.5	2.5	2.5	2.5	2.5	2.5	2.5	2.5	2.5	2.5
	ROOTA	0.65	0.65	0.65	0.65	0.65	0.65	0.65	0.65	0.65	0.65	0.65	0.65
	COIAM	0.35	0.35	0.35	0.35	0.35	0.35	0.35	0.35	0.35	0.35	0.35	0.35
FOREST PLANTATIONS PINE	CAY	0.85	0.85	0.85	0.85	0.85	0.85	0.85	0.85	0.85	0.85	0.85	0.85
	VEGINT	3.5	3.5	3.5	3.5	3.5	3.5	3.5	3.5	3.5	3.5	3.5	3.5
	ROOTA	0.66	0.66	0.66	0.66	0.66	0.66	0.66	0.66	0.66	0.66	0.66	0.66
	COIAM	0.35	0.35	0.35	0.35	0.35	0.35	0.35	0.35	0.35	0.35	0.35	0.35
FOREST PLANTATIONS WATTLE	CAY	0.9	0.9	0.9	0.88	0.85	0.86	0.89	0.9	0.92	0.92	0.9	0.9
	VEGINT	2	2	2	2	1.9	1.85	1.85	1.85	1.9	1.95	2	2
	ROOTA	0.83	0.83	0.83	0.83	0.83	0.83	0.83	0.83	0.83	0.83	0.83	0.83
	COIAM	0.25	0.25	0.25	0.3	0.3	0.3	0.3	0.3	0.3	0.3	0.25	0.25
WETLAND	CAY	0.8	0.8	0.8	0.7	0.6	0.5	0.4	0.4	0.4	0.5	0.6	0.7
	VEGINT	0.6	0.6	0.6	0.6	0.6	0.6	0.6	0.6	0.6	0.6	0.6	0.6
	ROOTA	1	1	1	1	1	1	1	1	1	1	1	1
	COIAM	0.2	0.2	0.2	0.2	0.3	0.3	0.3	0.3	0.3	0.3	0.2	0.2
DEGRADED THICKET AND BUSHLAND	CAY	0.55	0.55	0.55	0.45	0.3	0.3	0.3	0.3	0.4	0.45	0.55	0.55
	VEGINT	1.2	1.2	1.2	1.2	1	1	1	1	1	1.2	1.2	1.2
	ROOTA	0.85	0.85	0.85	0.85	0.9	0.9	0.9	0.9	0.9	0.85	0.85	0.85
	COIAM	0.1	0.1	0.1	0.15	0.2	0.2	0.2	0.2	0.2	0.15	0.1	0.1
DEGRADED UNIMPROVED GRASSLAND	CAY	0.55	0.55	0.55	0.45	0.2	0.2	0.2	0.2	0.4	0.45	0.55	0.55
	VEGINT	0.8	0.8	0.8	0.7	0.6	0.6	0.6	0.6	0.65	0.75	0.8	0.8

	ROOTA	0.9	0.9	0.9	0.94	1	1	1	1	0.95	0.92	0.9	0.9
	COIAM	0.1	0.1	0.1	0.15	0.15	0.2	0.2	0.2	0.2	0.15	0.1	0.1
CULTIVATED PERM. COMM.L SUGAR CANE	CAY	0.86	0.86	0.86	0.86	0.86	0.86	0.86	0.86	0.86	0.86	0.86	0.86
	VEGINT	1.9	1.9	1.9	1.9	1.9	1.9	1.9	1.9	1.9	1.9	1.9	1.9
	ROOTA	0.75	0.75	0.75	0.75	0.75	0.75	0.75	0.75	0.75	0.75	0.75	0.75
	COIAM	0.35	0.35	0.35	0.35	0.35	0.35	0.35	0.35	0.35	0.35	0.35	0.35
CULTIVATED TEMP. COMM. IRRIGATED	CAY	0.2	0.2	0.4	0.7	0.7	0.7	0.7	0.7	0.8	0.8	0.3	0.2
	VEGINT	0.5	0.5	0	0.5	0.7	0.8	1	1.2	1.2	0.5	0.5	0.5
	ROOTA	1	1	1	0.92	0.75	0.65	0.55	1	1	1	1	1
	COIAM	0.15	0.15	0.35	0.2	0.3	0.3	0.3	0.3	0.3	0.3	0.2	0.15
CULTIVATED TEMP. COMM. DRYLAND	CAY	1.07	1.01	0.55	0.35	0.35	0.35	0.35	0.35	0.35	0.35	0.36	0.75
	VEGINT	0.82	1.27	1.25	1.06	0.33	0.3	0.3	0.3	0.3	0.3	0.3	0.35
	ROOTA	0.77	0.75	0.81	0.93	1	1	1	1	1	1	0.99	0.86
	COIAM	0.2	0.2	0.25	0.3	0.3	0.3	0.3	0.3	0.3	0.35	0.3	0.25
CULTIVATED TEMP.SEMI-COMM. SUB. AGRIC.	CAY	0.87	0.81	0.45	0.35	0.2	0.2	0.2	0.2	0.2	0.2	0.3	0.6
	VEGINT	1.1	1.1	1	0.95	0.55	0.5	0.5	0.5	0.5	0	0.5	1
	ROOTA	0.8	0.8	0.85	0.93	1	1	1	1	1	1	1	0.86
	COIAM	0.2	0.2	0.25	0.3	0.3	0.3	0.2	0.2	0.2	0.35	0.3	0.25
URBAN RES. HIGH-DENSITY	CAY	0.7	0.7	0.6	0.5	0.45	0.4	0.4	0.4	0.4	0.6	0.7	0.7
	VEGINT	1.4	1.4	1.3	1.2	1.1	1	1	1	1	1.3	1.4	1.4
	ROOTA	0.9	0.9	0.9	0.95	0.95	0.95	0.95	0.95	0.92	0.92	0.9	0.9
	COIAM	0.2	0.2	0.2	0.25	0.3	0.3	0.3	0.3	0.3	0.3	0.2	0.2
URBAN RES. HIGH-DEN. (MORE RURAL THAN URBAN)	CAY	0.45	0.45	0.45	0.35	0.3	0.2	0.2	0.2	0.35	0.45	0.45	0.45

	VEGINT	0.5	0.5	0.5	0.5	0.5	0.5	0.5	0.5	0.5	0.5	0.5	0.5
	ROOTA	1	1	1	1	1	1	1	1	1	1	1	1
	COIAM	0.15	0.15	0.15	0.15	0.15	0.15	0.15	0.15	0.15	0.15	0.15	0.15
URBAN RES. MED. DENSITY (COASTAL)	CAY	0.8	0.8	0.8	0.7	0.6	0.5	0.5	0.5	0.5	0.6	0.8	0.8
	VEGINT	1.5	1.5	1.5	1.5	1.3	1.2	1.2	1.2	1.2	1.3	1.5	1.5
	ROOTA	0.85	0.85	0.85	0.9	0.95	0.95	0.95	0.95	0.9	0.85	0.85	0.85
	COIAM	0.25	0.25	0.25	0.3	0.3	0.3	0.3	0.3	0.3	0.3	0.25	0.25
URBAN INDUSTRIAL/TRANSPORT (COASTAL)	CAY	0.75	0.75	0.75	0.65	0.45	0.45	0.45	0.45	0.5	0.7	0.75	0.75
	VEGINT	1.5	1.5	1.5	1.5	1.3	1.3	1.3	1.3	1.4	1.5	1.5	1.5
	ROOTA	0.8	0.8	0.8	0.9	0.9	0.9	0.9	0.9	0.85	0.8	0.8	0.8
	COIAM	0.25	0.25	0.25	0.3	0.3	0.3	0.3	0.3	0.3	0.3	0.25	0.25
MINES AND QUARRIES	CAY	0.45	0.45	0.45	0.35	0.3	0.2	0.2	0.2	0.3	0.35	0.45	0.45
	VEGINT	0.5	0.5	0.5	0.5	0.5	0.5	0.5	0.5	0.5	0.5	0.5	0.5
	ROOTA	1	1	1	1	1	1	1	1	1	1	1	1
	COIAM	0.15	0.15	0.15	0.15	0.15	0.15	0.15	0.15	0.15	0.15	0.15	0.15
Langkloof Thicket-Renosterveld Severely Degraded	CAY	0.2	0.2	0.2	0.2	0.2	0.2	0.2	0.2	0.2	0.2	0.2	0.2
	VEGINT	0.2	0.2	0.2	0.2	0.2	0.2	0.2	0.2	0.2	0.2	0.2	0.2
	ROOTA	1	1	1	1	1	1	1	1	1	1	1	1
	COIAM	0.15	0.15	0.15	0.15	0.15	0.15	0.15	0.15	0.15	0.15	0.15	0.15

ACRU Simulations vs. WR2005:

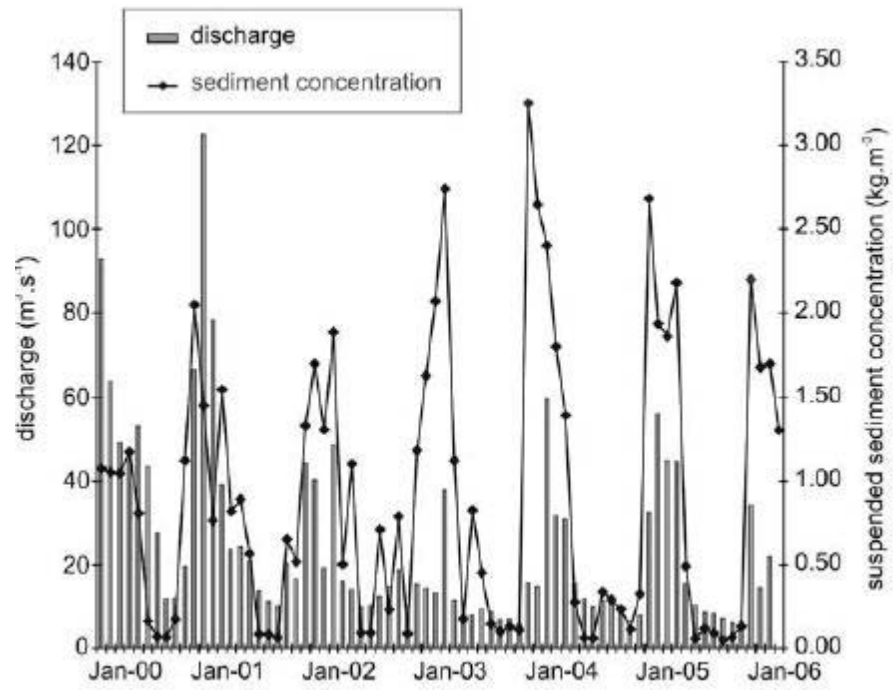


Summary of sedimentary and hydrological data:

TABLE 1 Summary of sedimentary and hydrological data																
Sampling date	Sample site	Transect	Cross-sectional area (m ²)	Weighted average velocity (m ² s ⁻¹)	Discharge (m ³ s ⁻¹)	Channel width (m)	Average depth (m)	Average discharge for sample site (m ³ s ⁻¹)	Average velocity for sample site (m ² s ⁻¹)	Average turbidity (ntu)	Total suspended sediment discharge (kg s ⁻¹)	Average suspended sediment concentration (kg m ⁻³)	Total bedload discharge (kg s ⁻¹)	Bedload discharge per width unit (kg m ⁻¹ s ⁻¹)	Suspended load (kg s ⁻¹): bedload (kg s ⁻¹)	Channel gradient (%)
11-Mar-06	A	A	11.2	0.4	4.44	38	0.26	3.13	0.31	297.33	1.95	0.44	0.45	0.0154	4.38 : 1	0.06
		Ax	10.03	0.35	3.47											
		Ay	7.97	0.19	1.49											
10-Mar-06	B	B	9.04	0.53	4.79	29	0.32	4.64	0.5	422.71	2.75	0.57	1.02	0.0428	2.70 : 1	0.03
		Bx	9.31	0.51	4.74											
		By	9.65	0.46	4.39											
09-Mar-06	C	C	13.17	0.57	7.62	32	0.39	6.72	0.54	520.29	4.36	0.57	1.08	0.0423	4.05 : 1	0.05
		Cx	11.6	0.53	6.17											
		Cy	12.21	0.52	6.37											
07-Mar-06	D	D	22.08	0.41	9	41	0.51	8.89	0.42	880.4	8.47	0.94	0.82	0.0218	10.32 : 1	0.02
		Dx	22.53	0.42	9.48											
		Dy	18.42	0.44	8.19											
08-Mar-06	E	E	17.14	0.37	6.25	40	0.4	6.78	0.43	673	4.57	0.73	0.84	0.0254	5.41 : 1	0.02
		Ex	14.7	0.46	6.74											
		Ey	15.89	0.46	7.34											

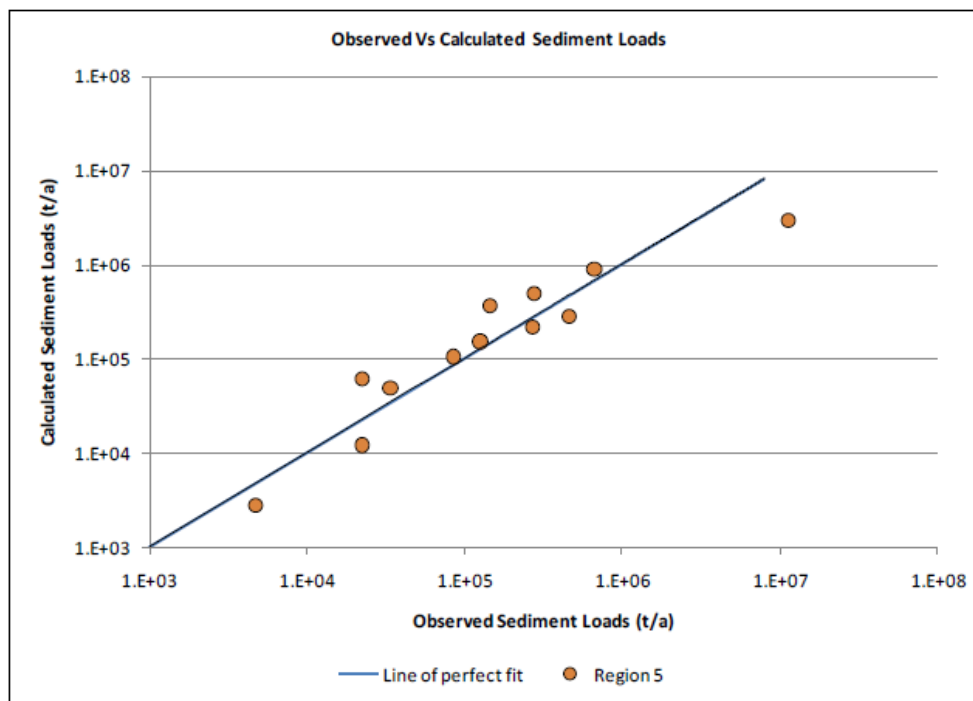
Summary of sedimentary and hydrological data (Source: Grenfell & Ellery, 2009).

Variation in sediment concentration and discharge:



Variation in sediment concentration and discharge from 2000-06 (Source: Grenfell & Ellery, 2009).

Simulated and observed data for Region 5 (KwaZulu-Natal):



Simulated and observed sediment loads for Region 5 (KwaZulu-Natal) using the empirical method (Msadala *et al.*, 2010)

APPENDIX E: COMPONENTS OF THE SHETRAN MODEL

Table E-1: Main components, processes and data required for the SHETRAN model (Source: Ewen *et al.*, 2000):

Component	Process	Data
<p><i>Water flow:</i> Surface water flow on ground surface and in stream channels; soil-water and ground-water flow in unsaturated and saturated zones, including systems of confined, unconfined, and perched aquifers</p>	<ul style="list-style-type: none"> • Canopy interception of rainfall • Evaporation and transpiration • Infiltration to subsurface • Surface runoff (overland, overbank, and in channels) • Snowpack development and snowmelt • Storage and 3D flow in variably saturated subsurface • Combinations of confined, unconfined, and perched aquifers • Transfers between subsurface water and river water • Ground-water seepage discharge • Well abstraction • River augmentation and abstraction • Irrigation 	<ul style="list-style-type: none"> • Precipitation and meteorological data for each station • Station numbers for each column and river link • Size and location of columns, river links, and finite-difference cells • Soil/rock types and depths for each column • Land-use/vegetation for each column • Man-controlled channel flow diversions and discharges • Rates of borehole pumping, artificial recharge, flow diversions, and so forth • Initial hydraulic potentials for subsurface • Initial overland and channel flow depths • Initial snowpack thicknesses and temperatures • Boundary hydraulic potentials (or flow rates) • Boundary stream inflow rates • Canopy drainage parameters and storage capacities • Ground cover fractions • Canopy resistances and aerodynamic resistances (for PME) • Vegetation root density distribution over depth • Porosity and specific storage of soils/rocks • Matric potential functions for soils/rocks • Unsaturated hydraulic conductivity functions for soils/rocks • Saturated hydraulic conductivity of soils/rocks • Snow density, zero-plane displacement, and roughness height

<p><i>Sediment transport</i> : Soil erosion and multifraction transport on ground surface and in stream channels</p>	<ul style="list-style-type: none"> • Erosion by raindrop and leaf drip impact and overland flow • Deposition and storage of sediments on ground surface • Total-load convection with overland flow • Overbank transport • Erosion of river beds and banks • Deposition on river bed • Down-channel advection • Infiltration of fine sediments into river bed 	<ul style="list-style-type: none"> • Raindrop size distribution • Drop sizes and fall distances for canopy drainage • Proportion of canopy drainage falling as leaf drip • Initial thickness of sediments and channel bed materials • Sediment concentrations in waters entering via inflowing streams • Sediment porosities and particle size distributions • Erodibility coefficients
<p><i>Solute transport</i> : Multiple, reactive solute transport on ground surface and in stream channels and subsurface</p>	<ul style="list-style-type: none"> • 3D advection with water flow • Advection with sediments • Dispersion • Adsorption to soils, rocks, and sediments • Two-region mobile/immobile effects in soils and rocks • Radioactive decay and decay chains • Deposition from atmosphere • Point or distributed surface or subsurface sources • Erosion of contaminated soils • Deposition of contaminated sediments • Plant uptake and recycling (simple representation only) • Exchanges between river water and river bed 	<ul style="list-style-type: none"> • Initial concentrations in surface and subsurface waters • Concentrations in rainfall • Dry deposition rates • Concentrations in flows entering at boundaries • Dispersion coefficients for soils/rocks • Adsorption distribution coefficients (and exponents, if nonlinear) • Mobile fractions for soils/rocks • Fractions of adsorption sites within mobile regions in soils/rocks • Exchange coefficients for mobile and immobile regions in soils/rocks • Decay constants (e.g., for radioactive decay) • Plant-uptake constants

APPENDIX F: GCMs GLOBAL CLIMATE CHANGE SCENARIOS (SOURCE: WARBURTON, 2012)

Institute	GCM	Acronym used & SRES Scenario	Downscaling Institute	Time period(s)
Canadian Center for Climate Modelling and Analysis (CCCma), Canada	Name: CGCM3.1 (T47) First published: 2005 Website: www.cccma.bc.ec.gc.ca/models/cgcm3.shtml	CCC A2	CSAG	1971 – 1990 2046 – 2065 2071 – 2100
		CCC B1	CSAG	1971 – 1990 2046 – 2065 2071 – 2100
Meteo-France/Centre for National de Recherches Meteorologiques (CRM), France	Name: CNRM-CM3 First published: 2004 Website: www.cnrm.meteo.fr/scenario2004/indexenglish.html	CRM A2	CSAG	1971 – 1990 2046 – 2065 2071 – 2100
		CRM B1	CSAG	1971 – 1990 2046 – 2065 2071 – 2100
Centre for Australian Weather and Climate Research: A partnership between CSIRO and the Bureau of Meteorology	Name: CSIRO Mk3.5 First published: 2005 Website: www.cawcr.gov.au/publications/technicalreports/CTR_021.pdf	CSIRO A2	CSAG	1971 – 1990 2046 – 2065 2071 – 2100
		CSIRO B1	CSAG	1971 – 1990 2046 – 2065 2071 – 2100
		CSIRO (CSIR) A2	CSIR	1961 - 2100
National Centre of Atmospheric Research, USA	Name: Community Climate Systems Model (CCSM3)	CCSM A1B	SMHI	1961 - 2100
		CCSM B2	SMHI	1961 - 2050

Geophysical Dynamics NOAA, USA	Fluid Laboratory, NOAA, USA	Name: GFDL-CM2.0 First published: 2005 Website: http://nomads.gfdl.noaa.gov/CM2.X/references/	GFDL2.0 A2	CSAG	1971 – 1990 2046 – 2065 2071 – 2100
			GFDL2.0 B1	CSAG	1971 – 1990 2046 – 2065 2071 – 2100
			GFDL2.0 (CSIR) A2	CSIR	1961 - 2100
Geophysical Dynamics NOAA, USA	Fluid Laboratory, NOAA, USA	Name: GFDL-CM2.1 First published: 2005 Website: http://nomads.gfdl.noaa.gov/CM2.X/references/	GFDL2.1 A2	CSAG	1971 – 1990 2046 – 2065 2071 – 2100
			GFDL2.1 B1	CSAG	1971 – 1990 2046 – 2065 2071 – 2100
			GFDL2.1 (CSIR) A2	CSIR	1961 - 2100
Goddard Institute for Space Studies (GISS), NASA, USA		Name: GISS MODELE-R First published: 2006 Website: www.giss.nasa.gov/tools/modelE/	GISS A2	CSAG	1971 – 1990 2046 – 2065 2071 – 2100
			GISS B1	CSAG	1971 – 1990 2046 – 2065 2071 – 2100
Max Planck Institute for Meteorology (MPI-M), Germany		Name: ECHAM4 First published: Website:	ECH4 A2	SMHI	1961 - 2050
			ECH4 B2	SMHI	1961 - 2050
Meteorological Institute University of Bonn (MIUB),		Name: MIUB ECHO-G First published: 2005	ECHO A2	CSAG	1971 – 1990 2046 – 2065

Germany				2071 – 2100
Max Planck Institute for Meteorology (MPI-M), Germany	Name: ECHAM5/MPI-OM First published: 2005 Website: www.mpimet.mpg.de/en/wissenschaft/modelle.html	ECHO B1	CSAG	1971 – 1990 2046 – 2065 2071 – 2100
Institut Pierre Simon Laplace (IPSL), France	Name: IPSL-CM4 First published: 2005 Website: mc2.ipsl.jussieu.fr/simules.html	ECH5 A2	CSAG	1971 – 1990 2046 – 2065 2071 – 2100
		ECH5 B1	CSAG	1971 – 1990 2046 – 2065 2071 – 2100
Meteorological Research Institute, Japan Meteorological Agency, Japan	Name: MRI CGCM2.3.2a First published: 2003 Website: www.mri-jma.go.jp/Dep/cl/cl4/publications/yukimoto_pap2001.pdf	ECH5 (CSIR) A2	CSIR	1961 - 2100
		ECH5 A1B	SMHI	1961 - 2100
		IPSL A2	CSAG	1971 – 1990 2046 – 2065 2071 – 2100
		IPSL B1	CSAG	1971 – 1990 2046 – 2065 2071 – 2100
		MRI A2	CSAG	1971 – 1990 2046 – 2065 2071 – 2100
		MRI B1	CSAG	1971 – 1990 2046 – 2065 2071 – 2100

<p>Hadley Centre for Climate Prediction and Research</p> <p>Met Office, United Kingdom</p>	<p>Name: UKHADcm3</p> <p>First published: 2000</p> <p>Website: www.metoffice.gov.uk/research/modelling-systems/unified-model/climate-models/hadcm3</p>	<p>UKHAD A2</p>	<p>CSIR</p>	<p>1961 - 2100</p>
<p>Center for Climate System Research (CCSR), University of Tokyo; National Institute for Environmental Studies (NIES); Frontier Research Center for Global Change (FRCGC)</p>	<p>Name: MIROC 3.2</p> <p>First published: 2004</p> <p>Website: www.ccsr.u-tokyo.ac.jp/kyosei/hasumi/MIROC/tech-repo.pdf</p>	<p>MIROC A2</p>	<p>CSIR</p>	<p>1961 - 2100</p>